

**MECHANISTIC STUDIES OF CHONDROITIN AC LYASE
FROM *FLAVOBACTERIUM HEPARINUM***

By

CARL S. RYE

B.Sc., The University of Victoria, 1997

A THESIS SUBMITTED IN PARTIAL FULFILMENT OF
THE REQUIREMENTS FOR THE DEGREE OF
DOCTOR OF PHILOSOPHY

in

THE FACULTY OF GRADUATE STUDIES
(Department of Chemistry)

We accept this thesis as conforming
to the required standard

THE UNIVERSITY OF BRITISH COLUMBIA

September 2002

© Carl S. Rye, 2002

In presenting this thesis in partial fulfilment of the requirements for an advanced degree at the University of British Columbia, I agree that the Library shall make it freely available for reference and study. I further agree that permission for extensive copying of this thesis for scholarly purposes may be granted by the head of my department or by his or her representatives. It is understood that copying or publication of this thesis for financial gain shall not be allowed without my written permission.

Department of Chemistry

The University of British Columbia
Vancouver, Canada

Date Sept. 23, 2002

Abstract

Chondroitin AC lyase from *Flavobacterium heparinum* degrades chondroitin sulfate glycosaminoglycans via an elimination mechanism resulting in disaccharides or oligosaccharides with $\Delta 4,5$ -unsaturated uronic acid residues at their non-reducing end. A general mechanism for all polysaccharide lyases has been proposed, however no mechanistic details exist, mainly due to the inhomogeneous nature of the polymeric substrates available, which renders impossible the collection of reliable and reproducible data. Thus, three different types of substrate were developed that can be monitored by three different techniques: UV/Vis spectroscopy, fluorescence spectroscopy, and by the use of a fluoride ion-selective electrode. These synthetic substrates have allowed the measurement of defined and reproducible kinetic parameters previously unavailable using the polymeric natural substrates.

The creation of this new class of structurally defined substrates has allowed their modification in order to carry out a variety of mechanistic analyses aimed at deciphering the exact catalytic mechanism of chondroitin AC lyase. A combination of primary and secondary deuterium kinetic isotope effects together with a linear free energy relationship has revealed the details regarding the order of the bond breaking and making steps of the enzymatic reaction. These mechanistic studies have revealed the reaction mechanism to be stepwise, including a rate-limiting proton abstraction followed by a facile elimination of the C4-linked leaving group. In addition, a solvent isotope exchange experiment has revealed that the exchange of deuterium at C5 does not compete with the departure of the leaving group, thus classifying the elimination mechanism as (E1cb)_{irr} or (E1cb)_I in which the proton abstraction step is essentially irreversible.

Tight binding inhibitors, in conjunction with X-ray crystallography, may allow the identification of key catalytic residues responsible for binding and catalysis. There are no known specific inhibitors of polysaccharide lyases reported in the literature, prompting investigation into this area. Two potential inhibitors of chondroitin AC lyase were synthesized, based on two different design concepts. The first, a disaccharide molecule containing a pre-formed C4-C5 alkene moiety in combination with an intact hexosamine leaving group sugar residue, surprisingly showed no inhibition. The second

potential inhibitor was a novel 5-nitro sugar, designed to mimic the *aci*-carboxylate intermediate along the reaction pathway. This compound was found to be a competitive inhibitor of the enzyme with a K_i value of ~ 0.7 mM. Unfortunately this relatively large inhibition constant is not representative of a transition state analogue, which would be expected to bind much tighter to the enzyme.

Table of Contents

Abstract	ii
Table of Contents	iv
List of Figures	ix
List of Tables	xii
List of Schemes	xiii
List of Abbreviations	xv
Acknowledgments	xvii
 Chapter 1 – Introduction	 1
1.1 Glycosaminoglycans and Proteoglycans	2
1.1.1 Structure	2
1.1.1.1 Chondroitin Sulfate and Dermatan Sulfate	5
1.1.1.2 Hyaluronic Acid	7
1.1.1.3 Heparin and Heparan Sulfate	8
1.1.1.4 Keratan Sulfate	9
1.1.2 Biological Roles of GAGs and Proteoglycans	10
1.1.3 GAG Degradation	14
1.1.3.1 Hydrolytic Mechanism	14
1.1.3.2 Eliminative Mechanism	16
1.2 Chondroitin AC Lyase	20
1.2.1 Three Dimensional Structure	21
1.2.2 Previous Research on Chondroitin AC Lyase	23
1.3 Other Enzymes Performing Elimination Reactions	25
1.4 Aims of This Thesis	31

Chapter 2 – Development of an Assay for Chondroitin AC Lyase

.....	32
2.1 Historical Assays	32
2.2 Development of Synthetic Substrates	34
2.3 Chromogenic Substrate (1)	36
2.4 Fluorogenic Substrate (2).....	37
2.5 Fluoride-Releasing Substrate (3).....	40
2.6 Conclusions.....	41
2.7 Methods	41
2.7.1 UV/Vis Spectroscopy.....	41
2.7.2 Fluorescence Spectroscopy.....	42
2.7.3 Fluoride Ion-Selective Electrode.....	42

Chapter 3 – Mechanistic Studies 43

3.1 Aims of This Research.....	43
3.2 Mechanistic Considerations	43
3.2.1 Rate Enhancement and the pK_a of the α -Proton.....	43
3.2.2 Modified Substrates	47
3.3 Synthetic Substrates	47
3.3.1 Synthesis	49
3.3.1.1 <i>Synthesis of the Fluorinated Substrates</i>	49
3.3.1.2 <i>Synthesis of the Chromogenic Substrates</i>	58
3.3.1.3 <i>Synthesis of the Fluorogenic Substrate</i>	62
3.3.1.4 <i>Synthesis of the Substrates for the Kinetic Isotope Effects</i>	63
3.4 Fluoride-Releasing Substrates and the Effect of the Aglycone Moiety	65
3.4.1 Monosaccharide Substrates.....	65
3.4.2 Disaccharide Substrate.....	66
3.4.3 Incompetent Fluorinated Substrates as Competitive Inhibitors	67
3.5 pH Dependence.....	68
3.6 Linear Free Energy Relationship.....	72
3.6.1 Background and Theory.....	72

3.6.2 Results and Discussion.....	74
3.7 Kinetic Isotope Effects.....	78
3.7.1 Primary Kinetic Isotope Effects	79
3.7.1.1 Background and Theory.....	79
3.7.1.2 Results and Discussion.....	80
3.7.2 Secondary Kinetic Isotope Effects	83
3.7.2.1 Background and Theory.....	83
3.7.2.2 Results and Discussion.....	85
3.8 Deuterium Exchange.....	88
3.8.1 Results and Discussion.....	88
3.8.2 Mechanistic Classification	92
3.9 Conclusions.....	92
 Chapter 4 – Potential Inhibitors of Chondroitin AC Lyase.....	95
4.1 Background.....	95
4.2 Inhibitor Design	97
4.3 Synthesis	101
4.3.1 Synthesis of the Disaccharide Inhibitor.....	101
4.3.2 Synthesis of the 5-Nitro Inhibitor.....	105
4.4 Inhibition Studies.....	107
4.4.1 Inhibition of Chondroitin AC Lyase by Compound 88	107
4.4.2 Inhibition of Chondroitin AC Lyase by Compound 89	108
4.5 Conclusions.....	113
 Chapter 5 - Materials and Methods	114
5.1 Isolation and Purification of Chondroitin AC Lyase from <i>Flavobacterium</i> <i>heparinum</i>	114
5.2 Enzymology	117
5.2.1 pH Analyses.....	117
5.2.1.1 pH Profiles for Chondroitin 6-Sulfate.....	117
5.2.1.2 pH Profile for the Synthetic Substrate 4 (k_{cat}/K_m).....	118

5.2.2 Kinetic Isotope Effects	118
5.2.3 Inhibition Studies	118
5.2.3.1 Inhibition by Compounds 88 and 89	118
5.2.3.2 Inhibition by Compounds 52 and 58	119
5.3 General Synthesis	120
5.3.1 General Acetylation Procedure	120
5.3.2 General Zemplén Deprotection	120
5.3.3 General Acetyl Chloride Deprotection	121
5.4 Synthesis of the Fluorinated Substrates	121
5.4.1 Phenyl 4-deoxy-4-fluoro- β -D-glucopyranosiduronic acid (3) (Scheme 3.1) ..	121
5.4.2 Benzyl 4-deoxy-4-fluoro- β -D-glucopyranosiduronic acid (4) (Scheme 3.1) ..	125
5.4.3 Methyl 4-deoxy-4-fluoro- β -D-glucopyranosiduronic acid (5) (Scheme 3.1) ..	128
5.4.4 Benzyl <i>O</i> -(4-deoxy-4-fluoro- β -D-glucopyranosiduronic acid)-(1 \rightarrow 3)-2- acetamido-2-deoxy- β -D-galactopyranoside (6) (Schemes 3.2, 3.3 and 3.4)	130
5.4.5 Benzyl 4-deoxy-4-fluoro- β -D-galactopyranosiduronic acid (52) (Scheme 3.5)	141
5.4.6 Phenyl 4-deoxy-4,4-difluoro- β -D- <i>xylo</i> -hexopyranosiduronic acid (58) (Scheme 3.6)	145
5.5 Synthesis of the Chromogenic Substrates	150
5.5.1 Benzyl 4- <i>O</i> -(2',4'-dinitrophenyl)- β -D-glucopyranosiduronic acid (1) (Scheme 3.7)	150
5.5.2 Benzyl 4- <i>O</i> -(4'-chloro-2'-nitrophenyl)- β -D-glucopyranosiduronic acid (8) (Scheme 3.8)	152
5.5.3 Benzyl 4- <i>O</i> -(2',5'-dinitrophenyl)- β -D-glucopyranosiduronic acid (10) (Scheme 3.8)	154
5.5.4 Benzyl 4- <i>O</i> -(4'-nitrophenyl)- β -D-glucopyranosiduronic acid (12) (Scheme 3.8)	155
5.5.5 Benzyl 4- <i>O</i> -(3',4'-dinitrophenyl)- β -D-glucopyranosiduronic acid (7) (Scheme 3.9)	157
5.5.6 Benzyl 4- <i>O</i> -(2'-nitrophenyl)- β -D-glucopyranosiduronic acid (9) (Scheme 3.9)	160

5.5.7 Benzyl 4- <i>O</i> -(2',4',6'-trichlorophenyl)- β -D-glucopyranosiduronic acid (11) (Scheme 3.9)	161
5.6 Synthesis of the Fluorogenic Substrate	163
Phenyl 4-methylumbelliferyl- β -D-glucopyranosiduronic acid (2) (Scheme 3.10) .	163
5.7 Synthesis of the Substrates for the Deuterium Kinetic Isotope Effects	167
5.7.1 Phenyl 4-deoxy-4-fluoro-5- $\{^2\text{H}\}$ - β -D-glucopyranosiduronic acid (83) (Scheme 3.11).....	167
5.7.2 Phenyl 4-deoxy-4-fluoro-4- $\{^2\text{H}\}$ - β -D-glucopyranosiduronic acid (87) (Scheme 3.12).....	169
5.8 Synthesis of the Potential Inhibitors.....	172
5.8.1 Methyl <i>O</i> -(2-acetamido-2-deoxy- β -D-galactopyranosyl)-(1 \rightarrow 4)- α -L-threo-hex- 4-enopyranoside (88) (Schemes 4.1, 4.2, and 4.3)	172
5.8.2 Phenyl (5S)-5-nitro- β -D-xylopyranoside (89) (Scheme 4.4)	180
Appendix 1.....	184
Appendix 2.....	185
Appendix 3.....	186
Appendix 4.....	187
Appendix 5.....	188
References.....	189

List of Figures

Figure 1.1. The general structure of the GAGs. The chondroitin sulfates containing <i>N</i> -acetylgalactosamine and glucuronic acid residues are shown	3
Figure 1.2. Illustration of a proteoglycan	5
Figure 1.3. The structures of the common chondroitin sulfates	6
Figure 1.4. The structure of hyaluronic acid	7
Figure 1.5. The structures of heparin and heparan sulfate, showing the significant heterogeneity of these polymers introduced by the minor sequence	9
Figure 1.6. The structure of keratan sulfate.....	10
Figure 1.7. Structure of the specific pentasaccharide sequence in heparin responsible for its high affinity to antithrombin III	12
Figure 1.8. Simplified blood coagulation scheme	14
Figure 1.9. Schematic showing the proposed three-step mechanism of chondroitin AC lyase	16
Figure 1.10. Possible mechanism of elimination (E1) involving the formation of a carbonium ion intermediate	18
Figure 1.11. Possible mechanism of elimination involving the formation of a covalent intermediate by an active site nucleophile	18
Figure 1.12. Hydrolysis of the disaccharide product of the lyase reaction by a glycuronidase to produce an α -keto acid and an amino sugar.....	19
Figure 1.13. Three dimensional crystal structure of chondroitin AC lyase	22
Figure 1.14. Representative examples of reactions catalyzed by enzymes of the enolase superfamily	26
Figure 1.15. The reactions catalyzed by crotonase, fumarase and cis,cis-muconate cycloisomerase.....	28
Figure 1.16. The elimination reaction catalyzed by 6-phosphogluconate dehydrase	29
Figure 1.17. The overall reaction catalyzed by L-2-keto-3-deoxyarabonate dehydrase... ..	29
Figure 1.18. The reaction Scheme for the conversion of 2-keto-3-deoxyarabonate to α -ketoglutaric semialdehyde by L-2-keto-3-deoxyarabonate dehydrase	30
Figure 2.1. The thiobarbituric acid reaction as an assay for polysaccharide lyases.....	33

Figure 2.2. (A) Three substrates designed for the assay of chondroitin AC lyase representing three separate assay techniques. (B) The conversion of substrate to products by chondroitin AC lyase.....	35
Figure 2.3. Kinetic data for the chromogenic substrate 1 fitted to the Michaelis-Menten equation	37
Figure 2.4. Kinetic Scheme for substrate inhibition	38
Figure 2.5. (A) Kinetic data for the fluorogenic substrate 2 fitted to Equation 1 showing substrate inhibition at high concentrations of substrate. (B) Low substrate concentration data for 2 fitted to the Michaelis-Menten equation.....	39
Figure 2.6. Kinetic data for the fluoride-releasing substrate 3 fitted to the Michaelis-Menten equation	40
Figure 3.1. Scheme illustrating how the mechanisms of polysaccharide lyases and epimerases differ only in the final proton delivery step	44
Figure 3.2. Illustration of how a hydrogen bond may preferentially stabilize the reaction intermediate (or transition state that resembles it) compared to the substrate	46
Figure 3.3. The fluoride-releasing substrates	48
Figure 3.4. The chromogenic and fluorogenic substrates.....	48
Figure 3.5. Competitive inhibitors of chondroitin AC lyase	67
Figure 3.6. pH Profiles for chondroitin AC lyase. (A) V_{\max} vs pH profile for chondroitin 6-sulfate. (B) k_{cat}/K_m vs pH profile for compound 4 . (C) K_m vs pH for chondroitin 6-sulfate. (D) k_{cat}/K_m vs pH profile for chondroitin 6-sulfate.....	71
Figure 3.7. Two step mechanism of a glycosidase shown cleaving a series of substituted phenyl glycosides.....	74
Figure 3.8. Linear free energy relationship for chondroitin AC lyase produced using substrates with substituted phenol leaving groups	76
Figure 3.9. Substrates for primary (83) and secondary (87) deuterium kinetic isotope effects.....	78
Figure 3.10. Primary deuterium KIE data	81
Figure 3.11. The first step of the enzyme catalyzed elimination reaction to give the enolic intermediate	82

Figure 3.12. Illustration of a transition state for a concerted <i>syn</i> -elimination process where a non-linear arrangement of proton donor, proton, and proton acceptor (X) may result in a less than maximal 1° KIE.....	83
Figure 3.13. Energy profiles illustrating the changes in zero-point energy differences between hydrogen- (H) and deuterium- (D) labelled substrates upon going to the transition state	85
Figure 3.14. Secondary deuterium KIE data. Plots of rate vs concentration for (A) the protio compound (3), and (B) the deutero compound (87).....	86
Figure 3.15. The interconversion of (+)-muconolactone and <i>cis,cis</i> -muconate by <i>cis,cis</i> -muconate cycloisomerase	87
Figure 3.16. Stacked plot of the partial ¹ H NMR spectra of compound 4 as it is turned over to product by chondroitin AC lyase	89
Figure 3.17. Deuterium exchange experiment. Partial ¹ H NMR spectra of (A) the monosaccharide substrate (4), and (B) its partial enzymatic digestion to product by chondroitin AC lyase in D ₂ O.	91
Figure 4.1. Schematic showing how the catalytic acid and base could be one common or two separate amino acid residues	96
Figure 4.2. The proposed inhibitors of chondroitin AC lyase	98
Figure 4.3. Schematic showing show a nitro group mimics a carboxyl group	99
Figure 4.4. The substrates and their nitro analogues for several non-carbohydrate lyases	100
Figure 4.5. X-ray crystal structure of compound 104 showing the ⁴ S ₀ conformation ...	107
Figure 4.6. Spectrophotometric titration of compound 89	108
Figure 4.7. Rates of protonation (descending curves) of the preformed carbanion of 89 and deprotonation (ascending curves) of 89 at pH 8.0 and 6.8	109
Figure 4.8. Graph illustrating the increased protonation rates of the nitronate anion in the presence of chondroitin AC lyase. The nitronate anion absorbs at 242 nm whereas the conjugate acid does not	111
Figure 4.9. Dixon plot showing the inhibition by the anion of compound 89	112
Figure 5.1. SDS-PAGE gel of fractions from the SP Sepharose column	116
Figure 5.2. SDS-PAGE gel of fractions from the ceramic hydroxyapatite column.....	116

List of Tables

Table 2.1. Kinetic parameters for selected synthetic substrates	36
Table 3.1. Kinetic data for fluoride-releasing substrates	66
Table 3.2. Size comparison between hydrogen and fluorine	68
Table 3.3. Kinetic data for chromogenic and fluorogenic substrates.....	75

List of Schemes

Scheme 3.1. Synthesis of the fluoride-releasing monosaccharide substrates	49
Scheme 3.2. Synthesis of 2,3,6-tri- <i>O</i> -benzoyl-4-deoxy-4-fluoro- α -D-glucopyranosyl bromide (29), the donor molecule for the disaccharide substrate	51
Scheme 3.3. Synthesis of benzyl 2-acetamido-4,6-di- <i>O</i> -acetyl-2-deoxy- β -D- galactopyranoside (40), the acceptor molecule for the disaccharide substrate	52
Scheme 3.4. Synthesis of benzyl <i>O</i> -(4-deoxy-4-fluoro- β -D-glucopyranosiduronic acid)- (1 \rightarrow 3)-2-acetamido-2-deoxy- β -D-galactopyranoside (6), the fluoride-releasing disaccharide substrate	54
Scheme 3.5. Synthesis of benzyl 4-deoxy-4-fluoro- β -D-galactopyranosiduronic acid (52)	56
Scheme 3.6. Synthesis of phenyl 4-deoxy-4,4-difluoro- β -D-xylo-hexopyranosiduronic acid (58)	57
Scheme 3.7. Synthesis of benzyl 4- <i>O</i> -(2',4'-dinitrophenyl)- β -D-glucopyranosiduronic acid (1)	58
Scheme 3.8. Synthesis of the chromogenic substrates containing 4-chloro-2-nitro-, 2,5- dinitro-, and 4-nitrophenolate leaving groups	60
Scheme 3.9. Synthesis of chromogenic substrates containing 3,4-dinitro-, 2-nitro-, and 2,4,6-trichlorophenolate leaving groups	60
Scheme 3.10. Synthesis of phenyl 4-methylumbelliferyl- β -D-glucopyranosiduronic acid (2)	62
Scheme 3.11. Synthesis of phenyl 4-deoxy-4-fluoro-5- $\{^2\text{H}\}$ - β -D-glucopyranosiduronic acid (83)	63
Scheme 3.12. Synthesis of phenyl 4-deoxy-4-fluoro-4- $\{^2\text{H}\}$ - β -D-glucopyranosiduronic acid (87)	64
Scheme 4.1. Synthesis of 3,4,6-tri- <i>O</i> -acetyl-2-deoxy-2-trichloroacetamido- α -D- galactopyranosyl trichloroacetimidate (91), the donor molecule of the disaccharide inhibitor	102

Scheme 4.2. Synthesis of methyl (methyl 2,3-di- <i>O</i> -acetyl- β -D-glucopyranosid)uronate (95), the acceptor molecule for the disaccharide inhibitor	102
Scheme 4.3. Synthesis of methyl <i>O</i> -(2-acetamido-2-deoxy- β -D-galactopyranosyl)- (1 \rightarrow 4)- α -L-threo-hex-4-enopyranoside (88), the disaccharide inhibitor	104
Scheme 4.4. Synthesis of phenyl (5 <i>S</i>)-5-nitro- β -D-xylopyranoside (89)	105

List of Abbreviations

AcCl:	acetyl chloride
AcOH:	acetic acid
AgOTf:	silver trifluoromethanesulfonate
AIBN:	2,2'-azobisisobutyronitrile
CAN:	ceric ammonium nitrate
Da:	dalton
DABCO:	1,4-diazobicyclo[2.2.2]octane
DBU:	1,8-diazabicyclo[5.4.0]undec-7-ene
DMDO:	dimethyldioxirane
DMF:	<i>N,N</i> -dimethyl formamide
ECM:	extracellular matrix
EtOAc:	ethyl acetate
EtOH:	ethanol
ESMS:	electrospray mass spectrometry
Gal:	galactose
GalNAc:	<i>N</i> -acetylgalactosamine
GAG:	glycosaminoglycan
GlcA:	glucuronic acid
GlcNAc:	<i>N</i> -acetylglucosamine
h:	hour(s)
HEWL:	hen egg white lysozyme
IdoA:	iduronic acid
<i>k</i> _{cat} :	catalytic rate constant (turnover number)
<i>k</i> _H / <i>k</i> _D :	ratio of rate constants for protio and deuteuro substrates
KIE:	kinetic isotope effect
<i>K</i> _m :	Michaelis constant of a substrate
<i>k</i> _{obs} :	pseudo-first order rate constant
LBHB:	low-barrier hydrogen bond
<i>m</i> -CPBA:	<i>m</i> -chloroperbenzoic acid

MeOH:	methanol
min:	minute(s)
NBS:	<i>N</i> -bromosuccinimide
NMO:	<i>N</i> -methylmorpholine
NMR:	nuclear magnetic resonance
NOE:	nuclear Overhauser effect
PE:	petroleum ether
PhOH:	phenol
Piv:	pivaloyl
ppm:	parts per million
rt:	room temperature
SDS-PAGE:	sodium dodecyl sulfate polyacrylamide gel electrophoresis
Ser:	serine
TBAB:	tetrabutylammonium bromide
TBAF:	tetrabutylammonium fluoride
TBAHS:	tetrabutylammonium hydrogen sulfate
TBTH:	tributyltin hydride
TEMPO:	2,2,6,6-tetramethyl-1-piperidinyloxy
Tf:	trifluoromethanesulfonate, or triflate
TFA:	trifluoroacetic acid
THF:	tetrahydrofuran
TMSOTf:	trimethylsilyl trifluoromethanesulfonate
TPAP:	tetrapropylammonium perruthenate
UV:	ultraviolet light
Vis:	visible light
Xyl:	xylose
1°:	primary
2°:	secondary

Acknowledgments

I would like to thank a number of people who are responsible for steering me down the right path during my studies at the University of British Columbia. First and foremost I would like to thank my supervisor, Professor Stephen Withers, for providing an ideal work place, full of guidance, encouragement, and freedom. I would like to extend my gratitude to IBEX Technologies Inc. of Montreal and Dr. Mirek Cygler at the Biotechnology Research Institute of the National Research Council for their generous donation of chondroitin AC lyase and *Flavobacterium heparinum* cells, which provided the engine for this research. My thanks also go to Lianne Diarge and Marietta Austria for their time and guidance with NMR spectroscopy, and to Peter Borda for his excellence and patience in the microanalytical laboratory. For her help with enzyme kinetics and keeping the shelves stocked with goodies, I would like to thank Karen Rupitz. I would also like to thank Shouming He for the prompt mass spectrometry analyses of many of my compounds. For financial support during my graduate career I would like to thank NSERC, the University of British Columbia, and Dr. Paul Trussell along with the British Columbia Science Council. A special thank-you goes to the members of the Withers' group, past and present, who have made my time at UBC most enjoyable. In particular, I would like to thank Dr. David Zechel for making the benchwork an interesting and entertaining experience, along with Hoa Ly and Dr. Spencer Williams for helpful discussions.

Now that I have covered my time spent in the laboratory, I would like to thank my friends for many great years here in Vancouver, outside the confines of the chemistry lab. Michael, Rob B., Rob G., Mark, Art, Todd, Roger – we've done so much and gone so many places. Hopefully luck will be on our sides and we will meet up once we have all 'grown up'. I would also like to thank my parents for their love, support, and generosity over the years.

Chapter 1 – Introduction

Cakes, pies, fudge, and cells – no matter how you slice it, carbohydrates are everywhere. Carbohydrates are one of life's most important biological molecules, although somewhat overshadowed by the notoriety of DNA, RNA, and proteins. In terms of mass, carbohydrates are the most abundant organic molecules, providing structure, support, energy storage, and intricate recognition systems for nearly all cells on earth.

The variety of carbohydrate structures found in nature is immense. The complexity of these polymers stems not only from the wide selection of monomers, but also from the seemingly endless combination of ways in which these can be linked together. The choice of anomeric configuration, the different epimers, including D and L forms, as well as the variety of linkage positions all contribute to this immense diversity. Aside from the linear array of monomers, a feature shared with DNA and proteins, carbohydrates may have a multitude of differently branched structures. In addition, sugars may be substituted with a number of groups including acyl, alkyl, sulfate, sulfonate, phosphate, phosphonate, and pyruvyl, adding even more complexity.¹ The amount of potential information content in carbohydrate polymers far outweighs that of any other biological polymer.

The enzymes responsible for the degradation of carbohydrates perform this task with rate accelerations amongst the highest of any known enzyme.^{2,3} The half-life of a common glycosidic linkage in the absence of enzymes is on the order of five million years under physiological conditions,² presenting an enormous barrier for these enzymes. However, it is one that is overcome with profound efficiency. The vast majority of our knowledge on carbohydrate-degrading enzymes has come through research on glycosidases, enzymes that use water to hydrolyse the glycosidic bond. This thesis presents research into a class of enzymes still in their infancy of mechanistic investigation, the polysaccharide lyases. Although responsible for the catabolism of carbohydrate polymers, the lyases do not actually cleave glycosidic bonds, but instead perform an elimination reaction to cleave the C4-oxygen bonds in a class of biologically important polymers termed the glycosaminoglycans. The detailed understanding of the

lyase mechanism at the molecular level is of the utmost importance in expanding not only our knowledge of this enzyme class, but also to harness the clinical and industrial applications that may present themselves.

1.1 Glycosaminoglycans and Proteoglycans

1.1.1 Structure

Animal tissues are composed of millions of specialized cells that perform an astounding array of biochemical processes. Within these cells a multitude of chemical reactions occur on an ongoing basis, providing the machinery and energy required to sustain life. Often overlooked is the extracellular space that surrounds, supports, and connects these cells. This crucial part of every tissue consists of a gel-like material and is termed the extracellular matrix (ECM). The ECM provides a physical and chemical connection between cells, allowing the diffusion of nutrients and oxygen, as well as providing the structural support necessary to maintain the specific spatial arrangement of the cells comprising each tissue. A variety of glycosaminoglycans (GAGs) constitute the majority of the ECM and perform a wide spectrum of biological roles.

The GAGs are long, unbranched, highly sulfated, acidic polysaccharides that are markedly heterogeneous along their length, and between individual GAG chains. GAGs consist of a sequence of repeating disaccharide units of uronic acid and hexosamine residues, sulfated at various positions through the polymer (Figure 1.1). The high degree of *N*- and *O*-sulfation, combined with the uronic acid moieties, makes GAGs among the most negatively charged biopolymers, a feature that is key to many of their functions. The uronic acid moiety can either be D-glucuronic acid (GlcA), or its C5 epimer, L-iduronic acid (IdoA). The hexosamine residue can either be D-galactosamine or D-glucosamine, and is most often *N*-acetylated, however, this amino sugar may also be esterified with sulfate. The marked heterogeneity of GAG chains arises from the various *N*- and *O*-sulfation patterns, and from the frequency of occurrence of the C5 epimers of uronic acids. Specific enzymes are responsible for this heterogeneity, and often produce

specifically modified disaccharides that are segregated into regions constituting functional sites in the polysaccharide.⁴ However, the source of this purposeful clustering is unknown.

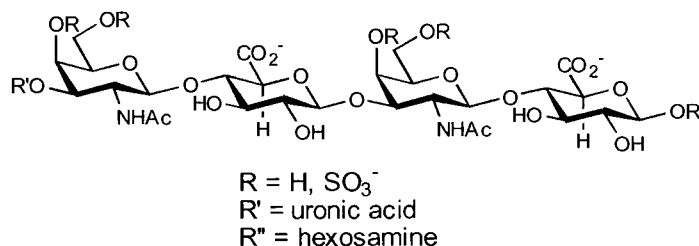


Figure 1.1. The general structure of the GAGs. The chondroitin sulfates containing *N*-acetylgalactosamine and glucuronic acid residues are shown.

Although not strictly GAGs by definition, there are other polysaccharides containing uronic acid residues that should be mentioned. These acidic polymers are degraded by polysaccharide lyases in a fashion similar to that of the GAG-degrading enzymes and are postulated to share a common mechanism, making them relevant to this discussion. The striking difference in these polysaccharides to those of GAGs, is that they are homopolymers of uronic acid residues, rather than consisting of repeating disaccharide units including a hexosamine moiety. Three of the most well-known and highly studied polysaccharides of this class are pectate, pectin, and alginate. Pectate is a polymer of α -(1 \rightarrow 4) linked galacturonate units, and is one of three major polysaccharide components of the plant cell wall, the other two being cellulose and hemicellulose.⁵ Pectin is very similar to pectate, although the carboxylate groups in pectin are usually esterified as the methyl ester. Enzymes capable of interconverting pectate and pectin, such as pectin methyl esterase, are commonly found in many lyase-producing organisms.⁶ Alginate, mainly from brown seaweeds, consists of 1 \rightarrow 4 linked residues of β -D-mannuronic acid or its C5 epimer α -L-guluronic acid, arranged randomly or in contiguous blocks within the linear molecule.⁷

With the exception of hyaluronic acid, all GAGs are synthesized covalently linked

to a core protein via its reducing end, forming a proteoglycan. The polysaccharides are synthesized in the Golgi, initially as a repeating sequence of identical disaccharide units, with the sulfation and C5-epimeric heterogeneity being introduced enzymatically as post-synthetic modifications. These subsequent modifications are incomplete, yielding GAGs with dramatic differences along their length and between individual GAG chains. The region that links the GAG chain to the core protein of most proteoglycans has been identified as [GAG]-GlcA- β (1 \rightarrow 3)-Gal- β (1 \rightarrow 3)-Gal- β (1 \rightarrow 4)-Xyl- β (1 \rightarrow O)-Serine, however slight modifications such as phosphorylation or O-sulfation of various hydroxyls has been noted.⁸ A single protein core may have as few as one, or more than 150 GAG chains covalently attached, making the sequence analysis of these important proteins difficult (Figure 1.2). Based on sequence information, a number of core protein families have been identified. However, these proteins are often inconsistently substituted with GAG chains, making the prediction of whether a particular protein will carry GAG chains based on sequence data extremely difficult. The core protein may also carry other functional domains besides GAGs, designed for the interaction with other proteins, or for anchoring the proteoglycan to the cell surface or to macromolecules of the ECM. The core proteins often contain specific regions that are devoid of GAG chains, yet play pivotal roles in the biological function of the proteoglycans. Interestingly, proteoglycans are not only found in the ECM, but may also occur intracellularly (usually in secretory granules) or at the cell surface.⁸

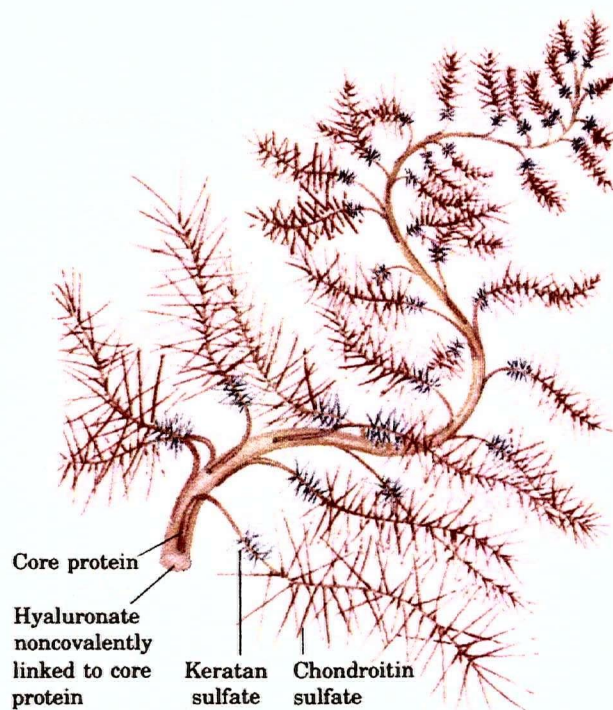


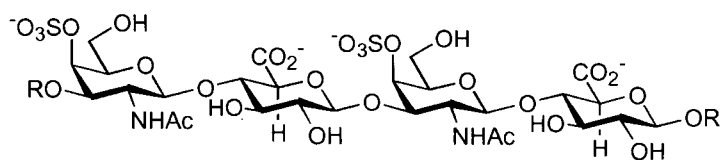
Figure 1.2. Illustration of a proteoglycan. A single molecule of hyaluronic acid is associated non-covalently with many molecules of core protein, shown here with covalently bound keratan sulfate and chondroitin sulfate GAGs. Adapted from ⁹.

GAGs may be divided up into four main classes: (1) chondroitin sulfate and dermatan sulfate, (2) hyaluronic acid, (3) heparin and heparan sulfate, and (4) keratan sulfate. A brief overview of their structures, illustrating the similarities and differences, is warranted.

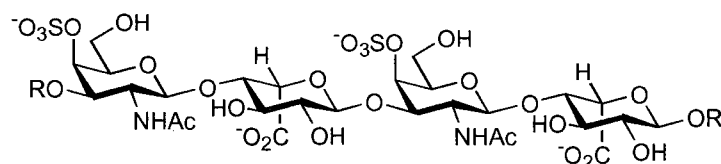
1.1.1.1 Chondroitin Sulfate and Dermatan Sulfate

The chondroitin sulfates are the most common type of GAG chain consisting of three major classes: (1) chondroitin sulfate A (chondroitin 4-sulfate), (2) chondroitin sulfate B (dermatan sulfate), and (3) chondroitin sulfate C (chondroitin 6-sulfate) (Figure 1.3). These polysaccharides consist of an *N*-acetyl-D-galactosamine (GalNAc) residue (usually *O*-sulfated at C4 or C6) attached through a β -(1 \rightarrow 4) linkage to D-GlcA or L-

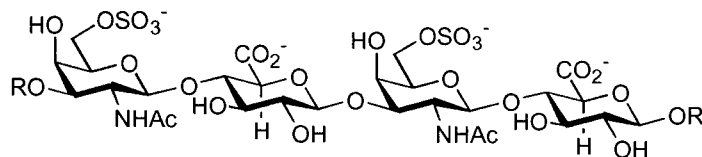
IdoA (dermatan sulfate) that is in turn attached via a β -(1 \rightarrow 3) linkage (α -(1 \rightarrow 3) for dermatan sulfate) to the next hexosamine residue. The C2 hydroxyl of the uronic acid residue may also be sulfated to some small degree. Of course, these are merely the most common sequences in each specific polymer. Marked heterogeneity occurs along each GAG chain, particularly with regards to the sulfation patterns, but also due to the ratio of GlcA to IdoA residues. It is most likely the presence of a small percentage of glucuronic acid residues in dermatan sulfate that has caused some confusion in the literature as to whether dermatan sulfate can or cannot be degraded by certain chondroitinases.¹⁰⁻¹³ Chondroitin sulfate GAGs have also been identified which are sulfated at both the C4 and C6 positions of the hexosamine moiety. Conversely, unsulfated GAG chains of the chondroitin type also exist, and they have been given the name chondroitin.



Chondroitin sulfate A (chondroitin 4-sulfate)



Chondroitin sulfate B (dermatan sulfate)



Chondroitin sulfate C (chondroitin 6-sulfate)

Figure 1.3. The structures of the common chondroitin sulfates. R = uronic acid. R' = hexosamine. The L-iduronic acid moieties of dermatan sulfate have been drawn in the 4C_1 chair conformation for simplicity, and may not represent their actual conformation in the GAG.

The secondary structural elements of the chondroitin sulfate class of GAGs vary significantly between dermatan sulfate and chondroitin sulfates A and C. In solution, dermatan sulfate has a flexible conformation, and forms no discrete secondary structures. This may be due to the iduronic acid moiety, which does not seem to have a particular preference between the 4C_1 chair, 1C_4 chair, and twist boat conformations.^{4,14} This ambiguity in the uronic acid conformation does not allow the dermatan sulfate chain to form defined secondary structures in solution. Chondroitin sulfates A and C, on the other hand, form helical structures in solution. However, the detailed characterisation of these structures is not well documented. In the solid state both dermatan sulfate and chondroitin sulfate A and C form helices of various periodicities, depending on the cation (Na^+ or Ca^{2+}) with which they are crystallized.

1.1.1.2 Hyaluronic Acid

Hyaluronic acid, discovered by Meyer and Palmer in 1934¹⁵ is unsulfated, and is structurally similar to chondroitin sulfates A and C in that the uronic acid residues are GlcA, however, the hexosamine residue is *N*-acetyl-D-glucosamine (GlcNAc) rather than the epimeric galactosamine (Figure 1.4). Hyaluronic acid is present in nearly all tissues of the vertebrates and lower marine organisms, and has also been found in some bacteria.¹⁶ Hyaluronic acid is considerably larger than the other GAGS, consisting of up to 50,000 sugar units, or 10^7 Da, which allows it to hold a large amount of water, contributing to its visco-elastic properties. The most unique feature of hyaluronic acid is that it is the only GAG not covalently attached to a protein core to form a proteoglycan.

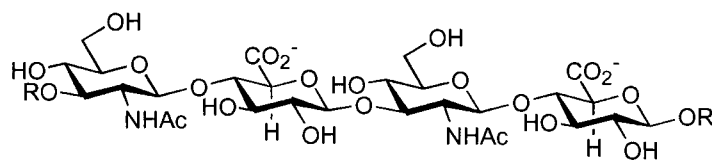


Figure 1.4. The structure of hyaluronic acid. R = uronic acid. R' = hexosamine.

1.1.1.3 Heparin and Heparan Sulfate

Arguably the best-known GAGs are heparin and heparan sulfate, due to their important functions in regulating blood coagulation and their clinical applications (*vide infra*). The distinction between heparin and heparan sulfate is cloudy at best, and the two are considered by some to be a family of molecules with a continuous range of compositions and properties. Generally, heparan sulfate is the less sulfated of the two GAGs, having one to two sulfates per disaccharide unit. Heparin, on the other hand, has the highest negative charge density of any known biological macromolecule, having four negative charges per disaccharide unit on average (3 sulfate and 1 carboxylate).^{6,17} The uronic acid residues of heparin are mainly L-IdoA, while those of heparan sulfate are mainly the C5 epimer, D-GlcA. Part of the reason for the cloudiness in the classification of this group is that the uronic acid identities are not as strict as in some of the other polysaccharides such as the chondroitin sulfates, with both L-IdoA and D-GlcA present in significant amounts. This makes heparin and heparan sulfate much more structurally complex, especially for heparan sulfate, which has between 25 and 80% IdoA content.⁴ Heparin and heparan sulfate consist of a D-glucosamine residue attached through an α -(1 \rightarrow 4) linkage to the uronic acid residue, which is in turn attached via a α/β -(1 \rightarrow 4) linkage to the next glucosamine residue (Figure 1.5).

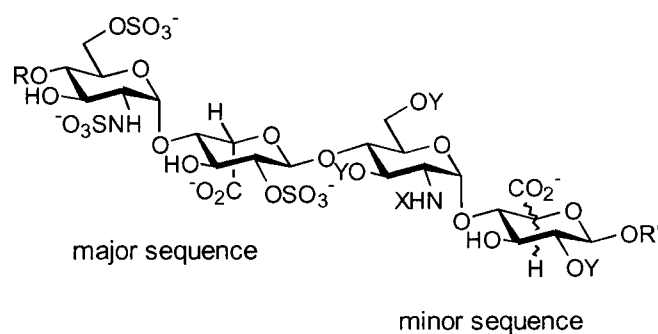
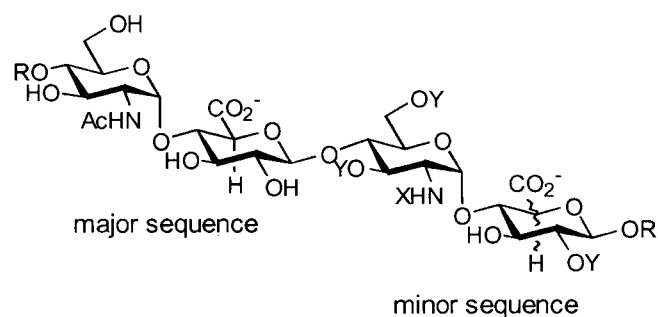
**Heparin****Heparan Sulfate**

Figure 1.5. The structures of heparin and heparan sulfate, showing the significant heterogeneity of these polymers introduced by the minor sequence. R = uronic acid. R' = hexosamine. X = SO₃⁻, Ac, or H. Y = H or SO₃⁻.

1.1.1.4 Keratan Sulfate

Keratan sulfate, although classed as a GAG, surprisingly doesn't contain any uronic acid residues. Instead, its primary structure consists of a GlcNAc moiety attached via a β-(1→3) linkage to D-galactose, which is in turn attached to the next GlcNAc residue via a β-(1→4) link (Figure 1.6). The C6 positions of the glucosamine residues are sulfated, as are the C6 positions of the galactose, although to a lesser degree. Disaccharide units containing zero, one, and two sulfate units have been identified in the polysaccharide, and may each contribute to various functions of the keratan sulfate GAG.

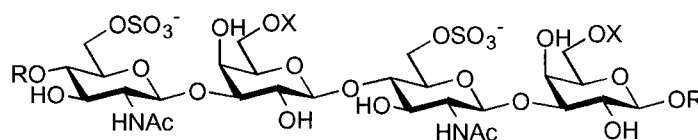


Figure 1.6. The structure of keratan sulfate. R = galactose. R' = GlcNAc. X = SO₃⁻ or H.

The main consequence of the lack of uronic acid moieties is that cleavage of the keratan sulfate chain does not occur via an eliminative mechanism. The degradation of this particular GAG thus occurs via a hydrolytic mechanism via glycosidases.

1.1.2 Biological Roles of GAGs and Proteoglycans

Defining specific roles for the proteoglycans and their associated GAGs has been hampered by the lack of detailed structure and sequence information available, and is further complicated by the marked heterogeneity between individual GAG chains. In addition, our knowledge of carbohydrate-protein interactions falls short of our understanding of the interactions that proteins have with nucleic acids and other proteins.

The majority of the biological roles of proteoglycans most certainly stem from the identity of the attached GAG chains. Thus, the protein core may simply serve as a scaffold for the appropriate immobilization and spacing of the GAG chains. For example, the protein core may assume an anchoring function when attached to the cell surface, which may be essential for the appropriate positioning of a GAG-bound ligand such as an enzyme or enzyme inhibitor. However, important roles specifically credited to the core proteins have also been demonstrated. For example, several core proteins have been found to bind fibronectin and collagen, interactions that influence collagen fibrillogenesis.⁸ Overall, the functions of proteoglycans are a result of the concerted contributions of the GAG and the core protein components.

One of the main functions of GAGs and proteoglycans is the mechanical support of various tissues. The combination of the sulfate groups and carboxylate groups of the

uronic acid moieties bestows GAGs with a high density of negative charge. In order to reduce the repulsive forces among neighbouring charged groups, the polymer adopts an extended linear conformation in solution. As a consequence, solutions of GAGs are highly viscous and thus provide an ideal scaffold for mechanical support. It is this high viscosity that allows GAGs to function as lubricants in the synovial fluid of joints, or to give the vitreous humour of the eye its jelly-like consistency. GAGs, as a part of the ECM of cartilage and tendons, contribute tensile strength and elasticity to these robust structural units.

Proteoglycans play important roles on cell surfaces, and may adhere via the interaction of the GAG components with specific anchoring proteins on the cell surface, or the core protein itself may be anchored in the lipid interior of the plasma membrane. Regardless of their mode of attachment, these cell surface-associated proteoglycans perform a variety of functions, including: (1) the regulation of cell-substrate adhesion, (2) the regulation of cell proliferation, (3) the participation in the binding and uptake of extracellular components, and (4) the regulation of ECM formation.¹⁸ The modes of interaction between GAG chains and components of the ECM are widely varied, and not well understood. The most obvious, and somewhat non-specific, interactions arise from the polyanionic character of the GAG chains, which bind to components with a sufficiently pronounced cationic domain (eg. proteins). The repulsive energy of multiple negative charges along the polysaccharide promotes cation binding (i.e., Na^+) in order to minimize these forces. However, the binding of Na^+ ions is entropically unfavourable, thus the binding of a protein (via positively charged amino acids) results in the entropically favoured release of Na^+ ions. This phenomenon has been termed the “polyelectrolyte effect”, and plays a significant role in the binding of proteins to GAGs at physiological salt concentrations.¹⁷ Other mainly non-specific interactions contribute to the binding to GAGs, such as hydrogen bonding and hydrophobic interactions. In contrast, numerous interactions having a much higher degree of specificity, based on specific GAG sequences, are known to play a major role in many biological functions. These arise from secondary structures within the GAG, with sulfate and carboxylate groups displayed at defined intervals and in defined orientations along the polysaccharide

backbone. For example, heparin displays a discrete pentasaccharide sequence required for the binding of antithrombin III, which is involved in the regulation of blood coagulation.¹⁷ This rare sequence occurs in only about one third of the chains in heparin, and is distinguished by an unusual tri-sulfated hexosamine residue in the internal portion of this pentasaccharide sequence, which is absolutely essential for its high affinity to antithrombin III (Figure 1.7). The discovery of this extremely specific sequence along the heparin chain has allowed the development of low molecular weight heparins, which have recently displaced heparin as the most commonly used clinical anticoagulant.

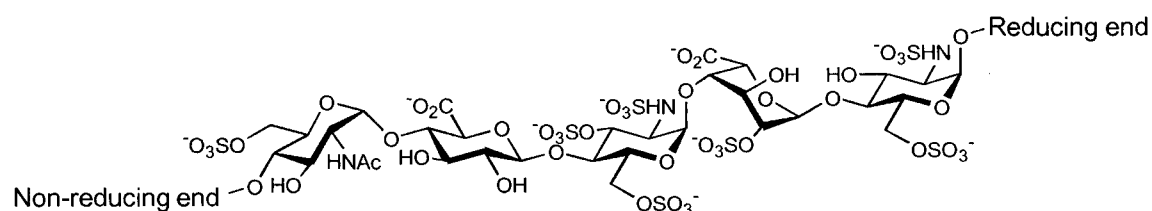


Figure 1.7. Structure of the specific pentasaccharide sequence in heparin responsible for its high affinity to antithrombin III. Particular attention should be paid to the absolutely essential tri-sulfated hexosamine moiety.

Proteoglycans are also found in basement membranes, which form the substratum for epithelial and endothelial cells. Three main biological roles have been ascribed to these basement membrane proteoglycans.¹⁹ The first function results from the high negative charge of the GAG polymers, which impede the passage of other negatively charged molecules and thus provide a filtration barrier. Secondly, proteoglycans contribute to the architecture of the basement membrane by binding with other components such as laminin, fibronectin, and collagen IV. A third function relates to the proteoglycan's high affinity for the serine protease inhibitor antithrombin. Thus, proteoglycans help to modulate blood coagulation after endothelial damage, and in processes such as tissue remodelling and the penetration of cells through basement membranes.¹⁹

Perhaps the most famous and biologically characterized role of GAGs is their part

in the regulation of blood coagulation, as briefly touched on in the previous paragraphs. Blood coagulation involves a complex cascade of many steps and enzymes (mainly serine proteases), eventually leading to the conversion of fibrinogen to fibrin by thrombin, to form a tightly woven clot (Figure 1.8). The GAGs that play a major part in interfering with blood coagulation are heparin, heparan sulfate, and dermatan sulfate. The main role of these GAGs is to accelerate the inactivation of the serine protease thrombin by antithrombin, in the last step of blood coagulation. Two modes of inactivation have been postulated, and it is likely that both mechanisms contribute to anticoagulation.²⁰ The first mode of inactivation is caused by a conformational change that occurs to antithrombin when heparin is bound to it, resulting in the greatly accelerated inactivation of thrombin. Following complex formation with thrombin, antithrombin loses its high affinity for heparin, which is subsequently released to affect another antithrombin molecule. Thus, the heparin is able to act as a catalyst and effectively block the coagulation cascade. The second mode of inactivation describes the GAG acting as a surface bridge to bring both thrombin and its inactivator, antithrombin, together by binding both proteins to the same GAG chain. GAGs can also impart their anticoagulant properties by activating a number of other inhibitors of the coagulation cascade apart from antithrombin. These include the activation of other serine protease inhibitors such as heparin cofactor II, protein C, and a protein known as tissue factor pathway inhibitor.²⁰ Regardless of their mode of action on the blood coagulation cascade, GAGs have been used for many years as clinical anticoagulants, with clinical tests beginning around 1935.¹⁷ In fact, heparin and its more recently developed and finely tuned cousin, low molecular weight heparin, are the most commonly used clinical anticoagulants.

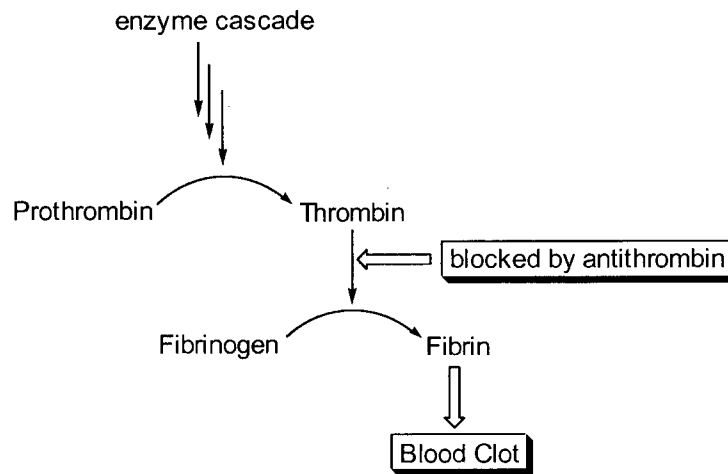


Figure 1.8. Simplified blood coagulation scheme.

1.1.3 GAG Degradation

Nature has provided two pathways for the degradation of GAGs. Enzymes employing hydrolytic and eliminative cleavage mechanisms have developed to efficiently degrade their GAG substrates.

1.1.3.1 Hydrolytic Mechanism

The hydrolytic mechanism, employed by a variety of enzymes found in eukaryotes employs water to cleave the glycosidic bonds. The examination of the GAG structures reveals two types of glycosidic bonds, the uronic acid-hexosamine bond, and the hexosamine-uronic acid bond. It follows that there are two general classes of polysaccharide hydrolases, which have evolved to cleave each of these glycosidic bonds.

The members of the first class are termed glucuronidases or iduronidases, and cleave the uronic acid-hexosamine bond with either retention or inversion of anomeric configuration. For simplicity, I will refer to these enzymes as glycosidases, a more general and commonly used term. The enzymatic mechanisms of these glycosidase enzymes have been well studied, and will be discussed only briefly. A short synopsis of

these mechanisms is included, as it nicely illustrates how nature has devised two completely separate mechanisms to degrade the same polysaccharide chain. For a more rigorous treatment of glycosidase mechanisms, interested readers are directed to a number of good reviews.²¹⁻²⁸ The retaining glycosidases utilize a double displacement mechanism, ensuring that the configuration at the anomeric centre is the same for both the starting material and the initially formed product. Two carboxylic acid residues in the enzyme active site, a nucleophile and a general acid/base, form the main catalytic machinery for this transformation. The first displacement results from the attack of the nucleophilic residue at the anomeric centre, with the departing saccharide unit leaving with assistance from the general acid catalyst. This results in the formation of a covalent glycosyl-enzyme intermediate with the nucleophilic carboxylate residue. The former acid catalyst residue is now deprotonated, and thus is ideally suited to assist a water molecule, via general base catalysis, to perform the second displacement reaction at the anomeric centre, hydrolysing the glycosyl-enzyme intermediate and releasing a product with net retention of anomeric configuration. The inverting enzymes utilize a slightly different mechanism that involves a direct displacement at the anomeric centre by a water molecule. As with the retaining enzymes, two carboxylic acid residues form the heart of the catalytic machinery, however, they play slightly different roles. One carboxylate residue acts as a general base catalyst, assisting the attack of water on the anomeric centre, while the other residue acts as a general acid by protonating the departing saccharide unit. This single displacement mechanism results in the inversion of stereochemistry at the anomeric centre.

The second class of GAG-degrading hydrolases consists of the hexosaminidases, which, as their name suggests, cleave the hexosamine-uronic acid bond. Many of these enzymes follow the same mechanisms outlined above for the glycosidases, resulting in products of retained or inverted anomeric configuration. However, there are a small number of hexosaminidases that are believed to utilize a variation of the double displacement mechanism in which the *N*-acetyl group takes on the role of the nucleophile, and forms an oxazolinium ion intermediate as opposed to a covalent glycosyl-enzyme intermediate.²⁹⁻³³ This non-covalent intermediate is then hydrolysed

by an incoming water molecule to generate the final products.

1.1.3.2 Eliminative Mechanism

Prokaryotes have developed enzymes that degrade GAGs via a completely different mechanism from that of the eukaryotic enzyme mechanisms outlined above. With few exceptions, eukaryotes utilize hydrolytic enzymes, whereas prokaryotic organisms utilize enzymes that perform an elimination mechanism to degrade GAGs and these latter enzymes are termed polysaccharide lyases. Unlike most other saccharide-degrading enzymes, the lyases do not cleave a glycosidic bond, but instead catalyze the cleavage of the 4-*O*-linked sugar from the uronic acid moiety, resulting in unsaturated sugar derivatives with a double bond between C4 and C5. This elimination mechanism was first suggested from the isolation of an unusual unsaturated sugar produced by the degradation of hyaluronic acid by a microbial polysaccharidase.³⁴ The now accepted mechanism, proposed by Gacesa,³⁵ is composed of three steps: (i) neutralization of the negative charge on the carboxylate anion of the glucuronic acid moiety, either by a divalent metal ion or an active site amino acid, (ii) general base-catalyzed abstraction of the C5 proton and finally, (iii) the β -elimination of the 4-*O*-linked sugar (Figure 1.9).

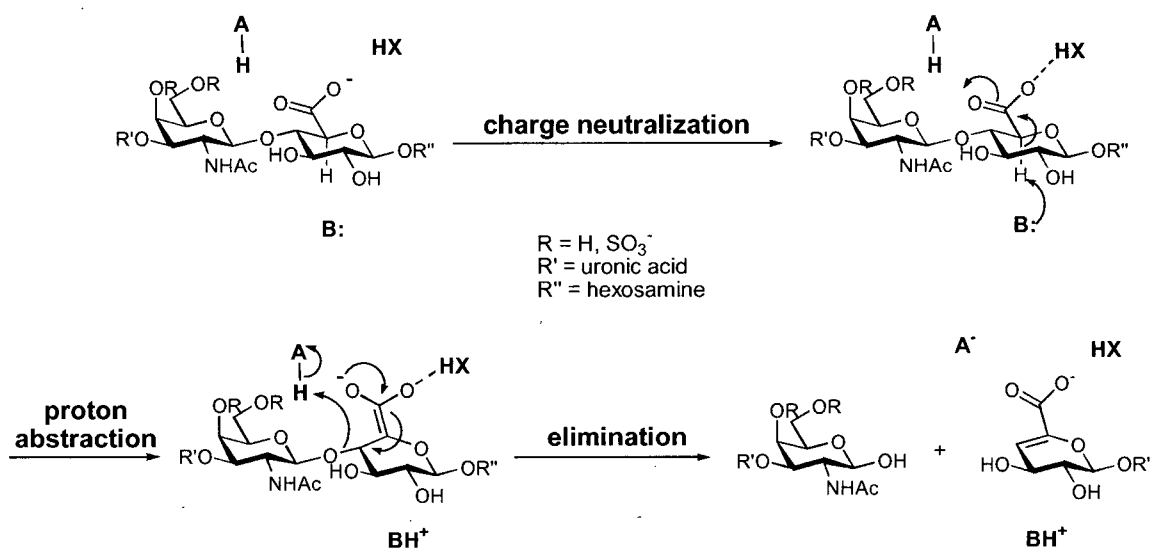


Figure 1.9. Schematic showing the proposed three-step mechanism of chondroitin AC lyase.

The carboxylic acid functionality is key in allowing this elimination to take place. Not only does it facilitate the abstraction of the neighbouring C5 proton by increasing its acidity, but it also stabilizes the anion subsequently formed, through resonance into the carboxyl group. This overall *syn*-elimination may be stepwise and follow an E1cb-like reaction scheme where the enolic (anion) species is a discrete intermediate along the reaction profile. On the other hand, the elimination may be a concerted process with concurrent proton abstraction and elimination of the 4-*O*-linked sugar. This latter mechanism represents a concerted *syn*-elimination, and although rare, has been postulated to occur in some reactions.^{36,37} The lyase reaction has been shown not to occur via a hydrolysis step followed by the elimination of water by establishing that ^{18}O from H_2^{18}O is not incorporated into the oligosaccharide products (ie. at the anomeric centre of the hexosamine residue).³⁵

Two other mechanistic schemes are possible, and should be considered. The first alternative mechanistic pathway is an E1 mechanism where a carbenium ion intermediate is formed through the cleavage of the C4-oxygen bond prior to the proton removal step, as illustrated in Figure 1.10. This mechanism seems unlikely, due to the formation of the unstabilized carbenium ion, and due to the lack of precedence for enzyme catalyzed E1 elimination reactions.

The last mechanism that should be considered is a double-displacement process where the leaving group sugar at C4 of the uronic acid moiety is displaced by an active site nucleophile to form a covalent intermediate. This intermediate then breaks down by the abstraction of the C5 proton, resulting in the elimination of the nucleophile to generate the alkene product (Figure 1.11). This mechanistic possibility allows the reaction to proceed via a more favourable *anti*-elimination pathway rather than the *syn* stereochemical course.

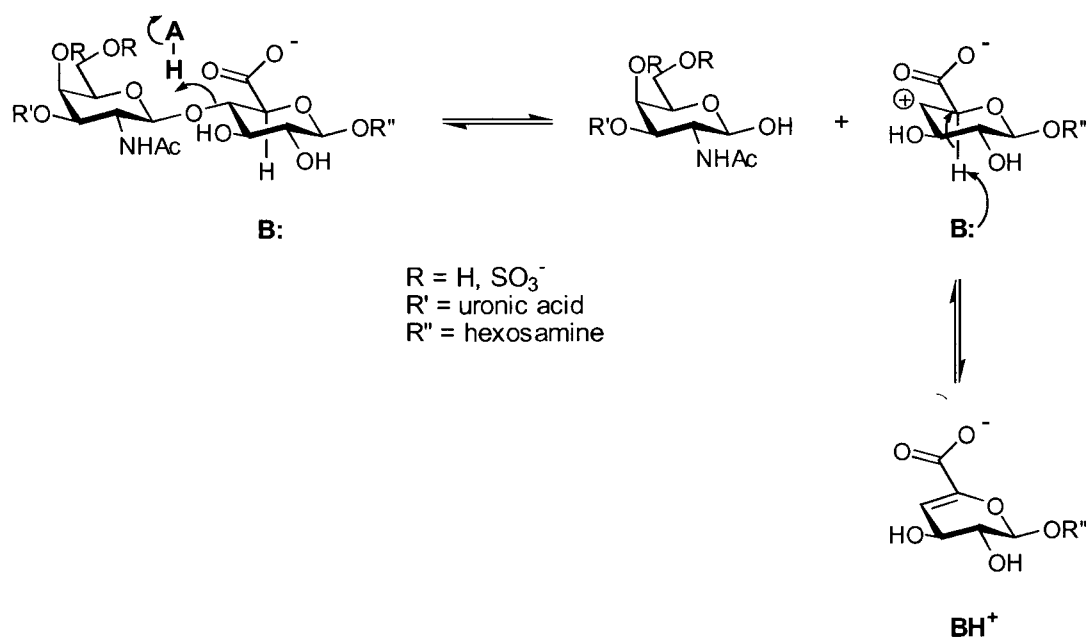


Figure 1.10. Possible mechanism of elimination (E1) involving the formation of a carbonium ion intermediate.

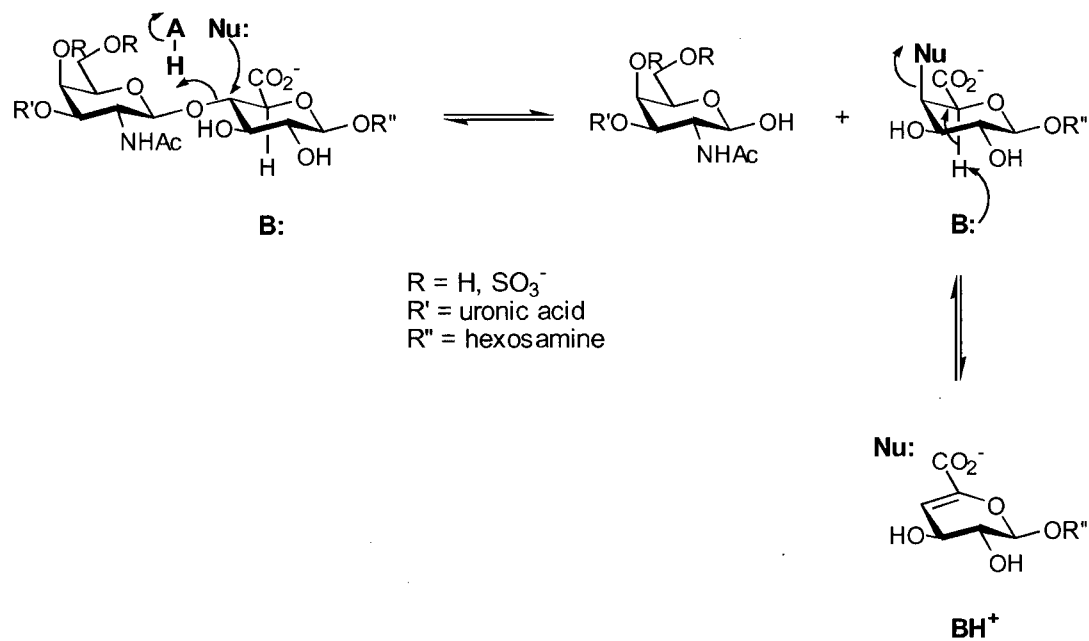


Figure 1.11. Possible mechanism of elimination involving the formation of a covalent intermediate by an active site nucleophile (Nu:).

With the final products of GAG degradation by the lyases being sulfated disaccharides, the requirement for other enzymes to complete the catabolism is obvious. Enzymes called glycuronidases act upon the unsaturated products generated by the degradation of GAGs by lyases. These enzymes are specific for the unsaturated uronic acid residues and produce an α -keto acid and an amino sugar by hydrolysing the disaccharide product of the lyase reaction (Figure 1.12). These enzymes are often found in conjunction with the lyases so that the organism can fully utilize the GAGs as an energy source. To complete the degradation, sulfoesterases and sulfamidases accomplish the removal of the sulfate groups from the oxygen and nitrogen centres respectively.

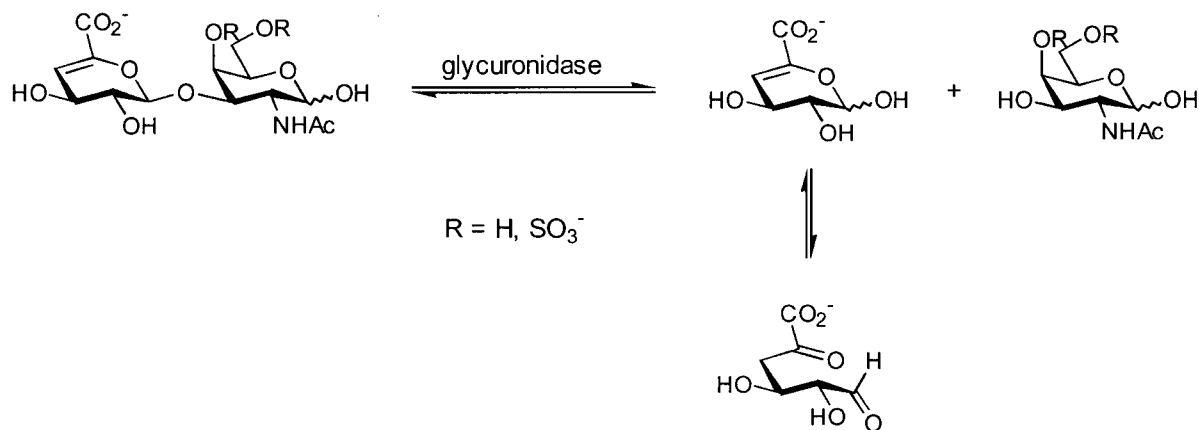


Figure 1.12. Hydrolysis of the disaccharide product of the lyase reaction by a glycuronidase to produce an α -keto acid and an amino sugar.

One of the main objectives of this thesis is to decipher the mechanistic scheme used by chondroitin AC lyase to degrade its substrates. This will be facilitated through the use of linear free energy relationships and both primary and secondary deuterium kinetic isotope effects, which provide valuable information on the order and nature of the bond breaking and forming steps.

1.2 Chondroitin AC Lyase

The enzyme under investigation in this thesis is chondroitin AC lyase (EC 4.2.2.5) from *Flavobacterium heparinum*, a Gram-negative soil bacterium. The first batches of enzyme used in this study were obtained as a generous donation from IBEX Technologies Inc. (Montreal) and Dr. Mirek Cygler at the Biotechnology Research Institute of the National Research Council. Later batches used were isolated and purified at the University of British Columbia as described in Chapter 5.

Flavobacterium heparinum produces a wide variety of enzymes designed to fully degrade GAGs, including four chondroitinases and three heparinases, as well as glycuronidases, sulfoesterases, and a sulfamidase.^{4,12,38} These enzymes are induced when utilising GAGs as the source of carbon, nitrogen, and sulfur, and illustrate how this soil bacterium may utilise the connective tissues of animal carcasses as a nutrient source. Chondroitin AC lyase as synthesized contains 700 amino acids, including a 22 residue long signal peptide. Thus, the mature enzyme contains 678 residues and starts at Gln23. It has a molecular weight of approximately 80 kDa, a pI of 8.85, and is glycosylated at two sites, Ser328 and Ser455. It degrades GAGs in a random endolytic fashion, which means that it cleaves the oligosaccharide substrates somewhere in the interior of the chain. Furthermore it does not simply progress along the chain producing disaccharides, but instead continuously binds a chain, cuts any cleavable site, and then releases the oligosaccharide products before binding a new chain to repeat the process. This produces larger polysaccharide products at first, including dodeca-, hexa- and tetra-saccharides, but eventually degrades the oligosaccharides completely to the disaccharide level.^{10,39} In contrast, many other enzymes show an exolytic action pattern where they cleave their substrates at either end of the polysaccharide chain, typically releasing mono- or disaccharides. Chondroitin AC lyase cleaves chondroitin 4- and 6-sulfate, as well as the unsulfated chondroitin and hyaluronic acid. However, its ability to cleave dermatan sulfate is inconclusive in the literature.¹⁰⁻¹³ This is most likely due to the presence of a small number of GlcA residues in the normally IdoA-containing polysaccharide, which are recognised by the AC lyase.

1.2.1 Three Dimensional Structure

The three dimensional structure of Chondroitin AC lyase has been recently determined, both as the free enzyme, and as various enzyme-oligosaccharide complexes.^{38,40,41} The infancy of the research on GAG lyases is illustrated by the fact that this was the first reported structure of a GAG-degrading lyase, and was published in 1998. The X-ray structure data provides valuable extra information and opportunities that can be used to research this enzyme's mechanism of action. It allows for the postulation of potentially essential catalytic residues and provides an opportunity to create enzyme inhibitors that may not only solidify the roles of these important catalytic and binding residues, but go on to be developed into therapeutic agents.

The enzyme is composed of two distinct domains of roughly equal size (Figure 1.13). The *N*-terminal domain is almost exclusively composed of α -helices that form a doubly-layered horseshoe. The *C*-terminal domain is a novel fold of β -strands arranged in a four-layered β -sheet sandwich. The region between the two domains forms a large cleft that is responsible for binding the substrate and contains the active site. Figure 1.13 shows the putative catalytic residues arginine, histidine, tyrosine, and asparagine in green within the active site cleft. This large cleft supports the finding that the enzyme acts in an endolytic fashion, binding to the middle of its polysaccharide substrate. In contrast are enzymes with exolytic modes of action that are often found to contain a pocket shaped active site cleft designed to bind only the end of a polysaccharide chain rather than its middle.²¹ The binding cleft of chondroitin AC lyase is lined with many positively charged residues such as histidine, arginine and lysine, which create a positive potential surface for the binding of the highly negatively charged substrate. There are also numerous aromatic residues including tryptophan, tyrosine, phenylalanine and histidine in the active site that form hydrophobic interactions important for substrate binding and selection of the cleavage site.

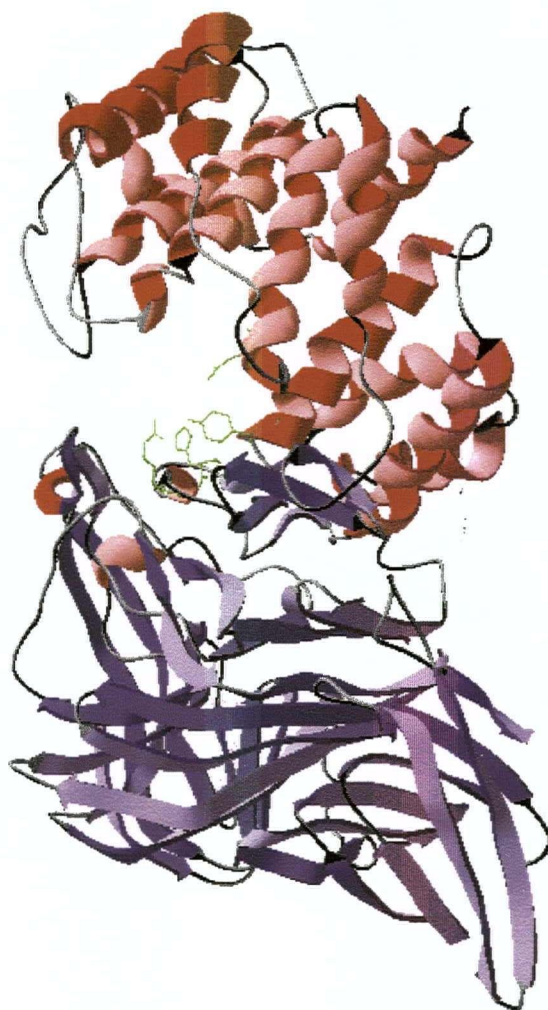


Figure 1.13. Three dimensional crystal structure of chondroitin AC lyase. Putative catalytic residues are shown in green, and include arginine, histidine, tyrosine, and asparagine.

Chondroitin AC lyase shows some homology with several sequences in the databases. The most homologous sequences are those from several bacterial hyaluronate lyases, having between 16 and 22% overall sequence identity.³⁸ This is not surprising, as not only are the chondroitin sulfates and hyaluronic acid similar in primary structure, but also each substrate can be degraded by the other enzyme. The overall three dimensional structure is similar to that of the hyaluronate lyase from *Streptococcus pneumoniae*, with the residues involved in substrate binding and degradation being highly conserved.^{42,43}

Based on the X-ray structures and site-directed mutagenesis studies, it appears likely that a histidine residue is responsible for the abstraction of the α -proton from the C5 carbon of the substrate, while a tyrosine residue is in the proper orientation to act as the acid catalyst that donates a proton to the departing C4 oxygen. However, the identity of the group responsible for neutralizing the charge on the carboxylate is not so clear. Proposals of either an arginine or an asparagine residue to play this role have been volunteered. Despite differences in the overall structures, the active site architectures of chondroitin AC lyase and hyaluronate lyase from *S. pneumoniae* are completely preserved with all potential catalytic residues overlapping one another when the two structures are overlayed.¹⁶ This homologous relationship most certainly stems from a common mechanism used to degrade the GAG substrates.

1.2.2 Previous Research on Chondroitin AC Lyase

Historically the role of polysaccharide lyases in research was not necessarily to investigate the enzymes themselves, but to gain knowledge regarding the structures of their substrates. The enzymes were used to degrade the unwieldy polymeric substrates into more manageable sized molecules that could then be analysed via a number of different methods. By using enzymes of differing specificity, a picture of the linkages and structural diversity of the polysaccharide could then be constructed.³⁹ Often the products of the enzymatic reactions were analysed simply by paper chromatography, allowing the identification of various disaccharides as well as tetra-, hexa-, and larger oligosaccharides. With the solvent systems employed, it was not uncommon for this chromatographic elution to take several days to yield results. These crude enzyme assays relied on techniques such as densitometry in combination with silver staining of the product spots.¹¹ However rudimentary these techniques may seem, they have allowed researchers to identify that chondroitin AC lyase degrades the chondroitin sulfates completely to disaccharides, ruling out a minimum substrate size requirement. Finally, to facilitate the complete characterisation of GAGs, various chemical methods were used to analyse the hexosamine, uronic acid, and sulfate content, as well as the reducing power of

starting materials and products.^{44,45}

The activity of chondroitin AC lyase was measured to be the highest at a temperature of about 40 °C, but denatures significantly with time at this temperature, showing a 50% decrease in activity after 6 hours.^{11,12} For this reason a temperature of 30 °C was chosen for the present research. Various studies into the pH optimum have concluded that the enzyme is most active between the pHs of 6 and 8, although the literature reports do not always agree.^{11,12}

The effect of various ions on the activity of chondroitin AC lyase has been studied, but again major discrepancies exist between experimenters. A calcium ion has been found in the three-dimensional crystal structure, however its remote location with respect to the active site leaves the exact function unknown.³⁸ In contrast, divalent metal ions play an active role in the mechanisms of other polysaccharide lyases, presumably to neutralise the charge on the carboxylate ion, and thus lower the pK_a value of the α -proton. The effect of added calcium has been reported to both increase⁴⁶ and decrease¹¹ the enzymatic activity. As a simple test, I found that up to 10 mM Ca^{2+} had no noticeable effect on enzyme activity. Sodium ions have been reported to have very little effect on chondroitinase AC up to at least 100 mM. However, other ions such as Fe^{3+} , Cu^{2+} , Sn^{2+} , and Pb^{2+} have been shown to have dramatic detrimental effects on the enzyme activity.^{11,46}

The action pattern of chondroitin AC lyase towards its substrates has been identified using viscosimetric measurements and gradient polyacrylamide gel electrophoresis.^{10,47} The rapid initial drop in molecular weight of the polymeric substrate shows the random endolytic action pattern as the enzyme cuts in the interior of the polysaccharide chains, thus significantly decreasing the molecular weight. In contrast, an exolytic action pattern would show a much slower decrease in molecular weight as the enzyme progressively removed disaccharide units from one end of the polysaccharide. This exolytic action pattern has been shown for the chondroitin AC lyase from *Arthrobacter aurescens*.⁴⁷

Despite investigations into the desired substrates of chondroitin AC lyase, the

effects of temperature, pH, and metal ions, along with the enzymatic action pattern, there have been no studies that delve into the actual mechanism of action. These mechanistic details are vital to our complete understanding of this enzyme and of polysaccharide lyases in general. Knowledge of the intricacies of the bond breaking and forming steps, together with the enzyme's catalytic machinery used to carry out this transformation, may eventually allow the harnessing of this enzyme's power for industrial applications, or the development of therapeutic agents. The paucity of details regarding the enzymatic mechanism is astounding, and provides the rationale for the present research.

1.3 Other Enzymes Performing Elimination Reactions

Apart from polysaccharide lyases, there are many enzymes that catalyze elimination reactions on a wide variety of substrates. A common feature of these reactions is the abstraction of a proton adjacent to a carbonyl group to form an anionic intermediate, which then breaks down to give products. This commonality is not limited to elimination reactions, which may be either of the *syn* or *anti* stereochemical course and involve the elimination of water, ammonia, or a carboxylic acid, but also occur in racemization, epimerization, and cycloisomerization reactions.

A large group of enzymes has been organized under the heading of the enolase superfamily, appropriately named for the enzyme whose function is "most central to living organisms".⁴⁸ Each of these enzymes catalyzes reactions that are initiated by the metal-assisted, general base-catalyzed abstraction of the α -proton of a carboxylate anion to generate a stabilized enolate anion intermediate. The members of this superfamily have been classified based on sequence similarities, yet catalyze a wide variety of reactions. A selection of examples from the enolase superfamily is illustrated in Figure 1.14.

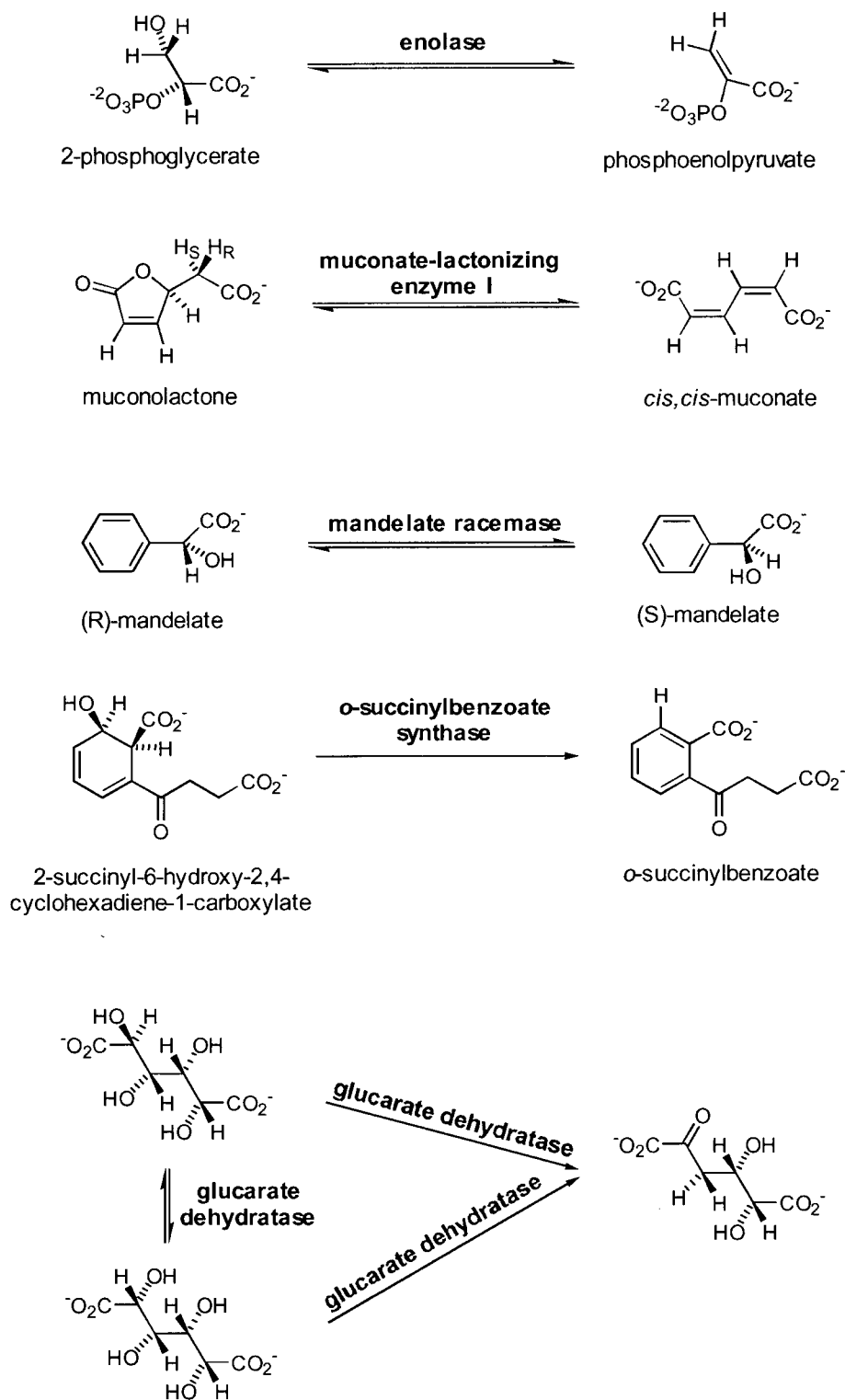


Figure 1.14. Representative examples of reactions catalyzed by enzymes of the enolase superfamily.

Four members of the enolase superfamily have been examined structurally: mandelate racemase, muconate-lactonizing enzyme I, enolase, and glucarate dehydratase.^{48,49} The three-dimensional structures along with mutagenesis studies have allowed the assignment of the catalytic residues responsible for the transformations. In all four enzymes, a lysine residue is responsible for the abstraction of the α -proton to generate the enolic intermediate. However, in the cases of mandelate racemase and glucarate dehydratase two active site bases are used to interconvert the enantiomers or epimers respectively, one on each side of the active site. In these enzymes a lysine residue abstracts the proton from either (S)-mandelate or (D)-glucarate, whereas a histidine abstracts the proton from (R)-mandelate or (L)-idarate. Interestingly, C5 has the (S)-absolute configuration in (D)-glucarate, and the (R)-absolute configuration in the epimeric (L)-idarate. In this superfamily it is almost always a glutamic acid residue that has been proposed as the acid catalyst in the elimination reactions.

Simple elimination reactions catalyzed by enzymes can be either of the *syn* or *anti* stereochemical course and vary greatly with respect to the order of the bond breaking and forming steps. As an illustration, consider the enzymes crotonase, fumarase and *cis,cis*-muconate cycloisomerase that catalyze the transformations illustrated in Figure 1.15. Primary and secondary deuterium kinetic isotope effect studies have been performed on each of the above enzyme systems in order to elucidate the details of the elimination mechanism. The crotonase-catalyzed reaction has been found to be an example of the extremely rare concerted *syn*-elimination.³⁶ The fumarase reaction is a stepwise *trans*-elimination of water in which the abstraction of the α -proton is fast, followed by a rate-limiting cleavage of the C-O bond.⁵⁰ In contrast, the reaction catalyzed by *cis,cis*-muconate cycloisomerase has been shown to be a stepwise *syn*-elimination where the abstraction of the α -proton is solely rate-limiting.⁵¹ Unfortunately there is not always such a clear distinction between the concerted and stepwise elimination pathways, with a seemingly continuous spectrum possible concerning the order of the bond breaking and forming steps. For example, *ab initio* calculations suggest that concerted *syn*-eliminations are possible, but will have a carbanion character arising from the greater extent of bond

cleavage to the α -proton than to the leaving group at the transition state.^{36,52}

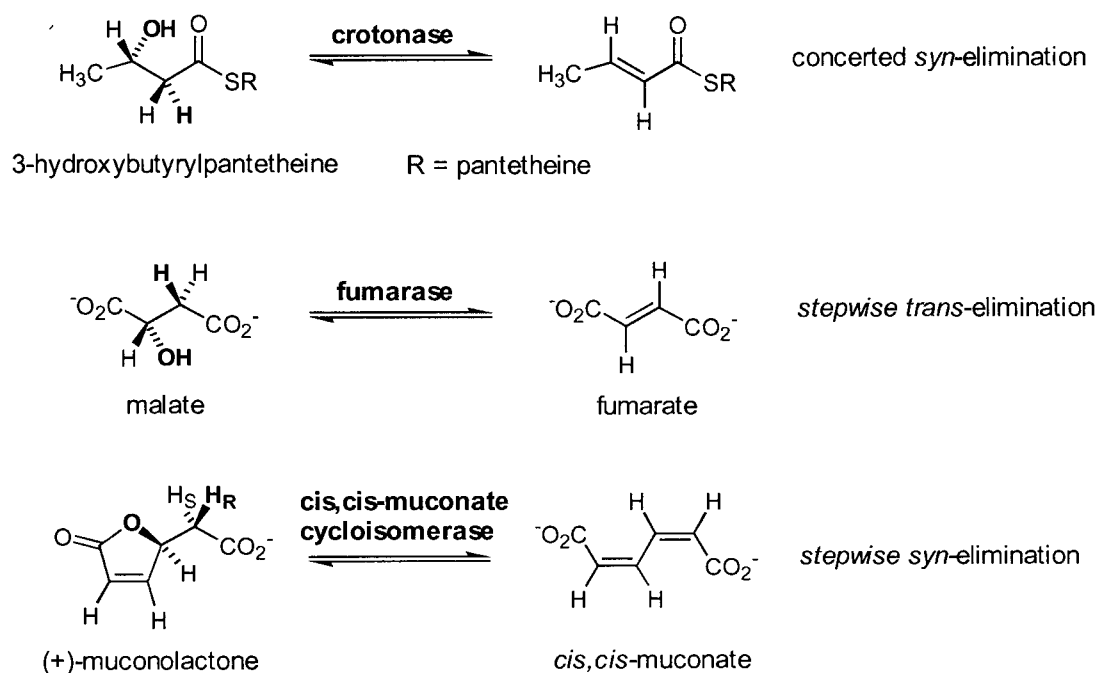


Figure 1.15. The reactions catalyzed by crotonase, fumarase and cis,cis-muconate cycloisomerase.

Polysaccharide lyases are not the only enzymes that act upon a carbohydrate substrate via an elimination mechanism. For example, there are a large number of hexose and pentose dehydrases, mostly for aldonic acids or their phosphate esters.⁵³ 6-Phosphogluconate dehydrase catalyzes the elimination of water from 6-phosphogluconate to form 2-keto-3-deoxy-6-phosphogluconate as illustrated in Figure 1.16. The enol-keto tautomerization reaction to form the 2-keto functionality has been shown to occur nonenzymatically once released from the enzyme.

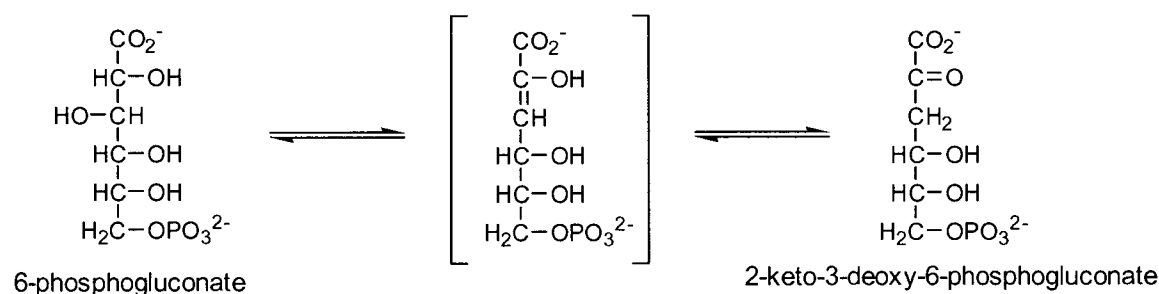


Figure 1.16. The elimination reaction catalyzed by 6-phosphogluconate dehydratase.

A second example of a carbohydrate based elimination reaction illustrates how enzymes can achieve a seemingly improbable reaction. The enzyme L-2-keto-3-deoxyarabonate dehydratase catalyzes the transformation of 2-keto-3-deoxyarabonate into α -ketoglutaric semialdehyde, illustrated in Figure 1.17. The astonishing feature of this reaction is that the elimination is occurring not between the α - and β -carbons, but across the β - and γ -carbons, where the proton being abstracted is γ to the carbonyl, and thus not activated towards abstraction. The removal of this C5 hydrogen would generate a carbanion that cannot be stabilised into an adjacent carbonyl, in contrast to all of the reactions previously discussed.

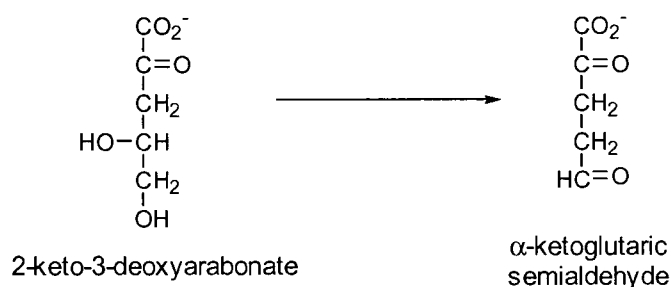


Figure 1.17. The overall reaction catalyzed by L-2-keto-3-deoxyarabonate dehydratase.

The enzyme has a clever way of increasing the acidity of the C5 proton in order for this elimination reaction to occur.⁵³ A lysine residue at the active site forms an iminium cation with the C2 keto group, which increases the acidity of the hydrogens at

C3 (Figure 1.18). A catalytic enzymatic base residue then abstracts this newly acidified C3 hydrogen to form an enamine, which then decomposes to expel the C4 hydroxyl group. This formal elimination of water has occurred α,β to the carbonyl, as in all of the previous examples. In this dehydrated cation, the C5 protons have been rendered acidic, due to their extended conjugation with the iminium nitrogen. Thus, a C5 hydrogen is abstracted by an active site base to form an enolic intermediate, which then ketonizes to yield a dehydrated enamine species. This dehydrated enamine consequently picks up a proton at C3, with the hydrolysis of the subsequent imine to generate the semialdehyde product. This amazing sequence of reactions shows how different enzymes have evolved to perform seemingly impossible elimination reactions. It also illustrates the vastly different reaction mechanism proposed for the polysaccharide lyases, which form only a small subset of the enzymes that perform elimination reactions.

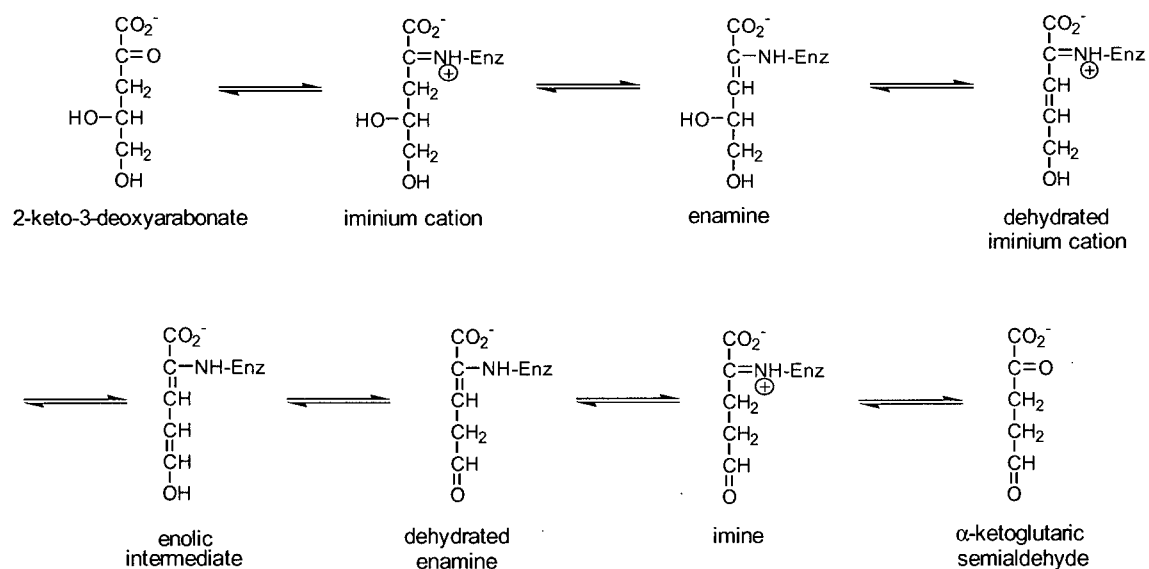


Figure 1.18. The reaction Scheme for the conversion of 2-keto-3-deoxyarabonate to α -ketoglutaric semialdehyde by L-2-keto-3-deoxyarabonate dehydrase.⁵³

1.4 Aims of This Thesis

In general, the polysaccharide lyases are a group of enzymes that are not well understood. They are most certainly overshadowed by their hydrolase cousins, the glycosidases, which are well studied and characterized both kinetically and mechanistically. Mechanistic studies of the lyases are in their infancy, hindered by the unwieldy size and heterogeneous nature of their natural substrates. The present research presents the first mechanistic studies of its kind on any polysaccharide lyase, and shows how the ideas and techniques successfully used to study a variety of other enzymes such as the glycosidases can be applied to this class of enzymes.

With the ultimate goal of elucidating the details of the catalytic mechanism of chondroitin AC lyase from *Flavobacterium heparinum* in mind, it is essential to have a simple assay of enzymatic activity. Historically, assays of these enzymes could not provide meaningful and reproducible kinetic parameters due to the inhomogeneous and polymeric nature of the substrates used. Thus, the first aim of this thesis is to develop a new assay that can be used in mechanistic studies. Secondly, through subsequent chemical modifications of successful candidate molecules, a variety of techniques can be employed to understand the order of the bond making and breaking steps of this elimination mechanism. These include primary and secondary deuterium kinetic isotope effects, linear free energy relationships, and isotope exchange experiments. Finally, tight binding inhibitors of chondroitin AC lyase are highly attractive targets that may help not only to further understand the catalytic mechanism, but also to provide additional insights into the structure of the transition state(s) along the reaction pathway. Furthermore, these inhibitors would be extremely helpful in structural studies of the enzyme, facilitating the identification of key residues involved in binding and catalysis. Thus, the third main aim of this thesis is the synthesis of several inhibitors for the enzyme.

It is the hope that the substrates, assays, and ideas developed in this study may aid researchers working with other polysaccharide lyases.

Chapter 2 – Development of an Assay for Chondroitin AC Lyase

2.1 Historical Assays

Research into any enzyme requires the use of an assay to monitor enzymatic activity. In addition, this assay must allow the measurement of defined and reproducible kinetic parameters, particularly if mechanistic studies are on the agenda. The heterogeneous and polymeric nature of the natural substrates for polysaccharide lyases has not allowed such an assay in the past, and has severely restricted the type of research conducted on this relatively poorly understood class of enzymes. Thus, the first goal of the present research was to develop a convenient and useful assay for chondroitin AC lyase to be used in subsequent mechanistic analyses. To appreciate the need for this assay, a survey of the antiquated assay techniques in prior use is appropriate.

Previous work with polysaccharide lyases has relied on a wide variety of assay techniques. Four main techniques form the majority of assays used to study these enzymes. (1) Viscometry.^{54,55} Glycosaminoglycans are long, negatively charged polymers that form highly viscous solutions, an important physical property that nicely explains some of their biological functions such as the cushioning of joints in the body. Thus, as an enzyme degrades this polymer, the viscosity of the solution decreases, and can be monitored over time. However, a large amount of material is usually necessary to obtain the viscosity measurements; (2) UV absorption of the alkene product at 230-240 nm.^{56,57} This region of the spectrum is often masked by absorbances of other species present in crude enzyme extracts such as aromatic amino acids; (3) The thiobarbituric acid reaction.^{56,58,59} This assay relies on the reactivity of the unsaturated uronic acid product towards periodate oxidation, forming β -formylpyruvate that subsequently forms a coloured species with thiobarbituric acid ($\lambda_{\text{max}} = 550 \text{ nm}$) (Figure 2.1);

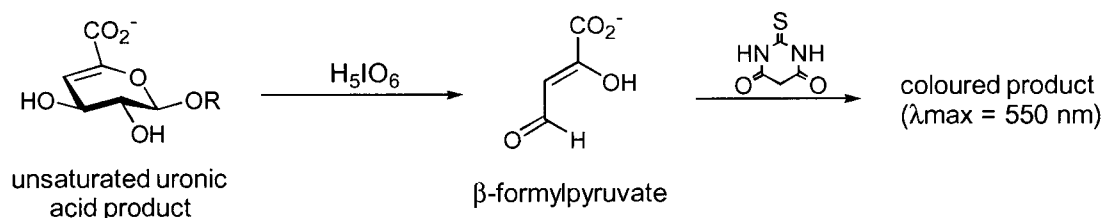


Figure 2.1. The thiobarbituric acid reaction as an assay for polysaccharide lyases.

(4) Measurement of reducing sugar.⁶⁰ Other assay techniques employed have included the preparation of covalently dye-labeled polymeric substrates,^{61,62} the colourimetric measurement of *N*-acetylamino sugars,^{63,64} and assays relying on the release of various non-covalently associated dyes that bind only to the polymeric substrates and not the smaller products.^{65,66} Many of these methods are time-consuming, difficult to perform, and are susceptible to errors arising from various substances present in crude enzyme preparations. In addition, all of these assays lack a defined substrate that can be used to extract meaningful and reproducible kinetic parameters such as k_{cat} and K_{m} . The heterogeneous and polymeric natural substrates are not defined in terms of their primary structure, with the sulfation pattern and uronic acid content (D-glucuronic acid or L-iduronic acid) varying along an individual polysaccharide chain as well as between chains. These polysaccharides, although available commercially, are often not available in a pure form. For example, chondroitin 6-sulfate purchased from Sigma is only about 90% pure, with the balance being made up of chondroitin 4-sulfate. The difficulties associated with using these substrates for the kinetic characterization of an enzyme should be immediately obvious. Previous studies have revealed that chondroitin AC lyase has a higher affinity for chondroitin 4-sulfate than for chondroitin 6-sulfate.¹⁰ The enzymatic reaction rate will obviously change as the reaction proceeds, with the enzyme presumably acting the fastest on certain specific sequences along the polysaccharide for which it has higher affinity, and then moving on to other cleavage sites for which the degradation rate is lower. All of these factors make data comparison unreliable between

experiments in which degradation occurs to different degrees of completion, or in which substrates are obtained from different sources or are simply different batches from the same supplier. In addition, the molecular weights of these substrates are not accurately known, thus, the essential kinetic parameters K_m and k_{cat}/K_m cannot be reliably defined. Further, as noted above, they will change during the course of the reaction. The development of simple substrates, defined in terms of their structure and molecular weight, have overcome these problems, and have allowed the measurement of defined and reproducible k_{cat} and K_m values. These substrates also have great potential to be used in a wide variety of mechanistic studies in order to elucidate the details of the catalytic mechanism, not only of chondroitin AC lyase, but also of many other polysaccharide lyases still at the infancy of their experimentation.

2.2 Development of Synthetic Substrates

The introduction of defined chromogenic substrates has considerably simplified the assay of glycosidases. This was particularly important with enzymes degrading polymeric substrates, such as cellulases and xylanases, since it allowed the measurement of defined k_{cat} and K_m values. The availability of these substrates facilitated a variety of mechanistic studies of glycosidases via the accurate measurement of kinetic isotope effects and linear free energy relationships produced by measuring the rates of hydrolysis of a series of substrates of differing reactivity. The equivalent analyses of polysaccharide lyases have not been possible due to the absence of defined substrates, especially since these polymeric substrates do not have regular repeating structures.

Consequently three different types of synthetic substrate were designed that can be monitored by three different techniques: UV/Vis spectroscopy, fluorescence spectroscopy, and by the use of a fluoride ion-selective electrode (Figure 2.2). Although this enzyme degrades substrates that are normally sulfated at various positions, the literature states that the enzyme actually acts faster on the unsulfated chondroitin and hyaluronic acid, than it does on chondroitin sulfates A and C.⁶ In addition, the uronic acid moiety of the chondroitin sulfates is not usually sulfated, thus unsulfated glucuronic

acid substrates that are easily synthesized seemed appropriate for the development of a convenient assay. Seven different chromogenic and four different fluoride-releasing substrates were synthesized, and are discussed in more detail in the following chapter. In order to focus on the development of these assays, and for simplicity, the following discussion will focus on three specific compounds as shown in Figure 2.2.

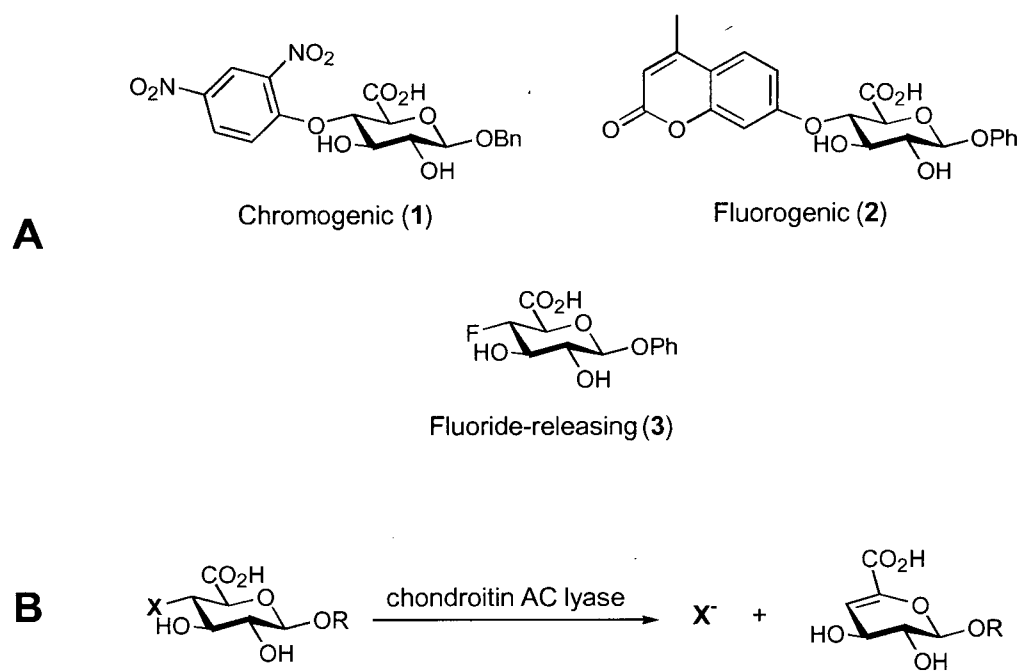


Figure 2.2. (A) Three substrates designed for the assay of chondroitin AC lyase representing three separate assay techniques. (B) The conversion of substrate to products by chondroitin AC lyase.

It is important to note that no artificial substrates for polysaccharide lyases have been synthesized and tested previously. These novel compounds represent a completely new class of synthetic substrate, akin to the highly successful aryl glycosides developed for the assay and mechanistic investigation of many glycosidases.

The pH chosen for the assay of the chromogenic and fluoride-releasing substrates (6.8) was based on the previous pH-rate analyses of this enzyme.^{11,12} In addition, the extinction coefficients of the various phenolate leaving groups are also available for this pH and phosphate buffer composition.⁶⁷ Conversely, a pH of 8 was chosen for the assay

of the fluorogenic substrate to ensure efficient fluorescence of the released 7-hydroxy-4-methylcoumarin, which is significantly more fluorescent at a pH above its pK_a of 7.8. The temperature optimum of chondroitin AC lyase has been reported to be around 40 °C.^{11,12} However, a temperature of 30 °C was chosen for all analyses due to the instability of the enzyme at its temperature optimum.

The kinetic parameters for the three substrates are summarized in Table 2.1. The syntheses and experimental details for all substrates can be found in subsequent chapters. By comparing the k_{cat}/K_m values, it is obvious that the fluoride-releasing substrate (**3**) is the most efficient substrate for chondroitin AC lyase, whereas the chromogenic (**1**) and fluorogenic (**2**) substrates display similar efficiencies. Clearly the significantly greater k_{cat} value of compound **3** over that of compounds **1** and **2** is responsible for this higher catalytic efficiency.

Table 2.1. Kinetic parameters for selected synthetic substrates.* Note: kinetics with **2** were performed at pH 8.0, whereas pH 6.8 was used for substrates **1** and **3**.

Substrate	k_{cat} (s ⁻¹)	K_m (mM)	k_{cat}/K_m (M ⁻¹ s ⁻¹)
Chromogenic (1)	0.019	7.0	2.7
Fluorogenic (2)	0.0016	1.0	1.5
Fluoride-releasing (3)	2.3	114	20

2.3 Chromogenic Substrate (**1**)

The release of the 2,4-dinitrophenolate anion is easily monitored at 400 nm, a wavelength well isolated from that of other absorbing species such as aromatic amino acids. The chromogenic substrate **1** was found to be stable under the assay conditions, with no measurable spontaneous elimination being observed (true also for the other two substrate types). However, upon addition of chondroitin AC lyase, the release of the 2,4-dinitrophenolate anion was observed by monitoring the absorbance at 400 nm. Figure 2.3

* Errors range from 7 to 25%

shows the kinetic data for **1** fitted to the Michaelis-Menten equation. The major drawback of the chromogenic substrate is the limited solubility in aqueous solutions. As a consequence, the maximum concentration of **1** attained (11 mM) fell short of twice the estimated K_m (7 mM). However the value of k_{cat}/K_m ($2.7 \text{ M}^{-1}\text{s}^{-1}$) derived from the individual parameters was consistent with the result obtained from the slope of the initial linear portion of the plot, indicating that the estimates are reasonable. The chromogenic substrate provides a facile assay, producing reproducible kinetic parameters in a short period of time.

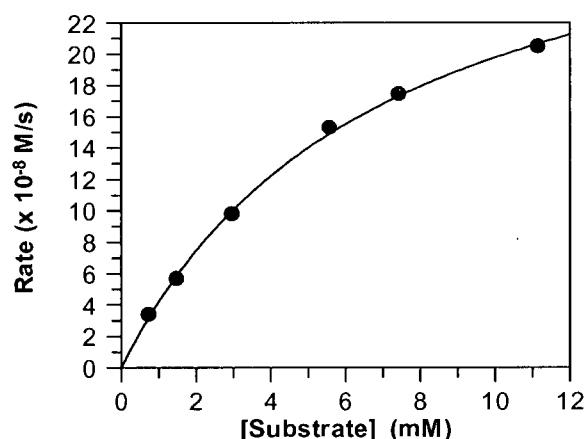


Figure 2.3. Kinetic data for the chromogenic substrate **1** fitted to the Michaelis-Menten equation.

2.4 Fluorogenic Substrate (2)

The use of the fluorescent leaving group 7-hydroxy-4-methylcoumarin (4-methylumbelliferone) allows a much more sensitive assay to be performed. Having an absorption maximum at 360 nm and emission maximum at 450 nm avoids interferences from other groups that may be present in the reaction mixture such as in crude enzyme preparations. A pH of 8.0 was chosen for this assay, rather than pH 6.8 as with the other substrates, because the fluorescence of 7-hydroxy-4-methylcoumarin is much greater at a pH above its pK_a (7.8). Chondroitin AC lyase shows a broad pH maximum,^{11,12} (see Chapter 3) and has sufficient activity at pH 8 to allow an efficient assay. Interestingly, the

fluorescent substrate showed substrate inhibition at high concentrations of substrate, something not observed with the other two classes of substrate. However, this may have been due to the lack of saturation achieved with the chromogenic and fluoride-releasing substrates due to either their limited solubilities or high K_m values. Substrate inhibition occurs when a second molecule of substrate binds to give an ES_2 complex that is catalytically inactive (Figure 2.4).⁶⁸ Chondroitin AC lyase normally binds a polysaccharide chain in a long active site cleft, and thus has potential to bind more than one substrate simultaneously, resulting in an unproductive ternary complex. Figure 2.5A shows the kinetic data for this fluorogenic substrate fitted to Equation 2.1, which corresponds to an uncompetitive substrate inhibition model. The kinetic parameters obtained from this curve fit are: $K_m = 2.5$ mM, $K_i = 1.4$ mM, and $k_{cat}/K_m = 1.3$ M⁻¹s⁻¹. However, there may be factors other than substrate inhibition to consider when results of this type are observed. Thus the kinetic parameters resulting from the fit to the Michaelis-Menten equation (Equation 2.2) were used.

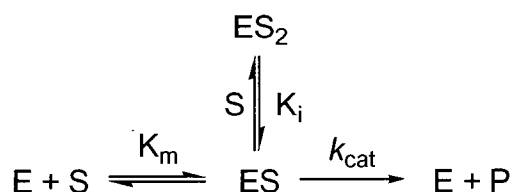


Figure 2.4. Kinetic Scheme for substrate inhibition. E = enzyme; S = substrate; ES = Michaelis complex; ES_2 = substrate inhibited Michaelis complex; K_i = inhibition (dissociation) constant for the second substrate molecule; P = product(s).

$$v_o = \frac{V_{\max}[S]}{K_m + [S] + ([S]^2 / K_i)} \quad (\text{Equation 2.1})$$

$$v_o = \frac{V_{\max}[S]}{K_m + [S]} \quad (\text{Equation 2.2})$$

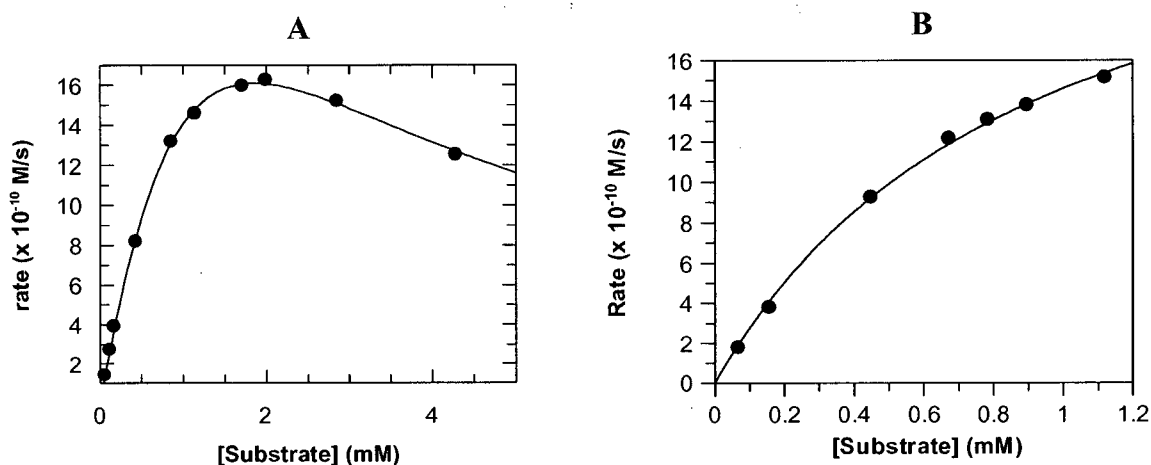


Figure 2.5. (A) Kinetic data for the fluorogenic substrate **2** fitted to Equation 2.1 showing substrate inhibition at high concentrations of substrate. (B) Low substrate concentration data for **2** fitted to the Michaelis-Menten equation.

Figure 2.5B shows only the lower substrate concentration portion of the curve fitted to the Michaelis-Menten equation. The K_m obtained from this curve for the fluorogenic substrate (1.0 mM) is considerably lower than that for the chromogenic substrate (7.0 mM). The increased binding of the chromogenic substrate may arise from extra base stacking interactions of the aromatic 7-hydroxy-4-methylcoumarin moiety with aromatic amino acids present at the active site, compared with those available to the smaller phenol moiety in the chromogenic substrate. Such interactions are commonly found in the active sites of polysaccharide-degrading enzymes, and the three-dimensional structure of chondroitin AC lyase has revealed several aromatic residues that line the active site.^{38,40} The smaller K_m value for the fluorogenic substrate is even more pronounced when the effect of the anomeric substituent upon binding is examined. It has been shown that substrates substituted with a phenyl aglycone display significantly weaker binding than those with a benzyl aglycone (see Chapter 3). The overall catalytic efficiency with the fluorogenic substrate as measured by k_{cat}/K_m ($1.5 \text{ M}^{-1}\text{s}^{-1}$) is similar to that of the chromogenic substrate. The slightly lower value may be explained by the increased pH of the assay, which has been shown to not only decrease k_{cat} but also to increase K_m (see Chapter 3). Overall, the fluorescent assay remains a much more

sensitive assay, utilizing much less enzyme and substrate.

2.5 Fluoride-Releasing Substrate (3)

The use of a fluoride ion-selective electrode allows a continuous assay to be performed with substrates that release the fluoride ion. Figure 2.6 shows the kinetic data for this substrate fitted to the Michaelis-Menten equation. The fluoride-releasing substrate has a significantly higher k_{cat} value than do the chromogenic or fluorogenic substrates (Table 2.1). This may be due to the stabilization of the developing negative charge by the highly electronegative fluorine atom. However, the K_m value of the fluoride-releasing substrate is also higher than those of the other substrate types, presumably due to the absence of the hydrophobic interactions provided by the aromatic leaving groups of the chromogenic and fluorogenic substrates. Nonetheless, the overall catalytic efficiency as measured by k_{cat}/K_m is greater for the fluoride-releasing substrate, owing to its much higher k_{cat} value.

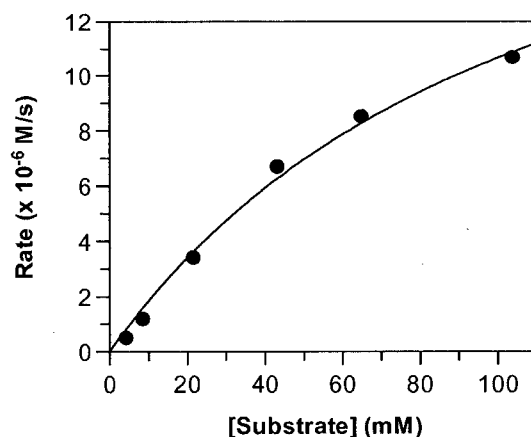


Figure 2.6. Kinetic data for the fluoride-releasing substrate 3 fitted to the Michaelis-Menten equation.

2.6 Conclusions

The development of three different types of structurally defined substrates that can be used to assay chondroitin AC lyase activity using three different techniques has been accomplished. These continuous assays involving UV/Vis spectroscopy, fluorescence spectroscopy, and the use of a fluoride ion-selective electrode are easily performed and are free from interferences caused by other components found in crude enzyme preparations. These substrates are the first artificial substrates developed for a polysaccharide lyase, and their defined structures have allowed the measurement of defined k_{cat} and K_{m} values that were previously unattainable using the heterogeneous and polymeric natural substrates. As a consequence, a variety of mechanistic studies of the enzyme are now possible, including the measurement of kinetic isotope effects and linear free energy relationships in order to decipher the nature of the catalytic mechanism. These substrates may also find applications with a wide variety of other polysaccharide lyases acting on GAGs containing glucuronic acid residues, and thus may facilitate the comparison of the enzymatic mechanisms of different GAG lyases.

2.7 Methods

2.7.1 UV/Vis Spectroscopy

Assays were carried out in quartz cuvettes (1 cm path length), total solution volume 200 μL . Mixtures containing buffer (50 mM sodium phosphate, 100 mM NaCl, pH 6.8) and the desired amount of substrate were incubated at 30 °C for at least 15 minutes to thermally equilibrate. Enzyme (30.0 μL of 1.0×10^{-4} M chondroitin AC lyase in buffer) was added and the change in absorbance was monitored over 1 minute using a Unicam 8700 or UV4 UV/Vis spectrophotometer equipped with a temperature-controlled cuvette holder. Enzymatic rates were calculated using an extinction coefficient of 10910 $\text{M}^{-1}\text{cm}^{-1}$.⁶⁷

2.7.2 Fluorescence Spectroscopy

Assays were carried out in disposable fluorescence cuvettes (1 cm path length), total solution volume 500 μL . Mixtures containing buffer (50 mM Tris-HCl, 100 mM NaCl, pH 8.0) and the desired amount of substrate (**2**) were incubated at 30 °C for at least 15 minutes to thermally equilibrate. Enzyme (25 μL of 3.6×10^{-5} M chondroitin AC lyase in buffer) was added and the change in fluorescence intensity was monitored at 30 °C over 5 minutes ($\lambda_{\text{excitation}}$ 360 nm, $\lambda_{\text{emission}}$ 450 nm) using a Varian Cary Eclipse fluorescence spectrometer equipped with a temperature-controlled cuvette holder. Rates were calculated using a standard curve of 7-hydroxy-4-methylcoumarin (4-methylumbelliferone).

2.7.3 Fluoride Ion-Selective Electrode

Assays were carried out in glass vials, total solution volume 300 μL . Mixtures containing buffer (50 mM sodium phosphate, 100 mM NaCl, pH 6.8) and the desired amount of substrate were incubated at 30 °C for at least 15 minutes to thermally equilibrate. Enzyme (30.0 μL of 1.0×10^{-4} M chondroitin AC lyase in buffer) was added and the change in fluoride ion concentration was monitored at 30 °C with an Orion fluoride ion-selective electrode interfaced with a computer.

Chapter 3 – Mechanistic Studies

3.1 Aims of This Research

To this date there have been no mechanistic studies published on polysaccharide lyases. The majority of investigations have centered on substrate specificity, action patterns and product compositions, and structural studies in combination with site-directed mutagenesis in order to identify the catalytic machinery of these unfamiliar enzymes. The present work focuses on utilizing techniques such as kinetic isotope effects and linear free energy relationships in order to elucidate the details of the catalytic mechanism of chondroitin AC lyase. The knowledge of the order of the bond breaking and forming steps and the nature of the transition states involved provides fuel for further research into these enzymes. These fundamental physical organic studies provide a solid foundation for the future development of potential therapeutic applications, as well as other more academic pursuits.

3.2 Mechanistic Considerations

3.2.1 Rate Enhancement and the pK_a of the α -Proton

The proposed mechanism, suggested by Gacesa,³⁵ is composed of three steps: (i) neutralization of the negative charge on the carboxylate anion of the glucuronic acid moiety, either by a divalent metal ion or an active site amino acid, (ii) general base-catalyzed abstraction of the C5 proton, and finally (iii) the β -elimination of the leaving group at C4. This mechanism was originally proposed as a modification of the route via which many C5 epimerases were believed to function (Figure 3.1). It is understandable that the epimerases and lyases may share the initial two steps, with the epimerase mechanism differing in that a proton is delivered back to the enolic intermediate from the opposite face to arrive at the epimerised product.

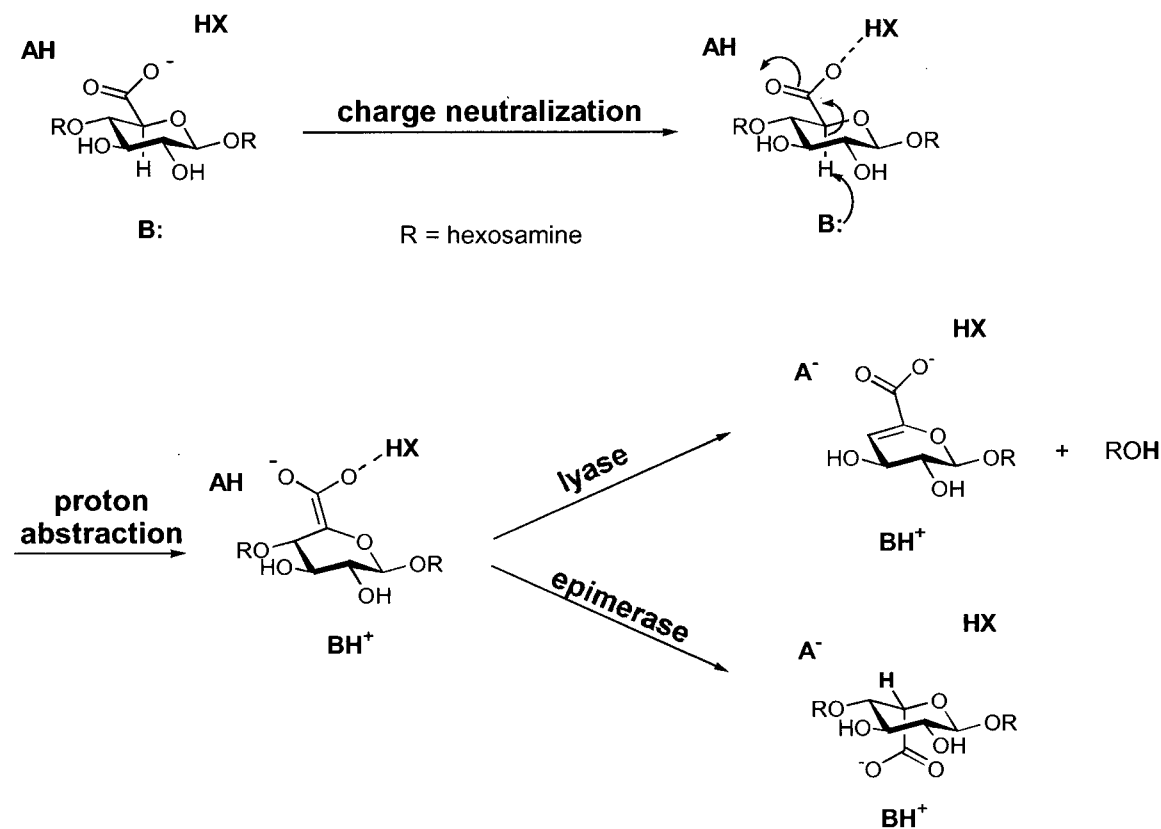


Figure 3.1. Scheme illustrating how the mechanisms of polysaccharide lyases and epimerases differ only in the final proton delivery step.

The ability of an active site general base to abstract the C5 α -proton is most often rationalised by the enhanced acidities of the α -protons of carbon acids relative to those of unactivated alkanes. The increased acidities are attributed to localisation of the resulting negative charge on the more electronegative oxygen, thereby generating a stabilised enolate anion rather than a highly unstable carbanion. However, the acidifying effect of the adjacent carbonyl group is not sufficient on its own to explain the high rates of the enzyme catalyzed reactions.^{69,70} The means of lowering the pK_a of the C5 proton of the uronic acid moiety ($pK_a \geq 22$) so that it can be abstracted by an active site base ($pK_a \sim 7$) is a matter of some contention. Gerlt and Gassman⁷⁰⁻⁷³ have proposed that concerted general acid – general base (electrophilic) catalysis involving a short, strong hydrogen bond to the carbonyl/enolic oxygen is sufficient to explain the observed rates of enzymatic catalysis. These short, strong or “low-barrier” hydrogen bonds have been

suggested to have exceptionally high strengths (up to 20 kcal/mol) and have been used to explain the high rates of many enzymatic reactions that involve the enolisation of carboxylate groups,^{71,74} as well as of serine proteases.⁷⁵ These low-barrier hydrogen bonds (LBHB) form when the pK_a values of the conjugate acid forms of the two groups sharing the proton are similar.⁷¹ Thus, a weak hydrogen bond in the enzyme-substrate complex can become one of the low-barrier type in the transition state or enzyme-intermediate complex if the pK_a values become matched during the reaction. This allows for the preferential stabilisation of the transition state, as predicted by transition state theory,⁷⁶ and helps to explain the great rate enhancements of many enzymes. To illustrate this point, it is appropriate to consider what residue in the enzyme active site is in a position to hydrogen bond with the carbonyl/enolic oxygen of the substrate and/or transition state or intermediate. In chondroitin AC lyase this residue may be arginine, which normally has a pK_a of ~ 12 . The pK_a value for the carbonyl oxygen of a carboxylic acid group is very low, ~ -8 ,⁷⁰ and a very strong hydrogen bond between this carbonyl oxygen of the substrate and the arginine residue in the active site is unlikely. However, the transition state is believed to resemble the enolic intermediate, and thus during the reaction we must consider the pK_a value of the OH group of the enol tautomer of the substrate carbon acid, which is estimated as 10-14 (Figure 3.2).⁷¹ Thus, for the transition state or the enolic intermediate, we can see that the pK_a values of the two groups are nearly matched, allowing for a LBHB to preferentially stabilize the transition state and/or reaction intermediate. A more in-depth analysis of this LBHB and how it contributes to the decrease in the pK_a of the α -proton is beyond the scope of this thesis, and the curious reader is directed to relevant papers in the literature.^{70,72,73,77}

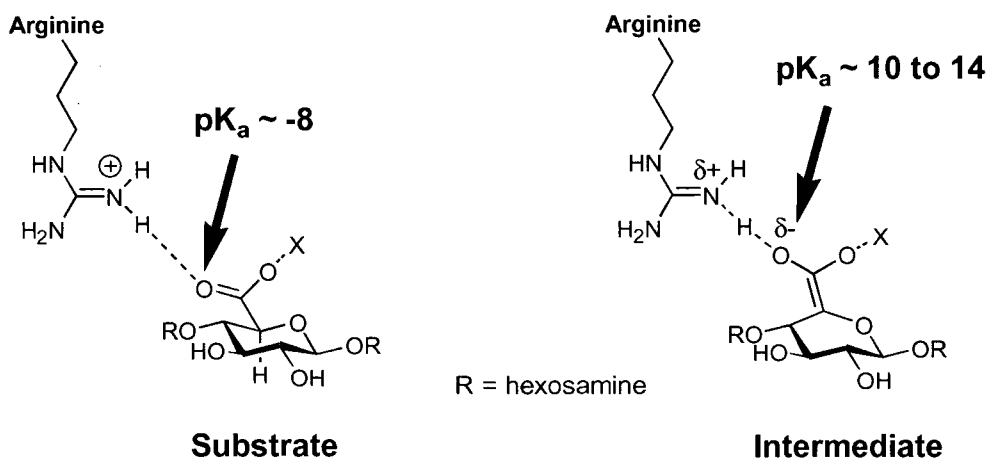


Figure 3.2. Illustration of how a hydrogen bond may preferentially stabilize the reaction intermediate (or transition state that resembles it) compared to the substrate. A low-barrier hydrogen bond may form between the OH group of the enolic intermediate and an arginine residue as their pK_a values become matched. X is a group that has neutralized the charge of the carboxylate group.

As promising as the LBHB may seem in explaining the remarkable catalysis of many enzymes, the existence of these unusually strong hydrogen bonds in solution or in enzyme active sites is doubted by some. With regards to enolisation reactions, Guthrie and Kluger^{78,79} propose that hydrogen bonding is insufficient to provide all of the stabilisation needed for the enol or enolate intermediate, and that electrostatic stabilization by a metal ion or positively charged amino acid is required to stabilize an enolate intermediate. Other researchers have used computer calculations to propose that it is mainly the orientation of the carboxylate group that determines the pK_a of the adjacent α -proton. These calculations have estimated that the rotation of a “perpendicular” carboxylate group so that its oxygen atoms lie in a plane formed by the carboxylate carbon and the adjacent α and β carbons may reduce the pK_a of the α -proton by as much as 40 pK_a units in certain cases!⁸⁰ This allows for efficient resonance stabilization of the carbanion, however, the validity of these arguments and calculations remains to be proven. Notwithstanding these arguments, the intent of this current research on chondroitin AC lyase is not to determine the specific mode of stabilization of the

proposed enolic intermediate, but to decipher the order and importance to catalysis of the bond breaking and forming steps.

3.2.2 Modified Substrates

The strategy of using modified substrates to study an enzymatic reaction has its limitations, simply because the substrates used are not the natural substrates for the enzyme. However, in a lot of the enzymes studied, a good deal of mechanistic information cannot be obtained by using the natural substrates, thus forcing the researcher to modify the substrates in one way or another. In particular, the substrates developed for this research all have activated leaving groups at C4, which could conceptually speed up the elimination of the leaving group, leading to a change in rate-limiting step. On the other hand, the increased electron withdrawing properties of the C4-linked fluorine or phenol moieties presumably increases the acidity of the proton at C5, and thus could increase the rate of the proton abstraction step, again leading to a change in rate-limiting step. Overall, the use of modified substrates with abnormal leaving groups may result in a change in mechanism or rate determining step. Thus it is not absolutely required that the lyase-catalyzed elimination of the polysaccharide substrate also occur in the manner deduced with the synthetic substrates. However, without these modified substrates, the mechanistic studies presented below would not be possible.

3.3 Synthetic Substrates

The use of heterogeneous polymeric substrates places immense limitations on the type of mechanistic studies that can be utilized to elicit the details of an enzymatic reaction. Chondroitin sulfates are commercially available; however, the sulfation patterns are not consistent throughout the polymer, the molecular weight is not accurately known and most likely varies between individual chains, and these substrates cannot easily be manipulated to allow the use of techniques such as kinetic isotope effects. Consequently the design and synthesis of a variety of synthetic substrates has allowed the measurement of defined and reproducible k_{cat} and K_{m} values, previously unattainable with the natural

polymeric substrates. The synthetic substrates are illustrated in Figure 3.3 (fluoride-releasing) and Figure 3.4 (chromogenic and fluorogenic).

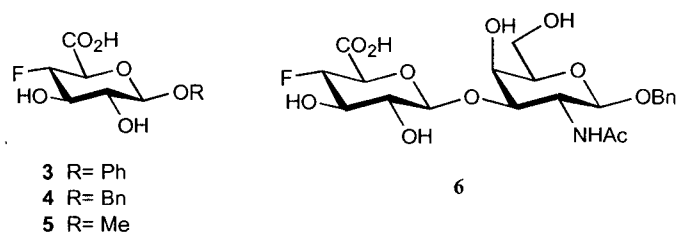


Figure 3.3. The fluoride-releasing substrates.

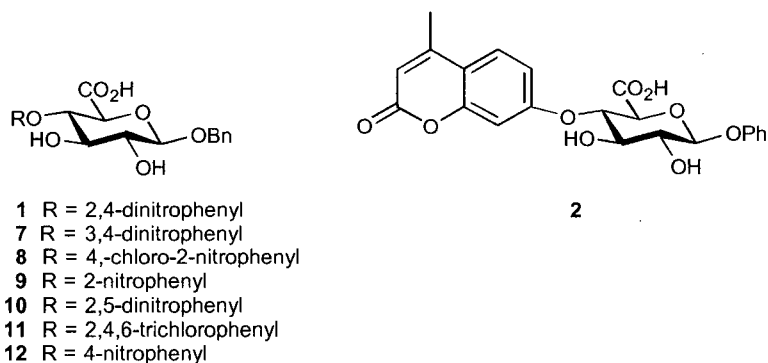


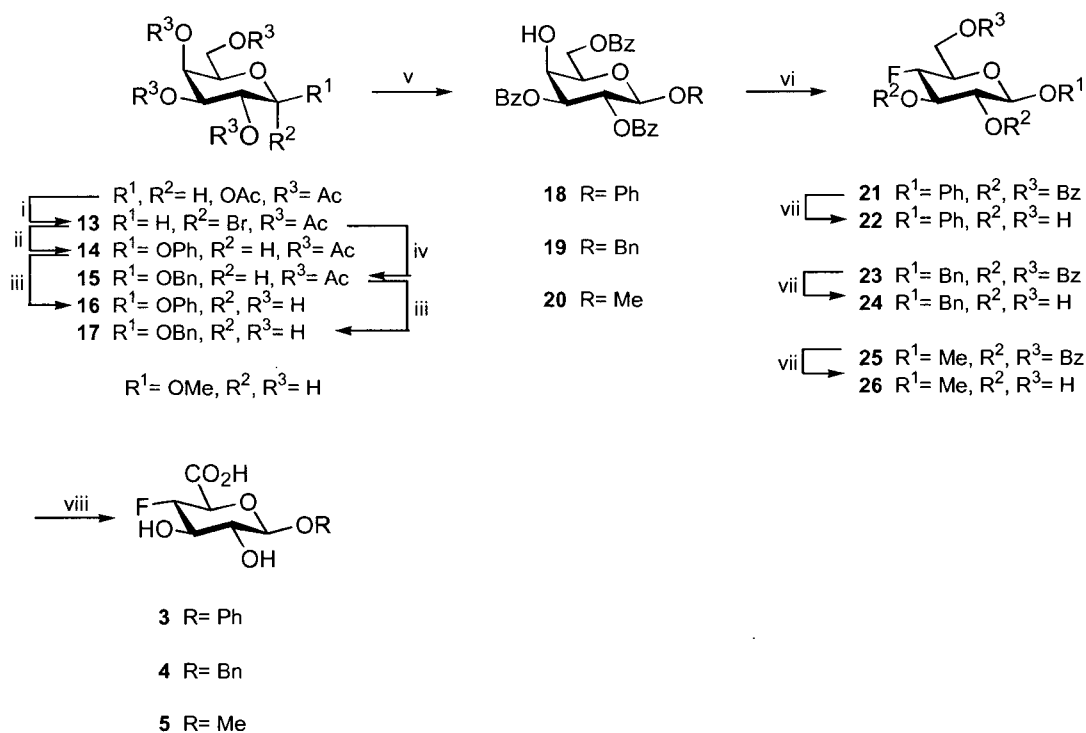
Figure 3.4. The chromogenic and fluorogenic substrates.

3.3.1 Synthesis

3.3.1.1 Synthesis of the Fluorinated Substrates

Phenyl 4-deoxy-4-fluoro-β-D-glucopyranosiduronic acid (3), benzyl 4-deoxy-4-fluoro-β-D-glucopyranosiduronic acid (4), and methyl 4-deoxy-4-fluoro-β-D-glucopyranosiduronic acid (5) (Scheme 3.1).

The synthesis of the three monosaccharide fluorinated substrates, differing only in their anomeric substituent is illustrated in Scheme 3.1.

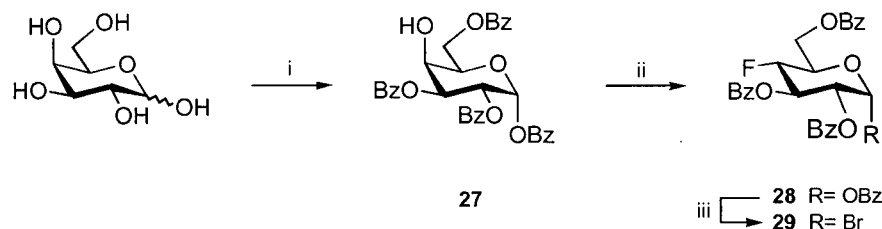


Scheme 3.1. Synthesis of the fluoride-releasing monosaccharide substrates. (i) HBr/AcOH, CH_2Cl_2 , $0^\circ\text{C} \rightarrow \text{rt}$; (ii) phenol, TBAHS, 1 M NaOH, CH_2Cl_2 ; (iii) NaOMe, MeOH; (iv) benzyl alcohol, Ag_2CO_3 , I_2 , CH_2Cl_2 ; (v) benzoyl chloride, pyridine, $-40^\circ\text{C} \rightarrow \text{rt}$; (vi) methyl DAST, CH_2Cl_2 , $-30^\circ\text{C} \rightarrow \text{rt}$; (vii) NaOMe, MeOH; (viii) For **3**: TEMPO, *t*-BuOCl, H_2O . For **4** and **5**: TEMPO, NaOCl, NaBr, TBAB, NaHCO_3 , EtOAc/ H_2O , 0°C .

Phenyl β -D-galactopyranoside (**16**)⁸¹ was prepared from *per*-O-acetylated galactose by first making the α -bromide (**13**) with HBr/AcOH and then introducing the phenyl aglycone via glycosylation using phase transfer catalysis with phenol and tetrabutylammonium sulfate (TBAHS) in a vigorously stirred mixture of 1 M NaOH and CH₂Cl₂ to give **14**. The acetate protecting groups were then removed via a Zemplén deprotection with sodium methoxide to give **16** as a white solid (40% overall). Benzyl β -D-galactopyranoside (**17**)⁸² was synthesized from **13** via a Königs-Knorr⁸³ reaction employing benzyl alcohol and Ag₂CO₃ to give **15**⁸⁴, followed by a Zemplén deprotection of the acetates to give the desired **17** as a white solid (79% from *per*-O-acetylated galactose). Methyl β -D-galactopyranoside was purchased commercially. Selective benzylation⁸⁵ of the galactosides at -40 °C afforded compounds **20**⁸⁵ (52%), **18**⁸⁶ (28%), and **19**⁸⁷ (40%) as white solids. Over-benzoylated products could be deprotected and re-benzoylated to give additional material. The 4-fluoro substituent was then easily introduced with (dimethylamino)sulfur trifluoride (methyl DAST) in CH₂Cl₂ to give **25**,⁸⁸ **21**, and **23**, in yields of 54%, 83%, and 60% respectively. The equatorial position of the 4-fluoro substituent was easily confirmed from the ¹H NMR coupling constant between H4 and H5 that ranged between 8.8 and 9.3 for the three compounds, showing the axial relationship between these two protons. After Zemplén deprotection of the benzoates the primary hydroxyl was selectively oxidized to the carboxylic acid using 2,2,6,6-tetramethyl-1-piperidinyloxy (TEMPO). The oxidation of the benzyl and methyl glucosides proceeded smoothly using NaOCl as the primary oxidant, giving **4** (93%) and **5** (74%) as white solids.⁸⁹ However, under the same conditions the phenyl glycoside (**22**) underwent an undesired side reaction, resulting in the *para*-chlorination of the aromatic ring, and gave an inseparable mixture of products. This was overcome by using *t*-butyl hypochlorite (*t*-BuOCl) in place of NaOCl, prepared as described in the literature,^{90,91} as the primary oxidant, to give **3** as a white solid (40%).

Benzyl *O*-(4-deoxy-4-fluoro- β -D-glucopyranosiduronyl)-(1 \rightarrow 4)-2-acetamido-2-deoxy- β -D-galactopyranoside (**6**) (Schemes 3.2, 3.3, and 3.4).

The synthesis of a disaccharide scaffold for the production of the desired substrate was attempted enzymatically with a β -glucuronidase from bovine liver. 4-Nitrophenyl β -D-glucopyranosiduronic acid was used as the donor, and either benzyl 2-acetamido-2-deoxy- β -D-galactopyranoside or the corresponding hemiacetal, 2-acetamido-2-deoxy-D-galactopyranose, was used as the acceptor. Unfortunately no desired products were isolated from these trials, and the disaccharide was subsequently produced chemically, via a much more laborious route than the enzymatic synthesis would have provided. The synthesis of the fluorinated disaccharide substrate is illustrated in Schemes 3.2 (donor), 3.3 (acceptor), and 3.4 (coupling).

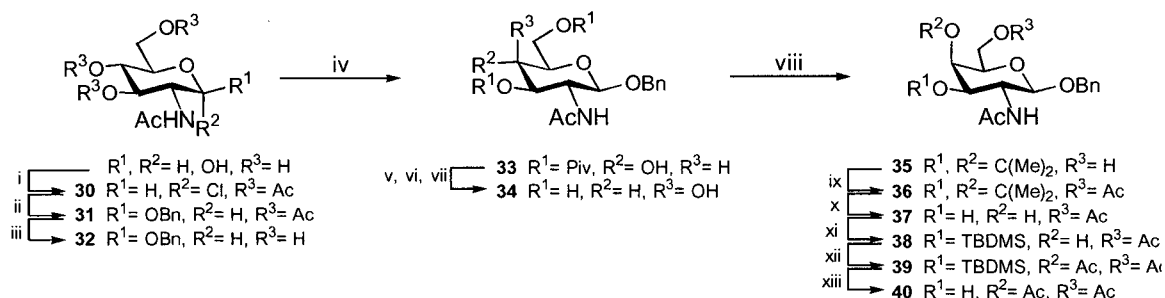


Scheme 3.2. Synthesis of 2,3,6-tri-*O*-benzoyl-4-deoxy-4-fluoro- α -D-glucopyranosyl bromide (**29**), the donor molecule for the disaccharide substrate. (i) BzCl , pyridine, 0°C ; (ii) methyl DAST, CH_2Cl_2 , $-30^\circ\text{C} \rightarrow \text{rt}$; (iii) HBr/AcOH , CH_2Cl_2 , $0^\circ\text{C} \rightarrow \text{rt}$.

The synthesis of the donor was accomplished in three facile steps. D-Galactose was selectively benzoylated with benzoyl chloride and pyridine at 0°C to give 1,2,3,6-tetra-*O*-benzoyl- α -D-galactopyranose (**27**)^{92,93} as an amorphous solid (15%) (Scheme 3.2). Side products could easily be deprotected and re-benzoylated to provide additional material. The 4-fluoro substituent was then easily introduced with methyl DAST in CH_2Cl_2 to give **28** as a white solid (63%), followed by treatment with HBr in acetic acid to give the α -bromide donor **29** as a white solid in a yield of 72%.

The obvious protection strategy to provide an acceptor *N*-acetylhexosamine sugar with the 3-hydroxyl free is through the one step benzylidenation of C4 and C6. However,

the glycosylation of this compound with the donor **29** proved to be problematic due to the low solubility of the acceptor, and the resulting cleavage of the *p*-methoxybenzylidene ring under the acidic coupling conditions (AgOTf), affording several products, including trisaccharides. An alternative protection strategy was employed (Scheme 3.3) that involved many more steps, however, a lot of the steps were high yielding and the products easily crystallized, thus eliminating the need for extensive chromatography. Another strategy that was not attempted, but may provide an appropriate acceptor molecule in a fewer number of steps, should also be mentioned. After the selective protection of the primary 6-hydroxyl group of the *N*-acetyl-D-galactopyranoside, the greater nucleophilicity of the equatorial 3-hydroxyl over that of the axial 4-hydroxyl might be employed to selectively couple to the donor via the desired 3-hydroxyl group. This strategy would avoid a lengthy synthetic sequence, but remains to be validated.



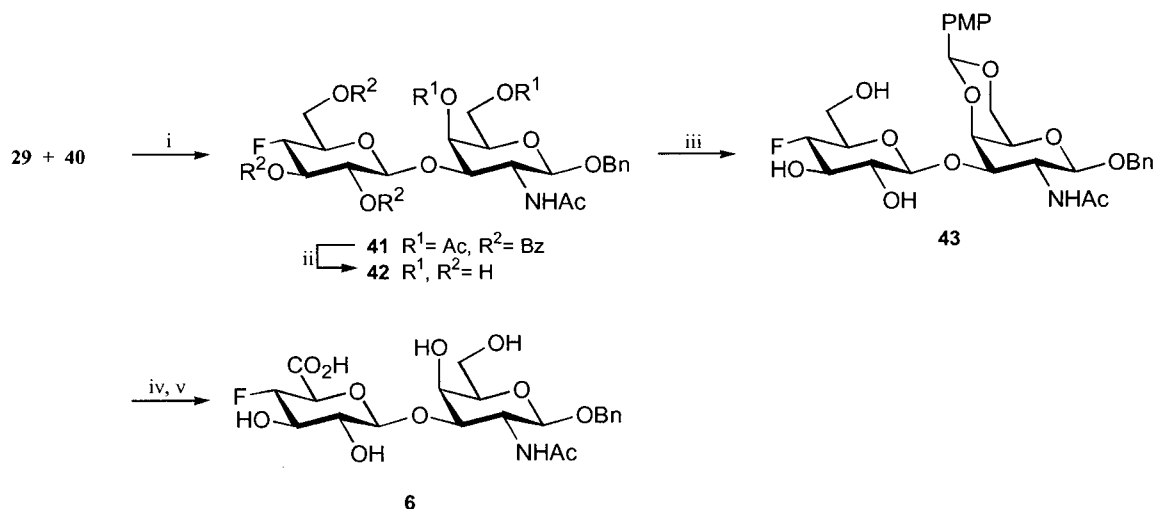
Scheme 3.3. Synthesis of benzyl 2-acetamido-4,6-di-*O*-acetyl-2-deoxy- β -D-galactopyranoside (**40**), the acceptor molecule for the disaccharide substrate. (i) acetyl chloride; (ii) benzyl alcohol, Ag_2CO_3 , I_2 , CH_2Cl_2 ; (iii) NaOMe, MeOH; (iv) pivaloyl chloride, pyridine, CH_2Cl_2 , 0 °C; (v) Tf_2O , pyridine, -15 °C; (vi) H_2O , 90 °C; (vii) NaOMe, MeOH; (viii) 2,2-dimethoxypropane, *p*-TsOH, then acetic acid, MeOH: H_2O (10:1), 45 °C; (ix) Ac_2O , pyridine; (x) acetic acid: H_2O (4:1), 50 °C; (xi) *t*-butyldimethylsilyl chloride, imidazole, DMF, 80 °C; (xii) Ac_2O , pyridine, 4-dimethylaminopyridine; (xiii) TBAF, THF.

Due to the significant cost difference between glucosamine and galactosamine sugars, the synthesis of the acceptor molecule started with the less expensive glucosamine and involved a conversion to the desired galacto-epimer as part of the synthesis. 2-Acetamido-2-deoxy-D-glucose was reacted with acetyl chloride for 3 days to give

30.⁹⁴ A Königs-Knorr reaction with benzyl alcohol and Ag_2CO_3 was employed to produce the benzyl glycoside **31**,⁹⁵ followed by a Zemplén deprotection with sodium methoxide to afford **32**⁹⁵ as a white solid. The conversion of the glucopyranoside derivative (**32**) into the galactopyranoside derivative (**34**) proceeded smoothly as described in the literature.⁹⁶ This involved the selective protection of the 3 and 6 hydroxyls as the pivaloyl esters to give **33**.⁹⁶ A triflate was then introduced at the remaining 4-hydroxyl group, which was subsequently displaced by water at 90 °C to give the product of inverted stereochemistry, followed by the deprotection of the pivaloyl esters with sodium methoxide in methanol to afford the desired benzyl 2-acetamido-2-deoxy- β -D-galactopyranoside (**34**)⁹⁶ as a white solid. The protection of the 3 and 4 hydroxyls with an isopropylidene group was accomplished using 2,2-dimethoxypropane and toluenesulfonic acid to give **35**,⁹⁶ followed by the protection of the remaining 6-hydroxyl with an acetate to give **36** in an overall 60% yield from **30** (8 steps). Removal of the isopropylidene moiety with aqueous acetic acid at 50 °C (80%) followed by the selective protection of the more reactive equatorial hydroxyl with *t*-butyldimethylsilyl chloride and imidazole in DMF at 80 °C gave crystalline **38** (79%). Acetylation of the remaining 4-hydroxyl group required a catalytic amount of 4-dimethylaminopyridine (DMAP) in the reaction mixture of pyridine and acetic anhydride to afford **39** as fine white crystals (95%). The silyl protecting group was removed with tetrabutylammonium fluoride (TBAF) in THF to give the acceptor **40** as a white crystalline solid in a moderate 49% yield. The yield of this final step was low due to the partial migration of the C4 acetate to C3.

Glycosylation of the donor **29** and the acceptor **40** was effected with silver triflate in CH_2Cl_2 to give the disaccharide **41** as a white crystalline solid in a yield of 32% (Scheme 3.4). The moderate yield of this reaction may be partly due to the electronegative fluorine atom disarming the donor molecule towards glycosylation by destabilizing the formation of the oxocarbenium ion. The concept of armed and disarmed donors and acceptors for glycosylation reactions was first brought forward by Fraser-Reid to rationalise, and expand the usefulness of various glycosylation reactions.⁹⁷ After a global Zemplén deprotection to give **42** (84%) a *p*-methoxybenzylidene group was

installed in the hexosamine residue using *p*-anisaldehyde dimethyl acetal and *p*-toluenesulfonic acid in DMF at 50 °C, affording **43** as a white crystalline solid (88%). The oxidation of the remaining primary hydroxyl group was accomplished with TEMPO and NaOCl under phase transfer conditions with TBAB in NaHCO_{3(aq)} and EtOAc. Under the reaction and/or work-up conditions employed, the cleavage of the *p*-methoxybenzylidene protecting group also occurred to some extent, affording the desired disaccharide substrate **6** as a white solid in a modest 25% yield.

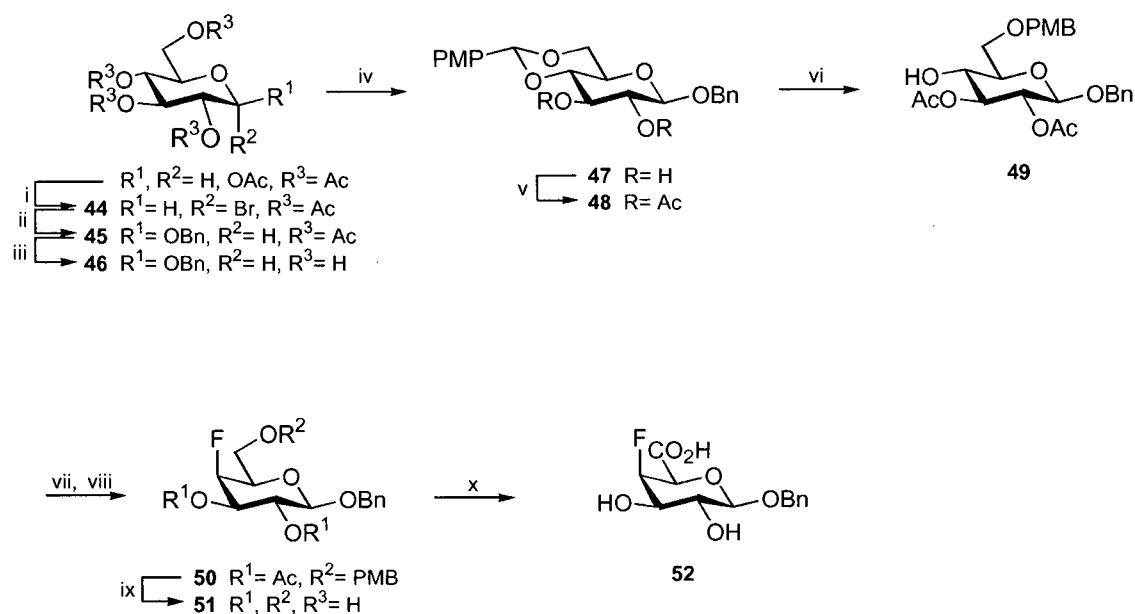


Scheme 3.4. Synthesis of benzyl *O*-(4-deoxy-4-fluoro- β -D-glucopyranosiduronic acid)-(1 \rightarrow 3)-2-acetamido-2-deoxy- β -D-galactopyranoside (**6**), the fluoride-releasing disaccharide substrate. (i) AgOTf, CH₂Cl₂; (ii) NaOMe, MeOH; (iii) *p*-anisaldehyde dimethyl acetal, *p*-TsOH, DMF, 50 °C; (iv) TEMPO, NaOCl, NaBr, TBAB, NaHCO₃, EtOAc/H₂O, 0 °C; (v) acetic acid, MeOH.

Benzyl 4-deoxy-4-fluoro- β -D-galactopyranosiduronic acid (52) (Scheme 3.5).

Benzyl β -D-glucopyranoside (**46**) was synthesized from *per-O*-acetylated glucose in a yield of 67% by first making the α -bromide (**44**) with HBr/AcOH, followed by glycosylation using a modified Königs-Knorr procedure with benzyl alcohol and Ag₂CO₃ (**45**), and finally a Zemplén deprotection with sodium methoxide.⁹⁸ A *p*-methoxybenzylidene protecting group was installed across C4 and C6 using *p*-anisaldehyde dimethyl acetal and a catalytic amount of camphorsulfonic acid in refluxing

CHCl_3 ,⁹⁹ to give **47** (63%) followed by the protection of the remaining hydroxyls with acetic anhydride and pyridine to give **48** as a white solid (57%). The benzylidene protecting group was selectively opened to the C6 position using sodium cyanoborohydride and trifluoroacetic acid (TFA) to give **49** as a colourless syrup (91%). An alternative method using triethylsilane¹⁰⁰ and TFA was not nearly as successful at the reductive opening of the *p*-methoxybenzylidene, producing mainly hydrolysis products according to the TLC analysis. Attempts to use the DAST reagent to introduce the axial fluorine at C4 as a route to the 4-fluorogalactopyranoside series of sugars were unsuccessful. Consequently, a C4-triflate was made from the suitably protected glucopyranoside (**49**) and was subsequently displaced with tetrabutylammonium fluoride (TBAF) to give the desired 4-fluoro-galactopyranoside, **50**, as a syrup in good yield (81% from **49**). Interestingly, the displacement of a C4 triflate from the analogous galactopyranoside epimer with TBAF was not successful at producing the 4-fluoro-glucopyranoside sugar under the conditions employed. After a facile global deprotection of **50** with acetyl chloride in methanol, the primary hydroxyl group was selectively oxidized with TEMPO and NaOCl to give **52** as a white solid (30% from **50**).

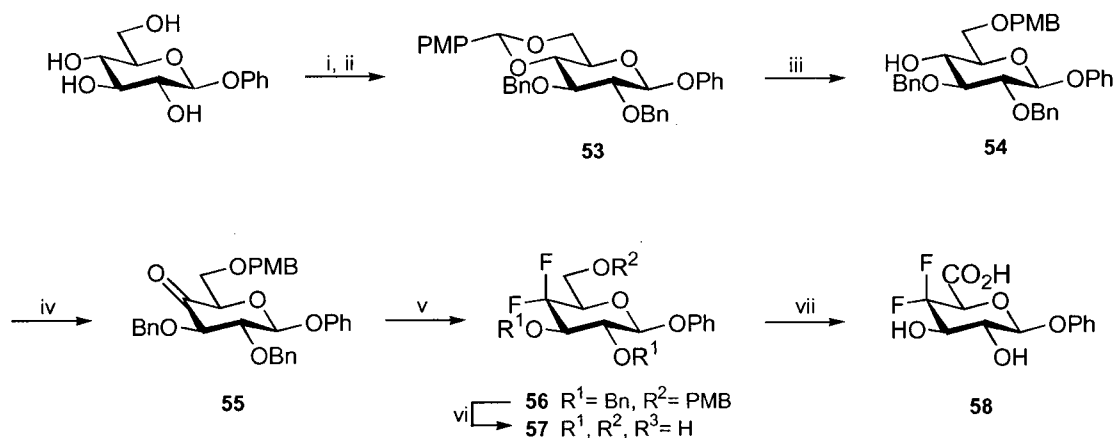


Scheme 3.5. Synthesis of benzyl 4-deoxy-4-fluoro- β -D-galactopyranosiduronic acid (**52**). (i) HBr/AcOH, CH₂Cl₂, 0 °C \rightarrow rt; (ii) benzyl alcohol, Ag₂CO₃, I₂, CH₂Cl₂; (iii) NaOMe, MeOH; (iv) *p*-anisaldehyde dimethyl acetal, camphorsulfonic acid, CHCl₃, reflux; (v) Ac₂O, pyridine; (vi) NaCNBH₃, TFA, THF/CH₂Cl₂; (vii) Tf₂O, pyridine, -15 °C \rightarrow rt; (viii) TBAF, THF; (ix) acetyl chloride, MeOH, 4 °C; (x) TEMPO, NaOCl, NaBr, TBAB, NaHCO₃, EtOAc/H₂O, 0 °C.

Phenyl 4-deoxy-4,4-difluoro- β -D-xylo-hexopyranosiduronic acid (58) (Scheme 3.6).

Commercially available phenyl β -D-glucopyranoside was reacted with *p*-anisaldehyde dimethyl acetal and *p*-toluenesulfonic acid in DMF at 50 °C, followed by the protection of the remaining hydroxyls as benzyl ethers using sodium hydride and benzyl bromide in DMF, to afford **53** as a white solid (39% isolated) (Scheme 3.6). After selectively opening the *p*-methoxybenzylidene ring with trifluoroacetic acid and sodium cyanoborohydride to leave the 4-hydroxyl free, the oxidation of this hydroxyl with DMSO and acetic anhydride¹⁰¹ gave **55** as a crystalline solid (75%). Benzyl ethers were employed as protecting groups at C2 and C3, rather than the usual acetates, because the oxidation of the C4 hydroxyl resulted in the elimination of the C2 acetate group, giving in an unsaturated product. Benzyl esters were also tried but were found to undergo the same

elimination as with the acetates. Other oxidation conditions were tried, such as oxalyl chloride and DMSO, and tetrapropylammonium perruthenate (TPAP) and *N*-methylmorpholine (NMO),¹⁰² however, none of the desired 4-keto product was isolated. It is also interesting that the oxidation with acetic anhydride and DMSO did not produce any product with the galacto-configured sugar after 18 h at rt. The introduction of two fluorines at C4 was accomplished by reacting the desired 4-keto compound (**55**) with DAST to give **56** in an 88% yield. The benzyl ethers were then removed by hydrogenation over Pd-C, and the removal of the *p*-methoxybenzyl ether was completed by a short treatment with ceric ammonium nitrate (CAN) to yield **57** (63%). The final step was the selective oxidation of the remaining primary hydroxyl with TEMPO and *t*-BuOCl to give **58** as a white solid in a moderate 27% yield.



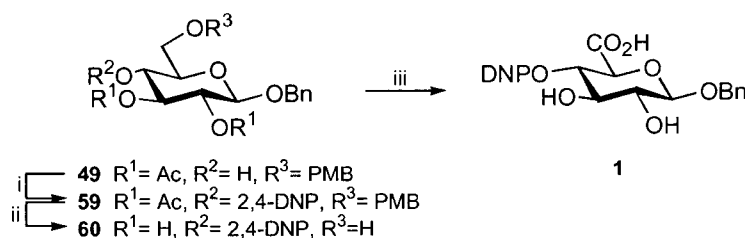
Scheme 3.6. Synthesis of phenyl 4-deoxy-4,4-difluoro- β -D-xylo-hexopyranosiduronic acid (**58**).

(i) *p*-anisaldehyde dimethyl acetal, *p*-TsOH, DMF, 50 °C; (ii) NaH, benzyl bromide, DMF; (iii) NaCNBH₃, TFA, THF/CH₂Cl₂; (iv) Ac₂O, DMSO; (v) methyl DAST, CH₂Cl₂, -30 °C \rightarrow rt; (vi) H₂, Pd-C, EtOAc/EtOH, followed by C.A.N., CH₃CN/H₂O; (vii) TEMPO, *t*-BuOCl, H₂O.

3.3.1.2 Synthesis of the Chromogenic Substrates

Benzyl 4-O-(2',4'-dinitrophenyl)-β-D-glucopyranosiduronic acid (1) (Scheme 3.7).

The synthesis of compound **1** is illustrated in Scheme 3.7.

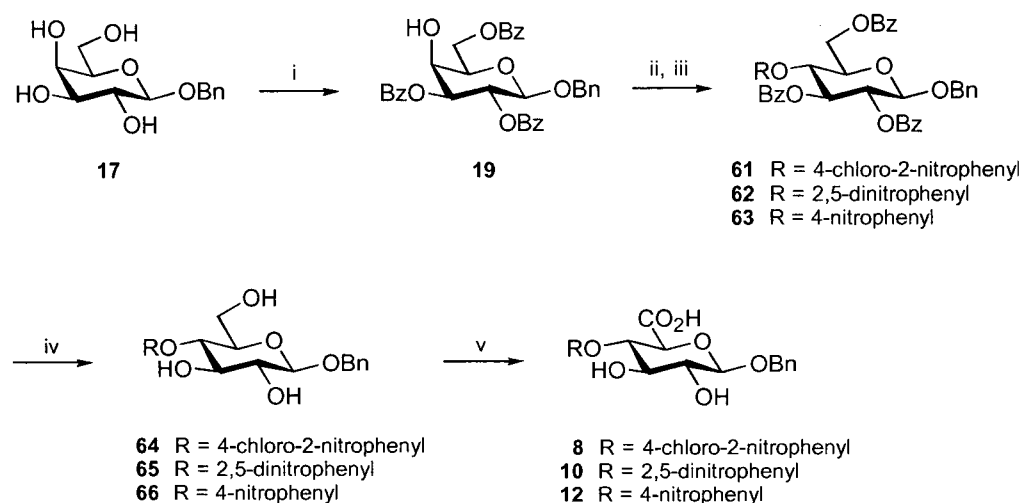


Scheme 3.7. Synthesis of benzyl 4-O-(2',4'-dinitrophenyl)-β-D-glucopyranosiduronic acid (**1**). (i) 2,4-dinitrofluorobenzene, DABCO, DMF; (ii) acetyl chloride, MeOH, 4 °C; (iii) TEMPO, NaOCl, NaBr, TBAB, NaHCO₃, EtOAc/H₂O, 0 °C.

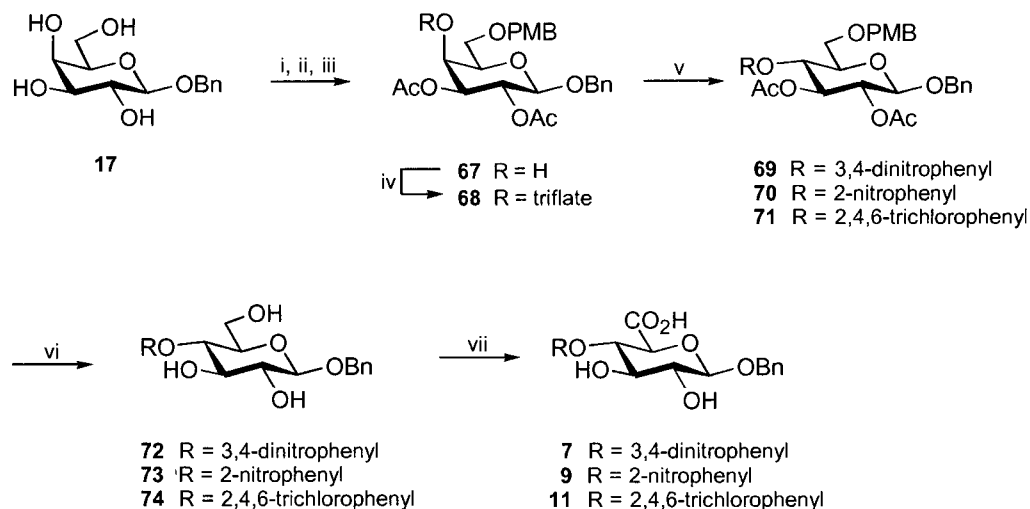
Beginning with the appropriately protected glucopyranoside (**49**, see Scheme 3.5) the dinitrophenol moiety at C4 was installed via a nucleophilic aromatic substitution reaction with 2,4-dinitrofluorobenzene and 1,4-diazobicyclo[2.2.2]octane (DABCO) in DMF to afford **59** as a pale yellow foam (80%). After deprotection of the acetates and the *p*-methoxybenzyl ether using acetyl chloride in methanol (89%), the primary hydroxyl group was selectively oxidized using TEMPO and NaOCl, affording **1** as a white solid (52%). An attempt at creating an even more reactive substrate with a 2,4,6-trinitrophenolate leaving group was attempted. However, this group was found to migrate from C4 to C6 upon deprotection of this primary hydroxyl group.

Benzyl 4-O-(4'-chloro-2'-nitrophenyl)- β -D-glucopyranosiduronic acid (8), benzyl 4-O-(2',5'-dinitrophenyl)- β -D-glucopyranosiduronic acid (10), benzyl 4-O-(4'-nitrophenyl)- β -D-glucopyranosiduronic acid (12), benzyl 4-O-(3',4'-dinitrophenyl)- β -D-glucopyranosiduronic acid (7), benzyl 4-O-(2'-nitrophenyl)- β -D-glucopyranosiduronic acid (9), and benzyl 4-O-(2',4',6'-trichlorophenyl)- β -D-glucopyranosiduronic acid (11) (Schemes 3.8 and 3.9).

Coupling of the aryl moiety to the 4-position through a nucleophilic aromatic substitution reaction proved impractical for less electron deficient reagents than 2,4-dinitrofluorobenzene. Thus, other phenol moieties were introduced via the S_N2 displacement of a C4-triflate using the potassium salt of the desired phenol. This required an appropriately protected galactoside, and for comparison purposes, two protecting group strategies were used in the synthesis of these chromogenic substrates. (1) Selective benzylation of benzyl β -D-galactopyranoside (**17**)⁸² provided the appropriately protected intermediate **19**⁸⁷ in one step in a moderate yield of 40% (Scheme 3.8). Overbenzoylated products could be easily deprotected and subjected to further benzylation to yield additional product. (2) The alternative protection strategy included the installation of a *p*-methoxybenzylidene group, acetylation of the remaining hydroxyls, and the selective opening of the benzylidene to afford the C6 *p*-methoxybenzyl ether using NaCNBH_3 and TFA to give **67** in an overall yield of 43% (Scheme 3.9). Chromatography was only necessary after the final ring-opening step.



Scheme 3.8. Synthesis of the chromogenic substrates containing 4-chloro-2-nitro-, 2,5-dinitro-, and 4-nitrophenolate leaving groups. (i) benzoyl chloride, pyridine, $-40\text{ }^{\circ}\text{C} \rightarrow \text{rt}$; (ii) TiF_2O , pyridine, $-15\text{ }^{\circ}\text{C} \rightarrow \text{rt}$; (iii) K^+ salt of appropriate phenol, DMF, $80\text{ }^{\circ}\text{C}$; (iv) NaOMe, MeOH; (v) TEMPO, NaOCl, NaBr, TBAB, NaHCO_3 , EtOAc/ H_2O , $0\text{ }^{\circ}\text{C}$.

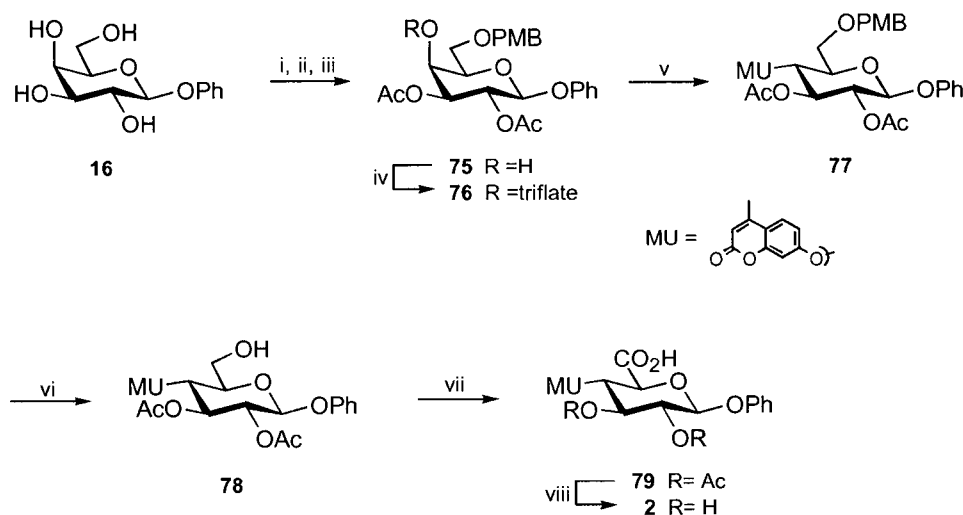


Scheme 3.9. Synthesis of chromogenic substrates containing 3,4-dinitro-, 2-nitro-, and 2,4,6-trichlorophenolate leaving groups. (i) *p*-anisaldehyde dimethyl acetal, *p*-TsOH, DMF, $50\text{ }^{\circ}\text{C}$; (ii) Ac_2O , pyridine; (iii) NaCNBH_3 , TFA, THF/ CH_2Cl_2 ; (iv) TiF_2O , pyridine, $-15\text{ }^{\circ}\text{C} \rightarrow \text{rt}$; (v) K^+ salt of appropriate phenol, DMF, $80\text{ }^{\circ}\text{C}$; (vi) acetyl chloride, MeOH, $4\text{ }^{\circ}\text{C}$; (vii) TEMPO, NaOCl, NaBr, TBAB, NaHCO_3 , EtOAc/ H_2O , $0\text{ }^{\circ}\text{C}$.

With the desired selectively protected compounds containing the free 4-hydroxyl in hand, the subsequent synthetic transformations to produce the coveted substrates were essentially the same for the two protecting group strategies employed. Triflic anhydride and pyridine were used to introduce the triflate leaving group at C4 that was subsequently displaced by the potassium salt of the desired phenol in DMF, giving the 4-substituted gluco-derivatives in moderate yields (37-47%). Elimination products containing a C4-C5 alkene were the other major component of these reactions, but could be easily separated by column chromatography. Zemplén deprotection of the benzoates with NaOMe proved problematic, with the phenol moieties partially migrating to the C3 position, leaving the desired compounds **64**, **65**, and **66** in yields of 53%, 26% and 71% respectively. Higher yields could have been achieved using the acidic global deprotection strategy (acetyl chloride in methanol) employed for the removal of the acetates and *p*-methoxybenzyl ether present in the intermediates formed with the other protecting group strategy. Thus, compounds **72**, **73**, and **74** were isolated in yields of 82%, 84%, and 86% respectively. The final transformation for all six compounds was the selective oxidation of the primary hydroxyl with TEMPO and NaOCl under phase transfer conditions with TBAB in $\text{NaHCO}_3(\text{aq})$ and EtOAc to give the desired uronic acids as white solids, with yields ranging from 53% to 83%

3.3.1.3 Synthesis of the Fluorogenic Substrate

Phenyl 4-methylumbelliferyl- β -D-glucopyranosiduronic acid (**2**) (Scheme 3.10).



Scheme 3.10. Synthesis of phenyl 4-methylumbelliferyl- β -D-glucopyranosiduronic acid (**2**). (i) *p*-anisaldehyde dimethyl acetal, *p*-TsOH, DMF, 50 °C; (ii) Ac₂O, pyridine; (iii) NaCNBH₃, TFA, THF/CH₂Cl₂; (iv) Tf₂O, pyridine, -15 °C → rt; (v) 7-hydroxy-4-methylcoumarin (K⁺ salt), DMF, 80 °C; (vi) C.A.N., CH₃CN:H₂O (9:1); (vii) CrO₃, H₂SO₄, acetone/H₂O, 35 °C, sonication; (viii) NaOMe, MeOH.

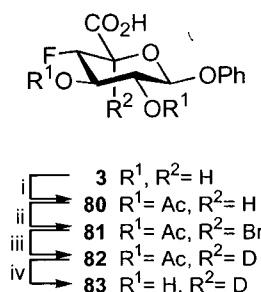
The preparation of compound **76** from phenyl β -D-galactopyranoside (**16**) proceeded in a manner similar to that described for **68** in the synthesis of the chromogenic substrates **7**, **9**, and **11** (Scheme 3.9), and is outlined in Scheme 3.10. The C4 triflate (**76**) was displaced with the potassium salt of 7-hydroxy-4-methylcoumarin (4-methylumbelliferone) in DMF at 80 °C to produce **77** as a white foam (29%). Selective deprotection of the *p*-methoxybenzyl group with ceric ammonium nitrate (CAN) gave **78** (87%) followed by a sonicated Jones oxidation¹⁰³ with CrO₃ and H₂SO₄ in acetone/H₂O to afford the acid **79** as glassy white solid. The Jones oxidation was used in place of the TEMPO oxidation employed in the other syntheses due to the fact that the methylumbelliferyl group was not compatible with the conditions of the TEMPO

oxidation. The facile Zemplén deprotection of the acetates afforded the desired compound, **2**, as a white solid (94%).

3.3.1.4 Synthesis of the Substrates for the Kinetic Isotope Effects

*Phenyl 4-deoxy-4-fluoro-5- $\{^2\text{H}\}$ - β -D-glucopyranosiduronic acid (**83**) (Scheme 3.11).*

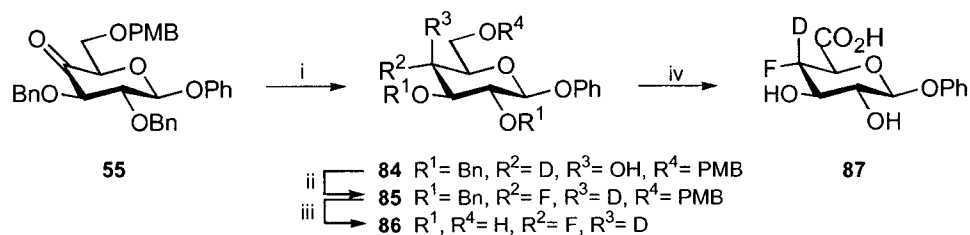
The synthesis of **83** carries on from the synthesis of **3** previously outlined in Scheme 3.1, and is illustrated in Scheme 3.11 below.



Scheme 3.11. Synthesis of phenyl 4-deoxy-4-fluoro-5- $\{^2\text{H}\}$ - β -D-glucopyranosiduronic acid (**83**).
(i) Ac_2O , H_2SO_4 ; (ii) NBS, $h\nu$, CCl_4 ; (iii) tributyltin deuteride, toluene, reflux; (iv) NaOMe-d_3 , CD_3OD .

Compound **3** was acetylated with acetic anhydride and sulfuric acid to give **80** as a white solid (79%), followed by a radical bromination with *N*-bromosuccinimide (NBS) in CCl_4 , directed by the adjacent carbonyl, to give the 5-bromo compound, **81**, as a white solid (39%). Deuterium incorporation at C5 proceeded smoothly with tributyltin deuteride in refluxing toluene to give both the D-gluco- and L-ido-configured sugars in roughly equal amounts. ^1H NMR analysis confirmed the expected $^4\text{C}_1$ chair conformation for the desired D-gluco compound and $^1\text{C}_4$ chair for the L-ido compound. The impurity corresponding to the protonated compound could not be detected by ^1H NMR. Unfortunate purification problems reduced the isolated yield of **82** to 5%, which was then deprotected with NaOMe-d_3 in CD_3OD to give the desired substrate **83** as a white solid (92%).

Phenyl 4-deoxy-4-fluoro-4- $\{^2\text{H}\}$ - β -D-glucopyranosiduronic acid (**87**) (Scheme 3.12).



Scheme 3.12. Synthesis of phenyl 4-deoxy-4-fluoro-4- $\{^2\text{H}\}$ - β -D-glucopyranosiduronic acid (**87**).

(i) sodium borodeuteride, MeOH; (ii) methyl DAST, CH_2Cl_2 , $-30^\circ\text{C} \rightarrow \text{rt}$; (iii) H_2 , Pd-C, EtOAc/EtOH, followed by C.A.N., $\text{CH}_3\text{CN}/\text{H}_2\text{O}$; (iv) TEMPO, *t*-BuOCl, H_2O .

Sodium borodeuteride in methanol was used to reduce the ketone of **55** and introduce the deuterium functionality at C4, giving the galactoside **84** as a white crystalline solid (94%) (Scheme 3.12). The stereochemistry at C4 was confirmed by analysis of the ^1H NMR signals arising from the protio compound also present as a result of the less than 100% deuterium incorporation. A broad doublet at 4.07 ppm with a coupling constant of 3.0 Hz (H3-H4) shows the equatorially disposed H4 (or D4) of this galactoside. After the incorporation of fluorine at C4 with DAST to give **85**, global deprotection was effected by hydrogenolysis over Pd-C in EtOAc/EtOH. However, the presence of trace amounts of sulfur from the previous DAST reaction poisoned the hydrogenation catalyst, and made the deprotection problematic, despite extensive purification. The *p*-methoxybenzyl ether was removed with ceric ammonium nitrate (CAN) in $\text{CH}_3\text{CN}/\text{H}_2\text{O}$ to afford **86** as a white solid (58%). The final step was the selective oxidation of the primary hydroxyl with TEMPO and *t*-BuOCl to give the desired **87** as a white solid (50%).

3.4 Fluoride-Releasing Substrates and the Effect of the Aglycone Moiety

3.4.1 Monosaccharide Substrates

In order to optimize the structure of the monosaccharide substrates for mechanistic analyses, the effect of the aglycone moiety was investigated. Fluoride-releasing substrates with a phenyl (**3**), benzyl (**4**), or methyl (**5**) group at the anomeric centre were synthesized and tested with the enzyme. The kinetic results shown in Table 3.1 clearly show a preference of the enzyme for a substrate with an aromatic aglycone. These favourable hydrophobic interactions with aromatic amino acids such as tyrosine and tryptophan are commonly found at the active site of carbohydrate-processing enzymes. In fact, the three-dimensional structures of various enzyme-oligosaccharide complexes of chondroitin AC lyase reveal tyrosine, histidine, phenylalanine, and several tryptophan residues arranged throughout the active site. Lacking these interactions, the substrate with the methyl aglycone (**5**) showed very weak binding, and no saturation binding behaviour was observed, resulting in a $k_{\text{cat}}/K_{\text{m}}$ value 91 and 27 times smaller than those of the substrates with a phenyl or benzyl aglycone. The substrate with a phenyl group at the anomeric centre showed a surprisingly larger k_{cat} than did the benzyl-containing substrate, however the binding of the phenyl substrate was poorer as reflected by its larger K_{m} value. Where synthesis is concerned, phenyl glycosides are more readily commercially available and are generally easier to synthesize than their benzyl counterparts. However, kinetic analyses of the phenyl-containing substrates are somewhat compromised by the high K_{m} values of these substrates, requiring more material for each analysis.

Table 3.1. Kinetic data for fluoride-releasing substrates.*

Substrate (aglycone)	k_{cat} (s^{-1})	K_{m} (mM)	$k_{\text{cat}} / K_{\text{m}}$ ($\text{M}^{-1}\text{s}^{-1}$)
3 (Ph)	2.3	114	20
4 (Bn)	0.16	28	5.9
5 (Me)	No saturation observed		0.22
6 (GalNAc)	0.011	12.5	0.85

3.4.2 Disaccharide Substrate

The natural substrates for chondroitin AC lyase are long polysaccharide chains, with the enzyme releasing disaccharide or oligosaccharide products. Thus, one would expect that increasing the number of sugar units in the synthetic substrate would improve the binding interactions with the enzyme, thereby yielding faster turnover. Consequently, a disaccharide substrate (**6**) with a benzyl *N*-acetylgalactosaminide residue connected via a β -1,3 linkage to the reducing end of 4-deoxy-4-fluoro- β -D-glucuronic acid, was synthesized in order to investigate the contribution of this extra sugar residue to catalysis. Surprisingly, the binding of this disaccharide to the enzyme was only slightly tighter than that of the monosaccharide substrates, yet the k_{cat} value was reduced at least 10-fold, resulting in a much less efficient substrate as measured by the low $k_{\text{cat}}/K_{\text{m}}$ value (Table 3.1). This may indicate that binding interactions towards the non-reducing end of the active site are more important for binding and catalysis. Unfortunately the addition of extra sugar units to occupy the -1, and -2 enzyme binding sites is not compatible with the design of this class of substrates. The primary natural substrates for chondroitin AC lyase contain a sulfate moiety at the 4 or 6 position of the hexosamine residue, whereas this synthetic disaccharide lacks any sulfation. It is conceivable that this seemingly stark lack

* Errors range from 5 to 25%

of sulfation could prevent the realization of all the extra binding energy potentially provided by the hexosamine residue. However, this enzyme is also highly active towards the unsulfated polymers chondroitin and hyaluronic acid, illustrating that the sulfation is not completely necessary for activity.¹² In fact, the literature states that chondroitin AC lyase acts at higher rates on chondroitin and hyaluronic acid than on chondroitin 4- or 6-sulfate.⁶ This was one of the main reasons that sulfation of the synthetic substrates was deemed unnecessary in the development of a disaccharide substrate for this enzyme. With regards to the monosaccharide substrates, the C2 position of the GlcA residue of the chondroitin sulfates has been found to be sulfated, but only to a very small degree. Thus, it was concluded that the substrates need not be sulfated at C2.

3.4.3 Incompetent Fluorinated Substrates as Competitive Inhibitors

The higher k_{cat} values of the fluoride-releasing substrates compared to those of the chromogenic or fluorogenic substrates (Tables 3.1 and 3.3) are thought to arise from the stabilization of the developing negative charge by the highly electronegative fluorine atom. With this in mind, a 4,4-difluoro substrate (**58**) was synthesized in the hope that it would be a superior substrate (Figure 3.5). However, no cleavage whatsoever of this compound was observed. Similarly, a 4-fluoro-galactopyranoside analogue (**52**) was also synthesized and was not a substrate for the enzyme, even though the leaving group is anti-periplanar to the abstracted hydrogen, and could conceivably be eliminated via an E2 mechanism.

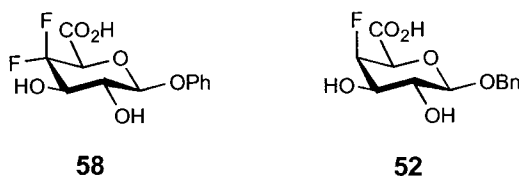


Figure 3.5. Competitive inhibitors of chondroitin AC lyase.

A trivial explanation for this otherwise surprising finding would be that the compounds with an axial fluorine substituent do not bind to the active site. However,

both of these compounds were shown to be competitive inhibitors of the enzyme with K_i values of 24 mM and 3 mM for the 4,4-difluoro (**58**) and 4-fluorogalacto (**52**) compounds respectively. Despite the small difference in size of fluorine and hydrogen atoms, the introduction of the axial C4-fluorine must either introduce enough additional steric bulk or result in an unfavourable dipolar interaction of sufficient magnitude to cause an unproductive mode of binding. Although the van der Waals radius of a fluorine atom is greater than that of a hydrogen by only 0.15 Å, the carbon-fluorine bond length is considerably greater than that of the carbon-hydrogen bond (Table 3.2). This combination causes the substitution of a fluorine atom for a hydrogen to increase the steric bulk significantly more than it may at first appear. It is not unreasonable to see how a change from 2.29 Å (radius + bond length) for a C-H group to 2.74 Å for a C-F group causes the fluorine-substituted compound to bind incorrectly, or not at all, in a finely tuned enzyme active site. An alternative explanation for the lack of activity shown by the difluoro compound (**58**) may rest at least partly with the greater than 10 kcal/mol ground-state stabilisation afforded by geminal fluorine atoms.^{104,105} The greater inhibition by compound **52** is most likely due to the fact that compounds with a benzyl aglycone have been shown to bind tighter to the enzyme than do those with phenyl aglycone moieties, as found in compound **58** (*vide supra*).

Table 3.2. Size comparison between hydrogen and fluorine.¹⁰⁶

Group	van der Waals radius (Å)	Bond Length (Å)
C-H	1.20	1.09
C-F	1.35	1.39

3.5 pH Dependence

One of the most common enzymatic investigations is to determine the pH at which the enzyme is the most active. Not only is this pH the most relevant to the enzyme, conducting research at this optimal pH ensures the efficient use of enzyme stocks by

allowing the least amount of enzyme to be used to achieve a maximal rate in enzymatic assays. Profiles of activity vs pH often provide clues about enzymatic machinery and reveal the pK_a values of catalytically important amino acids. Plots of enzymatic rate against pH frequently take the form of simple single or double ionization curves, even though the enzyme contains many ionizable groups. This is because it is usually only the ionization of groups directly involved in catalysis at the active site that is important to the pH profile. However, in some circumstances, such as with chymotrypsin, the pH profile reveals the pK_a of an amino acid which is not directly involved in catalysis, but holds the enzyme in a catalytically active conformation.⁶⁸

Previous studies^{11,12} have investigated the pH optimum for chondroitin AC lyase. However, the literature results do not agree with one another. For this reason analyses of pH-dependence were performed using the enzyme's natural substrate (chondroitin 6-sulfate) as well as a synthetic monosaccharide fluoride-releasing substrate (**4**) for comparison. A simple analysis of V_{max} vs pH was obtained with chondroitin 6-sulfate using saturating substrate concentrations. Figure 3.6A shows the V_{max} to be maximal at a pH of 6.8, and this was the pH chosen for subsequent enzymatic analyses. Two pK_a values can be extracted from this figure, 5.3 and 7.9, which may represent two ionizable groups important for catalysis in the enzyme-substrate complex such as the general base and general acid residues. These pK_a values may also reflect the ionization of the substrate within the enzyme-substrate complex. However, the pK_a values of the substrate carboxylic acid moieties free in solution have been shown to be much lower than either of these values (*vide infra*). A similar analysis of the dependence of V_{max} on pH with the synthetic substrate **4** was not possible due to its high K_m value. Instead a k_{cat}/K_m vs pH analysis was performed using low substrate concentrations where the rate vs $[S]$ profile is approximately linear. Figure 3.6B shows the second order rate constant for the synthetic substrate **4** to be maximal at around pH 6, close to the maximum found for the V_{max} profile of the natural substrate. The one clear pK_a value that can be abstracted from this curve is 7.2, closely matching that deduced from the study with the natural substrate, and implying the presence of an essential group that must remain protonated for activity, possibly the acid catalyst. On the basis of the X-ray crystallographic analysis, a tyrosine residue has been implicated as the acid catalyst.^{40,43}

The pK_a of a tyrosine residue is normally around 10, however a decrease of 2 to 3 pK_a units is not unheard of for amino acids at the active site of enzymes. The pK_a value of 5.3 abstracted from the V_{max} profile may represent a group that must be deprotonated for activity, such as the base catalyst. This residue has been proposed to be a histidine, as in other polysaccharide lyases, which normally has a pK_a value 6.5. Thus, these data correlate with the pH profile expected for an enzyme with essential histidine and tyrosine groups acting as catalytic base and acid residues, respectively.

Perhaps the most surprising finding was the remarkable change in K_m for the natural substrate with a change in pH. The K_m was measured to be 1.23 mg/mL at pH 8.8, and only 7.0×10^{-3} mg/mL at pH 5.0, corresponding to a change by a factor of 175 (Figure 3.6C). Conversely, for the synthetic substrate **4**, the K_m dropped by only 33% upon changing from pH 6.8 to pH 5.2. The substantial decrease in K_m observed with chondroitin 6-sulfate resulted in a significantly different pH profile for k_{cat}/K_m from that seen with the synthetic substrate, or from the profile of V_{max} vs pH with the same substrate. Figure 3.6D shows how the k_{cat}/K_m value increases with decreasing pH for chondroitin 6-sulfate.

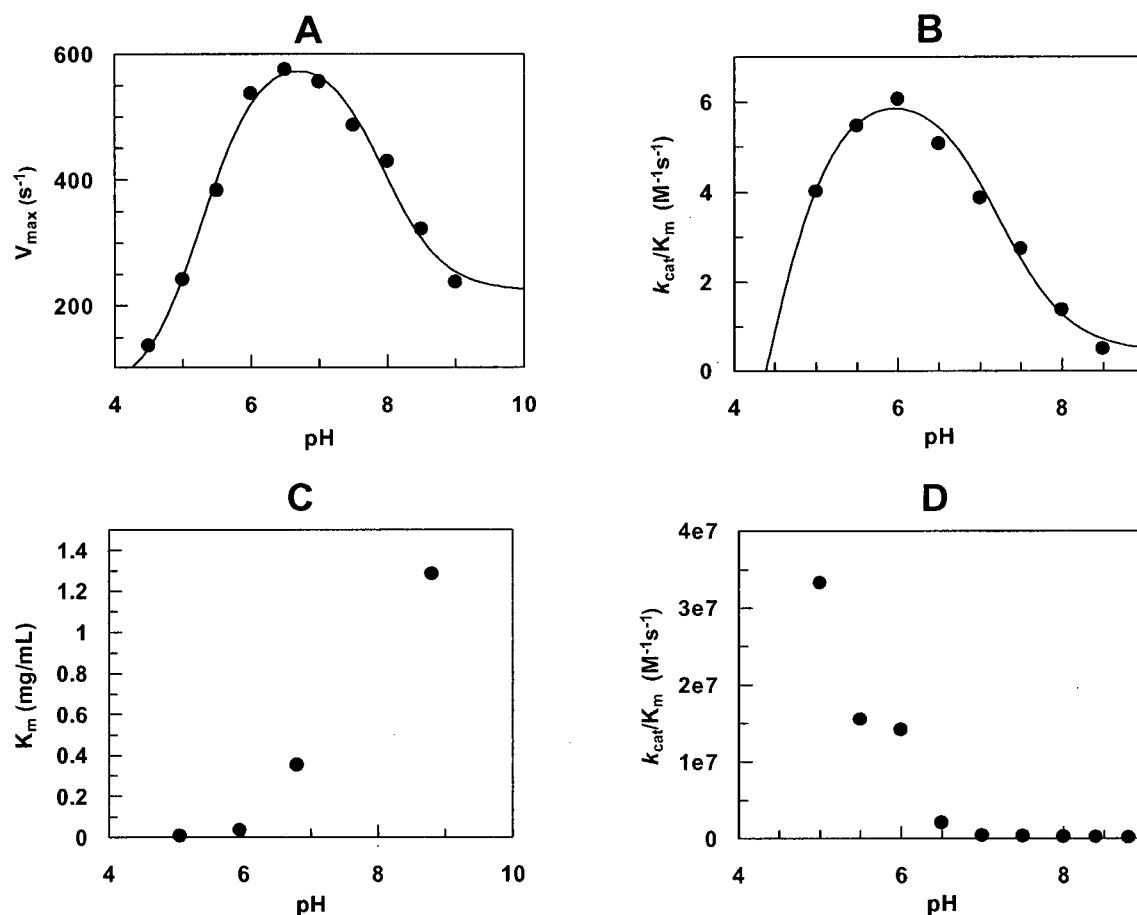


Figure 3.6. pH Profiles for chondroitin AC lyase. (A) V_{\max} vs pH profile for chondroitin 6-sulfate. (B) k_{cat}/K_m vs pH profile for compound 4. (C) K_m vs pH for chondroitin 6-sulfate. (D) k_{cat}/K_m vs pH profile for chondroitin 6-sulfate. The curves in A and B are fit to an equation describing the ionization for two groups that results in a bell shaped curve. No equation has been used to fit the data in C and D, and thus no curve has been included.

The above graphs illustrate the dramatic difference in the k_{cat}/K_m pH profiles between the synthetic substrate and that of the natural substrate. The main differences between the synthetic and natural substrates are three-fold: (i) the synthetic substrate has a fluoride leaving group which doesn't require acid catalysis, whereas the leaving group in chondroitin 6-sulfate is a sugar that requires acid catalysis, (ii) the synthetic substrate is not sulfated, whereas chondroitin 6-sulfate is, and (iii) the synthetic substrate is a monosaccharide, whereas the natural substrate is a large polysaccharide. The dependence of the leaving group on acid catalysis is not expected to affect the binding of the substrate

to the enzyme, and thus should not result in a dependence of K_m upon pH. The pK_a of the sulfate group is expected to be sufficiently low that the ionization of this group should not affect the results in the pH range of 5 to 9. With the use of Gran plots,¹⁰⁷⁻¹⁰⁹ the pK_a values of chondroitin 6-sulfate and the synthetic substrate **4** were measured to be 2.9 and 2.7 respectively. The pK_a value measured for chondroitin 6-sulfate may only be an approximate or average pK_a , as this polysaccharide contains many carboxylic acid groups dispersed along its length. One can envision the pK_a value of each individual carboxylic acid group being perturbed as the ionization state of neighbouring acids is changed by altering the pH during the titration. However, the small difference between the pK_a values of the carboxylic acid groups of the synthetic and natural substrates is not sufficient to explain the dramatically different effects of pH on the K_m that were observed. Inspection of the 3-dimensional structure of chondroitin AC lyase reveals that the proposed binding cleft on the enzyme is positively charged, presumably in order to bind this polyanionic substrate.^{38,40} It therefore seems reasonable that a decrease in pH may afford a more positively charged binding pocket on the enzyme which may well lead to enhanced binding only of a long polysaccharide chain such as the natural substrate, but not of the monosaccharide synthetic substrate. It is also conceivable that chondroitin 6-sulfate undergoes a pH-dependent conformational change that affects its binding to the enzyme active site and thus might be expected to change the K_m value.^{4,14}

3.6 Linear Free Energy Relationship

3.6.1 Background and Theory

Linear free energy relationships are popular tools used by the physical enzymologist to help decipher the nature of a reaction mechanism. The concepts originally arose from the observation of the differing acid strengths of substituted benzoic acids, and were first quantified by Hammett, thus linear free energy relationships are often referred to as 'Hammett relationships'. It was noticed that there were linear relationships between the rates of various reactions of aromatic compounds with the acid dissociation constants of the corresponding benzoic acids. A plot of the logarithms of the

rate constants of a reaction against the pK_a values of the substituted aromatic groups produces a straight line, hence the term 'linear' relationship. The 'free energy' portion of the title comes from the fact that the logarithm of a rate constant is proportional to the Gibbs free energy of activation of the reaction in question, and the logarithm of an equilibrium constant (such as a pK_a) is proportional to the Gibbs free energy change of the reaction involved.⁶⁸

The free energy correlations tell us about the charge development at various centres during the reaction. In this study, a series of substituted phenols will be used as leaving groups and the free energy relationship will provide information about the charge development on the phenolic oxygen during the transition state for the cleavage of the phenolic oxygen-carbon bond. From this information we may deduce the pathway, or mechanism, that the reaction is following. For multi-step enzymatic reactions, substituent effects will only be realized on the observed reaction rate if the charge development at that centre occurs during a rate-limiting step. Thus, information regarding which step(s) is/are rate limiting can be gained.

The use of linear free energy relationships in enzymatic systems has some limitations. Firstly, all enzymatic reactions involve at least two steps (binding and catalysis), each of which may react differently to structural alterations in the substrate. Due to the finely tuned structure of the enzyme active site, many enzymes simply may not accommodate the structural changes within the substrates. In addition, the variation of substituent groups on a common substrate scaffold may generate differential interactions that affect binding of the substrate and may alter the precise special orientations of the catalytic group(s) and reactive bond(s) of the substrate. Thus, these binding effects may obscure the changes brought about by the differential electronic substitutions made on the substrates. Despite these limitations, mechanistic details regarding enzymatic reactions have routinely been abstracted from linear free energy relationships.

Hammett relationships often show a non-linear pattern over a wide range of substituent reactivities. There are two main possibilities that can shed light on some interesting mechanistic considerations. Firstly, the plot may have an inflection point and be concave upward. This result arises when a substrate can follow two different pathways to arrive at the same product, and indicates a change in reaction mechanism as the

electron withdrawing or donating properties of the substituent are changed. Secondly, the plot may have an inflection point and be concave downward. This generally arises from a multi-step reaction in which the rate-determining step changes as the electronic nature of the substituent changes. This has been shown to be the case with many glycosidases that cleave a series of substituted phenyl glycosides. With the β -glucosidase from *Agrobacterium faecalis*, a plot of the logarithm of k_{cat} vs pK_{a} is flat for phenols of low pK_{a} , and has a negative slope for phenols of high pK_{a} .¹¹⁰ This reflects a change in the rate-determining step from being glycosylation (1st step) with phenols of high pK_{a} (> 8), to deglycosylation (2nd step) with phenols of low pK_{a} (< 8) (Figure 3.7). This may seem intuitively reasonable, in that as the leaving group ability of the phenol increases (with decreasing pK_{a}) the step involving the cleavage of this leaving group (1st step) becomes faster, and thus ultimately not rate limiting, resulting in a Hammett plot that is flat in this low pK_{a} region, and shows no dependence of reaction rate on leaving group reactivity.

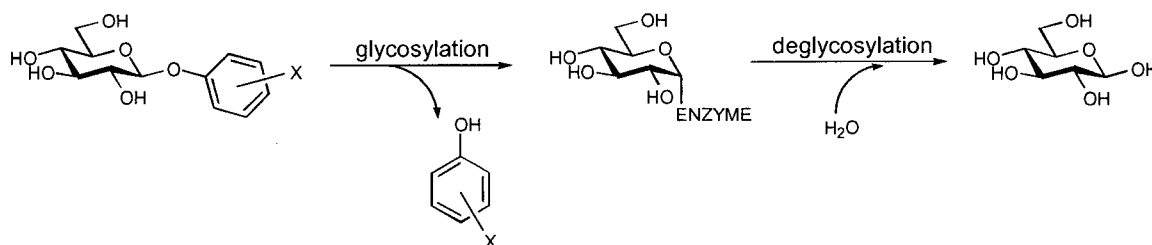


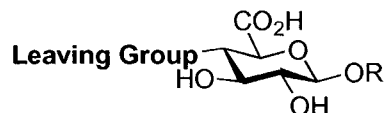
Figure 3.7. Two step mechanism of a glycosidase shown cleaving a series of substituted phenyl glycosides.

3.6.2 Results and Discussion

Seven synthetic substrates containing phenol leaving groups with nucleofugalities (leaving group abilities) defined by their pK_{a} values were synthesized (Figure 3.4). Of these, only 4 provided useful kinetic data, with the other 3 each having their own problems (*vide infra*). Table 3.3 summarises the kinetic parameters of the chromogenic substrates, and also includes the data from the fluorogenic substrate **2** for comparison. The resulting linear free energy relationship (Figure 3.8) showed that the rate of

enzymatic degradation of these substrates had virtually no dependence on the pK_a of the phenols.

Table 3.3. Kinetic data for chromogenic and fluorogenic substrates.* Note: analyses of **2** were performed at pH 8, while all others were done at pH 6.8. Extinction coefficients used to calculate rates were obtained from ⁶⁷.



R = Bn for chromogenic substrates
R = Ph for fluorogenic substrate **2**

Substrate	Leaving Group	Leaving Group pK_a	k_{cat} (s^{-1})	K_m (mM)	k_{cat} / K_m ($M^{-1}s^{-1}$)
1	2,4-dinitrophenolate	3.96	0.019	7.0	2.7
7	3,4-dinitrophenolate	5.36	0.019	9.0	2.1
8	4-chloro-2-nitrophenolate	6.45	0.035	12.2	2.8
9	2-nitrophenolate	7.22	0.027	16.9	1.6
10	2,5-dinitrophenolate	5.15	no activity		
11	2,4,6-trichlorophenolate	6.45	low solubility, no results obtained		
12	4-nitrophenolate	7.18	variable kinetic results		
2	4-methylumbelliferyl	7.8	0.0016	1.0	1.5

* Errors range from 7 to 16%

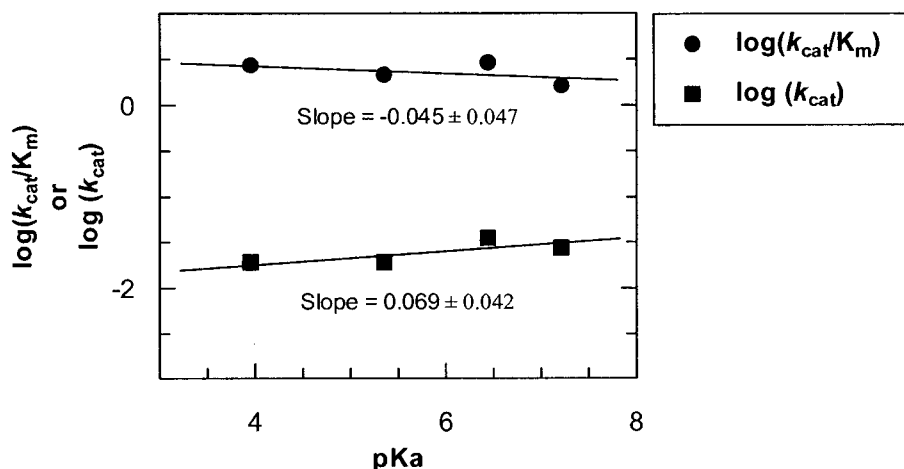


Figure 3.8. Linear free energy relationship for chondroitin AC lyase produced using substrates with substituted phenol leaving groups.

The flat linear free energy relationship shows that there is no significant charge development on the C4 oxygen at the transition state of the rate-limiting step. There are two main possibilities to explain this result. The first is that there is highly effective proton donation to the departing phenol by a general acid catalyst at the transition state, which neutralizes any charge development at the C4 oxygen. If this is the case it is impossible to tell whether the reaction is concerted or stepwise using this analysis. The second possibility is that the reaction is stepwise with the breaking of the C4-O4 bond not occurring in a rate-limiting step, thus ruling out a concerted *syn*-elimination. This second explanation is more likely, not only due to the rarity of concerted *syn*-elimination processes, but also due to its agreement with the near unity secondary deuterium kinetic isotope effect (KIE) that was measured with a substrate containing deuterium at C4 (*vide infra*).

The fluorogenic substrate **2** was found to bind more tightly to the enzyme than any of the chromogenic substrates, despite the phenyl aglycone moiety, which has been shown to increase the K_m relative to those of substrates with a benzyl aglycone (*vide supra*). This again may be due to the increased size of the aromatic 4-methylumbelliferone group allowing it to form more favourable hydrophobic interactions with aromatic amino acids known to be present in the active site. Thus, the lower K_m value is also a bit surprising given that the K_m values for substrates have been shown to

increase as the pH is increased (*vide supra*), and the kinetic constants for the fluorogenic substrate were obtained at pH 8.0 as opposed to pH 6.8 for the chromogenic substrates. However, the k_{cat} value for the fluorogenic substrate was at least ten-fold lower than that of the chromogenic substrates. This resulted in the overall catalytic efficiency, as measured by $k_{\text{cat}}/K_{\text{m}}$, being similar to that of the chromogenic substrates, correlating nicely with the flat linear free energy relationship seen for $k_{\text{cat}}/K_{\text{m}}$. These Hammett relationships, especially with enzymatic systems, should be constructed under identical reaction conditions and using the smallest structural perturbations of the leaving group while still allowing the desired activity range to be obtained. This prevents the enzyme from acting in a different manner based on the substrate's physical architecture rather than its electronic properties. However, as discussed below it is not always possible to avoid this. Additionally, as noted above, the pH of the fluorogenic assay was different from that of the chromogenic substrates. Thus, although the data point for the fluorogenic substrate would have fit nicely in Figure 3.8, it was not included.

Three substrates that were synthesized for use in the linear free energy analysis each had their own unique problems that prevented them from generating useful data. The extremely low solubility of the substrate with a 2,4,6-trichlorophenyl leaving group (**11**) (pK_{a} 6.39) precluded its use in enzymatic assays. Attempts at using organic cosolvents in the reaction mixtures to increase the solubility resulted in substantial rate decreases when performed with the other competent substrates. The substrate with a 2,5-dinitrophenyl leaving group (**10**) (pK_{a} 5.15) surprisingly showed no activity in enzymatic assays. NMR and elemental analysis confirmed the structure and purity of compound **10**. It is postulated that the position of the two nitro substituents being *para* to one another creates a much bulkier phenol group that cannot be accommodated in the enzyme's active site. This particular arrangement of nitro groups may cause the substrate to bind in an unproductive mode, or not at all. Inhibition studies with this compound may have facilitated an answer to whether the substrate was in fact binding to the enzyme, however, the compound had decomposed by the time the inhibition study was attempted. The substrate with a 4-nitrophenyl leaving group (**12**) (pK_{a} 7.18) was cleaved by the enzyme, however, the plot of product versus time had an unusual inflection point, preventing accurate analysis of the data. Compound **12** was re-purified and the structure and purity

of this compound were confirmed using NMR and elemental analysis. Subsequent analyses with the enzyme resulted in the same unusual kinetic behaviour. The source of, and explanation for, these kinetic results remains a mystery. Despite the failure of three compounds to produce useful kinetic data, 4 substrates containing leaving groups spanning a pK_a range of 3.96 to 7.22 (3 orders of magnitude in reactivity) were sufficient to generate a linear free energy relationship from which some mechanistic insight was gained.

3.7 Kinetic Isotope Effects

Kinetic isotope effects (KIEs) are one of the most useful tools used to elucidate the mechanisms of chemical reactions and probe transition state structure, including those catalyzed by enzymes. KIE studies are ideally suited to mechanistic investigations because isotopic substitution has no effect on the qualitative chemical reactivity of the substrate, yet often has an easily measured effect on the reaction rate. Both primary (1°) and secondary (2°) KIEs are useful tools, although the accurate measurement of the latter is more difficult, simply due to their lower magnitude.

Substrates were synthesized with deuterium incorporated at C5 (**83**) and C4 (**87**) of monosaccharide substrates, in order to measure potential primary and secondary deuterium KIEs (Figure 3.9).

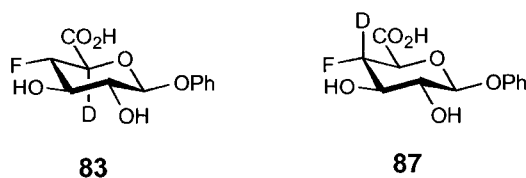


Figure 3.9. Substrates for primary (**83**) and secondary (**87**) deuterium kinetic isotope effects.

When interpreting the magnitude of KIEs measured on enzymatic systems, one must realize that the chemical interconversion step may no longer be rate-limiting. Indeed, product-release steps are often at least partially rate-limiting as a result of evolutionary pressure on the enzyme to accelerate chemical steps until they are just

slightly faster than the release of product.^{111,112} However, KIEs remain as extremely useful tools in describing enzymatic reaction mechanisms.

3.7.1 Primary Kinetic Isotope Effects

3.7.1.1 Background and Theory

A primary KIE results from the cleavage of a bond to the substituted atom. Two main pieces of information can be provided by primary KIEs. First, the existence of a primary KIE shows that the bond to that substituted atom is cleaved in a rate-limiting step. Second, the magnitude of the primary KIE provides information about the structure of the transition state for the cleavage of that bond. For example, if the bond to a substituted hydrogen is either only slightly or is nearly completely broken at the transition state, the KIE will be relatively low. On the other hand, a primary deuterium KIE near the theoretical maximum (~ 7) can indicate that the transition state involves the substituted hydrogen strongly bonded to both its new and its old bonding partner. It should be pointed out that deuterium KIEs much higher than 7 have been observed, and are a result of quantum mechanical tunnelling.¹¹³

The origin of isotope effects lies with the difference in zero-point vibrational energy between bonds to different isotopes. Heavier isotopes have lower zero-point energies than do their lighter counterparts. Equation 3.2 describes the vibrational energy levels of a diatomic molecule, where h is Planck's constant, ν is the frequency of the stretching vibration, and n is the vibrational quantum number ($n = 0$ for zero-point energy).

$$E = h(n + \frac{1}{2})\nu \quad \text{(Equation 3.2)}$$

If we assume that the diatomic molecule behaves as a simple harmonic oscillator, its frequency is given by Equation 3.3, where F is the force constant describing the stiffness of the bond, and μ is the reduced mass, equal to the product of the masses of the two atoms (A and B) divided by their sum (Equation 3.4).¹¹³

$$v = \frac{1}{2\pi} \left(\frac{F}{\mu} \right)^{\frac{1}{2}} \quad (\text{Equation 3.3})$$

$$\mu = \frac{m_A m_B}{m_A + m_B} \quad (\text{Equation 3.4})$$

From the above equations, it is intuitively obvious that the replacement of one of the atoms by a heavier isotope will increase μ , decrease v , and thus the energy levels will be lower (F is essentially unaffected by isotopic substitution since it depends on the nature of the A-B bond). Thus, for a reaction involving the abstraction of a hydrogen (deuterium), as in the elimination mechanism proposed for chondroitin AC lyase, a vibrational degree of freedom in the substrate is converted, at least partially, to a translational degree of freedom on passing through the transition state. If the hydrogen (deuterium) is equally bonded between the old and new bonding partners, the transition state has the same energy for the protonated and deuterated species, and thus the activation energy is necessarily higher for the deuterated substrate, which had a lower zero-point energy. In the situation where the hydrogen (deuterium) being abstracted is not equally disposed between bonding partners, the two species will not have exactly the same energy at the transition state, but will be closer in energy than at the ground state, resulting in a less than maximal KIE.

3.7.1.2 Results and Discussion

Using substrate concentrations well below K_m , the 1° deuterium KIE on k_{cat}/K_m for abstraction of the proton α to the carbonyl in compound **83** was measured to be 1.67 ± 0.07 . The data for the protio (**3**) and deutero (**83**) compounds are shown in Figure 3.10. The presence of a 1° deuterium KIE demonstrates that the C5-H5 bond is broken in a rate-limiting step, and suggests that an E1 elimination mechanism is not operating. This result, along with the flat linear free energy relationship suggests a stepwise mechanism with rate-limiting proton abstraction. This is consistent with the fact that proton transfers to and from carbon acids are usually much slower than those to and from oxygen,

nitrogen and sulfur (refer also to Figure 4.7 in Chapter 4).¹¹⁴ This slow transfer has been ascribed to the need for structural reorganization accompanying the delocalization of the negative charge, solvent reorganization, and from the poor hydrogen bonding capability of carbon acids and of the carbanionic carbon.¹¹⁵

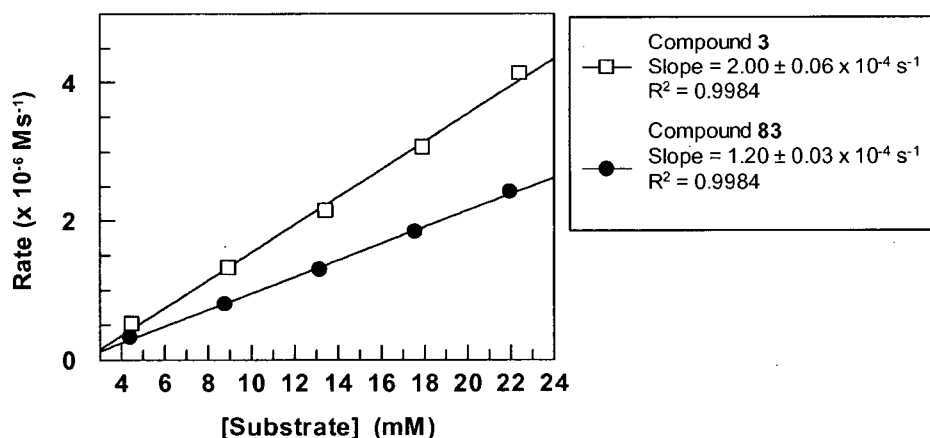


Figure 3.10. Primary deuterium KIE data. Plot of rate vs concentration for the protio (3) and deutero (83) compounds.

The Hammond postulate tells us that the transition state leading to the formation of a high energy species, such as the enolic intermediate proposed for this elimination mechanism, occurs late on the reaction coordinate and resembles the enolic intermediate. Consequently the extent of hydrogen transfer from the substrate at the transition state is large, and one might expect a KIE much less than the maximal value. This correlates nicely with the low 1° KIE observed. Thus, the conclusion made from the small 1° KIE observed is that the transition state is highly dissociated, with the C5 proton nearly completely abstracted by the catalytic base, therefore closely resembling the proposed enolic intermediate (Figure 3.11).

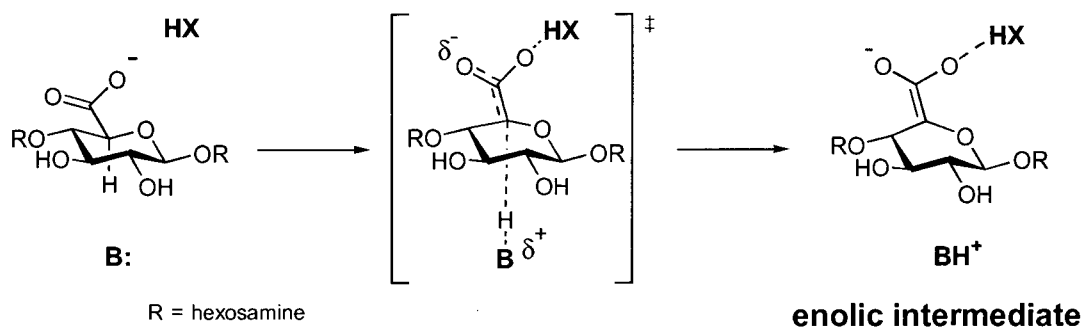


Figure 3.11. The first step of the enzyme catalyzed elimination reaction to give the enolic intermediate. The proposed transition state resembles the enolic intermediate as dictated by the nearly complete abstraction of H5 by the active site catalytic base (B:).

As noted earlier, kinetic isotope effects measured on enzymatic systems may be misleading, with product release steps being rate-limiting rather than the chemical interconversion step(s). This would be another possible explanation for the measurement of such a small 1° KIE since a less than maximal KIE may be expected if more than a single step in the catalytic sequence is rate-limiting, thereby decreasing the contribution of any single step. However, the flat linear free energy relationship observed, combined with the near unity 2° KIE (*vide infra*) strongly suggests that the elimination step is not rate-limiting. Small 1° KIEs may also arise from a non-linear arrangement of the proton donor, proton, and the proton acceptor, in the transition state for the transfer of the proton (Figure 3.12). Such an occasion is conceivable if the catalytic base residue responsible for the abstraction of the proton is the same residue responsible for delivering a proton to the leaving group. However, this requires that the reaction occur in a concerted fashion, otherwise the single residue may be involved in two separate but linearly disposed proton transfers. This is postulated to be the case with alginate lyase A1-III from *Sphingomonas* species, an enzyme that degrades a poly- β -D-mannuronic acid substrate. From the X-ray crystal structure of the enzyme complexed with a trisaccharide product, a tyrosine residue has been implicated as both the catalytic base that abstracts the C5 proton and the general acid which protonates the leaving sugar unit.¹¹⁶ However, no KIE studies have been performed, nor has any concerted mechanism been postulated for this enzyme at this time.

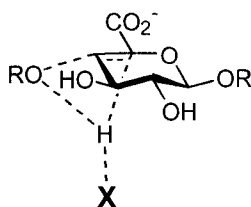


Figure 3.12. Illustration of a transition state for a concerted *syn*-elimination process where a non-linear arrangement of proton donor, proton, and proton acceptor (X) may result in a less than maximal 1° KIE.

Small 1° deuterium KIEs are not uncommon, and have been measured with other enzyme systems undergoing elimination reactions. For enolase, the 1° KIE for the abstraction of the proton α to the carbonyl group is dependent on both the pH and Mg^{2+} concentration, and ranges from ~ 1.2 to ~ 3.3 .^{117,118} The crotonase-catalyzed dehydration of 3-hydroxybutyrylpantetheine shows a 1° KIE of 1.60,³⁶ and that for *o*-succinylbenzoate synthase has been measured to be 2.7.¹¹⁹ The reaction catalyzed by UDP-*N*-acetylglucosamine 2-epimerase also shows a small 1° KIE of 1.8.¹²⁰ Although not an overall elimination process, there is strong evidence for the elimination of the UDP moiety as part of the proposed reaction mechanism. The 1° KIE for an antibody catalyzed elimination of HF adjacent to a ketone has been measured to be 2.35.¹²¹

3.7.2 Secondary Kinetic Isotope Effects

3.7.2.1 Background and Theory

Secondary KIEs occur when no bonds to the isotopically substituted atom are broken or formed during the course of the reaction. These effects are normally much smaller than 1° KIEs and occur in the range of $k_H/k_D = 0.7$ to 1.5. Secondary effects, like their primary cousins, arise from relative changes in the zero-point energies of the bonds to the isotopically substituted atoms. However, the changes in the secondary case are not the result of this bond being broken, but are due to the change in force constant in the

bond to the isotopically substituted atom at the transition state. For the sake of simplicity and its application to the present research, the following discussion will focus on the substitution of deuterium for hydrogen, but it is applicable to other isotopes. Figure 3.13 illustrates the changes in the zero-point energies of isotopically labelled compounds upon reaching the transition state for a reaction.¹²² Changes in bond strength or force constant may arise from a change in hybridization or a change in the extent of hyperconjugation. For example, if an sp^3 hybridized carbon changes to sp^2 , a hydrogen attached to this carbon will experience a decreased resistance to C-H bending. This is illustrated by the decreased frequency of C-H bending modes of alkenes compared to those in aliphatic compounds as observed in infrared spectra. In other words, the force constant decreases (case 1) and the curvature of the potential energy well is decreased, forcing the proton and deuterium energy levels closer together in the transition state.¹²² From here it is easily seen that the activation energy for the deuterated species is larger than that for the protonated species, and as a consequence the deuterated compound will have a smaller rate constant. This is referred to as a normal isotope effect where $k_H/k_D > 1$. Conversely, a change from sp^2 to sp^3 hybridization results in the force constant to increase (case 2) causing the proton and deuterium energy levels to move further apart in the transition state, and resulting in an inverse isotope effect where $k_H/k_D < 1$.

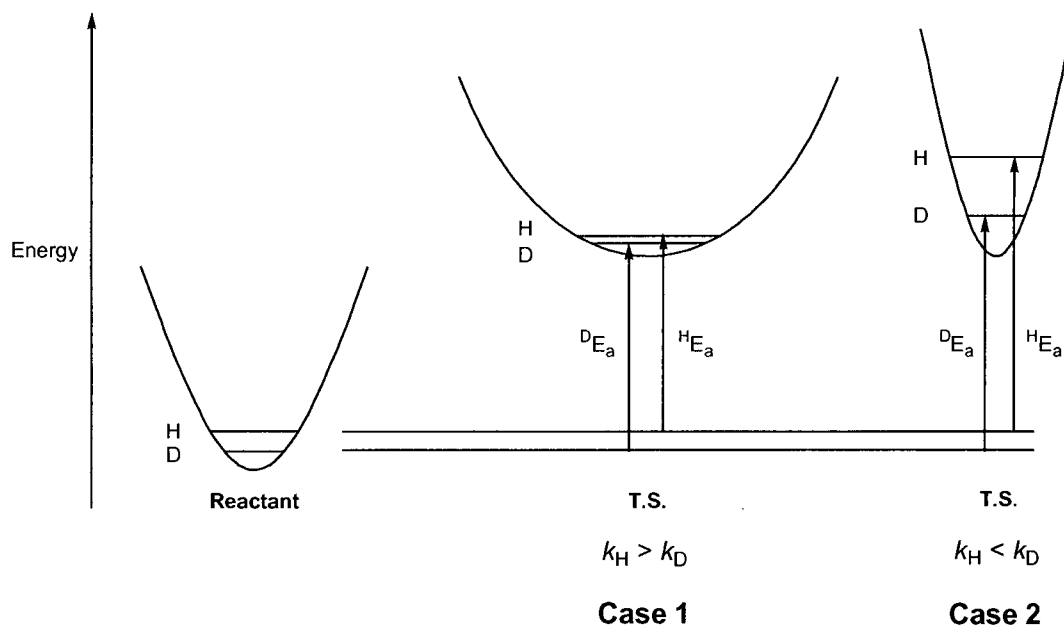


Figure 3.13. Energy profiles illustrating the changes in zero-point energy differences between hydrogen- (H) and deuterium- (D) labelled substrates upon going to the transition state (T.S.). $^{\text{D}}E_a$ and $^{\text{H}}E_a$ represent the activation energies for the deuterium- and hydrogen-labelled substrates respectively. Case 1 would give rise to a normal 2° KIE, whereas Case 2 would give an inverse 2° KIE. This Figure was adapted from ¹²².

From the above discussion it should be clear that 2° KIEs could be used to detect changes in geometry at the transition state as a reaction proceeds. This is pertinent to the present research because the substrate undergoes a change from sp^3 to sp^2 hybridization at carbons 4 and 5 as the reaction proceeds. As with 1° effects, an isotope effect will only be measured if the changes are occurring in the rate-limiting step of a multi-step reaction.

3.7.2.2 Results and Discussion

Using compound **87** with a deuterium incorporated at C4, the secondary deuterium KIE was measured to be 1.01 ± 0.03 at pH 6.8. The data for the protio (**3**) and deutero (**87**) compounds are shown in Figure 3.14. A secondary deuterium KIE value close to unity is expected if the rate-limiting step is solely the proton abstraction, hence formation of the enolic intermediate, due to the lack of sp^2 character at C4 during this

step. On the other hand, a partially rate-limiting departure of the leaving group where C4 takes on partial sp^2 character at the transition state is expected to show a secondary KIE greater than one, up to about $k_H/k_D = 1.5$ as a maximal value (as in an E2 elimination). The elimination of water by the enzymes fumarase and crotonase has been shown to involve kinetically significant departure of the leaving group with secondary kinetic isotope effects ranging from 1.13 to 1.23, illuminating the significant sp^2 character at this center.^{36,50} The low value of the 2° deuterium KIE measured for chondroitin AC lyase supports a stepwise mechanism in which the bond to the C4 leaving group is not broken in a rate-limiting step, and is consistent with the flat linear free energy relationship (*vide supra*).

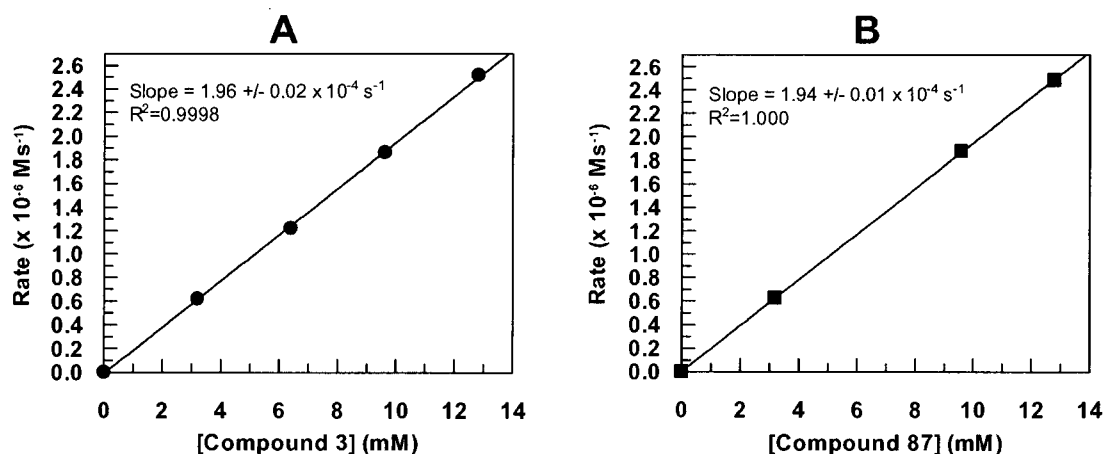


Figure 3.14. Secondary deuterium KIE data. Plots of rate vs concentration for (A) the protio compound (3), and (B) the deutero compound (87).

The absence of a significant 2° deuterium KIE in combination with the detection of a rate-limiting proton abstraction step rules out the double-displacement reaction mechanism involving the formation of a covalently bound intermediate (Figure 1.10). The second step in this reaction mechanism (elimination) cannot be rate-limiting, due to the absence of a 2° KIE since the hybridization at C4 changes from sp^3 to sp^2 in this step (assuming an E2 pathway for this *anti*-elimination). Thus, the first step (nucleophilic attack) would have to be rate-limiting. However, if the reaction were occurring through this mechanism, no 1° KIE would be observed for the abstraction of the C5 proton since

in the first step of the double-displacement mechanism there is no involvement of the C5 hydrogen in the formation of the covalent intermediate. It should be noted that this reaction mechanism might be more complicated than just described. The second step of the covalent intermediate reaction scheme could conceivably be composed of two separate steps and occur via an E1cb-like mechanism in which proton abstraction is rate-limiting. In this case a 1° KIE may be expected if the proton abstraction is at least partially rate-limiting in conjunction with the nucleophilic step (the proton abstraction step may also be completely rate-limiting). However, the C5 proton and the leaving group are arranged in an anti-periplanar arrangement, thus the elimination is expected to occur via an E2 mechanism.

Research on *cis,cis*-muconate cycloisomerase, an enzyme that catalyzes the interconversion of (+)-muconolactone and *cis,cis*-muconate, has found similar results to those presented here for chondroitin AC lyase (Figure 3.15).⁵¹ For the formation of *cis,cis*-muconate (*syn*-elimination), the 2° deuterium KIE was measured to be unity, and the 1° deuterium KIE was measured to be ~ 2.3. This strongly suggests a similar stepwise mechanism in which proton abstraction to form a carbanion intermediate is solely rate-limiting.

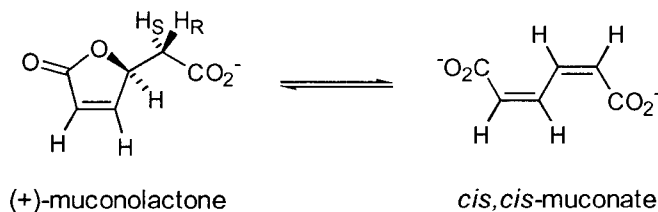


Figure 3.15. The interconversion of (+)-muconolactone and *cis,cis*-muconate by *cis,cis*-muconate cycloisomerase. Note, it is only the *pro-R* hydrogen that is abstracted, and is a *syn*-elimination in the forward direction.

The synthesis of 100% isotopically labelled compounds is not always possible in practice. There are a couple of approaches that may be taken to correct for this, depending on the situation. If the amount of ‘contaminating’ unlabelled material is small, and the isotope effect is large, most of the unlabelled material will be consumed early in

the reaction. Thus, data points taken later during the reaction will represent the ‘pure’ labelled material. A mathematical approach may also be used to correct results obtained with partially deuterated reactants so as to obtain the isotope effect that would be observed with isotopically pure material. This was the approach used in the present research, as the enzymatic reaction is quite slow, and the 2° KIE was expected to be very low. From the ^1H NMR spectrum of the labelled substrate (**87**), the amount of unlabelled compound was calculated to be 10.9%. Equation 3.5 was used to correct for this unlabelled substrate, where k_{obs} is the measured rate for the labelled substrate, k_{H} is the rate for the unlabelled substrate, N_{H} is the mole fraction of unlabelled material, and k_{D} is the true isotope effect.¹¹³ Due to the low value of the isotope effect, employing Equation 3.5 only increased the value of the isotope effect by 0.08% over that of the uncorrected value.

$$k_{\text{D}} = \frac{k_{\text{obs}} - k_{\text{H}}N_{\text{H}}}{1 - N_{\text{H}}} \quad (\text{Equation 3.5})$$

3.8 Deuterium Exchange

3.8.1 Results and Discussion

The deuterium exchange experiment, performed in D_2O buffer, attempts to observe the incorporation of deuterium at C5 of the substrate while it is in the active site of the enzyme. The incorporation of deuterium by the enzyme, or lack thereof, may provide some insight into the nature of the catalytic mechanism. The concept is that if the proton abstraction step is much faster than the elimination step, then the return of a proton (or deuterium) to this position may also be faster than the elimination. If so, the ‘wash in’ of deuterium at this position from the D_2O solvent may be observable.

The enzyme and substrate (**4**) were dissolved in a buffered D_2O solution and the reaction progress was monitored through ^1H NMR. Figure 3.16 shows a stacked plot of the partial ^1H NMR spectra, illustrating the course of the enzymatic reaction from starting material to product.

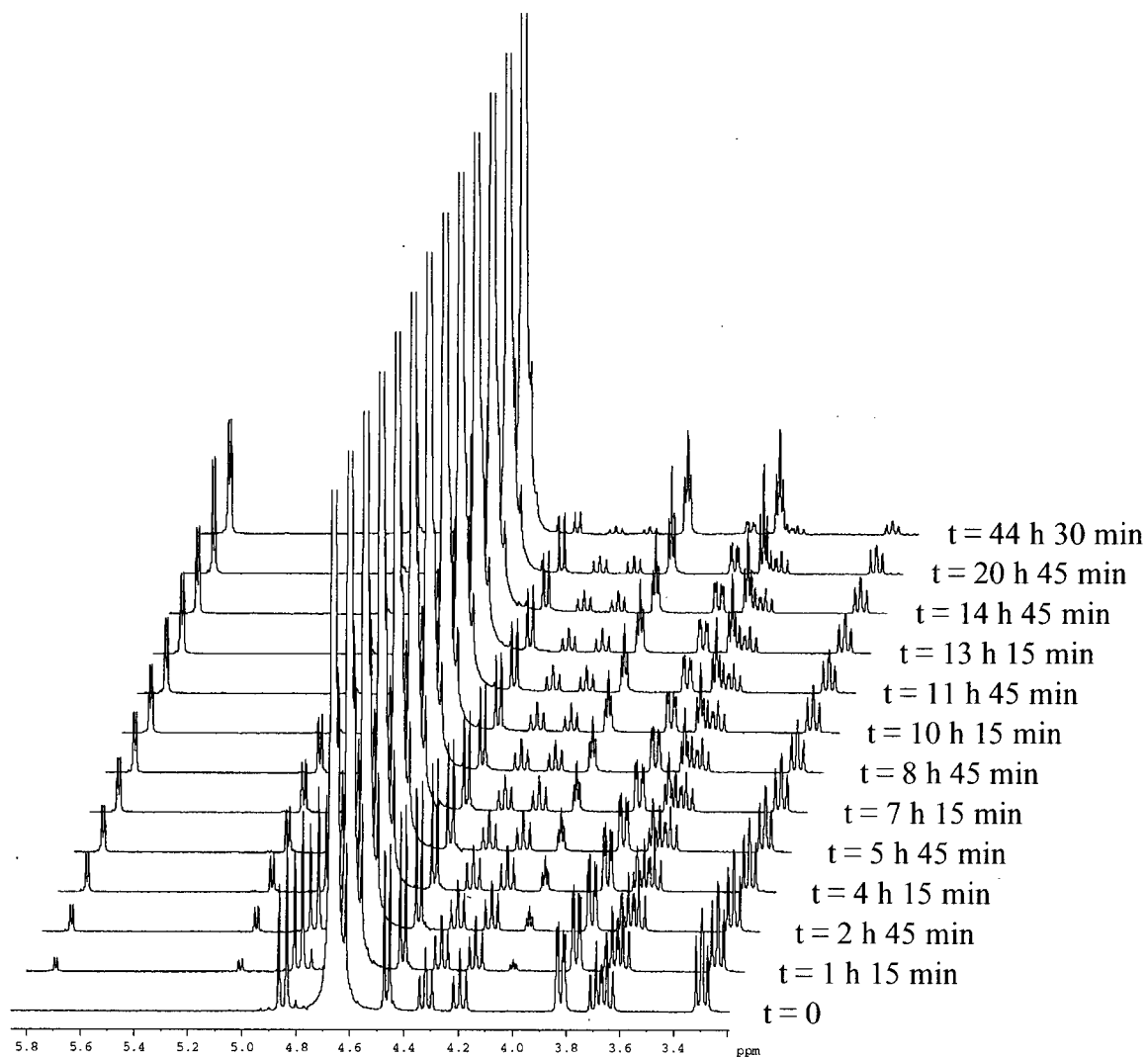


Figure 3.16. Stacked plot of the partial ¹H NMR spectra of compound **4** as it is converted to product by chondroitin AC lyase. For peak identities, refer to Figure 3.17.

The KIE and linear free energy analyses have shown that the initial proton abstraction step is rate limiting, while the elimination step is not. From these results we would not expect to see any deuterium incorporation into the starting material. Indeed, no deuterium exchange at C5 was observed before the elimination of the C4 substituent. This is illustrated in Figure 3.17, which shows the partial ^1H NMR spectra of the monosaccharide substrate (**4**) (Figure 3.17A) and that of the substrate and product mixture after partial conversion by chondroitin AC lyase (Figure 3.17B) in D_2O . If deuterium exchange at C5 occurred faster than the elimination of the 4-fluoro group (and in a reversible manner), then the integration of H5 of the starting material would decrease relative to that of H1, H2, and H3. However, this is clearly not the case as shown by the integrations in Figure 3.17. This is consistent with a mechanism that involves the swift elimination of the C4 substituent after a rate-limiting proton abstraction. However, this experiment does not constitute proof that exchange of this C5 proton is not occurring since enzyme active sites have long been proposed to be sequestered from bulk solvent, and thus the residues located there may not be accessible to the D_2O solvent as required for deuterium exchange.

Other enzymes, such as enolase, show rapid exchange of the proton α to the carbonyl group with solvent, and are believed to use a stepwise mechanism in which proton abstraction and leaving group departure are both rate-limiting.¹¹⁸ On the other hand the crotonase-catalyzed β -elimination, which is thought to be concerted, shows almost no deuterium exchange ($\leq 3\%$).³⁶

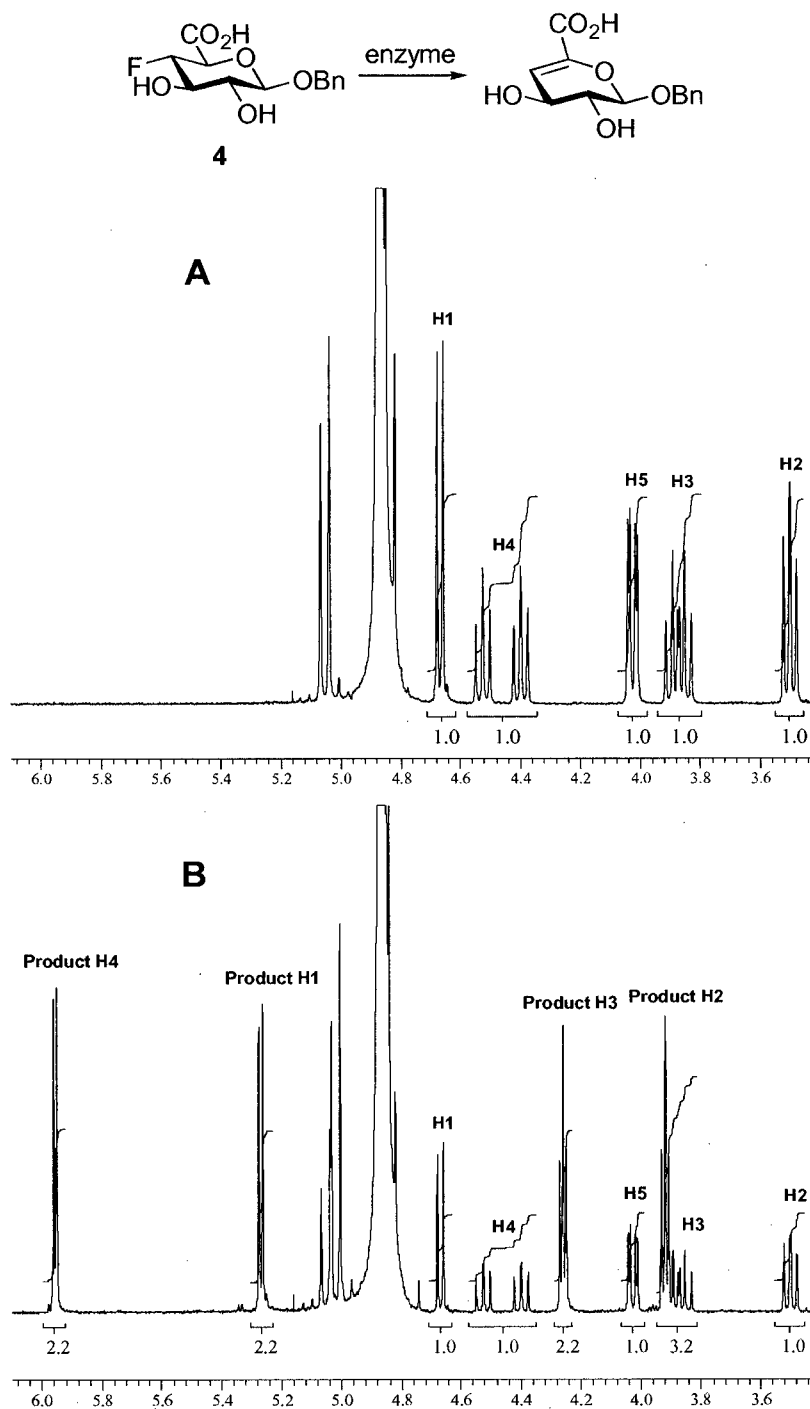


Figure 3.17. Deuterium exchange experiment. Partial ^1H NMR spectra of (A) the monosaccharide substrate (**4**), and (B) its partial enzymatic digestion to product by chondroitin AC lyase in D_2O . The large peak in the centre is H_2O , and is flanked by the doublets of the methylene hydrogens of the benzyl group. Integrations are shown beneath the peaks.

3.8.2 Mechanistic Classification

The definition of an E1cb reaction as generally accepted in the scientific community is formally one that involves the formation of a kinetically significant intermediate, and for which solvent deuterium exchange successfully competes with departure of the leaving group (ie. leaving group departure is rate-limiting).⁷² Thus, the mechanism of chondroitin AC lyase, as well as other enzymes such as *cis,cis*-muconate cycloisomerase (Figure 3.15), cannot be described by the simple E1cb scheme that has generally been proposed. More correctly, the mechanism is a subset of the E1cb class and can be referred to as (E1cb)_I or (E1cb)_{irr}.¹²³ The subscripts refer to the fact that the proton abstraction is essentially irreversible, and that deuterium exchange does not compete with the departure of the leaving group. What is normally referred to as an E1cb reaction is more correctly termed (E1cb)_R, in which proton abstraction is fast and reversible, with rate-limiting departure of the leaving group. Alternatively, another type of E1cb mechanism exists that is termed (E1)_{anion}, which is characterized by a fast yet essentially irreversible proton abstraction followed by a rate-limiting elimination step (ie. the formation of a stable carbanion).

3.9 Conclusions

The development of a variety of synthetic substrates along with convenient assay techniques has allowed an assortment of enzymological and mechanistic studies to be performed with chondroitin AC lyase. Taken together, these paint a detailed portrait of the steps involved in this elimination mechanism, and illuminates the nature and structure of the transition states involved.

By altering the aglycone moiety of the fluoride-releasing substrates it was found that the enzyme has a significant preference for substrates with aromatic appendages. This is not surprising from the three-dimensional structure, which shows many aromatic amino acids at the active site that may form favourable hydrophobic interactions with the aromatic ligands of the synthetic substrates. The position of the aromatic aglycone with respect to the glucuronic acid sugar ring also seems to be important, with the benzyl-

containing substrate binding much tighter than the 'shorter' phenyl-containing substrate. Despite the increased binding observed for a disaccharide substrate, the overall catalytic efficiency was lower than that of the monosaccharide substrates. Thus the more involved synthesis of the disaccharide molecules is not warranted for the development of simple substrates for the study of this polysaccharide lyase. The structurally-confined architecture of the active site was demonstrated by the incompetent 'substrates' with an axially-disposed fluorine at C4. Despite the small size difference between hydrogen and fluorine atoms and the anti-periplanar arrangement of the α -proton and fluorine atom, these molecules were not degraded by the enzyme. However, these competitive inhibitors may prove useful in conjunction with X-ray crystallographic studies in order to clearly establish the identity of the catalytic residues of chondroitin AC lyase. Samples of compounds **52** and **58** have been sent to our collaborators, who have solved the three-dimensional structure of this enzyme, in the hope of obtaining a structure of a complex. However, at the time of writing no results have been obtained.

Chondroitin AC lyase was found to be most active at pH 6.8 when acting on the natural substrate chondroitin 6-sulfate, and at pH 6 with the synthetic substrate **4**. The bell-shaped pH profiles imply the presence of two catalytically essential residues having pK_a values of ~ 5.3 and ~ 7.9 . These may represent the catalytic base and acid residues respectively in the enzyme active site, which, based on the three dimensional structure and site-directed mutagenesis studies have been proposed to be histidine and tyrosine. A remarkable dependence of K_m on a change in pH was observed for the natural polymeric substrate, with a much smaller effect observed on a synthetic monosaccharide substrate. The pH profiles also showed that the enzyme activity was sufficient at pH 8 to allow the use of the fluorescent assay with compound **2**, which requires a pH of at least 8 to ensure efficient fluorescence of the released 4-methylumbelliferone group.

The linear free energy analysis has provided substantial clues to the mechanism of chondroitin AC lyase. The flat linear free energy relationship produced by using substrates with leaving groups of differing nucleofugalities showed that there is no charge development on the C4 oxygen at the transition state of the rate-limiting step, and strongly suggests a step-wise mechanism in which the elimination step is not rate limiting. This conclusion was further solidified by the measurement of a near unity 2°

deuterium KIE. This showed that there was no change in the sp^3 hybridization at C4 during the rate-limiting step, indicating that the C4-leaving group bond is not broken during a rate-limiting step, and ruling out a concerted *syn*-elimination mechanism.

The measurement of a 1° deuterium KIE of 1.67 ± 0.07 illustrates that the reaction mechanism involves the rate-limiting abstraction of the α -proton to form a high energy enolic intermediate via a transition state where the C5 proton is nearly fully abstracted by the active site base.

Chapter 4 – Potential Inhibitors of Chondroitin AC Lyase

4.1 Background

The development of enzyme inhibitors has long been a staple of the investigation into enzyme functions and mechanisms. As one of the most important diagnostic tools of the enzymologist, inhibition studies often reveal the chemical and physical architecture of the active site and impart clues to the mechanism of the enzymatic reaction. A massive amount of time and effort is spent each year in the discovery and development of new and/or better enzyme inhibitors that may be useful as drug candidates, or as potential toxins and poisons to kill off undesired pests. With the advent of X-ray crystallography came about a real drive to crystallize some of nature's largest and most complex molecules, the enzymes. Since hen egg white lysozyme (HEWL), the first enzyme to have its tertiary structure solved using X-ray diffraction methods,¹²⁴ an enormous number of structures have been solved, often with inhibitors bound at the active site(s). Interestingly, the use of enzyme inhibitors can also often aid in the crystallization of enzymes that are difficult to crystallise on their own. The structures of enzyme-inhibitor complexes can reveal the catalytic machinery responsible for the enzyme's amazing rate acceleration, providing important information to the enzymologist as well as to the synthetic organic chemist looking for drug candidates.

The development of tight binding inhibitors for chondroitin AC lyase would be extremely helpful in conjunction with three-dimensional structural studies, facilitating the identification of key residues involved in binding and catalysis. At the present time there are no known specific inhibitors of polysaccharide lyase enzymes. Inhibitors of these lyase enzymes have potential as antibiotics since these enzymes are only known to be present in bacterial sources, not in mammalian cells. The mammalian enzymes degrade glycosaminoglycans via a well-studied hydrolytic mechanism, and can either be inverting or retaining glycosidases.

The proposed mechanism of chondroitin AC lyase (Figure 1.9) involves several key catalytic acid and base residues at the enzyme active site. The first step is the

neutralisation of the negative charge of the carboxylate anion of the glucuronic acid moiety by an amino acid residue (positively charged or neutral). In many polysaccharide lyases, this function is performed by a divalent metal ion such as calcium; however, the calcium ion in chondroitinase AC is not located in the active site and thus cannot perform this role. This charge neutralisation is a key feature of the lyase mechanism and plays a part in lowering the pK_a of the adjacent H5 proton sufficiently enough to be abstracted by an active site general base catalyst ($pK_a \sim 7$). The leaving group for this elimination reaction is a sugar unit, and thus requires the assistance of a general acid catalyst to protonate the departing C4 oxygen atom. Additional ambiguity concerning the catalytic machinery of chondroitin AC lyase is introduced by the identity of this acid catalyst. With the elimination following the *syn* stereochemical course, it is not difficult to imagine how the conjugate acid form of the catalytic base residue (now protonated after abstracting the C5 hydrogen) could serve as the acid catalyst. Both the C5 proton and the departing C4 oxygen atom are on the same side of the sugar ring plane. Conversely, the acid and base residues may be two separate amino acids (Figure 4.1).

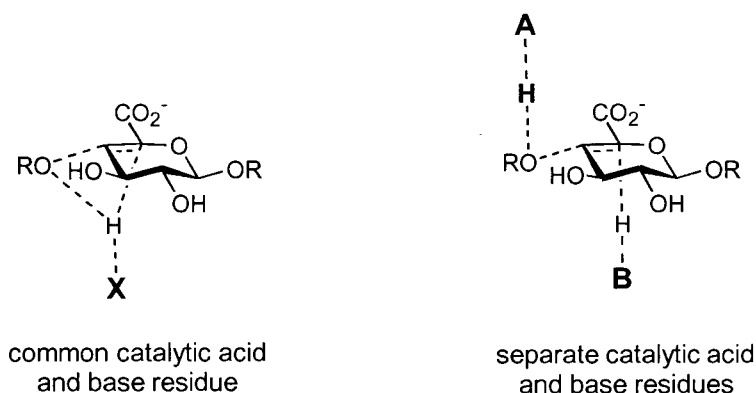


Figure 4.1. Schematic showing how the catalytic acid and base could be one common or two separate amino acid residues. Note: a concerted elimination process is depicted for simplicity and the proton abstraction and donation steps may be two separate events. R = hexosamine.

The identity of the catalytic residues remains elusive despite site directed mutagenesis studies and the high resolution X-ray crystal structures of the free enzyme^{38,41} and various enzyme-oligosaccharide complexes.⁴⁰ Unfortunately many of

these structures have been solved with dermatan sulfate polysaccharides that possess the iduronic acid moiety (C5 epimer of glucuronic acid), thus making identification of catalytic base and charge neutralization residues extremely difficult. Potential candidate amino acid residues responsible for the neutralisation or dispersion of the negative charge on the carboxylate are arginine,⁴⁰ or asparagine as suggested by a very similar active-site architecture with a hyaluronate lyase.^{42,43} The active site architectures of the two enzymes are completely preserved and clearly indicate a common catalytic mechanism. A histidine residue in chondroitin AC lyase has been implicated as the catalytic base responsible for abstracting the relatively acidic H5 proton of the glucuronic acid moiety. The variety of amino acids named as potential base catalysts in various polysaccharide lyases is quite large and diverse. Apart from histidine,^{40,43,125} candidates such as tyrosine,¹¹⁶ glutamate, arginine,¹²⁶ and cysteine^{127,128} have been named. The most likely candidate for the general acid catalyst in chondroitin AC lyase is tyrosine, as has been implicated in a number of other polysaccharide lyases.^{42,43,116,125,129} Although structural and mutagenesis studies have been performed with chondroitin AC lyase, the identity of the key catalytic amino acids is certainly not iron-clad, with different research groups forming different conclusions. Thus, the development of tight binding inhibitors may solve this ambiguity.

4.2 Inhibitor Design

Transition state theory⁷⁶ predicts that an enzyme should bind the transition state several orders of magnitude more strongly than the ground state via protein-substrate interactions that are optimized only at the transition state. The short-lived nature of the transition state with partially formed and/or broken bonds presents an insurmountable barrier to the synthetic organic chemist who cannot recreate perfectly these non-equilibrium bond lengths with stable compounds. Thus, the design of transition state analogues as enzyme inhibitors takes advantage of the differences in electronic and geometric characteristics of the ground and transition states in order to capture a fraction of the immense binding energy for the transition state species. In fact, an ideal transition

state analogue should bind to the enzyme more tightly than it does to the ground state species by a factor equal to the ratios of the rate constants for the enzyme-catalyzed and uncatalyzed reaction.^{76,130} However, transition state similarity is not necessary for the tight-binding inhibition of enzymes. A variety of favourable interactions such as hydrogen, ionic, or hydrophobic bonds between an enzyme and substrate may lead to tight-binding inhibition. Perhaps one of the best examples of fortuitous binding is that of methotrexate, an inhibitor of dihydrofolate reductase with $K_i = 0.15$ pM, which is bound upside down with respect to substrate in the catalytic site.^{131,132} Experimental approaches to determine whether or not a tight-binding inhibitor is actually a transition state analogue have been developed, but are beyond the scope of this thesis.^{76,133}

Two separate concepts for inhibitor design were explored, based upon mimics of reaction intermediates or transition states. The formation of the proposed *aci*-carboxylate intermediate yields sp^2 hybridisation at C5 of the uronic acid moiety. The potential inhibitor **88** (Figure 4.2) attempts to take advantage of this tetrahedral sp^3 to planar sp^2 transformation that takes place between substrate and intermediate and/or product. Compound **88** cannot be cleaved by the enzyme due to the lack of a proton at C5, satisfies the trigonal geometric requirements of the carbanion intermediate and/or transition state, and contains the hexosamine 'leaving group' sugar moiety from which it can derive binding interactions.

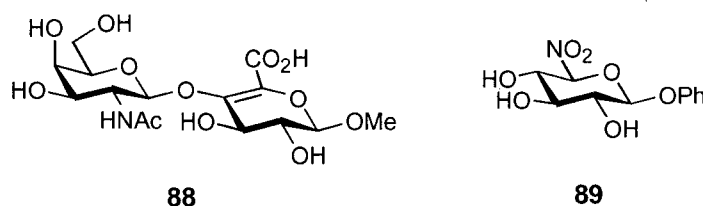


Figure 4.2. The proposed inhibitors of chondroitin AC lyase.

The second approach to an inhibitor was the synthesis of the novel 5-nitro sugar **89** (Figure 4.2). This design was based on the remarkable stability of the anion formed by the loss of a proton from the carbon acid (C5) adjacent to a nitro group. It was hoped that the anion of **89** would mimic the anionic transition state and thus bind tightly to the

enzyme. The nitronate anion thus formed is a mimic of the *aci*-carboxylate anion due to the fact that sp^2 hybridization of C5 has already occurred as a result of the delocalization of electrons from the carbanion to the oxygens of the nitro group (Figure 4.3). Nitro analogs of the substrates of several non-carbohydrate lyases¹³⁴⁻¹³⁷ have been shown to bind more tightly to these enzymes than do the corresponding substrates, acting as potent inhibitors. Invariably, it has been found that the inhibitory species was the ionized form of these nitroalkanes (pK_a values from 9 to 11).

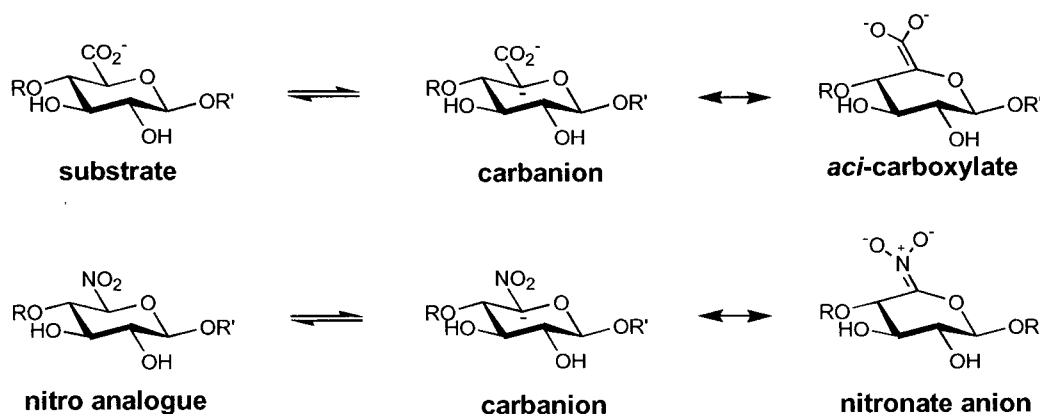


Figure 4.3. Schematic showing show a nitro group mimics a carboxyl group.

The anions of the nitro analogues of the substrates for fumarase,¹³⁵ aspartase,¹³⁵ aconitase,¹³⁶ and enolase¹³⁴ show inhibition constants in the low nanomolar range (Figure 4.4). The substrates for these enzymes are small molecules, and thus the nitro analogue contains all the same structural moieties as the parent substrate (minus the carboxylate). This allows the anionic nitro analogues to mimic the transition state or reaction intermediate ideally. However, chondroitin AC lyase degrades a large polysaccharide that makes many contacts in the binding pocket and active site of the enzyme. The potential inhibitor target is only a monosaccharide, and therefore would not be expected to bind as tightly as do the analogues of the other enzyme substrates. Nonetheless, compound **89** is hoped to bind reasonably tightly and therefore provide insight into the reaction mechanism as well as provide the opportunity for further three dimensional structural analyses of enzyme-inhibitor complexes.

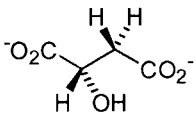
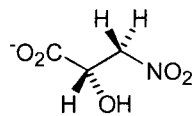
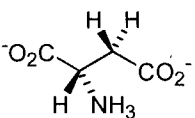
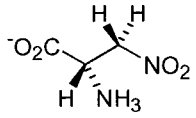
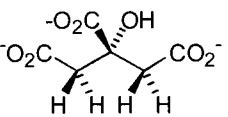
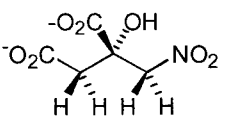
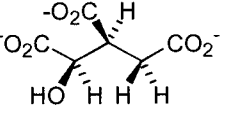
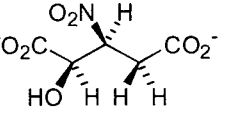
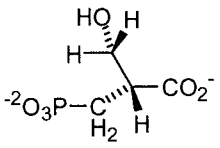
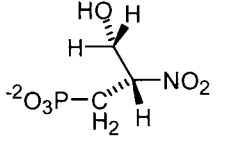
	Substrate	Nitro Analogue
fumarase	 L-malate	
aspartase	 L-aspartate	
aconitase	 citrate	
	 isocitrate	
enolase	 methylene-phosphoglycerate	 (3-hydroxy-2-nitropropyl)phosphonate

Figure 4.4. The substrates and their nitro analogues for several non-carbohydrate lyases. Note: the normal substrate for enolase is 2-phosphoglycerate, however, the nitro analogue of this would be an unstable α -nitrophosphate.¹³⁴

An interesting and somewhat perplexing phenomenon exists with carbon acids. Proton transfers to and from carbon acids are usually much slower than those to and from oxygen, nitrogen and sulfur.¹¹⁴ This results from the need for structural reorganization accompanying the delocalization of the negative charge, from solvent reorganization, and

from the poor hydrogen bonding capability of carbon acids and of the carbanionic carbon.¹¹⁵ This remarkable phenomenon allows the use of a preformed nitronate carbanion in initial steady state velocity measurements without significant interference from the conjugate carbon acid.

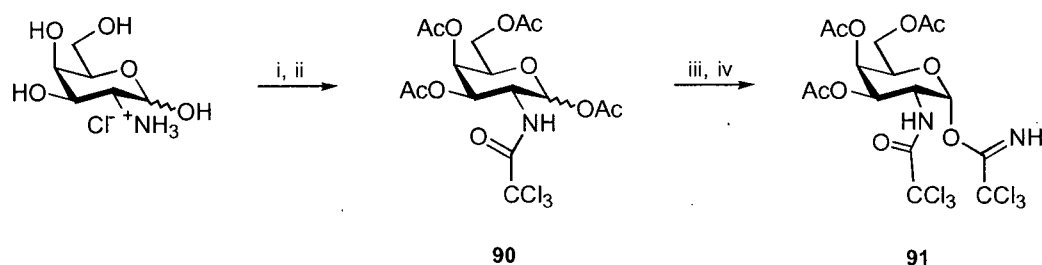
4.3 Synthesis

4.3.1 Synthesis of the Disaccharide Inhibitor.

Methyl O-(2-acetamido-2-deoxy- β -D-galactopyranosyl)-(1 \rightarrow 4)- α -L-threo-hex-4-enopyranoside, 88 (Schemes 4.1, 4.2, and 4.3).

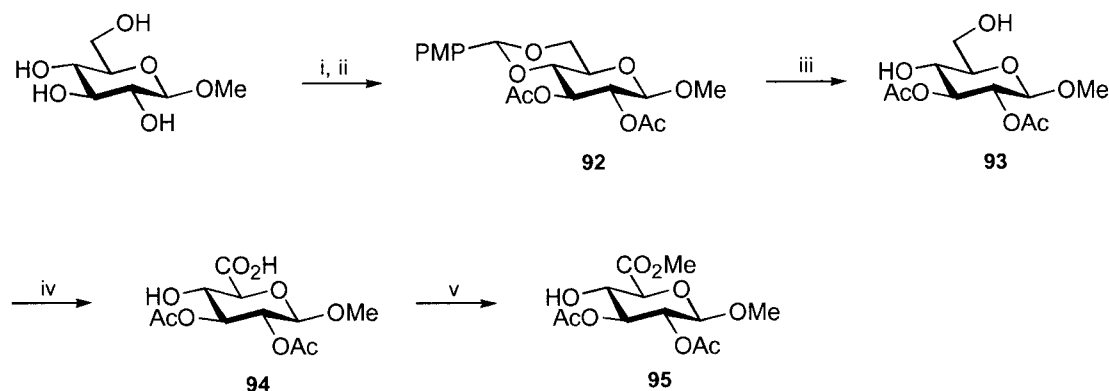
An expedient route to the disaccharide scaffold of the desired inhibitor was attempted using the β -N-acetylhexosaminidase from *Aspergillus oryzae*. Enzymatic syntheses were attempted using 4-nitrophenyl 2-acetamido-2-deoxy- β -D-galactopyranoside as the donor and either methyl β -D-glucopyranosiduronic acid or the corresponding methyl ester, methyl (methyl β -D-glucopyranosid)uronate, as acceptors. Unfortunately no reaction took place, as judged by TLC. There have been several literature reports that outline the synthetic applications of this enzyme to build disaccharide and trisaccharide molecules with a variety of acceptors.¹³⁸⁻¹⁴⁰ As a control, methyl β -D-glucopyranoside was used as a donor and the TLC indicated that a reaction had indeed taken place as described in the literature, indicating that the enzyme was in fact active and that the enzyme would simply not accept the C6-oxidized sugars as acceptors. Thus, the synthesis of the desired disaccharide inhibitor was achieved through purely chemical methods.

The synthesis of the donor is outlined in Scheme 4.1. The trichloroacetimidate donor methodology was chosen due to the facile synthesis of the desired donor and for the good yields of their subsequent glycosylation reactions.



Scheme 4.1. Synthesis of 3,4,6-tri-*O*-acetyl-2-deoxy-2-trichloroacetamido- α -D-galactopyranosyl trichloroacetimidate (**91**), the donor molecule of the disaccharide inhibitor. (i) trichloroacetyl chloride, NaHCO₃, H₂O; (ii) Ac₂O, pyridine; (iii) hydrazine acetate, DMF; (iv) trichloroacetonitrile, DBU, CH₂Cl₂.

Commercially available D-galactosamine hydrochloride was first selectively *N*-trichloroacetylated with trichloroacetyl chloride in aqueous NaHCO₃, followed by the acetylation of the hydroxyl groups to give **90**¹⁴¹ (32%) (Scheme 4.1). Hydrazine acetate then was employed to selectively deprotect the anomeric center, after which a trichloroacetimidate functionality was installed with trichloroacetonitrile and 1,8-diazabicyclo[5.4.0]undec-7-ene (DBU), to give the desired donor **91** (57%).

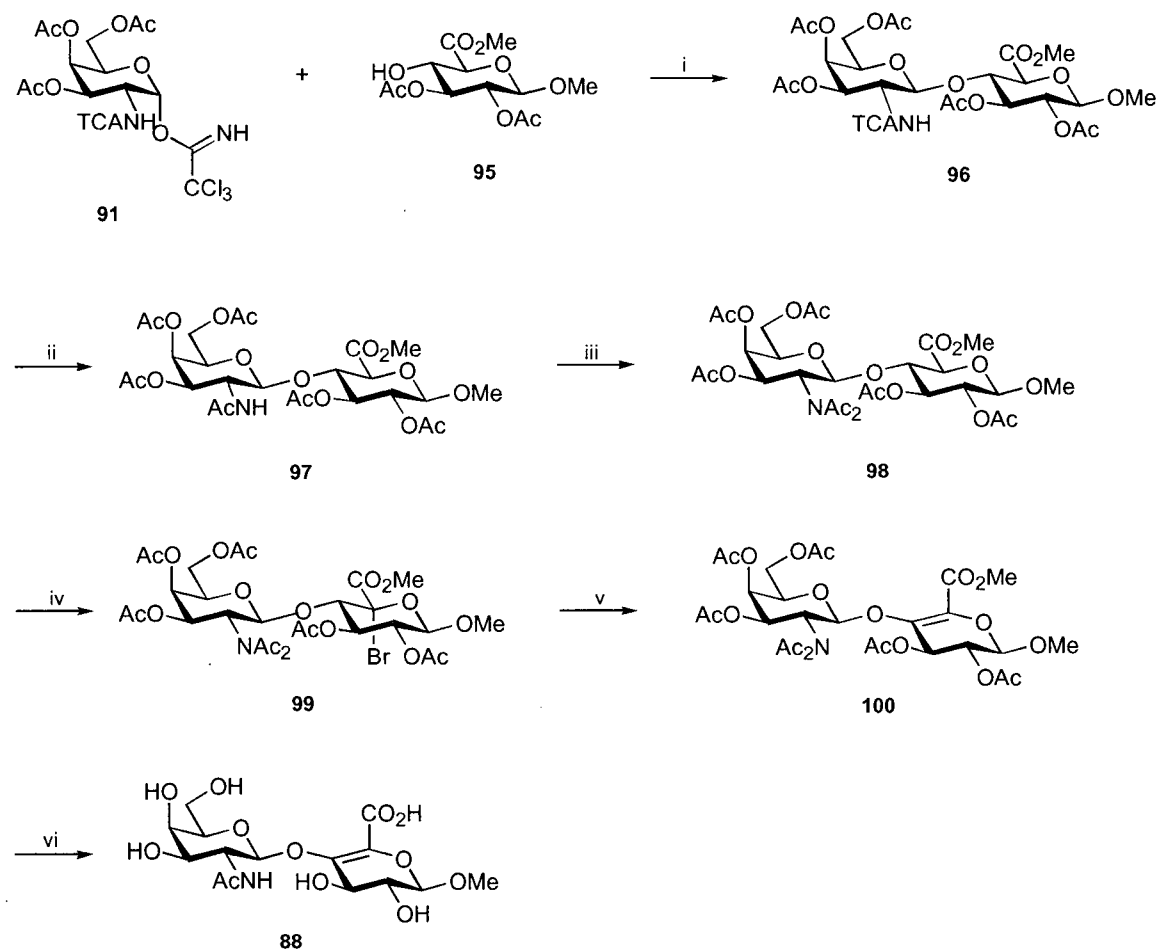


Scheme 4.2. Synthesis of methyl (methyl 2,3-di-*O*-acetyl- β -D-glucopyranosid)uronate (**95**), the acceptor molecule for the disaccharide inhibitor. (i) *p*-anisaldehyde dimethyl acetal, *p*-TsOH, DMF, 50 °C; (ii) Ac₂O, pyridine; (iii) I₂, MeOH, reflux; (iv) TEMPO, NaOCl, NaBr, TBAB, NaHCO₃(aq), EtOAc, 0 °C; (v) H⁺ resin, MeOH.

The acceptor **95** was prepared in five steps as follows (Scheme 4.2). Commercially available methyl β -D-glucopyranoside was reacted with *p*-anisaldehyde dimethyl acetal and catalytic *p*-toluenesulfonic acid in DMF at 50 °C under aspirator pressure¹⁴² and the resulting crude material was treated with pyridine and acetic anhydride to give **92** as a white crystalline solid (80%). The *p*-methoxybenzylidene protecting group was removed using a 1% (w/v) solution of iodine in methanol at reflux¹⁴³ to afford **93**¹⁴⁴ (87%). Selective oxidation of the primary hydroxyl group was accomplished using 2,2,6,6-tetramethyl-1-piperidinyloxy (TEMPO) and NaOCl under phase transfer conditions with tetrabutylammonium bromide (TBAB) in NaHCO₃(aq) and EtOAc.⁸⁹ Formation of the methyl ester using acidic ion exchange resin in methanol yielded the acceptor **95** (25% from **93**). The low yield of the final step was due to the partial deprotection of the acetates under the acidic conditions employed.

Glycosylation of the acceptor, **95**, with the donor, **91**, was accomplished using a catalytic amount of trimethylsilyl triflate (TMSOTf) in 1,2-dichloroethane at 0 °C, affording the disaccharide **96** as a white foam (78%) (Scheme 4.3). The ¹H NMR spectrum of **96** showed a doublet with a coupling constant of 8.4 Hz for the anomeric proton of the hexosamine sugar (H1'), confirming that the newly formed linkage was of the β -configuration. Conversion of the *N*-trichloroacetate to an *N*-acetate was effected by treating **96** with tributyltin hydride (TBTH) and 2,2'-azobisisobutyronitrile (AIBN) in refluxing benzene¹⁴⁵ to give **97** as a white crystalline solid (78%). Since the next key step involved a radical bromination, which is not compatible with an acetamide, it was necessary to introduce a second acetyl group onto the nitrogen. This second acetate group was easily established onto the nitrogen centre by treating **97** with isopropenyl acetate and catalytic *p*-toluenesulfonic acid¹⁴⁶ at 65 °C to afford the *N,N*-diacetate compound **98** (98%). Directed by the adjacent carbonyl functionality, bromination¹⁴⁷ at C5 of the glucopyranosiduronate moiety using NBS and light in refluxing CCl₄ proceeded smoothly to give **99** as a colourless foam (64%). The alkene functionality was then introduced by the elimination of HBr with DBU in DMF¹⁴⁸ to afford **100** as a white foam (75%). Global deprotection of **100** using NaOH in 5:1 MeOH:H₂O¹⁴⁹ afforded the desired methyl *O*-(2-acetamido-2-deoxy- β -D-galactopyranosyl)-(1 \rightarrow 4)- α -L-threo-hex-4-

enopyranoside **88** (48%). Purification of **88** proved to be somewhat problematic and thus lowered the isolated yield; successive separations by silica gel and size exclusion chromatography (Sephadex G-10) were necessary to obtain a pure product.

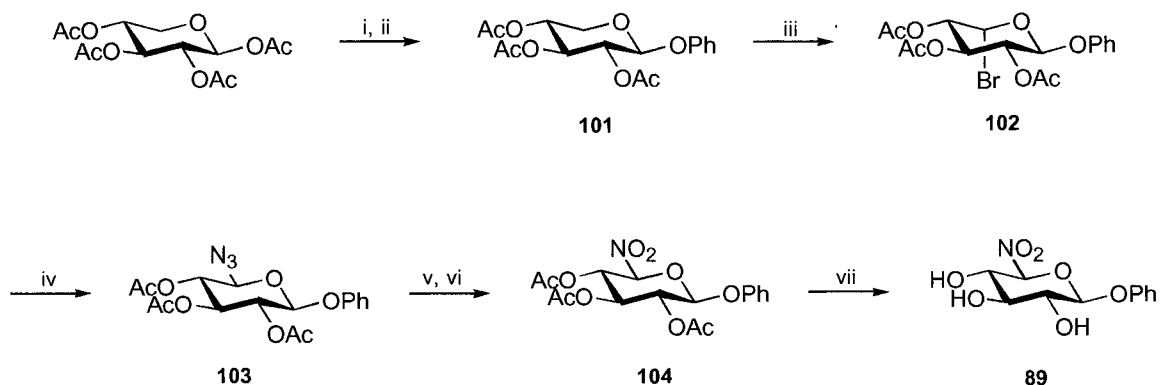


Scheme 4.3. Synthesis of methyl *O*-(2-acetamido-2-deoxy- β -D-galactopyranosyl)-(1 \rightarrow 4)- α -L-threo-hex-4-enopyranoside (**88**), the disaccharide inhibitor. (i) TMSOTf, 1,2-dichloroethane, 0 °C; (ii) TBTH, AIBN, benzene, reflux; (iii) p-TsOH, isopropenyl acetate, 65 °C; (iv) NBS, CCl₄, light, reflux; (v) DBU, DMF; (vi) NaOH, MeOH/H₂O.

4.3.2 Synthesis of the 5-Nitro Inhibitor

Phenyl (5*S*)-5-nitro- β -D-xylopyranoside, **89** (Scheme 4.4).

The synthesis of the novel 5-nitro sugar, **89**, is illustrated in Scheme 4.4 below.



Scheme 4.4. Synthesis of phenyl (5*S*)-5-nitro- β -D-xylopyranoside (**89**). (i) HBr/AcOH; (ii) PhOH, TBAHS, 1 M NaOH, CH₂Cl₂; (iii) NBS, CCl₄, light, reflux; (iv) NaN₃, DMF; (v) PtO₂, H₂, EtOAc/EtOH; (vi) DMDO, acetone; (vii) AcCl, MeOH.

Phenyl 2,3,4-tri-O-acetyl- β -D-xylopyranoside (**101**)¹⁵⁰ was prepared from 1,2,3,4-tetra-O-acetyl- β -D-xylopyranose by first making the α -bromide with HBr/AcOH, followed by glycosylation using phase transfer catalysis with phenol and tetrabutylammonium sulfate (TBAHS) in a vigorously stirred mixture of 1 M NaOH and CH₂Cl₂ (42%) (Scheme 4.4). Bromination¹⁵¹ at C5 using NBS and light in refluxing CCl₄ gave **102** as a pale yellow solid (25%). A coupling constant of 4.0 Hz was measured for the H4-H5 protons, indicating that the bromine was in the axial orientation. Extended reaction times not only resulted in bromination of one or more of the acetate groups, but also gave a *p*-bromophenyl derivative that was extremely difficult to separate from the desired compound. The first attempt at introducing a nitro functionality at C5 was the direct S_N2 displacement of the 5-bromine with NaNO₂ in DMF, both with and without

phloroglucinol. Phloroglucinol is an effective scavenger of nitrite esters that may react with aliphatic nitro compounds and reduce the yield of these desired compounds.¹⁵² Unfortunately this transformation did not produce any 5-nitro product. However, S_N2 displacement of the bromide with sodium azide in DMF¹⁵¹ was successful in giving the product of inverted stereochemistry, **103**, as a crystalline solid (45%). The ¹H NMR spectrum of **103** showed the expected upfield shift of H5 relative to that in **102**, and the H4-H5 coupling constant was measured to be 7.6 Hz, as compared to 4.0 Hz for **102**, indicating the equatorial stereochemistry of the C5-azido group. The transformation of the azide into the nitro functionality was accomplished via the reduction of the azide with hydrogen over Adam's catalyst (PtO₂) in ethanol/EtOAc, followed by the immediate oxidation with a freshly prepared solution of dimethyldioxirane (DMDO)¹⁵³ in acetone to afford the crystalline 5-nitro compound **104** (42%). The oxidation with DMDO was performed without purification of the intermediate amine to avoid epimerisation and hydrolysis of this newly formed glycosylamine. Other methods were investigated to perform the azide to nitro transformation, with little success. The reaction of the azide with tri-*n*-butylphosphine (Staudinger reaction), followed by the oxidation of the resulting phosphine imine with ozone¹⁵⁴ in CH₂Cl₂ at -78 °C led to no detectable amount of the desired nitro compound **104**. Alternatively, after the reduction of the azide with hydrogen over PtO₂, *m*-chloroperbenzoic acid (*m*-CPBA) was used to oxidize the resulting amine to the nitro functionality.¹⁵⁵ Although some desired product was isolated, the yield was low, precluding its use as an efficient synthetic transformation. From the standard 1D ¹H NMR data, the stereochemistry of the nitro group at C5 of **104** and assignment of each proton signal was not obvious. Selective NOE and COSY NMR experiments (CDCl₃) allowed the assignment and indicated that the sugar ring was not in the normal ⁴C₁ chair conformation. The X-ray crystal structure of **104** was obtained (crystallized from ethanol), confirming the structure of the sugar and revealing a twist boat conformation (⁴S₀), with C1, C2, C3, and C5 defining a plane (Figure 4.5). The coupling constants in the ¹H NMR spectrum correlated nicely with the X-ray structure, indicating that the conformation in solution was nearly the same as that in the crystal. Deprotection of the acetates with HCl/MeOH provided the desired phenyl (5S)-5-nitro-β-

D-xylopyranoside **89** as a white solid (78%). Selective NOE and COSY NMR experiments (methanol) facilitated the assignment of the ^1H spectrum and showed that the conformation of **89** was a normal $^4\text{C}_1$ chair.

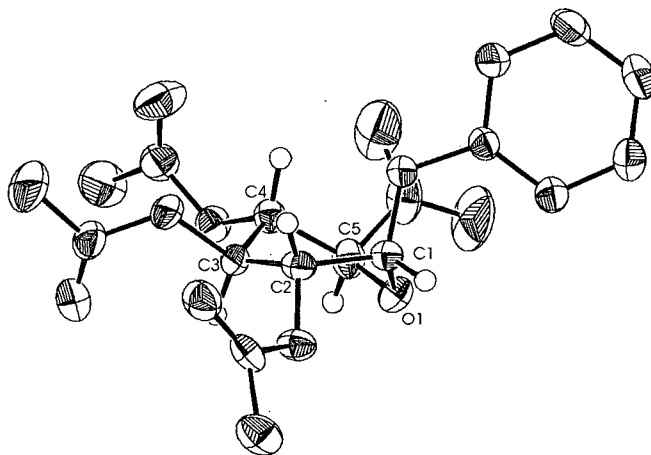


Figure 4.5. X-ray crystal structure of compound **104** showing the $^4\text{S}_0$ conformation. Atoms C1, C2, C3, and C5 define a plane.

4.4 Inhibition Studies

4.4.1 Inhibition of Chondroitin AC Lyase by Compound **88**

Despite possessing the leaving group hexosamine sugar, and having sp^2 hybridization at C5 of the uronic acid moiety, no inhibition was observed with the disaccharide compound **88** at concentrations up to 25 mM. The transition state for this elimination mechanism is predicted to carry an additional partial negative charge at C5, delocalized into the *aci*-carboxylate form of the acid. The lack of additional anionic character in **88** may provide a rationale for the surprising lack of inhibition observed. Alternatively, the pre-formed C4-C5 alkene structure may be too product-like to be tightly bound by the enzyme, or perhaps a β -1,3 linked hexosamine residue is required at the reducing end of the chain to afford proper recognition and binding. This latter point is emphasized by the fact that chondroitinases do not cleave heparin or heparan sulfate,

which are entirely 1,4 linked, suggesting that the 1,3 linkage may be a strong determinant for enzymatic activity.⁴ However, the activities of synthetic monosaccharide substrates with benzyl, phenyl, and methyl aglycone moieties suggests that some inhibition might have been expected.

4.4.2 Inhibition of Chondroitin AC Lyase by Compound 89

The novel 5-nitro sugar, **89**, was synthesized with the hope that the carbon acid would have a pK_a sufficiently low, and the anion be sufficiently stable, to be used in inhibition studies. As a first step it was necessary to measure the pK_a of this molecule to ensure that the anion could be easily formed. Fortunately this was easily achieved since the formation of the anion of the carbon acid can be monitored by the absorbance of this species at 242 nm. In this way, the pK_a of the carbon acid **89** (H5) was spectrophotometrically measured to be 8.8 (Figure 4.6), which is well within the expected range.

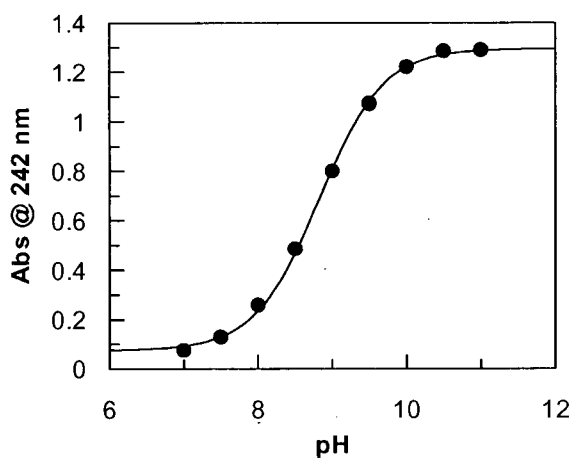


Figure 4.6. Spectrophotometric titration of compound **89** ($pK_a = 8.8$). For each point, an aliquot of a solution of **89** was equilibrated at the desired pH (buffered) at 30 °C for 75 minutes. Corrections were made for buffer effects caused by the different buffers used at each pH.

A second consideration in using **89** as an inhibitor is the kinetic stability of the anion. Rates of deprotonation and reprotonation were determined simply by monitoring changes in absorbance at 242 nm after altering the solution pH. Figure 4.7 shows the data for the deprotonation of **89** and the protonation of its conjugate base at pH 6.8 and 8.0 in 50 mM buffer and 100 mM NaCl at 30 °C. At pH 6.8, $k_{\text{prot}} = 3.7 \times 10^{-3} \text{ s}^{-1}$ ($t_{1/2} = 4$ minutes) and at pH 8.0, $k_{\text{prot}} = 1.7 \times 10^{-3} \text{ s}^{-1}$ ($t_{1/2} = 15$ minutes). The deprotonation and reprotonation rates were found to be dependent on the concentration of the buffer. A change to 200 mM buffer and 100 mM NaCl at pH 8 reduced the half-life of the anion to 7 minutes. These kinetic results show that the anion of **89** is sufficiently stable at pH 8.0 to be used directly as a preformed carbanion in initial steady state velocity measurements (performed within a few minutes) without significant interference from its conjugate carbon acid.

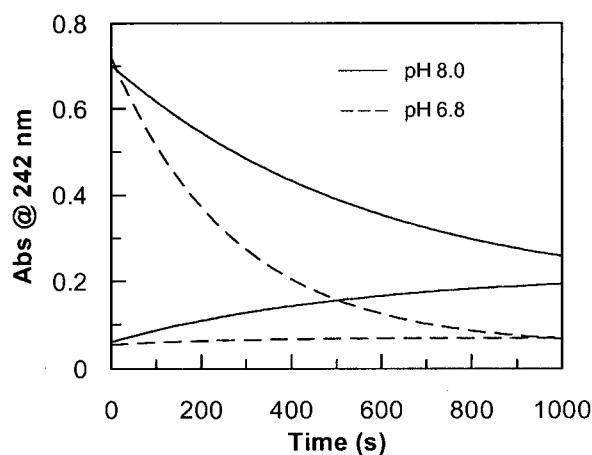


Figure 4.7. Rates of protonation (descending curves) of the preformed carbanion of **89** and deprotonation (ascending curves) of **89** at pH 8.0 and 6.8. The reactions were carried out at 30 °C in 50 mM sodium phosphate (pH 6.8) or Tris (pH 8.0) buffers and 100 mM NaCl.

Despite the promising outlook provided by both the ease of formation of the nitronate anion as well as by its stability in solution, it is the interesting interaction with the enzyme that has resolved its usefulness as an inhibitory compound. The argument that due to its resemblance to the transition state or reaction intermediate the nitronate anion might be bound tightly by the enzyme and thus be a potent inhibitor certainly seems

reasonable. This, as alluded to earlier, is undoubtedly the case for the enzymes such as fumarase,¹³⁵ aspartase,¹³⁵ aconitase,¹³⁶ and enolase¹³⁴ for which nanomolar inhibition constants are observed for the corresponding nitronate anions. The observation of these low inhibition constants dictates that the enzymes are not carrying out the simple reprotonation of the nitronate anions back to the conjugate acids (on the time scale of the inhibition tests), which should not be potent inhibitors. However, in the presence of chondroitin AC lyase, the nitronate anion of compound **89** was observed to be quickly converted back to the conjugate acid, with the final ratio of conjugate acid and base species being dictated by the solution pH and by the pK_a of compound **89**. Conversely, the enzyme also catalyzes the formation of the nitronate anion from the conjugate acid. This may seem intuitively reasonable, as the enzyme is simply lowering the activation energy for both the forward (deprotonation) and reverse (protonation) reactions, without changing the value of the equilibrium constant for this step. Thus, when a solution of the nitronate anion (at pH 11) or the conjugate acid (at pH 4.5) is added to a solution of chondroitin AC lyase buffered at pH 6.8, the rate of protonation or deprotonation is greatly increased over that without the enzyme, and is dependent on the concentration of enzyme. Figure 4.8 shows how the protonation rate increases as the concentration of enzyme is increased, when a solution of the anion is added to 50 mM sodium phosphate buffer at pH 6.8. For the solid green curve in Figure 4.8 ($[enzyme] = 2.8 \times 10^{-7} \text{ M}$) the enzyme had converted all of the nitronate anion to the conjugate acid by the time the solution was completely mixed and placed into the spectrometer. Thus, at the enzyme concentrations necessary for the inhibition analyses with chondroitin AC lyase ($\geq 1.8 \times 10^{-6} \text{ M}$), the lifetime of the anion is not sufficient for it to be used as a preformed carbanion. It is unclear whether the authors of the papers concerning the non-carbohydrate lyase enzymes and their nitro inhibitors investigated the possibility that those enzymes were also catalyzing the protonation and deprotonation reactions.

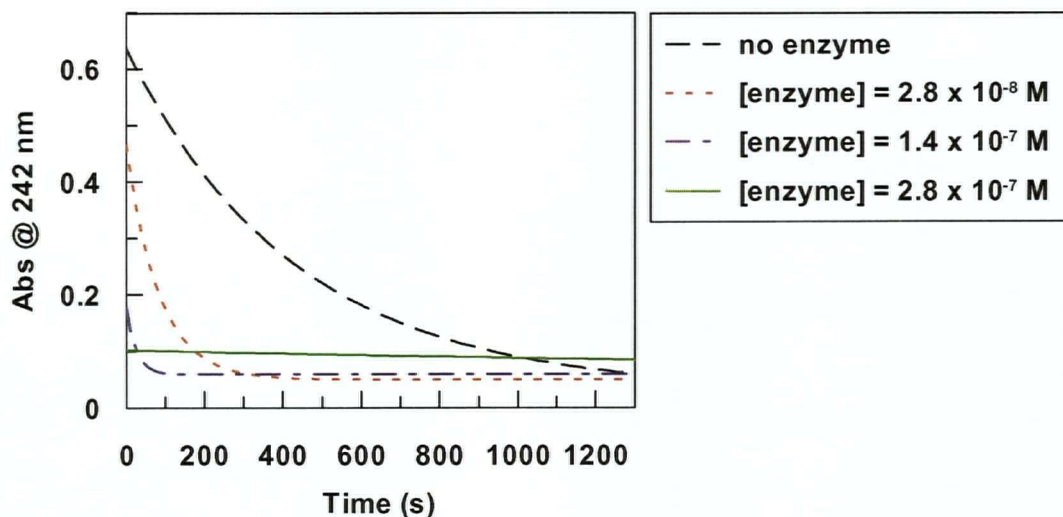


Figure 4.8. Graph illustrating the increased protonation rates of the nitronate anion in the presence of chondroitin AC lyase. The nitronate anion absorbs at 242 nm whereas the conjugate acid does not. The concentration of compound **89** used in each experiment was $\sim 5 \times 10^{-5}$ M. The final absorbance of the solutions correspond to the absorbance of the enzyme plus nitronate anion as dictated by the pK_a and the solution pH of 6.8.

Despite the efficient enzymatic protonation of the nitronate anion, an inhibition constant for this anion remains attainable. The pK_a of compound **89** dictates the concentration of conjugate acid and base forms present at a certain pH. Thus, assuming it is solely the anionic form that is responsible for inhibition of the enzyme, it is possible to estimate the inhibition afforded by the nitronate anion. Of course this assumption is not perfect in that the parent compound **89** may exhibit some weak binding to the enzyme, but may still allow an estimation of the inhibitory power of the nitronate anion.

Using the concentration of nitronate anion calculated from the pK_a of compound **89**, inhibition studies at pH 8 showed the nitronate anion of **89** to be a competitive inhibitor with a K_i of 0.7 mM, as shown by the Dixon plot in Figure 4.9. A similar analysis at pH 6.8 showed the inhibition constant for this anion to be 0.35 mM. This factor of two decrease in inhibition constant at the lower pH is not significant, and correlates nicely with the increased binding observed with the substrates as the pH is lowered (see Chapter 3). Disappointingly, the inhibition shown by the anion of **89** is not representative of a transition state analogue, which would be expected to bind much more tightly to the enzyme. Possibly this is a consequence of the inhibitor being a

monosaccharide derivative, thus not gaining binding interactions by occupying other important binding sites on the enzyme. Inhibition might therefore be increased dramatically by combining the inhibitory strategy of compound **88** in which the hexosamine 'leaving group' is present, as well as more saccharide units at the reducing end with the hope of increasing the binding to an enzyme that normally prefers a polymeric substrate. The observation of roughly the same K_i value at pH 6.8 and pH 8, determined by using the equilibrium concentration of the anion as dictated by the pK_a of **89**, strongly suggests that it is indeed the nitronate anion that is the inhibitory species.

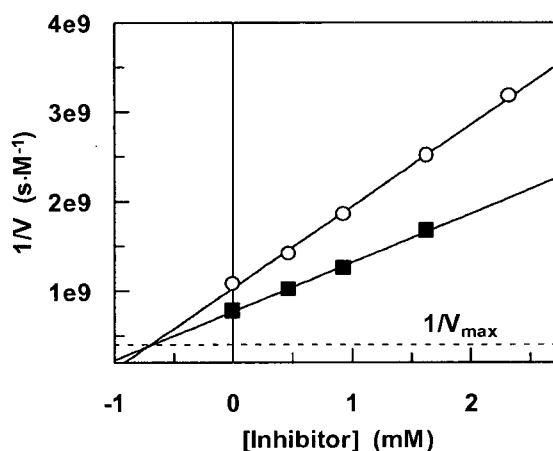


Figure 4.9. Dixon plot showing the inhibition by the anion of compound **89**. Kinetics were carried out in 200 mM Tris buffer and 100 mM NaCl, pH 8.0, 30 °C, using the fluorescent substrate **2** at concentrations of $0.75 K_m$ and $1.5 K_m$.

4.5 Conclusions

Unfortunately the compounds designed as potential inhibitors did not live up to their expectations, and possible explanations for their lack of inhibitory power are provided in the above discussions. Perhaps one of the biggest stumbling blocks in designing simple yet competent inhibitors of chondroitin AC lyase lies in the enzyme's random endolytic mode of action. The requirement of a long polysaccharide chain for efficient binding and catalysis provides a substantial barrier to the synthetic organic chemist. Thus, it is conceivable that the inhibitor designs presented here, in particular the novel 5-nitro sugar, may be applicable to other polysaccharide lyases that act in an exolytic fashion, and thus may have a higher affinity for a smaller substrate.

Chapter 5 - Materials and Methods

5.1 Isolation and Purification of Chondroitin AC Lyase from *Flavobacterium heparinum*

CompleteTM, Mini, EDTA-free protease inhibitor cocktail tablets were from Roche Diagnostics GmbH. Benzonase[®] Nuclease was from Novagen. SP Sepharose[®] Fast Flow cation exchange media was from Amersham Pharmacia Biotech. Ceramic hydroxyapatite, type A, 40 µm was from American International Chemical, Inc. Sodium phosphate buffers were obtained from J. T. Baker. Tris buffers were obtained from Sigma. Sodium dodecyl sulfate polyacrylamide gel electrophoresis (SDS-PAGE) was performed on a Pharmacia PhastSystem using preprepared PhastGels (homogeneous 7.5), and the proteins were detected with silver stain.

Much of the chondroitinase AC used in this research was obtained as generous donations from IBEX Technologies Inc. (Montreal) and Dr. Mirek Cygler at the Biotechnology Research Institute of the National Research Council. Due to the high demand for enzyme, its purification was also undertaken at UBC, and is described below.

Chondroitin sulfate-degrading strains of *Flavobacterium heparinum* were grown and isolated in the laboratory of Dr. Mirek Cygler as described in the literature.¹² The cell pellet obtained by fermentation (96 g) was re-suspended in 90 mL buffer consisting of 10 mM sodium phosphate, pH 7. To this was added 8 CompleteTM, Mini, EDTA-free protease inhibitor cocktail tablets and 10 µL of Benzonase[®] Nuclease (25 U/µL). The cells were lysed by French pressing (2x), and cell debris was removed by centrifugation (10000 rpm, 30 min, 4 °C). The supernatant was filtered through a 0.45 µm disk filter, diluted 1:1 with cold 10 mM sodium phosphate buffer, pH 7, and loaded onto a SP Sepharose[®] Fast Flow cation exchange column (2.6 x 30 cm), equilibrated with 10 mM sodium phosphate buffer, pH 7, at 4 °C. After washing with 3 column volumes of equilibration buffer (5 mL/min), the bound proteins were eluted with 25 mM sodium phosphate buffer, 150 mM NaCl, pH 7 (5 mL/min). Eluted proteins were monitored with a UV detector (280 nm) coupled to a chart recorder. Additional material was removed

from the column by flushing with 25 mM sodium phosphate buffer, 1.0 M NaCl, pH 7 (5 mL/min). Fractions (5 mL each) were assayed for lyase AC activity and analyzed for purity via SDS-PAGE. Figure 5.1 shows the SDS-PAGE gels of the column fractions. Fractions containing chondroitin AC lyase were pooled and applied to a ceramic hydroxyapatite column (2.6 x 33 cm) equilibrated with 10 mM sodium phosphate buffer, pH 7, at 4 °C. After loading, the column was washed with 3 column volumes of 15% (v/v) 25 mM sodium phosphate buffer, 1.0 M NaCl, pH 7, (10 mL/min) and the bound proteins eluted in a linear gradient over 130 minutes of (15-70%) 25 mM sodium phosphate buffer, 1.0 M NaCl, pH 7, (10 mL/min). Chondroitin AC lyase eluted when the eluent was ~ 50% of the 25 mM buffer. Additional material was removed with 100% 25 mM sodium phosphate buffer, 1.0 M NaCl, pH 7. Fractions containing purified protein as judged by SDS-PAGE (Figure 5.2) were pooled, concentrated and desalted with an Amicon stir cell. The final concentration and buffer exchange into 50 mM sodium phosphate, 100 mM NaCl, pH 6.8 was accomplished using a centriprep concentrator. Using an extinction coefficient of $141020 \text{ M}^{-1}\text{cm}^{-1}$ and a molecular weight of 79693.88 gmol^{-1} , the amount of purified protein isolated was calculated to be ~ 90 mg.

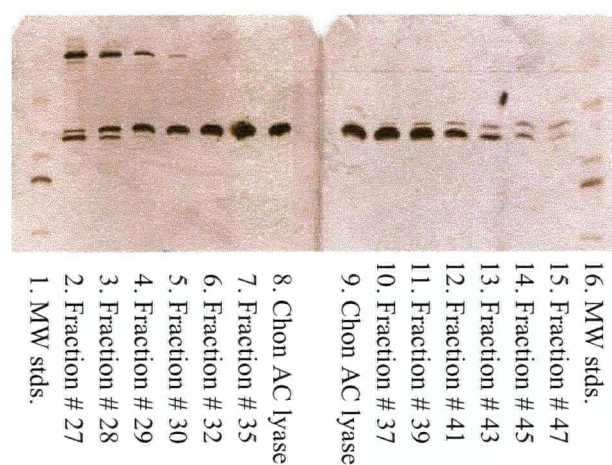


Figure 5.1. SDS-PAGE gel of fractions from the SP Sepharose column. The MW standards are: (top to bottom) myosin (200,000), *E. coli* β -galactosidase (116,250), rabbit muscle phosphorylase b (97,400), bovine serum albumin (66,200), and hen egg white ovalbumin (45,000). Lanes 8 and 9 labelled Chon AC lyase are an authentic sample of the enzyme.

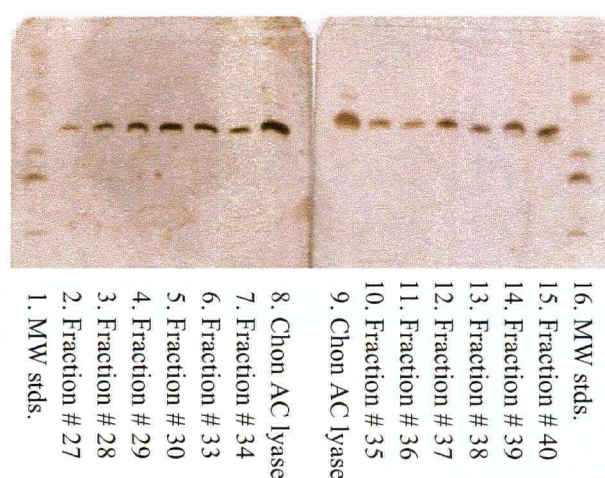


Figure 5.2. SDS-PAGE gel of fractions from the ceramic hydroxyapatite column. The MW standards are: (top to bottom) myosin (200,000), *E. coli* β -galactosidase (116,250), rabbit muscle phosphorylase b (97,400), bovine serum albumin (66,200), and hen egg white ovalbumin (45,000). Lanes 8 and 9 labelled Chon AC lyase are an authentic sample of the enzyme.

5.2 Enzymology

5.2.1 pH Analyses

The buffers used in the pH analyses (50 mM + 100 mM NaCl) were MES (2-[N-morpholino]ethanesulfonic acid, pH 4.5-6.0), sodium phosphate (pH 6.0-7.5), and Tris (tris[hydroxymethyl]-aminomethane, pH 7.5-9.0). Corrections were made for buffer effects caused by the different buffers used.

5.2.1.1 pH Profiles for Chondroitin 6-Sulfate

Enzymatic activity was monitored by the change in absorbance at 232 nm ($\epsilon = 3800 \text{ M}^{-1}\text{cm}^{-1}$ for unsaturated products)¹² in quartz cuvettes (path length 1 cm) at 30 °C, total volume 200 μL . Enzyme stock solutions ($\sim 2 \times 10^{-8} \text{ M}$) were made up in 10 mM sodium phosphate buffer, 100 mM NaCl, pH 6.8, containing 0.1% bovine serum albumin (BSA). Mixtures of buffer and the desired amount of substrate were incubated at 30 °C for at least 15 minutes to thermally equilibrate before the enzyme was added to initiate the reaction. V_{max} analyses were performed at two different high substrate concentrations to ensure that complete saturation had been reached, and the initial rates were measured over 30 seconds. The k_{cat}/K_m analyses were performed by the depletion method using low substrate concentrations and by monitoring the change in absorbance at 232 nm over ~ 15 minutes. The data were fitted to a first-order rate equation using the program GraFit 4.0,¹⁵⁶ giving values for the pseudo-first-order rate constant at each pH. Equation 5.1 shows a modified Michaelis-Menten equation for the conditions of low substrate concentration ($[S] \ll K_m$). The k_{obs} values correspond to $[E]k_{\text{cat}}/K_m$, and thus the k_{cat}/K_m values can be extracted dividing the observed rate constants by the enzyme concentration.

$$v = \frac{k_{\text{cat}}[E][S]}{K_m} \quad (\text{Equation 5.1})$$

5.2.1.2 pH Profile for the Synthetic Substrate 4 (k_{cat}/K_m)

The assays were carried out in glass vials, total solution volume 300 μL . Mixtures containing buffer and the desired amount of substrate were incubated at 30 °C for at least 15 minutes to thermally equilibrate. Enzyme (30.0 μL of 1.0×10^{-4} M chondroitin AC lyase in 10 mM sodium phosphate, 100 mM NaCl, pH 6.8) was added and the change in fluoride ion concentration was monitored at 30 °C with an Orion fluoride ion-selective electrode interfaced with a computer. Initial rates were measured at low substrate concentrations and k_{cat}/K_m was calculated by dividing by the enzyme concentration. The pH of the reaction mixtures was confirmed at the conclusion of each analysis.

5.2.2 Kinetic Isotope Effects

Kinetic isotope effects were measured using direct methods. In order to minimize errors, measurements were alternated between the deuterated and undeuterated compounds with the same reagents and in the same constant-temperature bath. Assays were carried out in glass vials, total solution volume 300 μL . Mixtures containing buffer (50 mM sodium phosphate, 100 mM NaCl, pH 6.8) and the desired amount of substrate were incubated at 30 °C for at least 15 minutes to thermally equilibrate. Enzyme (30.0 μL of 1.0×10^{-4} M chondroitin AC lyase in buffer) was added and the change in fluoride ion concentration was monitored at 30 °C with an Orion fluoride ion-selective electrode interfaced with a computer. A correction was made for the less than 100% incorporation of deuterium in compound **87** as described in the text (see Chapter 3).

5.2.3 Inhibition Studies

5.2.3.1 Inhibition by Compounds **88** and **89**

pH 6.8: The assays were carried out in glass vials, total solution volume 300 μL . Mixtures containing buffer (50 mM sodium phosphate, 100 mM NaCl, pH 6.8) and desired amounts of substrate (benzyl 4-deoxy-4-fluoro- β -D-glucopyranosiduronic acid, **4**)

and inhibitor were incubated at 30 °C for at least 15 min to thermally equilibrate. Compound **89** was equilibrated in buffer for at least 1.5 h prior to testing to ensure that a consistent ionization state of the carbon acid had been reached. Enzyme (30 μ L of 1.0×10^{-4} M chondroitin AC lyase in buffer) was added and the change in fluoride ion concentration was monitored at 30 °C with an Orion fluoride ion-selective electrode interfaced with a computer. The rates were constant over a period of at least 10 minutes. The pH of the solutions was measured both at the beginning and at the end of the reaction.

pH 8.0: The assays were carried out in fluorescence cuvettes (1 cm path length), total solution volume 500 μ L. Mixtures containing buffer (200 mM Tris, 100 mM NaCl, pH 8.0) and desired amount of substrate (phenyl 4-methylumbelliferyl- β -D-glucopyranosiduronic acid, **2**) were incubated at 30 °C for at least 15 min to thermally equilibrate. Desired amounts of compound **89** (at pH 8.0) and enzyme (25 μ L of 3.5×10^{-5} M chondroitin AC lyase in buffer) were then added and the change in fluorescence intensity was monitored at 30 °C over 5 min ($\lambda_{\text{excitation}}$ 360 nm, $\lambda_{\text{emission}}$ 450 nm) using a Varian Cary Eclipse fluorescence spectrometer equipped with a temperature-controlled cuvette holder. Rates were calculated using a standard curve of 7-hydroxy-4-methylcoumarin (4-methylumbelliferone). The pH of the solutions was measured both at the beginning and at the end of the reaction.

5.2.3.2 Inhibition by Compounds **52** and **58**

Inhibition studies of compounds **52** and **58** were performed at pH 8 as described for compound **89** above.

5.3 General Synthesis

Unless otherwise stated, all reagents were obtained from commercial suppliers and were used without further purification. Column chromatography was performed with silica gel (230-400 mesh). TLC was performed on Merck pre-coated 60 F-254 silica plates and visualized using UV light (254 nm) and/or by applying a solution of 10% ammonium molybdate in 2 M H₂SO₄ followed by heating. The NMR spectra were recorded on Bruker AC200 (200 MHz), AV300 (300 MHz) or AV400 (400 MHz) spectrometers. All ¹⁹F NMR spectra are referenced to trifluoroacetic acid as zero ppm. Elemental analyses were carried out at the University of British Columbia microanalytical laboratory. High resolution mass spectra were measured by the mass spectrometry laboratory at the University of British Columbia. Melting points were recorded using a Laboratory Devices Mel-Temp II melting point apparatus and are uncorrected. Anhydrous solvents were prepared as follows: CH₂Cl₂, CCl₄, pyridine, and benzene were distilled over CaH₂. THF was distilled over sodium benzophenone. Methanol was distilled over magnesium and iodine. DMF was dried successively over 4 Å molecular sieves (3x). Deionized water, purified with a Barnstead NANOpure system, was used for all aqueous solutions.

5.3.1 General Acetylation Procedure

The starting material was dissolved in a solution of acetic anhydride and pyridine (2:3) and stirred at rt until TLC indicated a complete reaction. The solution was concentrated under vacuum, and the residue dissolved in CH₂Cl₂, washed with 1 M HCl (3x), saturated NaHCO₃ (2x), dried over MgSO₄, and concentrated under vacuum to leave a relatively pure product.

5.3.2 General Zemplén Deprotection

Starting material was dissolved in dry methanol and a catalytic amount of sodium methoxide was added. The reaction mixture was stirred at rt until TLC indicated a

complete reaction. The solution was then neutralized with Amberlite IR-120 (H^+) resin, filtered, and concentrated under vacuum to leave a relatively pure product.

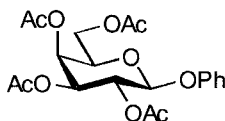
5.3.3 General Acetyl Chloride Deprotection

Acetyl chloride (10% v/v) was added to a solution of the starting material in dry methanol at 0 °C, then stirred at 4 °C until TLC indicated a complete reaction. The solution was then concentrated under vacuum to leave a relatively pure product.

5.4 Synthesis of the Fluorinated Substrates

5.4.1 Phenyl 4-deoxy-4-fluoro- β -D-glucopyranosiduronic acid (3) (Scheme 3.1)

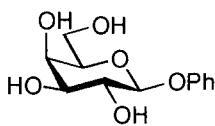
Phenyl 2,3,4,6-tetra-O-acetyl- β -D-galactopyranoside (14)



A solution of HBr in acetic acid (60 mL, 45% w/v) was added to a solution of *per-O*-acetylated galactose (34 g, 87 mmol) at 0 °C. Upon completion of the addition the reaction mixture was allowed to warm up to ambient temperature, and stirred for 2 h, before pouring onto an ice/water mixture. The mixture was diluted with CH_2Cl_2 , and the aqueous phase was extracted once with CH_2Cl_2 . The combined organic phases were washed with saturated $NaHCO_3$ (3x), H_2O (1x), dried over $MgSO_4$ and concentrated under vacuum to give 2,3,4,6-tetra-*O*-acetyl- α -D-galactopyranosyl bromide (**13**)⁸² as a colourless oil. Crude **13** was dissolved in CH_2Cl_2 (250 mL) and added to a solution of phenol (16.4 g, 174 mmol, 2 eq) and tetrabutylammonium hydrogensulfate (TBAHS) (29.6 g, 87.1 mmol, 1eq) in 1 M NaOH (250 mL). The reaction mixture was stirred vigorously at rt for 2 h. The phases were then separated, and the aqueous phase extracted with CH_2Cl_2 (2x). The combined organic phases were washed with 1 M NaOH (5x), brine (2x), dried over $MgSO_4$, and concentrated under vacuum, leaving a dark syrup which begins to crystallize. The syrup was passed down a short plug of silica using

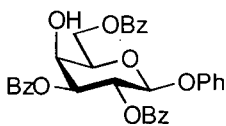
PE:EtOAc 2:1, then 1:1, to give **14** as colourless crystals (15.0 g, 40%): ^1H NMR (400 MHz, CDCl_3) δ 7.28 (2 H, dd, J 8.5, J 7.3 Hz, Ph_{meta}), 7.05 (1 H, tt, J 7.3, J 0.9 Hz, Ph_{para}), 6.98 (2 H, dd, J 8.5, J 0.9 Hz, Ph_{ortho}), 5.47 (1 H, dd, $J_{2,3}$ 10.3, $J_{2,1}$ 7.9 Hz, H2), 5.44 (1 H, dd, $J_{4,3}$ 3.3, $J_{4,5}$ 0.9 Hz, H4), 5.09 (1 H, dd, $J_{3,2}$ 10.3, $J_{3,4}$ 3.3 Hz, H3), 5.02 (1 H, d, $J_{1,2}$ 7.9 Hz, H1), 4.21 (1 H, dd, $J_{6a,6b}$ 11.3, $J_{6a,5}$ 7.0 Hz, H6_a), 4.14 (1 H, dd, $J_{6b,6a}$ 11.3, $J_{6b,5}$ 6.1 Hz, H6_b), 4.03 (1 H, ddd, $J_{5,6a}$ 7.0, $J_{5,6b}$ 6.1, $J_{5,4}$ 0.9 Hz, H5), 2.16, 2.05, 2.04, 1.99 (12 H, 4 s, 4 Ac).

Phenyl β -D-galactopyranoside (**16**)⁸¹



Zemplén deprotection of **14** with sodium methoxide was carried out according to the general procedure to yield **16**⁸¹ as a white solid (96%): ^1H NMR (200 MHz, CD_3OD) δ 7.27 (2 H, dd, J 8.5, J 7.1 Hz, Ph_{meta}), 7.09 (2 H, dd, J 8.5, J 0.9 Hz, Ph_{ortho}), 6.99 (1 H, tt, J 7.1, J 0.9 Hz, Ph_{para}), 4.86 (1 H, d, $J_{1,2}$ 7.6 Hz, H1), 3.89 (1 H, dd, $J_{4,3}$ 3.4, $J_{4,5}$ 1.0 Hz, H4), 3.78 (1 H, dd, $J_{2,3}$ 9.8, $J_{2,1}$ 7.6 Hz, H2), 3.78-3.71 (2 H, m, H6_a, H6_b), 3.66 (1 H, ddd, $J_{5,6a}$ 7.3, $J_{5,6b}$ 4.6, $J_{5,4}$ 1.0 Hz, H5), 3.56 (1 H, dd, $J_{3,2}$ 9.8, $J_{3,4}$ 3.4 Hz, H3).

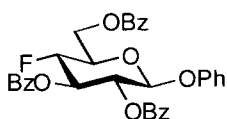
Phenyl 2,3,6-tri-O-benzoyl- β -D-galactopyranoside (**18**)⁸⁶



Benzoyl chloride (4.64 mL, 40.0 mmol, 3.2 eq) in dry pyridine (8 mL) was added dropwise to a stirred solution of **16** (3.2 g, 12.5 mmol) in dry pyridine (22 mL) at -40°C . The reaction mixture was maintained at $\leq -20^\circ\text{C}$ for 1 h, and was then allowed to attain ambient temperature and stirred overnight. The reaction was then diluted ice/ H_2O and EtOAc, and the organic phase was washed with H_2O (1x), 1 M HCl (3x), saturated NaHCO_3 (2x), dried over MgSO_4 , and concentrated under vacuum. The residue was purified by column chromatography (Tol:EtOAc 15:1). First eluted was phenyl 2,3,4,6-tetra-O-benzoyl- β -D-galactopyranoside, followed by phenyl 3,4,6-tri-O-benzoyl- β -D-

galactopyranoside, and finally **18**⁸⁶ as a white solid (2.0 g, 28%, 53% based on recovered **16** obtained from the deprotection of the other ‘incorrectly’ benzoylated products with sodium methoxide): ¹H NMR (200 MHz, CDCl₃) δ 8.10-7.90 (6 H, m, Ar), 7.65-7.30 (9 H, m, Ar), 7.20-6.90 (5 H, m, Ar), 6.06 (1 H, dd, J_{2,1} 8.0, J_{2,3} 10.5 Hz, H₂), 5.44 (1 H, dd, J_{3,4} 3.4, J_{3,2} 10.5 Hz, H₃), 5.29 (1 H, d, J_{1,2} 8.0 Hz, H₁), 4.76 (1 H, dd, J_{6eq-6ax} 11.6, J_{6eq,5} 5.5 Hz, H_{6eq}), 4.65 (1 H, dd, J_{6ax-6eq} 11.6, J_{6ax,5} 7.2 Hz, H_{6ax}), 4.45 (1 H, d, J_{4,3} 3.4 Hz, H₄), 4.24 (1 H, m, H₅); ¹³C NMR (75 MHz, CDCl₃) δ 166.38, 165.83, 165.36 (3 C=O), 157.07 (C), 133.55, 133.33, 133.22, 129.96, 129.74, 129.71 (6 CH), 129.50 (C), 129.39 (CH), 129.28, 128.82 (2 C), 128.49, 128.45, 128.40, 128.35, 1263.12, 117.2 (6 CH), 99.96 (CH, C₁), 74.13, 72.77, 69.29, 67.27 (4 CH), 63.00 (CH₂); **Anal. calc. for** C₃₃H₂₈O₉: C, 69.71; H, 4.96. Found: C, 69.46; H, 4.99.

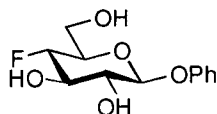
Phenyl 2,3,6-tri-O-benzoyl-4-deoxy-4-fluoro-β-D-glucopyranoside (**21**)



(Diethylamino)sulfur trifluoride (DAST, 2.78 mL, 21.1 mmol, 6 eq) was added dropwise to a solution of **18** (2.0 g, 3.5 mmol) in dry CH₂Cl₂ (20 mL) at –30 °C. Upon completion of the addition the reaction was allowed to attain ambient temperature, and was stirred for 4 h, cooled to –5 °C, and methanol then added to quench. The reaction mixture was diluted with CH₂Cl₂, washed with saturated NaHCO₃ (3x), and the aqueous phases extracted once with CH₂Cl₂. The combined organic phases were washed once with H₂O, dried over MgSO₄, and concentrated under vacuum. The residue was purified by column chromatography (PE:Et₂O 2:1) to give **21** as a white solid (83%): **mp** 153-156 °C; ¹H NMR (200 MHz, CDCl₃) δ 8.15-7.90 (6 H, m, Ar), 7.70-7.30 (9 H, m, Ar), 7.27-7.10 (2 H, m, Ar), 7.10-6.90 (3 H, m, Ar), 5.92 (1 H, ddd, J_{3,2} 9.6, J_{3,4} 8.8, J_{3,F} 14.1 Hz, H₃), 5.72 (1 H, dd, J_{2,1} 7.8, J_{2,3} 9.6 Hz, H₂), 5.34 (1 H, d, J_{1,2} 7.8 Hz, H₁), 4.76 (1 H, ddd, J_{4,5} = J_{4,3} 8.8, J_{4,F} 50.5 Hz, H₄), 4.82 (1 H, ddd, J_{6eq-6ax} 12.2, J_{6eq,5} = J_{6eq,F} 2.3 Hz, H_{6eq}), 4.60 (1 H, ddd, J_{6ax-6eq} 12.2, J_{6ax,5} 6.4, J_{6ax,F} 1.2 Hz, H_{6ax}), 4.22 (1 H, ddd, J_{5,4} 8.8, J_{5,6ax} 6.4, J_{5,6eq} 2.3 Hz, H₅); ¹³C NMR (75 MHz, CDCl₃) δ 165.98, 165.53, 165.08 (3 C=O), 156.79 (C, OPh), 133.49, 133.41, 133.34, 129.90, 129.80, 129.76, 129.50 (7 CH), 128.88,

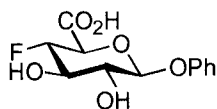
128.82 (2 C, 2 OBz), 128.47, 128.42 (2 CH), 99.51 (CH, C1), 87.31 (CH, d, $J_{4,F}$ 189.3 Hz, C4), 72.82 (CH, d, $J_{3,F}$ 19.9 Hz, C3), 71.80 (CH, d, $J_{5,F}$ 23.6 Hz, C5), 71.14 (CH, d, $J_{2,F}$ 7.8 Hz, C2), 62.65 (CH₂, C6); ^{19}F NMR (188 MHz, CDCl₃) δ -123.14 (dd, $J_{F,4}$ 50.5, $J_{F,3}$ 14.1 Hz); **Anal. calc. for** C₃₃H₂₇FO₈: C, 69.47; H, 4.77. Found: C, 69.80; H, 4.89.

Phenyl 4-deoxy-4-fluoro- β -D-glucopyranoside (22)



Compound **21** was deprotected with sodium methoxide according to the general procedure. The crude product was washed with Et₂O to remove methyl benzoate, leaving **22** as a white solid (85%): mp 178-179 °C; ^1H NMR (200 MHz, CD₃OD) δ 7.35-7.20 (2 H, m, Ar), 7.15-6.95 (3 H, m, Ar), 4.96 (1 H, d, $J_{1,2}$ 7.8 Hz, H1), 4.34 (1 H, ddd, $J_{4,F}$ 50.7, $J_{4,3}$ 9.4, $J_{4,5}$ 8.5 Hz, H4), 3.90-3.60 (4 H, m, H3, H5, H6_a, H6_b), 3.48 (1 H, dd, $J_{2,3}$ 9.3, $J_{2,1}$ 7.8 Hz, H2); ^{13}C NMR (75 MHz, CD₃OD) δ 158.98 (C), 130.46, 123.49, 117.74 (3 CH), 102.06 (CH, C1), 90.25 (CH, d, $J_{4,F}$ 179.9 Hz, C4), 75.73 (CH, d, $J_{3,F}$ 17.9 Hz, C3), 75.30 (CH, d, $J_{5,F}$ 24.5 Hz, C5), 74.63 (CH, d, $J_{2,F}$ 8.7 Hz, C2), 61.49 (CH₂, C6); ^{19}F NMR (188 MHz, CD₃OD) δ -122.3 (ddd, $J_{F,4}$ 50.7, $J_{F,3}$ 13.6, $J_{F,5}$ 3.0 Hz); **Anal. calc. for** C₁₂H₁₅FO₅: C, 55.81; H, 5.85. Found: C, 55.85; H, 5.87.

Phenyl 4-deoxy-4-fluoro- β -D-glucopyranosiduronic acid (3)

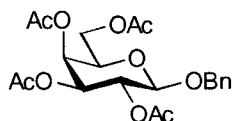


A solution of **22** (416 mg, 1.61 mmol) and TEMPO (3 mg, 0.019 mmol, 0.01 eq) in H₂O (33 mL) was made and the pH adjusted to 10 to 10.5 with 1 M NaOH. *t*-BuOC[⁹¹ (0.67 mL, 5.6 mmol, 3.5 eq) was added and the pH of the solution maintained between 10 and 10.5 with 2 M NaOH. The pH stabilizes after ~ 20 min. The reaction mixture was stirred at rt for 2.5 h, quenched with EtOH, and the pH reduced to 5 with 1 M H₂SO₄. The reaction mixture was then washed with CHCl₃ (3x) and concentrated under vacuum. The residue was stirred with MeOH, any remaining solids removed by filtration, and the filtrate concentrated under vacuum. The residue was purified by HPLC (amide-80

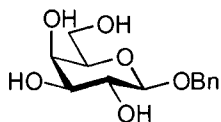
column, linear gradient from 100% CH₃CN to CH₃CN:H₂O 4:1 over 40 min, then CH₃CN:H₂O 4:1 until completely eluted), then passed down a cation exchange column (Bio-Rad[®] AG 50W-X2, H⁺, 200-400 mesh) to give **3** as a white solid (175 mg, 40%): ¹H NMR (300 MHz, CD₃OD) δ 7.31 (2 H, dd, J 8.3, J 7.8 Hz, Ph_{meta}), 7.11 (2 H, d, J 7.8 Hz, Ph_{ortho}), 7.05 (1 H, tt, J 8.3, 0.9 Hz, Ph_{para}), 5.06 (1 H, d, J_{1,2} 7.9 Hz, H1), 4.47 (1 H, ddd, J_{4,F} 49.9, J_{4,5} 9.7, J_{4,3} 8.8 Hz, H4), 4.26 (1 H, dd, J_{5,4} 9.7, J_{5,F} 3.2 Hz, H5), 3.80 (1 H, ddd, J_{3,F} 16.2, J_{3,4} = J_{3,2} 8.8 Hz, H3), 3.55 (1 H, dd, J_{2,3} 8.8, J_{2,1} 7.9 Hz, H2); HRMS (LSIMS-, 3-NBA) m/z: 271.06267. Calc. For C₁₂H₁₂FO₆ [M – H][–] 271.0618; Anal. calc. for C₁₂H₁₃FO₆ + 0.5 H₂O: C, 51.25; H, 4.66. Found: C, 51.06; H, 4.89.

5.4.2 Benzyl 4-deoxy-4-fluoro-β-D-glucopyranosiduronic acid (**4**) (Scheme 3.1)

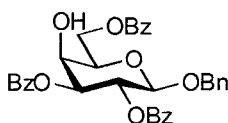
Benzyl 2,3,4,6-tetra-O-acetyl-β-D-galactopyranoside (**15**)⁸⁴



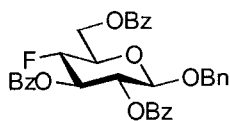
A mixture of Ag₂CO₃ (9.05 g, 32.8 mmol, 3 eq), benzyl alcohol (5.7 mL, 55 mmol, 5 eq), and a crystal of iodine in dry CH₂Cl₂ (10 mL) was stirred over 4 Å molecular sieves for 15 min before a solution of **13** (4.5 g, 10.9 mmol) in dry CH₂Cl₂ (10 mL) (also stirred over 4 Å molecular sieves for 15 min) was added dropwise. The reaction flask was covered in foil and stirred for 21 h, diluted with EtOAc, filtered through Celite, and concentrated under vacuum. Excess benzyl alcohol was removed by Kugelrohr distillation at ~80 °C and the residue then purified by column chromatography (PE:EtOAc 5:2) to give **15**⁸⁴ as a colourless syrup (3.83 g, 80%): ¹H (200 MHz, CDCl₃) δ 7.40-7.25 (5 H, m, Ar), 5.37 (1 H, dd, J_{4,3} 3.4, J_{4,5} 0.7 Hz, H4), 5.26 (1 H, dd, J_{2,3} 10.4, J_{2,1} 8.1 Hz, H2), 4.96 (1 H, dd, J_{3,2} 10.4, J_{3,4} 3.4 Hz, H3), 4.90 (1 H, d, J 12.1 Hz, OCH₂Ph), 4.61 (1 H, d, J 12.1 Hz, OCH₂Ph), 4.50 (1 H, d, J_{1,2} 8.1 Hz, H1), 4.21 (1 H, dd, J_{6a,6b} 11.0, J_{6a,5} 6.6 Hz, H6_a), 4.13 (1 H, dd, J_{6b,6a} 11.0, J_{6b,5} 6.6 Hz, H6_b), 3.87 (1 H, ddd, J_{5,6a} = J_{5,6b} 6.6, J_{5,4} 0.7 Hz, H5), 2.14, 2.05, 1.99, 1.96 (12 H, 4 s, 4 Ac).

Benzyl β -D-galactopyranoside (17)⁸²

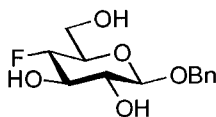
Zemplén deprotection of **15** with sodium methoxide was carried out according to the general procedure to yield **17**⁸² as a white solid in quantitative yield: ¹H NMR (200 MHz, CD₃OD) δ 7.50-7.20 (5 H, m, Ar), 4.95 (1 H, d, J 11.7 Hz, OCH₂Ph), 4.68 (1 H, d, J 11.7 Hz, OCH₂Ph), 4.34 (1 H, d, J_{1,2} 7.6 Hz, H1), 3.90-3.72 (3 H, m), 3.68-3.44 (3 H, m); ¹³C (75 MHz, CD₃OD) δ 139.09 (C), 129.21, 129.14, 128.60, 103.83, 76.64, 74.90, 72.51 (7 CH), 71.63 (CH₂), 70.26 (CH), 62.49 (CH₂).

Benzyl 2,3,6-tri-O-benzoyl- β -D-galactopyranoside (19)⁸⁷

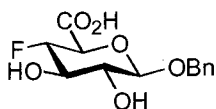
Prepared from **17**⁸² as described for **18**.⁸⁶ The crude residue was purified by column chromatography (PE:EtOAc 3.5:1). First eluted was the tetrabenzoate compound, followed by **19**⁸⁷ which was crystallized from EtOAc/hexanes to give a white solid (40%). The other 'incorrectly' benzoylated products formed in the reaction were deprotected with sodium methoxide and recycled through the synthesis): ¹H NMR (200 MHz, CDCl₃) δ 8.10-7.90 (6 H, m, Ar), 7.63-7.10 (14 H, m, Ar), 5.88 (1 H, dd, J_{2,3} 10.5, J_{2,1} 7.8 Hz, H2), 5.30 (1 H, dd, J_{3,2} 10.5, J_{3,4} 3.2 Hz, H3), 4.90 (1 H, d, J 12.4 Hz, OCH₂Ph), 4.79-4.58 (4 H, m, H1, OCH₂Ph, H6_a, H6_b), 4.36 (1 H, d, J_{4,3} 3.2 Hz, H4), 4.02 (1 H, dd, J_{5,6a} = J_{5,6b} 6.5 Hz, H5); **Anal. calc. for** C₃₄H₃₀O₉: C, 70.09; H, 5.19. Found: C, 69.97; H, 5.07. Last eluted was benzyl 3,6-di-O-benzoyl- β -D-galactopyranoside.

Benzyl 2,3,6-tri-O-benzoyl-4-deoxy-4-fluoro- β -D-glucopyranoside (23)

Prepared from **19**⁸⁷ as described for **21**. The residue was purified by column chromatography (PE:EtOAc 4:1) to give **23** as a white foam (60%): ¹H NMR (200 MHz, CDCl₃): δ 8.14-8.07 (2 H, m, Ar), 8.00-7.87 (4 H, m, Ar), 7.62-7.12 (15 H, m, Ar), 5.75 (1 H, ddd, $J_{3,F}$ 14.2, $J_{3,2}$ 9.5, $J_{3,4}$ 9.0 Hz, H3), 5.49 (1 H, dd, $J_{2,3}$ 9.5, $J_{2,1}$ 7.8 Hz, H2), 4.88 (1 H, d, J 12.5 Hz, OCH₂Ph), 4.82-4.52 (2 H, m, H6_a, H6_b), 4.80 (1 H, ddd, $J_{4,F}$ 50.0, $J_{4,3}$ = $J_{4,5}$ 9.0 Hz, H4), 4.76 (1 H, d, $J_{1,2}$ 7.8 Hz, H1), 4.65 (1 H, d, J 12.5 Hz, OCH₂Ph), 3.98 (1 H, ddd, $J_{5,4}$ 9.0, $J_{5,6a}$ 5.1, $J_{5,6b}$ 2.4 Hz, H5); ¹⁹F NMR (188 MHz, CDCl₃) δ -123.30 (dd, $J_{F,4}$ 50.0, $J_{F,3}$ 14.2 Hz).

Benzyl 4-deoxy-4-fluoro- β -D-glucopyranoside (24)

Zemplén deprotection of **23** with sodium methoxide according to the general procedure followed by recrystallization from EtOAc/PE gave **24** as a white solid (87%): ¹H NMR (200 MHz, (CD₃)₂CO) δ 7.42-7.15 (5 H, m, Ph), 4.86 (1 H, d, J 12.2 Hz, OCH₂Ph), 4.58 (1 H, d, J 12.2 Hz, OCH₂Ph), 4.42 (1 H, d, $J_{1,2}$ 7.9 Hz, H1), 4.26 (1 H, ddd, $J_{4,F}$ 51.1, $J_{4,5}$ 9.4, $J_{4,3}$ 8.8 Hz, H4), 3.87-3.54 (3 H, m, H3, H6_a, H6_b), 3.47 (1 H, ddd, $J_{5,4}$ 9.4, $J_{5,6a}$ 5.1, $J_{5,6b}$ 2.9 Hz, H5), 3.26 (1 H, dd, $J_{2,3}$ 9.0, $J_{2,1}$ 7.9 Hz, H2).

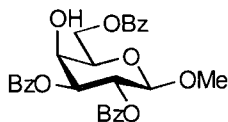
Benzyl 4-deoxy-4-fluoro- β -D-glucopyranosiduronic acid (4)

A solution of TEMPO (11 mg), **24** (734 mg, 2.7 mmol), sodium bromide (33 mg, 0.32 mmol, 0.12 eq), and tetrabutylammonium bromide (58 mg, 0.18 mmol, 0.067 eq) in saturated NaHCO₃ (7 mL) and EtOAc (16 mL) was cooled to 0 °C. To this was added a solution of commercial bleach (12.9 mL, 5.25% w/v NaOCl), saturated NaHCO₃ (6 mL),

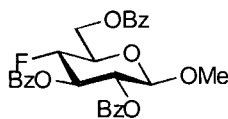
and brine (12 mL) also at 0 °C. The reaction mixture was stirred at this temperature for 2.5 h, diluted with EtOAc and H₂O, then the organic layer was extracted with saturated NaHCO₃ (3x). The combined aqueous phases were acidified with 2 M HCl, extracted with EtOAc (6x), dried over MgSO₄, and concentrated under vacuum. The residue was purified by column chromatography (PE:EtOAc 1:3 + 0.4% acetic acid), passed down an ion exchange column (Bio-Rad® AG 50W-X2, 200-400 mesh, H⁺ form), and freeze-dried to give **4** as a white solid (718 mg, 93%): ¹H NMR (200 MHz, (CD₃)₂CO) δ 7.41-7.16 (5 H, m, Ph), 4.86 (1 H, d, J 12.3 Hz, OCH₂Ph), 4.61 (1 H, d, J 12.3 Hz, OCH₂Ph), 4.56 (1 H, d, J_{1,2} 7.8 Hz, H1), 4.40 (1 H, ddd, J_{4,F} 50.3, J_{4,5} 9.5, J_{4,3} 8.8 Hz, H4), 4.10 (1 H, dd, J_{5,4} 9.5, J_{5,F} 3.6 Hz, H5), 3.72 (1 H, ddd, J_{3,F} 16.3, J_{3,4} = J_{3,2} 8.8 Hz, H3), 3.34 (1 H, dd, J_{2,3} 8.8, J_{2,1} 7.8 Hz, H2); ¹⁹F NMR (188 MHz, (CD₃)₂CO) δ -122.26 (dd, J_{F,4} 50.3, J_{F,3} 16.3 Hz); **Anal. calc. for** C₁₃H₁₅FO₆: C, 54.55; H, 5.28. Found: C, 54.43; H, 5.33.

5.4.3 Methyl 4-deoxy-4-fluoro-β-D-glucopyranosiduronic acid (**5**) (Scheme 3.1)

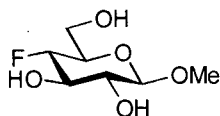
Methyl 2,3,6-tri-O-benzoyl-β-D-galactopyranoside (**20**)⁸⁵



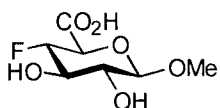
Prepared from methyl β-D-galactopyranoside according to the literature procedure⁸⁵: ¹H NMR (200 MHz, CDCl₃) δ 8.10-7.90 (6 H, m, Ar), 7.63-7.30 (9 H, m, Ar), 5.76 (1 H, dd, J_{2,3} 10.2, J_{2,1} 7.8 Hz, H2), 5.35 (1 H, dd, J_{3,2} 10.2, J_{3,4} 3.2 Hz, H3), 4.70 (1 H, dd, J_{6a,6b} 11.5, J_{6a,5} 6.6 Hz, H6_a), 4.65 (1 H, d, J_{1,2} 7.8 Hz, H1), 4.60 (1 H, dd, J_{6b,6a} 11.5, J_{6b,5} 6.4 Hz, H6_b), 4.34 (1 H, dd, J_{4,OH} 5.3, J_{4,3} 3.2 Hz, H4), 4.07 (1 H, dd, J_{5,6a} 6.6, J_{5,6b} 6.4 Hz, H5), 3.52 (3 H, s, OMe), 2.59 (1 H, d, J_{OH,4} 5.3 Hz, 4-OH).

Methyl 2,3,6-tri-O-benzoyl-4-deoxy-4-fluoro- β -D-glucopyranoside (25)⁸⁸

Prepared from **20** as described for **23**. Purified by column chromatography (toluene:EtOAc 31:1) to give **25** as a yellow-brown foam (54%): ¹H NMR (200 MHz, CDCl₃) δ 8.13-7.90 (6 H, m, Ar), 7.65-7.30 (9 H, m, Ar), 5.82 (1 H, ddd, $J_{3,F}$ 14.1, $J_{3,2}$ = $J_{3,4}$ 9.3 Hz, H3), 5.41 (1 H, dd, $J_{2,3}$ 9.3, $J_{2,1}$ 7.8 Hz, H2), 4.79 (1 H, ddd, $J_{4,F}$ 50.2, $J_{4,5}$ = $J_{4,3}$ 9.3 Hz, H4), 4.69 (1 H, d, $J_{1,2}$ 7.8 Hz, H1), 4.80-4.50 (2 H, m, H6_a, H6_b), 4.03 (1 H, dddd, $J_{5,4}$ 9.3, $J_{5,6a}$ 7.8, $J_{5,6b}$ 5.0, $J_{5,F}$ 2.6 Hz, H5), 3.50 (3 H, s, OMe); ¹⁹F NMR (188 MHz, CDCl₃) δ -123.50 (dd, $J_{F,4}$ 50.2, $J_{F,3}$ 14.1 Hz).

Methyl 4-deoxy-4-fluoro- β -D-glucopyranoside (26)⁸⁸

Zemplén deprotection of **25** with sodium methoxide was carried out according to the general procedure. The crude product was washed with Et₂O to remove methyl benzoate, leaving **26** as a white solid (81%): ¹H NMR (200 MHz, CD₃OD) δ 4.22 (1 H, ddd, $J_{4,F}$ 50.7, $J_{4,3}$ 9.6, $J_{4,5}$ 8.6 Hz, H4), 4.21 (1 H, d, $J_{1,2}$ 7.8 Hz, H1), 3.83 (1 H, ddd, $J_{6a,6b}$ 12.2, $J_{6a,5}$ = $J_{6a,F}$ 2.2 Hz, H6_a), 3.74-3.55 (2 H, m, H3, H6_b), 3.52 (3 H, s, OMe), 3.54-3.40 (1 H, m, H5), 3.17 (1 H, dd, $J_{2,3}$ 9.5, $J_{2,1}$ 7.8 Hz, H2); ¹⁹F NMR (188 MHz, CD₃OD) δ -122.31 (dd, $J_{F,4}$ 50.7, $J_{F,3}$ 14.1 Hz).

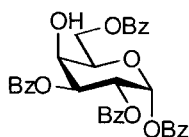
Methyl 4-deoxy-4-fluoro- β -D-glucopyranosiduronic acid (5)

Prepared from **26** as described for **4**. Purified by column chromatography (EtOAc:MeOH:H₂O 7:2:1 + 0.4% acetic acid), passed down an ion exchange column (Bio-Rad[®] AG 50W-X2, 200-400 mesh, H⁺ form), and freeze-dried to give **5** as a white solid (74%): ¹H NMR (200 MHz, CD₃OD) δ 4.33 (1 H, ddd, $J_{4,F}$ 50.4, $J_{4,5}$ 9.5, $J_{4,3}$ 8.7

H_z, H₄), 4.28 (1 H, d, $J_{1,2}$ 7.8 Hz, H₁), 3.99 (1 H, dd, $J_{5,4}$ 9.5, $J_{5,F}$ 3.1 Hz, H₅), 3.64 (1 H, ddd, $J_{3,F}$ 16.1, $J_{3,4}$ 8.7, $J_{3,2}$ 9.3 Hz, H₃), 3.52 (3 H, s, OMe), 3.23 (1 H, dd, $J_{2,3}$ 9.3, $J_{2,1}$ 7.8 Hz, H₂); ^{19}F NMR (188 MHz, CD₃OD) δ -121.12 (ddd, $J_{F,4}$ 50.4, $J_{F,3}$ 16.1, $J_{F,5}$ 3.1 Hz); **Anal. calc.** for C₇H₁₁FO₆ + 0.5 H₂O: C, 38.36; H, 5.52. Found: C, 38.44; H, 5.56.

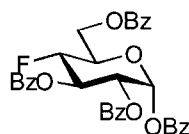
5.4.4 Benzyl *O*-(4-deoxy-4-fluoro- β -D-glucopyranosiduronic acid)-(1 \rightarrow 3)-2-acetamido-2-deoxy- β -D-galactopyranoside (**6**) (Schemes 3.2, 3.3 and 3.4)

1,2,3,6-Tetra-*O*-benzoyl- α -D-galactopyranose (**27**)^{92,93}



A solution of benzoyl chloride (52.85 mL, 455 mmol, 4.1 eq) in dry pyridine (20 mL) was added dropwise to a solution of galactose (20 g, 111 mmol) in dry pyridine (400 mL) at 0 °C. The reaction was stirred for 1 h at this temperature and then ice was added. The reaction was extracted with CH₂Cl₂ (4x) and the combined organic phases washed with 1 M HCl (4x), saturated NaHCO₃ (1x), half-saturated NaHCO₃ (2x), H₂O (1x), dried over MgSO₄, and concentrated under vacuum. The residue was purified by column chromatography (toluene:EtOAc 8:1) to give **27** as an amorphous solid (9.62 g, 15%): ^1H NMR (200 MHz, CDCl₃) δ 8.14-7.80 (10 H, m, Ar), 7.60-7.10 (10 H, m, Ar), 6.82 (1 H, d, $J_{1,2}$ 3.6 Hz, H₁), 6.07 (1 H, dd, $J_{2,3}$ 10.8, $J_{2,1}$ 3.6 Hz, H₂), 5.88 (1 H, dd, $J_{3,2}$ 10.8, $J_{3,4}$ 2.9 Hz, H₃), 4.77 (1 H, dd, $J_{6a,6b}$ 9.6, $J_{6a,5}$ 5.2 Hz, H_{6a}), 4.60-4.40 (3 H, m, H₄, H₅, H_{6b}).

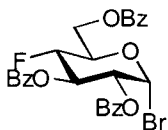
1,2,3,6-Tetra-*O*-benzoyl-4-deoxy-4-fluoro- α -D-glucopyranose (**28**)



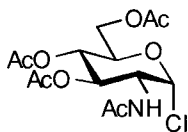
Compound **28** was prepared from **27** by reaction with DAST as described for **4**. The crude product was crystallized from EtOAc/PE to give **28** as a white solid (63%): ^1H NMR (200 MHz, CDCl₃) δ 8.20-7.90 (6 H, m, Ar), 7.85 (2 H, d, J 8.8 Hz, Ar), 7.75-7.20 (12 H, m, Ar), 6.76 (1 H, dd, $J_{1,2} = J_{1,F}$ 3.4 Hz, H₁), 6.25 (1 H, ddd, $J_{3,F}$ 13.4, $J_{3,2}$ 10.3, $J_{3,4}$

9.2 Hz, H3), 5.56 (1 H, dd, $J_{2,3}$ 10.3, $J_{2,1}$ 3.4 Hz, H2), 4.93 (1 H, ddd, $J_{4,F}$ 50.3, $J_{4,3} = J_{4,5}$ 9.2 Hz, H4), 4.70-4.62 (2 H, m, H6_a, H6_b), 4.50 (1 H, m, H5); ^{13}C NMR (75 MHz, CDCl_3) δ 166.02, 165.66, 165.35, 164.24 (4 C=O), 134.04, 133.57, 133.33, 130.03, 129.90, 129.72, 129.50, 128.91, 128.80, 128.74, 128.47, 128.36, 89.69 (CH, C1), 86.70 (CH, d, $J_{4,F}$ 190.8 Hz, C4), 70.42 (CH, d, $J_{3,F}$ 20.5 Hz, C3), 69.82 (CH, d, $J_{2,F}$ 7.6 Hz, C2), 69.81 (CH, d, $J_{5,F}$ 23.5 Hz, C5), 61.99 (CH_2 , C6); ^{19}F NMR (188 MHz, CDCl_3) δ -121.86 (dd, $J_{F,4}$ 50.3, $J_{F,3}$ 13.4 Hz); **Anal. calc. for** $\text{C}_{34}\text{H}_{27}\text{FO}_9$: C, 68.22; H, 4.55. Found: C, 68.52; H, 4.52.

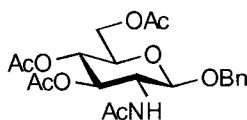
2,3,6-Tri-O-benzoyl-4-deoxy-4-fluoro- α -D-glucopyranosyl bromide (**29**)



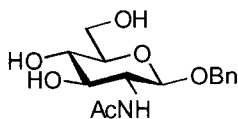
A solution of HBr (4.6 mL, 5.7 M in acetic acid) was added to a solution of **28** (2.63 g, 4.39 mmol) in dry CH_2Cl_2 (13 mL) at 0 °C. Upon completion of the addition the reaction mixture was allowed to warm to ambient temperature, and stirred overnight (15 hours). The reaction was then poured into an ice/water mixture, and extracted twice with CH_2Cl_2 . The combined organic phases were washed with saturated NaHCO_3 (3x), H_2O (1x), dried over MgSO_4 , and concentrated leaving a white solid which was recrystallized from EtOAc/PE to give **29** as a fine white solid (1.77 g, 72%). The supernatant was concentrated to give an additional 619 mg (25%) of **29**: ^1H NMR (200 MHz, CDCl_3) δ 8.15-7.90 (6 H, m, Ar), 7.70-7.30 (9 H, m, Ar), 6.74 (1 H, dd, $J_{1,2}$ 3.9, $J_{1,F}$ 2.8 Hz, H1), 6.20 (1 H, ddd, $J_{3,F}$ 13.5, $J_{3,2}$ 10.0, $J_{3,4}$ 9.0 Hz, H3), 5.21 (1 H, ddd, $J_{2,3}$ 10.0, $J_{2,1}$ 3.9, $J_{2,F}$ 0.7 Hz, H2), 4.88 (1 H, ddd, $J_{4,F}$ 49.0, $J_{4,5}$ 9.2, $J_{4,3}$ 9.0 Hz, H4), 4.80-4.55 (3 H, m, H5, H6_a, H6_b); ^{13}C NMR (75 MHz, CDCl_3) δ 165.94, 165.31, 165.27 (3 C=O), 133.89, 133.53, 133.42, 130.07, 129.84, 129.79 (6 CH), 129.38, 128.85 (2 C), 128.57, 128.53, 128.44 (3 CH), 128.16 (C), 86.10 (CH, C1), 85.98 (CH, d, $J_{4,F}$ 188.0 Hz, C4), 72.00 (CH, d, $J_{5,F}$ 24.2 Hz, C5), 70.86 (CH, d, $J_{2,F}$ 8.1 Hz, C2), 70.53 (CH, d, $J_{3,F}$ 20.2 Hz, C3), 61.54 (CH_2 , C6); ^{19}F NMR (188 MHz, CDCl_3) δ -121.90 (dd, $J_{F,4}$ 49.0, $J_{F,3}$ 13.5 Hz); **Anal. calc. for** $\text{C}_{27}\text{H}_{22}\text{BrFO}_7$: C, 58.18; H, 3.98. Found: C, 58.43; H, 4.01.

2-Acetamido-3,4,6-tri-O-acetyl-2-deoxy- α -D-glucosyl chloride (30)⁹⁴

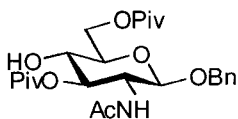
Acetyl chloride (25 mL, 352 mmol) was added to 2-acetamido-2-deoxy-D-glucose (10.0 g, 45.2 mmol) in a 100 mL round bottom flask equipped with a condenser. After ~ 4 hours the starting material had dissolved. The reaction was stirred for 3 days, diluted with CH_2Cl_2 and poured onto an ice/ H_2O mixture. The organic phase was washed with saturated NaHCO_3 (3x), dried over MgSO_4 , and concentrated to about 8 mL at 45 °C. Et_2O (75 mL) was then added with stirring, causing **30** to precipitate as a slightly yellow solid (12.14 g, 73 %): ^1H NMR (200 MHz, CDCl_3) δ 6.17 (1 H, d, $J_{1,2}$ 3.9 Hz, H1), 5.79 (1 H, d, $J_{\text{NH},2}$ 8.4 Hz, NH), 5.30 (1 H, dd, $J_{3,2} = J_{3,4}$ 10.0 Hz, H3), 5.19 (1 H, dd, $J_{4,3} = J_{4,5}$ 9.4 Hz, H4), 4.51 (1 H, ddd, $J_{2,3}$ 10.0, $J_{2,\text{NH}}$ 8.4, $J_{2,1}$ 3.9 Hz, H2), 4.32-4.05 (3 H, m, H5, H6_a, H6_b), 2.08, 2.03, 1.96 (12 H, 3 s, 4 Ac).

Benzyl 2-acetamido-3,4,6-tri-O-acetyl-2-deoxy- β -D-glucopyranose (31)⁹⁵

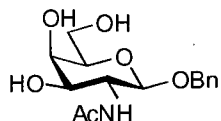
Prepared from **30** as described for **15**. The residue was purified by column chromatography (PE:EtOAc, 1:3 to 1:4.5), to yield **31** as a white solid (64%): ^1H (200 MHz, CDCl_3): δ 7.35-7.26 (5 H, m, Ar), 5.30 (1 H, d, $J_{\text{NH},2}$ 9.3 Hz, NH), 5.18 (1 H, dd, $J = J$ 9.3 Hz, H3 or H4), 5.07 (1 H, dd, $J = J$ 9.3 Hz, H3 or H4), 4.87 (1 H, d, J 12.2 Hz, OCH_2Ph), 4.60 (1 H, d, $J_{1,2}$ 8.3 Hz, H1), 4.57 (1 H, d, J 12.2 Hz, OCH_2Ph), 4.26 (1 H, dd, $J_{6\text{ax},6\text{eq}}$ 12.4, $J_{6\text{ax},5}$ 4.6 Hz, H6_{ax}), 4.14 (1 H, dd, $J_{6\text{eq},6\text{ax}}$ 12.4, $J_{6\text{eq},5}$ 2.2 Hz, H6_{eq}), 3.94 (1 H, ddd, $J_{2,3} = J_{2,\text{NH}}$ 9.3 Hz, $J_{2,1}$ 8.3 Hz, H2), 3.64 (1 H, ddd, $J_{5,4}$ 9.3, $J_{5,6\text{ax}}$ 4.6, $J_{5,6\text{eq}}$ 2.2 Hz, H5), 2.09, 2.00, 1.89 (9 H, 3 s, Ac).

Benzyl 2-acetamido-2-deoxy- β -D-glucopyranoside (32)⁹⁵

Zemplén deprotection of **31** with sodium methoxide according to the general procedure gave **32** as a white solid in a quantitative yield: ¹H NMR (200 MHz, CD₃OD) δ 7.30 (5 H, s, Ar), 4.85 (1 H, d, J 12.0 Hz, OCH₂Ph), 4.56 (1 H, d, J 12.0 Hz, OCH₂Ph), 4.42 (1 H, d, J_{1,2} 8.3 Hz, H1), 3.88 (1 H, dd, J_{6a,6b} 12.2, J_{6a,5} 2.0 Hz, H6_a), 3.74-3.62 (2 H, m), 3.48-3.20 (3 H, m), 1.94 (3 H, s, Ac).

Benzyl 2-acetamido-2-deoxy-3,6-di-O-pivaloyl- β -D-glucopyranoside (33)⁹⁶

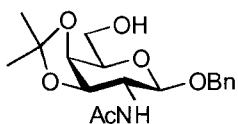
A mixture of **32** (6.17 g, 19.8 mmol) in dry CH₂Cl₂ (55 mL) and dry pyridine (65 mL) was cooled to 0 °C before pivaloyl chloride (6.8 mL, 55.5 mmol, 2.8 eq) was added dropwise. The reaction mixture was stirred at 0 °C for 3 h, diluted with CH₂Cl₂, washed with saturated NaHCO₃ (3x), H₂O (1x), dried over MgSO₄, and concentrated under vacuum leaving a white foam that was recrystallized from EtOAc/hexanes to give **33** as a white solid (8.36 g, 88%): ¹H (400 MHz, CDCl₃) δ 7.35-7.25 (5 H, m, Ar), 5.61 (1 H, d, J_{NH,2} 9.3 Hz, NH), 4.98 (1 H, dd, J_{3,2} 10.5, J_{3,4} 8.8 Hz, H3), 4.84 (1 H, d, J 12.3 Hz, OCH₂Ph), 4.56 (1 H, d, J 12.3 Hz, OCH₂Ph), 4.45 (1 H, d, J_{1,2} 8.4 Hz, H1), 4.42-4.34 (2 H, m, H6_a, H6_b), 4.00 (1 H, ddd, J_{2,3} 10.5, J_{2,NH} 9.3, J_{2,1} 8.4 Hz, H2), 3.54-3.46 (2 H, m, H4, H5), 3.03 (1 H, s, br, 4-OH), 1.84 (3 H, s, Ac), 1.23, 1.15 (18 H, 2 s, 2 C(CH₃)₃).

Benzyl 2-acetamido-2-deoxy- β -D-galactopyranoside (34)⁹⁶

Trifluoromethanesulfonic anhydride (3.84 mL, 22.8 mmol, 1.3 eq) was added dropwise to a solution of **33** (8.36 g, 17.4 mmol) in dry CH₂Cl₂ (100 mL) and dry pyridine (8.4 mL) at -15 °C. The reaction mixture was stirred at this temperature for 1 h

45 min, then allowed to warm to ambient temperature. H₂O (10 mL) was added, and the solution heated to 90 °C for 3 h. The reaction was cooled, diluted with CH₂Cl₂, washed with saturated NaHCO₃ (3x), H₂O (1x), dried over MgSO₄, and concentrated under vacuum. After drying under high vacuum for a couple of hours the residue was taken up in dry methanol (100 mL) and sodium methoxide added to make the solution basic. The mixture was stirred overnight, diluted with methanol to dissolve any solid present, neutralized with Amberlite® IR-120 (H⁺) resin, filtered, and concentrated under vacuum. The residue was recrystallized from 2-propanol or methanol/ether to yield **34** as a white solid (4.41 g, 81%): ¹H NMR (200 MHz, (CD₃)₂SO + D₂O) δ 7.73 (1 H, d, J_{NH,2} 9.2 Hz, NH), 7.40-7.20 (5 H, m, Ar), 4.76 (1 H, d, J 12.5 Hz, OCH₂Ph), 4.50 (1 H, d, J 12.5 Hz, OCH₂Ph), 4.34 (1 H, d, J_{1,2} 8.2 Hz, H1), 3.78 (1 H, ddd, J_{2,3} 10.8, J_{2,NH} 9.2, J_{2,1} 8.2 Hz, H2), 3.65 (1 H, d, J_{4,3} 2.9 Hz, H4), 3.60-3.50 (2 H, m, H_{6a}, H_{6b}), 3.44 (1 H, dd, J_{3,2} 10.8, J_{3,4} 2.9 Hz, H3), 3.34 (1 H, dd, J_{5,6a} = J_{5,6b} 5.9 Hz, H5), 1.82 (3 H, s, Ac).

Benzyl 2-acetamido-2-deoxy-3,4-isopropylidene-β-D-galactopyranoside (35)⁹⁶

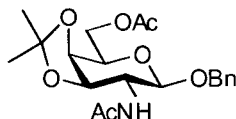


A solution of **34** (2.0 g, 6.4 mmol) and toluenesulfonic acid (75 mg, 0.4 mmol, 0.06 eq) in 2,2-dimethoxypropane (65 mL) was stirred at rt overnight. Acetone was added to clarify the solution, and after an additional 2.5 h triethylamine (0.4 mL) was added to quench the reaction. The solvent was removed under vacuum and the residue dissolved in 10:1 MeOH:H₂O (70 mL) and acetic acid (0.4 mL) and heated at 45 °C for 2.5 h at which time the TLC indicated the disappearance of the faster running C6-methoxyisopropyl compound. Triethylamine (1.75 mL) was added and the solvent removed under vacuum. The residue was crystallized from EtOAc/hexanes to give **35** as a white solid (1.92 g, 85%): ¹H NMR (200 MHz, CDCl₃) δ 7.30 (5 H, s, Ph), 5.87 (1 H, d, J_{NH,2} 7.5 Hz, NH), 5.03 (1 H, d, J_{1,2} 8.6 Hz, H1), 4.85 (1 H, d, J 11.8 Hz, CH₂Ph), 4.68 (1 H, dd, J_{3,2} 8.6, J_{3,4} 5.6 Hz, H3), 4.58 (1 H, d, CH₂Ph), 4.13 (1 H, dd, J_{4,5} 1.3, J_{4,3} 5.6 Hz, H4), 4.02-3.75 (3 H, m, H5, H_{6a}, H_{6b}), 3.17 (1 H, ddd, J_{2,1} = J_{2,3} 8.6, J_{2,NH} 7.5 Hz, H2), 1.95 (3 H, s, NAc), 1.50, 1.30 (6 H, 2 s, C(CH₃)₂); ¹³C NMR (100 MHz, CDCl₃) δ 170.74 (C=O), 137.38

(C), 128.80 (CH), 128.48 (CH), 128.41 (CH), 128.08 (CH), 127.95 (CH), 110.11 (C), 98.96 (CH, C1), 75.46 (CH), 73.68 (CH), 73.38 (CH), 71.44 (CH₂), 62.55 (CH₂), 57.70 (CH), 28.12 (CH₃), 26.21 (CH₃), 23.55 (CH₃).

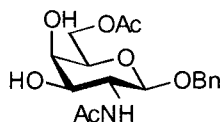
Benzyl 2-acetamido-6-O-acetyl-2-deoxy-3,4-isopropylidene-β-D-galactopyranoside

(36)

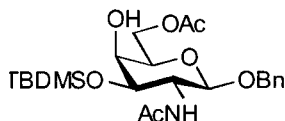


Zemplén deprotection of **35** with sodium methoxide according to the general procedure gave **36** as a white solid (99%): ¹H NMR (200 MHz, CDCl₃) δ 7.30 (5 H, s, Ph), 5.80 (1 H, d, J_{NH,2} 6.8 Hz, NH), 5.02 (1 H, s, J_{1,2} 8.6 Hz, H1), 4.87 (1 H, d, J 11.8 Hz, CH₂Ph), 4.71 (1 H, dd, J_{3,2} 8.3, J_{3,4} 5.4 Hz, H3), 4.55 (1 H, d, CH₂Ph), 4.37 (2 H, m, H6_a, H6_b), 4.07 (1 H, dd, J_{4,5} 2.2, J_{4,3} 5.4 Hz, H4), 4.05 (1 H, ddd, J_{5,6ax} 6.8, J_{5,6eq} 5.1, J_{5,4} 2.2 Hz, H5), 3.12 (1 H, ddd, J_{2,1} 8.3, J_{2,3} 8.3, J_{2,NH} 6.8 Hz, H2), 2.10, 1.93 (6 H, 2 s, 2 Ac), 1.50, 1.31 (6 H, 2 s, 2 CH₃).

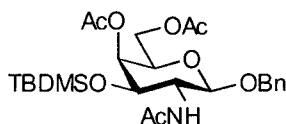
Benzyl 2-acetamido-6-O-acetyl-2-deoxy-β-D-galactopyranoside (37)



A solution of **36** (2.21 g, 5.62 mmol) in 4:1 acetic acid:H₂O (35 mL) was heated to 50 °C for 4 h, concentrated under vacuum, and the resulting solid crystallized from methanol/ether/hexanes to give **37** as a white solid (1.59 g, 80%): ¹H NMR (200 MHz, CD₃OD) δ 7.30 (5 H, m, Ph), 4.84 (1 H, d, J 12.2 Hz, CH₂Ph), 4.58 (1 H, d, CH₂Ph), 4.44 (1 H, d, J_{1,2} 8.3 Hz, H1), 4.29 (2 H, m, H6_a, H6_b), 3.98 (1 H, dd, J_{2,1} 8.3, J_{2,3} 10.8 Hz, H2), 3.81 (1 H, dd, J_{4,3} 3.4, J_{4,5} 0.6 Hz, H4), 3.70 (1 H, ddd, J_{5,6ax} 7.1, J_{5,6eq} 5.1, J_{5,4} 0.6 Hz, H5), 3.60 (1 H, dd, J_{3,4} 3.4, J_{3,2} 10.8 Hz, H3), 2.08, 1.95 (6 H, 2 s, 2 Ac); ¹³C NMR (75 MHz, CD₃OD + CD₂Cl₂) δ 173.60 (C=O), 172.18 (C=O), 138.35 (C), 128.94 (CH), 128.56 (CH), 128.46 (CH), 128.38 (CH), 101.10 (CH, C1), 73.33 (CH), 72.48 (CH), 71.15 (CH₂), 69.00 (CH), 64.27 (CH₂), 53.83 (CH), 22.98 (Ac), 20.90 (Ac); **Anal. calc. for** C₁₇H₂₃NO₇: C, 57.78; H, 6.56; N, 3.96. Found: C, 57.79; H, 6.58; N, 4.08.

Benzyl 2-acetamido-6-O-acetyl-2-deoxy-3-O-tert-butyldimethylsilyl-β-D-galactopyranoside (38)

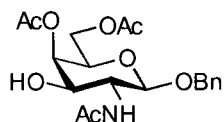
A solution of **37** (100 mg, 0.28 mmol), *t*-butyldimethylsilyl chloride (85 mg, 0.56 mmol, 2 eq), and imidazole (77 mg, 1.13 mmol, 4 eq) in dry DMF (1.6 mL) was heated to 80 °C under argon for 2 h, cooled, diluted with EtOAc, washed with saturated NaHCO₃ (2x), H₂O (1x), dried over MgSO₄, and concentrated. The residue was purified by column chromatography (PE:EtOAc 1:1) to yield **38** as a white crystalline solid (104 mg, 79%): ¹H NMR (200 MHz, CDCl₃) δ 7.30 (5 H, m, Ph), 5.53 (1 H, d, J_{NH,2} 7.3 Hz, NH), 5.05 (1 H, d, J_{1,2} 8.6 Hz, H1), 4.89 (1 H, d, J 11.8 Hz, OCH₂Ph), 4.57 (1 H, d, OCH₂Ph), 4.45 (1 H, dd, J_{3,2} 10.2, J_{3,4} 3.9 Hz, H3), 4.37 (2 H, d, J_{6,5} 6.0 Hz, H_{6a}, H_{6b}), 3.80-3.70 (2 H, m, H4, H5), 3.28 (1 H, ddd, J_{2,NH} 7.3, J_{2,1} 8.6, J_{2,3} 10.2 Hz, H2), 2.10, 1.90 (6 H, 2 s, 2 Ac), 0.88 (9 H, s, C(CH₃)₃), 0.08, 0.05 (6 H, 2 s, Si(CH₃)₂); ¹³C NMR (100 MHz, CDCl₃) δ 170.81 (C=O), 170.52 (C=O), 137.40 (C), 128.34 (CH), 128.14 (CH), 127.84 (CH), 98.26 (CH, C1), 71.74 (CH), 70.87 (CH₂), 70.06 (CH), 69.02 (CH), 63.40 (CH₂), 56.10 (CH), 25.60 (C(CH₃)₃), 23.67 (Ac), 20.90 (Ac), 17.86 (C(CH₃)₃), -4.74, -4.84 (Si(CH₃)₂); **Anal. calc. for** C₂₃H₃₇NO₇Si: C, 59.07; H, 7.97; N, 3.00. Found: C, 59.39; H, 7.93; N, 3.21.

Benzyl 2-acetamido-4,6-di-O-acetyl-2-deoxy-3-O-tert-butyldimethylsilyl-β-D-galactopyranoside (39)

4-Dimethylaminopyridine (DMAP) (85 mg, 0.70 mmol, 0.22 eq) was added to a solution of **38** (1.51 g, 3.23 mmol) in dry pyridine (12 mL) and acetic anhydride (3.4 mL), and the reaction mixture was stirred for 1 h at rt, and concentrated under vacuum. The residue was crystallized from EtOAc/hexanes to give **39** as fine white crystals (1.57 g, 95%): ¹H NMR (200 MHz, CDCl₃) δ 7.30 (5 H, s, Ph), 5.48 (1 H, d, J_{NH,2} 7.3 Hz, NH), 5.21 (1 H, d, J_{4,3} 3.4 Hz, H4), 5.13 (1 H, d, J_{1,2} 8.2 Hz, H1), 4.88 (1 H, d, J 12.1 Hz, OCH₂Ph), 4.58 (1 H, d, OCH₂Ph), 4.42 (1 H, dd, J_{3,2} 10.0, J_{3,4} 3.4 Hz, H3), 4.13 (2 H, m,

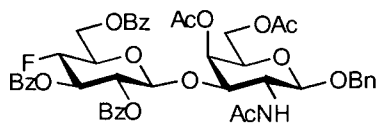
H_{6a}, H_{6b}), 3.87 (1 H, ddd, J_{5,6a} 5.6, J_{5,6b} 5.5, J_{5,4} 0.9 Hz, H5), 3.32 (1 H, ddd, J_{2,NH} 7.3, J_{2,1} 8.2, J_{2,3} 10.0 Hz, H2), 2.09, 2.07, 1.88 (9 H, 3 s, 3 Ac), 0.81 (9 H, s, C(CH₃)₃), 0.05, 0.00 (6 H, 2 s, Si(CH₃)₂); ¹³C NMR (75 MHz, CDCl₃) δ 170.55 (C=O), 170.35 (C=O), 170.14 (C=O), 137.26 (C), 128.38 (CH), 128.16 (CH), 127.93 (CH), 98.54 (CH, C1), 71.21 (CH₂), 70.95 (CH), 69.62 (CH), 68.51 (CH), 62.47 (CH₂), 56.75 (CH), 25.51 (C(CH₃)₃), 23.71 (Ac), 20.78 (Ac), 20.75 (Ac), 17.75 (C(CH₃)₃), -4.82, -5.12 (Si(CH₃)₂); **Anal. calc.** for C₂₅H₃₉NO₈Si: C, 58.92; H, 7.71; N, 2.75. Found: C, 58.92; H, 7.79; N, 2.88.

Benzyl 2-acetamido-4,6-di-O-acetyl-2-deoxy-β-D-galactopyranoside (40)



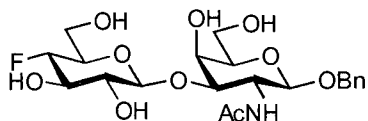
Tetrabutylammonium fluoride (1 M in THF, 6 mL, 6.0 mmol, 4 eq) was added dropwise to a solution of **39** (766 mg, 1.5 mmol) in THF (10 mL). The reaction mixture was stirred for 20 min at rt, diluted with CH₂Cl₂, washed with saturated NaHCO₃ (2x), H₂O (1x). The combined aqueous phases were extracted once with CH₂Cl₂. The combined organic phases were dried over MgSO₄, and concentrated under vacuum. The resulting solid was recrystallized twice from EtOAc/hexanes to give **40** as a white solid (164 mg, 28%). The supernatants were concentrated and purified by column chromatography (EtOAc:MeOH 14:1) to give an additional 126 mg of product (total yield 49%): mp 172-173 °C; ¹H NMR (200 MHz, CDCl₃) δ 7.45-7.30 (5 H, m, Ar), 5.48 (1 H, d, J_{NH,2} 5.2 Hz, NH), 5.30 (1 H, dd, J_{4,3} 3.5, J_{4,5} 0.9 Hz, H4), 4.91 (1 H, d, J 12.0 Hz, OCH₂Ph), 4.59 (1 H, d, OCH₂Ph), 4.59 (1 H, d, J_{OH,3} 3.5 Hz, 3-OH), 4.48 (1 H, d, J_{1,2} 8.2 Hz, H1), 4.18 (2 H, d, J_{6,5} 6.3 Hz, H_{6a}, H_{6b}), 3.90 (1 H, ddd, J_{3,2} 10.3, J_{3,4} = J_{3,OH} 3.5 Hz, H3), 3.81 (1 H, dt, J_{5,6} 6.3, J_{5,4} 0.9 Hz, H5), 3.71 (1 H, ddd, J_{2,3} 10.6, J_{2,1} 8.2, J_{2,NH} 5.2 Hz, H2), 2.15, 2.07, 1.95 (9 H, 3 s, 3 Ac); **Anal. calc.** for C₁₉H₂₅NO₈: C, 57.71; H, 6.37; N, 3.54. Found: C, 57.93; H, 6.35; N, 3.60.

Benzyl O-(2,3,6-tri-O-benzoyl-4-deoxy-4-fluoro- β -D-glucopyranosyl)-(1 \rightarrow 3)-2-acetamido-4,6-di-O-acetyl-2-deoxy- β -D-galactopyranoside (41**)**



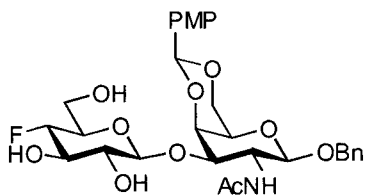
A mixture of **40** (425 mg, 1.08 mmol), **29** (1.198 g, 2.15 mmol, 2 eq), and powdered 4 Å molecular sieves in dry CH₂Cl₂ (25 mL) was stirred at rt under argon for 1 h before silver trifluoromethanesulfonate (828 mg, 3.22 mmol, 3 eq) was added. The reaction flask was covered in foil and stirred at rt for 4.5 h. Pyridine (0.6 mL) was added to quench, and the reaction mixture was diluted with CH₂Cl₂, filtered, washed with 5% Na₂S₂O₃ (1x), saturated NaHCO₃ (1x), H₂O (1x), dried over MgSO₄, and concentrated in vacuo. The residue was purified by column chromatography (PE:EtOAc 2:3) to yield **41** as a white crystalline solid (302 mg, 32%): ¹H NMR (400 MHz, CDCl₃) δ 8.12-8.07 (2 H, m, Ar), 7.96-7.88 (3 H, m, Ar), 7.70-7.60 (15 H, m, Ar), 5.76 (1 H, ddd, J_{3',F} 14.7, J_{3',4'} 9.1, J_{3',2'} 9.7 Hz, H3'), 5.45 (1 H, d, J_{4,3} 3.2 Hz, H4), 5.32 (1 H, dd, J_{2',1'} 7.8, J_{2',3'} 9.7 Hz, H2'), 5.25 (1 H, d, J_{NH,2} 6.3 Hz, NH), 5.03 (1 H, d, J_{1,2} 8.3 Hz, H1), 4.84 (1 H, d, J_{1',2'} 7.8 Hz, H1'), 4.80 (1 H, d, J 11.8 Hz, OCH₂Ph), 4.78 (1 H, dd, J_{3,2} 10.8, J_{3,4} 3.23 Hz, H3), 4.73 (1 H, ddd, J_{4',F} 50.1, J_{4',3'} = J_{4',5'} 6.3 Hz, H4'), 4.66 (1 H, m H_{6a}), 4.58 (1 H, dd, J_{6b,6a} 11.2, J_{6b,5} 4.2 Hz, H_{6b}), 4.48 (1 H, d, J 11.8 Hz, OCH₂Ph), 4.02-3.95 (3 H, m, H5, H_{6a}', H_{6b}'), 3.75 (1 H, ddd, J_{5',6a'} = J_{5',6b'} 6.2, J_{5',4'} 6.3 Hz, H5'), 3.12 (1 H, ddd, J_{2,3} 10.8, J_{2,1} 8.3, J_{2,NH} 6.3 Hz, H2), 2.01, 1.97 (6 H, 2 s, 2 OAc), 1.36 (3 H, s, NAc); ¹³C NMR (50 MHz, CDCl₃) δ 171.15, 170.58, 169.73, 166.15, 165.62, 164.86 (6 C=O), 137.10, 133.70, 133.56, 133.31, 129.95, 129.83, 129.17, 129.00, 128.74, 128.614, 128.53, 128.50, 128.28, 128.19, 101.50, 98.12, 87.10 (CH, d, J_{4',F} 187.0 Hz, C4'), 91.96, 75.13, 72.76 (CH, d, J 19.8 Hz), 71.81, 71.65, 71.54, 71.38, 69.24, 62.43, 55.62, 23.08, 20.87, 20.82 (3 Ac); ¹⁹F NMR (188 MHz, CDCl₃) δ -123.76 (dd, J_{F,4'} 50.1, J_{F,3'} 14.7 Hz); **Anal. calc. for** C₄₆H₄₆FNO₁₅: C, 63.37; H, 5.32; N, 1.61. Found: C, 63.34; H, 5.38; N, 1.63.

Benzyl O-(4-deoxy-4-fluoro- β -D-glucopyranosyl)-(1 \rightarrow 3)-2-acetamido-2-deoxy- β -D-galactopyranoside (42)



Zemplén deprotection of **41** with sodium methoxide was performed according to the general procedure. The product was crystallized from methanol/ether/hexanes to yield **42** as fine white crystals (75%). The supernatant was concentrated and purified by column chromatography (EtOAc:MeOH:H₂O 13:2:1) to yield an additional 15 mg of **42** (total yield 84%): decomposition at ~ 214 °C; ¹H NMR (400 MHz, D₂O) δ 7.50–7.30 (5 H, m, Ar), 4.87 (1 H, d, *J* 12.2 Hz, OCH₂Ph), 4.67 (1 H, d, *J* 12.2 Hz, OCH₂Ph), 4.51 (1 H, d, *J*_{1,2} 8.6 Hz, H1), 4.47 (1 H, d, *J*_{1',2'} 7.9 Hz, H1'), 4.29 (1 H, ddd, *J*_{4',F} 50.7, *J*_{4',3'} = *J*_{4',5'} 9.2 Hz, H4'), 4.14 (1 H, d, *J*_{4,3} 2.8 Hz, H4), 3.96 (1 H, dd, *J*_{2,3} 10.8, *J*_{2,1} 8.6 Hz, H2), 3.90–3.79 (6 H, m, H3, H3', H5, H6_a, H6_b, H6_{a'}), 3.79–3.55 (2 H, m, H5', H6_{b'}), 3.31 (1 H, dd, *J*_{2',3'} 9.3, *J*_{2',1'} 7.9 Hz, H2'), 1.92 (3 H, s, NAc); ¹³C NMR (75 MHz, D₂O) δ 174.88 (C=O), 136.99, 128.96, 128.86, 128.68, 104.42, 100.25 (2 CH), 88.94 (CH, d, *J*_{4',F} 179.2 Hz, C4'), 80.50, 75.04, 73.74 (CH, d, *J*_{3',F} 18.1 Hz, C3'), 73.24 (CH, d, *J*_{5',F} 24.2 Hz, C5'), 72.68 (CH, d, *J*_{2',F} 8.5 Hz, C2'), 71.60, 68.06, 61.17, 60.01, 51.42, 22.40 (NAc); ¹⁹F NMR (188 MHz, D₂O) δ -123.43 (dd, *J*_{F,4'} 50.7, *J*_{F,3'} 15.6 Hz); **Anal. calc.** for C₂₁H₃₀FNO₁₀: C, 53.05; H, 6.36; N, 2.95. Found: C, 53.10; H, 6.23; N, 2.75.

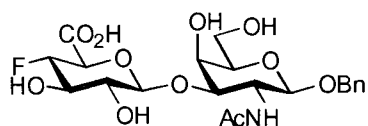
Benzyl O-(4-deoxy-4-fluoro- β -D-glucopyranosyl)-(1 \rightarrow 3)-2-acetamido-2-deoxy-4,6-O-paramethoxybenzylidene- β -D-galactopyranoside (43)



A solution of **42** (125 mg, 0.26 mmol), *p*-anisaldehyde dimethyl acetal (120 mg, 0.66 mmol, 2.5 eq) and *p*-toluenesulfonic acid monohydrate (1 mg, 0.005 mmol, 0.02 eq) in dry DMF (0.7 mL) was rotated under aspirator pressure at 50 °C for 7 h. The reaction mixture was poured slowly into a rapidly stirring mixture of water (2 mL) and NaOH (3

mg) causing **43** to precipitate as a white solid (3.92 g 99%), which was filtered off and washed with H₂O and PE (138 mg, 88%): ¹H NMR (400 MHz, CD₃OD) δ 7.45 (2 H, d, J 8.7 Hz, Ar), 7.37-7.29 (5 H, m, Ar), 6.90 (2 H, d, J 8.7 Hz, Ar), 5.58 (1 H, s, ArCH), 4.90 (1 H, d, J 12.1 Hz, OCH₂Ph), 4.65 (1 H, d, J_{1,2} 8.2 Hz, H1), 4.62 (1 H, d, OCH₂Ph), 4.41 (1 H, d, J_{4,3} 3.1 Hz, H4), 4.39 (1 H, d, J_{1',2'} 7.8 Hz, H1'), 4.30-4.10 (4 H, m, H2, H4', H6_a, H6_b), 3.99 (1 H, dd, J_{3,2} 11.1, J_{3,4} 3.1 Hz, H3), 3.85-3.75 (4 H, m, H6_a', OMe), 3.68 (1 H, dd, J_{6b',6a'} 12.0, J_{6b',5'} 5.3 Hz, H6_b'), 3.62-3.50 (2 H, m, H3', H5), 3.49-3.40 (1 H, m, H5'), 3.22 (1 H, dd, J_{2',3'} 9.0, J_{2',1'} 7.8 Hz, H2'), 1.92 (3 H, s, NAc); ¹³C NMR (100 MHz, CD₃OD) δ 175.28 (C=O), 161.63, 139.10, 132.16 (3 C), 129.38, 129.05, 128.95, 128.76, 114.27, 106.18 (6 CH), 102.32 (CH, d, J_{1',F} 3.0 Hz, C1'), 101.63 (CH, C1), 90.56 (CH, d, J_{4',F} 180.9 Hz, C4'), 78.66, 77.10 (2 CH), 75.47 (CH, d, J_{5',F} 22.4 Hz, C5'), 75.45 (CH, d, J_{3',F} 18.8 Hz, C3'), 74.41 (CH, d, J_{2',F} 8.6 Hz, C2'), 71.60, 70.16 (2 CH₂), 67.98 (CH), 61.88 (CH₂), 55.68, 52.91, 23.16 (NAc); ¹⁹F NMR (188 MHz, CD₃OD) δ -121.66 (dd, J_{F,4'} 51.5, J_{F,3'} 17.0 Hz); HRMS (LSIMS⁺, glycerol) m/z: 594.23492. Calc. For C₂₉H₃₇FNO₁₁ [M + H]⁺ 594.2351.

Benzyl O-(4-deoxy-4-fluoro-β-D-glucopyranosiduronic acid)-(1→3)-2-acetamido-2-deoxy-β-D-galactopyranoside (6)

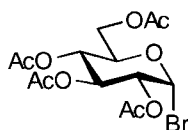


Prepared from **43** as described for **4**. Crude material was then dissolved in methanol and heated at reflux for 15 min, cooled to rt and added 1 drop of acetic acid, and let stand overnight at rt. The solution was concentrated and purified by column chromatography (EtOAc:MeOH:H₂O 7:2:1 + 0.4% AcOH to 6:3:1 + 0.4% AcOH). The solid was then dissolved in H₂O, passed down a cation exchange column (Bio-Rad[®] AG 50W-X2, H⁺, 200-400 mesh) to give **6** as a white solid (19 mg, 25%): ¹H NMR (400 MHz, CD₃OD) δ 7.35-7.20 (5 H, m, Ar), 4.87 (1 H, d, J 12.2 Hz, OCH₂Ph), 4.62 (1 H, d, J 12.2 Hz, OCH₂Ph), 4.52 (1 H, d, J_{1,2} 8.5 Hz, H1), 4.49 (1 H, d, J_{1',2'} 7.7 Hz, H1'), 4.32 (1 H, ddd, J_{4',F} 50.5, J_{4',3'} = J_{4',5'} 9.2 Hz, H4'), 4.08 (1 H, dd, J_{2,3} 10.7, J_{2,1} 8.5 Hz, H2), 4.04 (1 H, d, J_{4,3} 2.6 Hz, H4), 3.98 (1 H, dd, J_{5',4'} 9.2, J_{5',F} 2.6 Hz, H5'), 3.84-3.70 (3 H, m, H3,

H5, H6_a), 3.62 (1 H, ddd, $J_{3',F}$ 16.0, $J_{3',2'}$ 9.0, $J_{3',4'}$ 9.2 Hz, H3'), 3.50 (1 H, dd, $J_{6b,5} = J_{6b,6a}$ 6.0 Hz, H6_b), 1.90 (3 H, s, NAc); ^{13}C NMR (100 MHz, CD₃OD) δ 174.23 (C=O), 139.25, 129.32, 128.93, 128.67, 106.01, 101.77, 91.93 (CH, d, $J_{4',F}$ 184.7 Hz, C4'), 81.89, 76.54, 75.30 (CH, d, J 18.3 Hz), 74.18 CH, d, J 8.1 Hz), 71.41, 69.43, 62.60, 53.00, 10.45, 23.16 (NAc); ^{19}F NMR (188 MHz, CD₃OD) δ -120.84 (dd, $J_{F,4'}$ 50.5, $J_{F,3'}$ 16.0 Hz); HRMS (LSIMS+, glycerol) m/z : 490.1726. Calc. For C₂₁H₂₉FNO₁₁ [M + H]⁺ 490.1725.

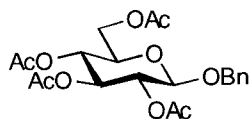
5.4.5 Benzyl 4-deoxy-4-fluoro- β -D-galactopyranosiduronic acid (52) (Scheme 3.5)

2,3,4,6-Tetra-O-acetyl- α -D-glucopyranosyl bromide (44)

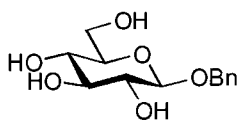


Prepared from *per*-O-acetylated glucose⁹⁸ as described for **29** to give **44** as a light yellow oil which crystallized under high vacuum (10.47 g, 99%): ^1H NMR (200 MHz, CDCl₃) δ 6.58 (1 H, d, $J_{1,2}$ 3.8 Hz, H1), 5.53 (1 H, dd, J = 9.5 Hz, H3 or H4), 5.13 (1 H, dd, J = 9.5 Hz, H3 or H4), 4.80 (1 H, dd, $J_{2,3}$ 9.5, $J_{2,1}$ 3.8 Hz, H2), 4.36-4.21 (2 H, m, H6_a, H6_b), 4.15-4.04 (1 H, m, H5), 2.07, 2.07, 2.02, 2.01 (12 H, 4 s, 4 Ac).

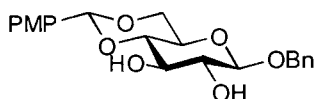
Benzyl 2,3,4,6-tetra-O-acetyl- β -D-glucopyranoside (45)¹⁵⁷



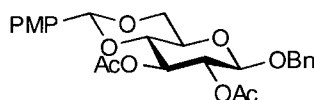
Prepared from **44** as described for **15**. The crude residue was purified by column chromatography (PE:EtOAc 2.5:1) giving **45**¹⁵⁷ as a white solid (68%): ^1H NMR (200 MHz, CDCl₃) δ 7.36-7.24 (5 H, m, Ar), 5.20-5.00 (2 H, m, H3, H4), 4.88 (1 H, d, J 12.2 Hz, OCH₂Ph), 4.60 (1 H, d, J 12.2 Hz, OCH₂Ph), 4.52 (1 H, d, $J_{1,2}$ 7.5 Hz, H1), 4.26 (1 H, dd, $J_{6ax,6eq}$ 12.3, $J_{6ax,5}$ 4.7 Hz, H6_{ax}), 4.14 (1 H, dd, $J_{6eq,6ax}$ 12.3, $J_{6eq,5}$ 2.7 Hz, H6_{eq}), 4.09 (1 H, dd, $J_{2,3}$ 9.8, $J_{2,1}$ 7.5 Hz, H2), 3.66 (1 H, ddd, $J_{5,4}$ 9.5, $J_{5,6eq}$ 4.7, $J_{5,6ax}$ 2.7 Hz, H5), 2.08, 1.99, 1.98, 1.98 (12 H, 4 s, 4 Ac); **Anal. Calc. for:** C₂₁H₂₆O₁₀: C, 57.53; H, 5.98. Found: C, 57.27; H, 6.00.

Benzyl β -D-glucopyranoside (46)

Zemplén deprotection of **45** with sodium methoxide according to the general procedure gave **46** as a white solid (99%): ^1H NMR (200 MHz, CD_3OD) δ 7.45-7.16 (5 H, m, Ar), 4.90 (1 H, d, J 11.8 Hz, OCH_2Ph), 4.63 (1 H, dd, J 11.8 Hz, OCH_2Ph), 3.32 (1 H, d, $J_{1,2}$ 7.3 Hz, H1), 3.87 (1 H, dd, $J_{6\text{eq},6\text{ax}}$ 12.1, $J_{6\text{eq},5}$ 1.9 Hz, H6_{eq}), 3.66 (1 H, dd, $J_{6\text{ax},6\text{eq}}$ 12.1, $J_{6\text{ax},5}$ 5.0 Hz, H6_{ax}), 3.39-3.18 (4 H, m, H2, H3, H4, H5).

Benzyl 4,6-O-(4-methoxybenzylidene)- β -D-glucopyranoside (47)

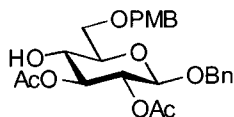
A solution of **46** (1.50 g, 5.55 mmol), *p*-methoxybenzaldehyde dimethyl acetal (2.02 g, 11.1 mmol, 2 eq) and a catalytic amount of camphorsulfonic acid in CHCl_3 was heated at reflux, and the solvent distilled off to remove the methanol generated, with fresh CHCl_3 added to keep the volume constant. After 2 h K_2CO_3 (~2 g) was added, and the hot solution was filtered, and concentrated under vacuum. The residue was purified by column chromatography (PE:EtOAc 2:3) to give **47** as a white solid (1.35 g, 63%): ^1H NMR (200 MHz, CDCl_3) δ 7.45-7.30 (7 H, m, Ar), 6.88 (2 H, d, J 8.8 Hz, Ar), 5.49 (1 H, s, ArCH), 4.93 (1 H, d, J 11.5 Hz, OCH_2Ph), 4.62 (1 H, d, J 11.5 Hz, OCH_2Ph), 4.49 (1 H, d, $J_{1,2}$ 7.5 Hz, H1), 4.34 (1 H, dd $J_{6\text{eq},6\text{ax}}$ 10.5, $J_{6\text{eq},5}$ 4.7 Hz, H6_{eq}), 3.90-3.73 (2 H, m), 3.78 (3 H, s, OMe), 3.60-3.37 (3 H, m); LRMS (DCI⁺) m/z : 388 $[\text{M}]^+$.

Benzyl 2,3-di-O-acetyl-4,6-O-(4-methoxybenzylidene)- β -D-glucopyranoside (48)

Compound **47** was subjected to the general acetylation procedure to give **48** as a white solid (90%): ^1H NMR (200 MHz, CDCl_3) δ 7.40-7.25 (7 H, m, Ar), 7.85 (2 H, d, J 8.8 Hz, Ar), 5.44 (1 H, s, ArCH), 5.25 (1 H, dd, $J_{3,4} = J_{3,2}$ 9.3 Hz, H3), 5.03 (1 H, dd, $J_{2,3}$ 9.3, $J_{2,1}$ 7.9 Hz, H2), 4.88 (1 H, d, J 12.1 Hz, OCH_2Ph), 4.62 (1 H, d, $J_{1,2}$ 7.9 Hz, H1),

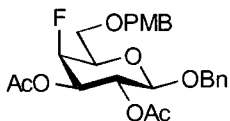
4.60 (1 H, d, J 12.1 Hz, OCH_2Ph), 4.35 (1 H, dd, $J_{6\text{eq},6\text{ax}}$ 10.4, $J_{6\text{eq},5}$ 4.9 Hz, $\text{H}_{6\text{eq}}$), 3.79 (1 H, dd, $J_{6\text{ax},6\text{eq}} = J_{6\text{ax},5}$ 10.4 Hz, $\text{H}_{6\text{ax}}$), 3.77 (3 H, s, OMe), 3.68 (1 H, dd, $J_{4,5} = J_{4,3}$ 9.3 Hz, H_4), 3.48 (1 H, ddd, $J_{5,6\text{ax}}$ 10.4, $J_{5,4}$ 9.3, $J_{5,6\text{eq}}$ 4.9 Hz, H_5), 2.02, 1.99 (6 H, 2 s, 2 Ac); **Anal. Calc. for:** $\text{C}_{25}\text{H}_{28}\text{O}_9$: C, 63.55; H, 5.97. Found: C, 63.39; H, 5.97.

Benzyl 2,3-di-O-acetyl-6-O-(4-methoxybenzyl)- β -D-glucopyranoside (49)



A solution of sodium cyanoborohydride (4.76 g, 75.7 mmol, 10 eq), in dry THF (75 mL) was added to a solution of **48** (3.58 g, 7.57 mmol) in dry CH_2Cl_2 (130 mL), and the solution stirred over 4 Å molecular sieves for 30 min before trifluoroacetic acid (11.7 mL, 151 mmol, 20 eq) was added dropwise. The reaction mixture was stirred at rt overnight (19 h), diluted with CH_2Cl_2 , and washed with saturated NaHCO_3 (3x). The combined aqueous phases were extracted once with CH_2Cl_2 . The combined organic phases were washed once with H_2O , dried over MgSO_4 , and concentrated under vacuum. The residue was purified by column chromatography (CH_2Cl_2 :EtOAc 6:1 to 5:1) to give **49** as a colourless syrup (3.26 g, 91%): $^1\text{H NMR}$ (200 MHz, CDCl_3) δ 7.40-7.22 (7 H, m, Ar), 6.88 (2 H, d, J 8.8 Hz, Ar), 5.04-4.97 (2 H, m, H_2 , H_3), 4.87 (1 H, d, J 12.3 Hz, OCH_2Ph), 4.59 (1 H, d, J 12.3 Hz, OCH_2Ph), 4.60-4.45 (3 H, m, H_1 , OCH_2Ar), 3.80 (3 H, s, OMe), 3.83-3.68 (3 H, m, H_4 , $\text{H}_{6\text{a}}$, $\text{H}_{6\text{b}}$), 3.50 (1 H, m, H_5), 2.98 (1 H, d, $J_{4,\text{OH}}$ 3.3 Hz, 4-OH), 2.07, 2.00 (6 H, 2 s, 2 Ac).

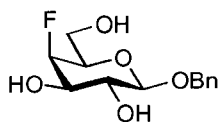
Benzyl 2,3-di-O-acetyl-4-deoxy-4-fluoro-6-paramethoxybenzyl- β -D-galactopyranoside (50)



Trifluoromethanesulfonic anhydride (0.79 mL, 4.68 mmol, 2 eq) was added dropwise to a solution of **49** (1.11 g, 2.34 mmol) in dry CH_2Cl_2 (13 mL) and dry pyridine (3.5 mL) at -15°C , and stirred for 15 min before the reaction mixture was allowed to warm to rt and stirred for one h. The reaction mixture was then concentrated under

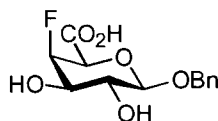
vacuum, and cooled on ice as as tetrabutylammonium fluoride (TBAF, 1 M in THF, 35 mL, 15 eq) was added dropwise. The reaction mixture was then stirred at rt for 3 h, diluted with CH₂Cl₂, and washed with 1 M HCl (3x). The combined aqueous phases were extracted once with CH₂Cl₂, and the combined organic phases washed with saturated NaHCO₃ (3x), H₂O (1x), dried over MgSO₄, and concentrated under vacuum. The residue was purified by column chromatography (PE:EtOAc 3:1) to yield **50** (895 mg, 81%) as a light yellow syrup: ¹H NMR (200 MHz, CDCl₃) δ 7.40-7.20 (7 H, m, Ar), 6.87 (2 H, d, J 8.8 Hz, Ar), 5.32 (1 H, dd, J_{2,3} 10.5, J_{2,1} 8.0 Hz, H2), 4.96 (1 H, ddd, J_{3,F} 27.8, J_{3,2} 10.5, J_{3,4} 2.7 Hz, H3), 4.89 (1 H, d, J 12.5 Hz, OCH₂Ph), 4.87 (1 H, dd, J_{4,F} 49.5, J_{4,5} 2.7 Hz, H4), 4.60 (1 H, d, J 12.5 Hz, OCH₂Ph), 4.54-4.46 (3 H, m, OCH₂Ar, H1), 3.80 (3 H, s, OMe), 3.76-3.60 (3 H, m, H5, H6_a, H6_b), 2.07, 1.99 (6 H, 2 s, 2 Ac); ¹⁹F NMR (188 MHz, CDCl₃) δ -141.42 (ddd, J_{F,4} 49.5, J_{F,3} = J_{F,5} 27.8 Hz).

Benzyl 4-deoxy-4-fluoro-β-D-galactopyranoside (**51**)



Compound **50** was deprotected according to the general acetyl chloride in methanol deprotection strategy, and then purified by column chromatography (EtOAc) to give **51** as a white solid (78%): ¹H NMR (200 MHz, (CD₃)₂CO) δ 7.40-7.15 (5 H, m, Ar), 4.85 (1 H, d, J 12.2 Hz, OCH₂Ph), 4.71 (1 H, dd, J_{4,F} 50.1, J_{4,3} 2.6 Hz, H4), 4.58 (1 H, d, J 12.2 Hz, OCH₂Ph), 4.37 (1 H, dd, J_{1,2} 7.3, J_{1,F} 1.0 Hz, H1), 3.73-3.44 (5 H, m, H2, H3, H5, H6_a, H6_b); ¹⁹F NMR (188 MHz, (CD₃)₂CO) δ -142.00 (ddd, J_{F,4} 49.6, J_{F,3} = J_{F,5} 28.0 Hz).

Benzyl 4-deoxy-4-fluoro-β-D-galactopyranosiduronic acid (**52**)

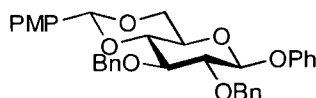


Prepared from **51** as described for **4**. The crude product was crystallized from EtOAc/PE, then passed down a cation exchange column (Bio-Rad® AG 50W-X2, 200-400 mesh, H⁺ form) and freeze-dried to give **52** as a white solid (39%): ¹H NMR (200

MHz, (CD₃)₂CO) δ 7.45-7.18 (5 H, m, Ar), 5.02 (1 H, dd, $J_{4,F}$ 48.2, $J_{4,3}$ 2.8 Hz, H4), 4.92 (1 H, d, J 12.2 Hz, OCH₂Ph), 4.62 (1 H, d, J 12.2 Hz, OCH₂Ph), 4.50 (1 H, d, $J_{1,2}$ 7.8 Hz, H1), 4.44 (1 H, d, $J_{5,F}$ 28.4 Hz, H5), 3.78 (1 H, ddd, $J_{3,F}$ 29.3, $J_{3,2}$ 9.8, $J_{3,4}$ 2.8 Hz, H3), 3.59 (1 H, ddd, $J_{2,3}$ 9.8, $J_{2,1}$ 7.8, $J_{2,F}$ 2.0 Hz, H2); ¹⁹F NMR (188 MHz, (CD₃)₂CO) δ -127.26 (ddd, $J_{F,4}$ 48.2, $J_{F,5}$ 28.4, $J_{F,3}$ 29.3 Hz); IR (KBr) 3700-2400, 1741 cm⁻¹; **Anal. calc. for** C₇H₁₁FO₆ + H₂O: C, 51.32; H, 5.63. Found: C, 51.51; H, 5.07.

5.4.6 Phenyl 4-deoxy-4,4-difluoro- β -D-xylo-hexopyranosiduronic acid (58) (Scheme 3.6)

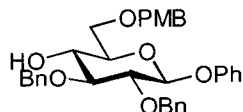
Phenyl 2,3-di-O-benzyl-4,6-O-paramethoxybenzylidene- β -D-glucopyranoside (53)



Phenyl 4,6-*O*-paramethoxybenzylidene- β -D-glucopyranoside was prepared from phenyl- β -D-glucopyranoside as for **75**. The crude material (14.6 g, 39.0 mmol) was dissolved in dry DMF (80 mL) was added to sodium hydride (3.74 g, 156 mmol, 4 eq) in dry DMF (170 mL). To this was added benzyl bromide (16.68 g, 97.5 mmol, 2.5 eq) dropwise and the reaction mixture stirred for 2 h at rt before methanol (33 mL) was added dropwise. The reaction mixture was diluted with EtOAc, washed with H₂O (3x), the combined aqueous phases were extracted once with ether, and the combined organic phases dried over MgSO₄, and concentrated under vacuum leaving a yellow solid which was crystallized from CH₂Cl₂/PE to give **53** as a white solid (8.45 g, 39%) (The filtrate containing more product was concentrated and saved): **mp** 114-116 °C; ¹H NMR (400 MHz, CDCl₃) δ 7.42 (2 H, d, J 8.5 Hz, Ar), 7.40-7.26 (12 H, m, Ar), 7.10-7.02 (3 H, m, Ar), 6.91 (2 H, d, J 8.8 Hz, Ar), 5.55 (1 H, s, ArCH), 5.14 (1 H, d, $J_{1,2}$ 7.3 Hz, H1), 4.98 (1 H, d J 11.0 Hz, OCH₂Ar), 4.94 (1 H, d, J 11.3 Hz, OCH₂Ar), 4.85 (1 H, d, J 11.0 Hz, OCH₂Ar), 4.82 (1 H, d, J 11.3 Hz, OCH₂Ar), 4.36 (1 H, dd, $J_{6eq,6ax}$ 10.4, $J_{6eq,5}$ 5.2 Hz, H6_{eq}), 3.90-3.74 (4 H, m, H2, H3, H4, H6_{ax}), 3.81 (3 H, s, OMe), 3.56 (1 H, ddd, $J_{5,4} = J_{5,6ax}$ 9.4, $J_{5,6eq}$ 5.2 Hz, H5); ¹³C NMR (75 MHz, CDCl₃) δ 160.05, 157.08, 138.43, 138.10, 129.73 (5 C), 129.58, 128.41, 128.32, 128.28, 128.17, 127.99, 127.75, 127.62,

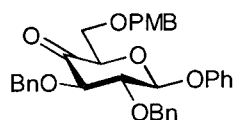
127.31, 122.98, 116.90, 113.60, 102.01, 101.12, 81.78, 81.22, 80.88 (17 CH), 75.48, 75.10, 68.66 (3 CH₂), 55.27 (CH₃); **Anal. calc. for** C₃₄H₃₄O₇: C, 73.63; H, 6.18. Found: C, 73.42; H, 6.22.

Phenyl 2,3-di-O-benzyl-6-O-paramethoxybenzyl-β-D-glucopyranoside (54)



Prepared from **53** as described for **49**. Purified by column chromatography (PE:EtOAc 3:1) to give **54** as a colourless syrup which slowly crystallized to a white solid (81%). A sample was recrystallized from EtOAc/hexanes for NMR and elemental analysis: **mp** 93-94 °C; ¹H NMR (400 MHz, CDCl₃) δ 7.39 (12 H, m, Ar), 7.24 (2 H, d, J 8.8 Hz, Ar), 7.11-7.03 (3 H, m, Ar), 6.86 (2 H, d, J 8.5 Hz, Ar), 5.10-5.02 (2 H, m, H1, OCH₂Ar), 5.97 (1 H, d, J 11.3 Hz, OCH₂Ar), 4.84 (1 H, d, J 11.6 Hz, OCH₂Ar), 4.79 (1 H, d, J 11.3 Hz, OCH₂Ar), 4.53 (1 H, d, J 11.6 Hz, OCH₂Ar), 4.49 (1 H, d, J 11.6 Hz, OCH₂Ar), 3.82-3.64 (4 H, m), 3.80 (3 H, s, OMe), 3.62-3.52 (2 H, m); ¹³C NMR (75 MHz, CDCl₃) δ 159.24, 157.27, 138.54, 138.16, 129.95 (5 C), 129.49, 129.27, 128.50, 128.35, 128.19, 127.91, 127.81, 127.74, 122.67, 116.85, 113.78 (11 CH), 101.66 (CH, C1), 84.01, 81.44 (2 CH), 75.28, 74.89 (2 CH₂), 74.32 (CH), 73.28 (CH₂), 71.47 (CH), 71.47 (CH), 69.83 (CH₂), 55.21 (CH₃); **Anal. calc. for** C₃₄H₃₆O₇: C, 73.36; H, 6.52. Found: C, 73.23; H, 6.65.

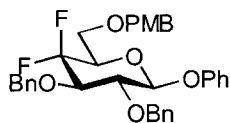
Phenyl 2,3-di-O-benzyl-6-O-paramethoxybenzyl-β-D-xylo-hexopyranosid-4-ulose (55)



Acetic anhydride (5.4 mL) was added to a solution of **54** (3.00 g, 5.39 mmol) in dry DMSO (20.2 mL) and stirred at rt for 24 h. Ethanol was added and the reaction mixture stirred for a further 1 h, diluted with EtOAc, washed with H₂O (1x), saturated NaHCO₃ (2x), H₂O (1x), dried over MgSO₄, and concentrated. The residue was purified by column chromatography (PE:EtOAc 6:1 to 5:1) giving **55** as a white solid (2.24 g,

75%). A small sample was recrystallized from EtOH/PE for elemental analysis: mp 79–81 °C; ^1H NMR (400 MHz, CDCl_3) δ 7.42 (2 H, dd, J 7.6, J 1.8 Hz, Ar), 7.37–7.26 (10 H, m, Ar), 7.17 (2 H, d, J 8.8 Hz, Ar), 7.12–7.04 (3 H, m, Ar), 6.83 (2 H, d, J 8.5 Hz, Ar), 5.45 (1 H, d, $J_{1,2}$ 6.1 Hz, H1), 4.96 (1 H, d, J 11.6 Hz, OCH_2Ar), 4.90 (1 H, d, J 11.3 Hz, OCH_2Ar), 4.83 (1 H, d, J 11.3 Hz, OCH_2Ar), 4.67 (1 H, d, J 11.6 Hz, OCH_2Ar), 4.42 (1 H, d, J 11.3 Hz, OCH_2Ar), 4.38 (1 H, d, J 11.3 Hz, OCH_2Ar), 4.30 (1 H, dd, $J_{5,6\text{ax}}$ 7.3, $J_{5,6\text{eq}}$ 3.6 Hz, H5), 4.28 (1 H, d, $J_{3,2}$ 9.1 Hz, H3), 4.07 (1 H, dd, $J_{2,3}$ 9.1, $J_{2,1}$ 6.1 Hz, H2), 3.93 (1 H, dd, $J_{6\text{eq},6\text{ax}}$ 10.7, $J_{6\text{eq},5}$ 3.6 Hz, H6eq), 3.79 (3 H, s, OMe), 3.66 (1 H, dd, $J_{6\text{ax},6\text{eq}}$ 10.6, $J_{6\text{ax},5}$ 7.3 Hz, H6ax); ^{13}C NMR (75 MHz, CDCl_3) δ 201.88 (C=O), 159.22, 156.85, 137.67, 137.35, 129.86 (5 C), 129.58, 129.33, 128.38, 128.35, 128.06, 127.92, 127.84, 122.84, 116.75, 113.73 (10 CH), 100.89 (CH, C1), 83.06, 82.84, 77.80 (3 CH), 74.56, 73.81, 73.27, 68.28 (4 CH_2), 55.20 (CH_3); Anal. calc. for $\text{C}_{34}\text{H}_{34}\text{O}_7$: C, 73.63; H, 6.18. Found: C, 73.43; H, 6.26.

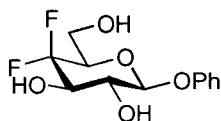
Phenyl 2,3-di-O-benzyl-4-deoxy-4,4-difluoro-6-O-paramethoxybenzyl- β -D-xylohexopyranoside (56)



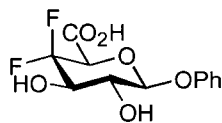
Prepared from **55** by DAST treatment as described for **23**. Purified by column chromatography (PE:EtOAc 7:1) to give **56** as a colourless oil which solidified over time (88%): ^1H NMR (400 MHz, CDCl_3) δ 7.40–7.18 (14 H, m, Ar), 7.09–7.03 (3 H, m, Ar), 6.83 (2 H, d, J 8.5 Hz, Ar), 5.01 (1 H, d, $J_{1,2}$ 7.6 Hz, H1), 4.98 (1 H, d, J 10.7 Hz, OCH_2Ar), 4.90 (1 H, d, J 11.3 Hz, OCH_2Ar), 4.80 (1 H, d, J 10.7 Hz, OCH_2Ar), 4.78 (1 H, d, J 11.3 Hz, OCH_2Ar), 4.52 (1 H, d, J 11.3 Hz, OCH_2Ar), 4.44 (1 H, d, J 11.3 Hz, OCH_2Ar), 3.96–3.74 (4 H, m, H3, H5, H6a, H6b), 3.78 (3 H, s, OMe), 3.71 (1 H, dd, $J_{2,3}$ 10.7, $J_{2,1}$ 7.6 Hz, H2); ^{13}C NMR (100 MHz, CDCl_3) δ 159.34, 158.62, 137.87, 137.37, 129.94 (5 C), 129.60, 129.26, 128.38, 128.20, 128.15, 127.99, 127.88, 123.05, 116.98, 113.86 (10 CH), 101.28 (CH, C1), 80.12 (CH, d, J 8.5 Hz, C2), 79.82 (CH, dd, J 19.7, J 19.7 Hz, C3), 75.73, 75.57 (2 CH_2), 74.33 (CH, dd, J 29.5, J 23.0 Hz, C5), 73.51 (CH_2),

66.10 (CH₂, d, J 3.8 Hz, C6), 55.28 (CH₃, OMe); ¹⁹F NMR (188 MHz, CDCl₃) δ -40.22 (dd, J_{F,F} 249.9, J 6.2 Hz, F4_{eq}), -55.58 (ddd, J_{F,F} 249.9, J 21.0, J 21.0 Hz, F4_{ax}).

Phenyl 4-deoxy-4,4-difluoro-β-D-xylo-hexopyranoside (57)



Hydrogenation to remove the protecting groups proved difficult. A solution of **56** (825 mg, 1.4 mmol) in EtOAc (10 mL), methanol (15 mL), ethanol (25 mL), and 1 drop acetic acid was stirred with 10% palladium on carbon catalyst (~70 mg) under 1 atm of H₂ overnight. The catalyst was replaced with fresh material and rehydrogenated (2x). At this time TLC indicated 2 products, the desired compound **57** (lower R_f), and phenyl 4-deoxy-4,4-difluoro-6-*O*-paramethoxybenzyl-β-D-xylo-hexopyranoside (higher R_f). The reaction mixture was filtered through a bed of Celite, and concentrated under vacuum. The residue was dissolved in 9:1 CH₃CN:H₂O (10 mL) to which was added ceric ammonium nitrate (700 mg), and the reaction stirred at rt for 1.5 h. The solvent was evaporated under vacuum, and the residue was purified by column chromatography (PE:EtOAc 1:1.75) to give **57** as a white solid (63%): ¹H NMR (400 MHz, (CD₃)₂CO + D₂O) δ 7.26 (2 H, dd, J 8.8, J 7.3 Hz, Ph_{meta}), 7.08 (2 H, dd, J 8.8, J 0.9 Hz, Ph_{ortho}), 6.99 (1 H, tt, J 7.3, J 0.9 Hz, Ph_{para}), 5.09 (1 H, dd, J_{1,2} 7.6, J_{1,F} 0.9 Hz, H1), 4.03-3.84 (3 H, m H2, H3, H5), 3.74-3.64 (2 H, m H6_a, H6_b); ¹³C NMR (100 MHz, (CD₃)₂CO + D₂O) δ 158.64 (C), 130.20, 123.15 (2 CH), 119.13 (C, dd, J 251.3, J 249.0 Hz, C4), 117.45 (CH), 101.60 (CH, C1), 76.20 (CH, dd, J 29.1, J 22.5 Hz, C5), 73.97 (CH, dd, J 20.1, J 20.1 Hz, C3), 73.83 (CH, d, J 8.5 Hz, C2), 59.14 (CH₂, d, J 5.2 Hz, C6); ¹⁹F NMR (188 MHz, (CD₃)₂CO + D₂O) δ -43.53 (dd, J_{F,F} 247.2, J 6.1 Hz, F4_{eq}), -58.33 (ddd, J_{F,F} 247.2, J 22.9, J 22.9 Hz, F4_{ax}); **Anal. calc. for** C₁₂H₁₄F₂O₅: C, 52.18; H, 5.11. Found: C, 52.16; H, 5.13.

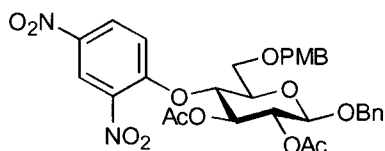
Phenyl 4-deoxy-4,4-difluoro- β -D-xylo-hexopyranosiduronic acid (58)

Prepared from **57** as described for **3**. The crude product was purified by column chromatography (PE:EtOAc 7:3 to EtOAc:MeOH 8:2), then HPLC (amide-80 column, linear gradient from CH₃CN:H₂O 95:5 to 4:1 over 45 min, then to 3:1 over the next 15 min, and then 3:1 until completely eluted), then passed down a column of acid resin (Bio-Rad[®] AG 50W-X2, 200-400 mesh) and freeze-dried to give to give **58** as a white solid (27%): ¹H NMR (300 MHz, (CD₃)₂CO) δ 7.30 (2 H, dd, J 8.8, J 7.4 Hz, Ph_{meta}), 7.12 (2 H, dd, J 7.4, J 1.0 Hz, Ph_{ortho}), 7.03 (1 H, tt, J 7.4, J 1.0 Hz, Ph_{para}), 5.30 (1 H, d, J_{1,2} 7.9 Hz, H1), 4.80 (1 H, d, J_{5,Fax} 24.6 Hz, H5), 4.05 (1 H, ddd, J_{3,Fax} 20.6, J_{3,2} 9.6, J_{3,Feq} 7.0 Hz, H3), 3.77 (1 H, ddd, J_{2,3} 9.6, J_{2,1} 7.9, J_{2,F} 1.8 Hz, H2); ¹³C NMR (75 MHz, (CD₃)₂CO) δ 165.46 (C=O), 158.36 (C), 130.26, 123.43 (2 CH), 117.85 (CH, dd, J_{4,Fax} = J_{4,Feq} 235.9 Hz, C4), 117.57 (CH), 101.05 (CH, C1), 74.03 (CH, dd, J_{3,Fax} = J_{3,Feq} 20.1 Hz, C3), 73.60-72.70 (2 CH, m, C2, C5); ¹⁹F NMR (282 MHz, (CD₃)₂CO) δ -42.24 (dd, J_{Feq,Fax} 246.4, J_{Feq,3} 7.0 Hz, F4_{eq}), -55.74 (ddd, J_{eq,Fax} 246.4, J_{Fax,5} 24.6, J_{Fax,3} 20.6, F4_{ax}); **Anal. calc. for** C₁₂H₁₂F₂O₆ + 0.5 H₂O: C, 48.17; H, 4.38. Found: C, 48.18; H, 4.48.

5.5 Synthesis of the Chromogenic Substrates

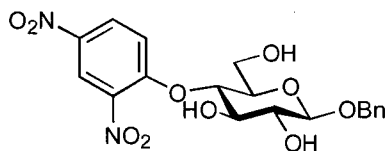
5.5.1 Benzyl 4-O-(2',4'-dinitrophenyl)- β -D-glucopyranosiduronic acid (**1**) (Scheme 3.7)

Benzyl 2,3-di-O-acetyl-4-O-(2',4'-dinitrophenyl)-6-O-(4-methoxybenzyl)- β -D-glucopyranoside (**59**)



A solution of 2,4-dinitrofluorobenzene (290 mg, 1.56 mmol, 1.8 eq), 1,4-diazobicyclo[2,2,2]-octane (DABCO, 533 mg, 4.75 mmol, 5.5 eq), and **49** (410 mg, 0.86 mmol) in dry DMF (2 mL) was stirred at rt for 24 h, diluted with CH_2Cl_2 , washed with half-saturated NaHCO_3 (6x), H_2O (2x), dried over MgSO_4 , and concentrated under vacuum. The residue was purified by column chromatography (PE:EtOAc 3:1 to 2:1) to give **59** as pale yellow foam (441 mg, 80%): ^1H NMR (200 MHz, CDCl_3) δ 8.55 (1 H, d, $J_{3',5'} 2.5$ Hz, H3'), 8.18 (1 H, dd, $J_{5',6'} 9.5$, $J_{5',3'} 2.5$ Hz, H5'), 7.40–7.22 (6 H, m, Ar), 6.97 (2 H, d, $J 8.3$ Hz, Ar), 6.66 (2 H, d, $J 8.5$ Hz, Ar), 5.33 (1 H, dd, $J_{3,4} = J_{3,2} 9.3$ Hz, H3), 5.05 (1 H, dd, $J_{2,3} 9.3$, $J_{2,1} 7.8$ Hz, H2), 4.94 (1 H, dd, $J_{4,3} = J_{4,5} 9.3$ Hz, H4), 4.91 (1 H, d, $J 12.4$ Hz, OCH_2Ph), 4.63 (1 H, d, $J 12.4$ Hz, OCH_2Ph), 4.60 (1 H, d, $J_{1,2} 7.8$ Hz, H1), 4.49 (1 H, d, $J 11.5$ Hz, OCH_2Ar), 4.14 (1 H, d, $J 11.5$ Hz, OCH_2Ar), 3.87–3.62 (6 H, m, H5, H6_a, H6_b, OMe), 1.99, 1.79 (6 H, 2 s, 2 Ac); **Anal. Calc. for:** $\text{C}_{31}\text{H}_{32}\text{N}_2\text{O}_{13}$: C, 58.12; H, 5.03; N, 4.37. Found: C, 58.17; H, 5.11; N, 4.33.

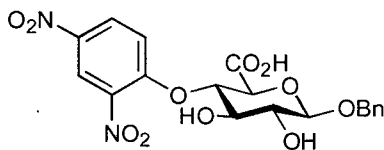
Benzyl 4-O-(2',4'-dinitrophenyl)- β -D-glucopyranoside (**60**)



Compound **59** was deprotected according to the general acetyl chloride in methanol deprotection strategy to give **60** (89%): ^1H NMR (200 MHz, CD_3OD) δ 8.68 (1

H, d, $J_{3',5'}$ 2.7 Hz, H3'), 8.41 (1 H, dd, $J_{5',6'}$ 9.5, $J_{5',3'}$ 2.7 Hz, H5'), 7.80 (1 H, d, $J_{6',5'}$ 9.5 Hz, H6'), 7.45-7.19 (5 H, m, Ph), 4.94 (1 H, d, J 12.0 Hz, OCH₂Ph), 4.76, (1 H, dd, $J_{4,3} = J_{4,5}$ 9.0 Hz, H4), 4.68 (1 H, d, J 12.0 Hz, OCH₂Ph), 4.49 (1 H, d, $J_{1,2}$ 7.8 Hz, H1), 3.90-3.57 (4 H, m, H3, H5, H6_a, H6_b), 3.42 (1 H, dd, $J_{2,3}$ 9.3, $J_{2,1}$ 7.8 Hz, H2); ¹³C NMR (50 MHz, CD₃OD) δ 158.70, 142.48, 139.67, 130.27, 130.07, 129.90, 128.52, 122.77, 119.82, 115.60, 104.19, 80.45, 77.52, 76.38, 76.03, 72.79, 62.04; **ESI-MS** m/z 459.2 [M + Na]⁺; **Anal. Calc. for:** C₁₉H₂₀N₂O₁₀: C, 52.30; H, 4.62; N, 6.42. Found: C, 52.19; H, 4.63; N, 6.25.

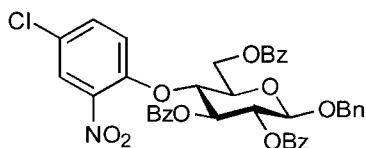
Benzyl 4-O-(2',4'-dinitrophenyl)- β -D-glucopyranosiduronic acid (1)



Prepared from **60** as described for **4**. The residue was purified by column chromatography (EtOAc:MeOH 40:2 to EtOAc:MeOH:H₂O 27:2:1), then dissolved in H₂O and passed down a cation exchange column (Bio-Rad[®] AG 50W-X2, 200-400 mesh, H⁺ form), and freeze-dried to give **1** as a white solid (52%): ¹H NMR (200 MHz, CD₃OD) δ 8.61 (1 H, d, $J_{3',5'}$ 2.7 Hz, H3'), 8.37 (1 H, dd, $J_{5',6'}$ 9.5, $J_{5',3'}$ 2.7 Hz, H5'), 7.76 (1 H, d, $J_{6',5'}$ 9.5 Hz, H6'), 7.47-7.20 (5 H, m, Ph), 4.92 (1 H, d, J 12.0 Hz, OCH₂Ph), 4.53 (1 H, d, $J_{1,2}$ 7.8 Hz, H1), 4.84 (1 H, dd, $J_{4,3} = J_{4,5}$ 9.3 Hz, H4), 4.67 (1 H, d, J 12.0 Hz, OCH₂Ph), 4.00 (1 H, d, $J_{5,4}$ 9.3 Hz, H5), 3.78 (1 H, dd, $J_{3,4} = J_{3,2}$ 9.3 Hz, H3), 3.45 (1 H, $J_{2,3}$ 9.3, $J_{2,1}$ 7.8 Hz, H2); ¹³C NMR (50 MHz, CD₃OD) δ 188.19 (C=O), 158.48, 141.64, 140.95, 138.81, 129.57, 129.31, 129.10, 128.78, 122.10, 119.54, 116.45, 103.85, 102.30, 82.51, 76.41, 76.23, 75.12, 72.24; **ESI-MS** m/z 473.2 [M + Na]⁺; **Anal. Calc. for:** C₁₉H₁₈N₂O₁₁: C, 50.67; H, 4.03; N, 6.22. Found: C, 50.32; H, 4.00; N, 5.96.

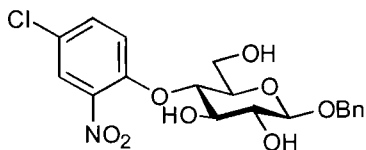
5.5.2 Benzyl 4-*O*-(4'-chloro-2'-nitrophenyl)- β -D-glucopyranosiduronic acid (**8**) (Scheme 3.8)

Benzyl 2,3,6-tri-*O*-benzoyl-4-*O*-(2'-nitro-4'-chlorophenyl)- β -D-glucopyranoside (**61**)



Trifluoromethanesulfonic anhydride (0.26 mL, 1.5 mmol, 3 eq) was added dropwise to a solution of **19** (300 mg, 0.5 mmol) in dry CH_2Cl_2 (3 mL) and dry pyridine (0.8 mL) at -15 to -20 $^\circ\text{C}$. After stirring for 15 min at this temperature the reaction was allowed to attain ambient temperature, and stirred for 2 h. The reaction mixture was diluted with H_2O and EtOAc, and the organic layer washed with 1 M HCl (3x). The combined aqueous phases were extracted with EtOAc (1x). The combined organic phases were washed with saturated NaHCO_3 (1x), H_2O (1x), dried over MgSO_4 , and concentrated under vacuum. The amber syrup and the potassium salt of 4-chloro-2-nitrophenol (327 mg, 1.5 mmol, 3 eq) was dissolved in dry DMF (3 mL) and heated to 80 $^\circ\text{C}$ for 3.5 h. The reaction mixture was cooled, diluted with CH_2Cl_2 and washed with H_2O (2x), saturated NaHCO_3 (7x), dried over MgSO_4 , and concentrated under vacuum. The residue was purified by column chromatography (PE:EtOAc 4:1) to give **61** as a pale yellow foam (142 mg, 37%): ^1H NMR (200 MHz, CDCl_3) δ 8.03-7.86 (4 H, m, Ar), 7.72-7.02 (19 H, m, Ar), 5.84 (1 H, dd, $J_{3,2} = J_{3,4}$ 9.5 Hz, H3), 5.53 (1 H, dd, $J_{2,3}$ 9.5, $J_{2,1}$ 7.8 Hz, H2), 4.93 (1 H, dd, $J_{4,3} = J_{4,5}$ 9.5 Hz, H4), 4.90 (1 H, d, J 12.4 Hz, OCH_2Ph), 4.83 (1 H, d, $J_{1,2}$ 7.8 Hz, H1), 4.75-4.63 (3 H, m, OCH_2Ph , H6_a, H6_b), 4.14 (1 H, ddd, $J_{5,4}$ 9.5, $J_{5,6a} = J_{5,6b}$ 3.0 Hz, H5).

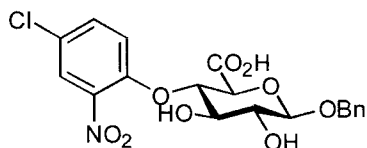
Benzyl 4-*O*-(2'-nitro-4'-chlorophenyl)- β -D-glucopyranoside (**64**)



Zemplén deprotection of **61** with sodium methoxide was carried out according to the general scheme. Purified by column chromatography (PE:EtOAc 1:1) to give **64** as a

white solid (53%): $^1\text{H NMR}$ (200 MHz, $(\text{CD}_3)_2\text{CO}$) δ 7.78 (1 H, d, $J_{3',5'}$ 2.5 Hz, H3'), 7.67 (1 H, d, $J_{6',5'}$ 9.1 Hz, H6'), 7.56 (1 H, dd, $J_{5',6'}$ 9.1, $J_{5',3'}$ 2.5 Hz, H5'), 7.40-7.22 (5 H, m, Ph), 4.87 (1 H, d, J 11.9 Hz, OCH_2Ph), 4.66 (1 H, d, br, OH), 4.61 (1 H, d, J 11.9 Hz, OCH_2Ph), 4.59 (1 H, dd, $J_{4,5} = J_{4,3}$ 9.1 Hz, H4), 4.49 (1 H, d, $J_{1,2}$ 7.8 Hz, H1), 3.96-3.50 (4 H, m, H3, H5, H6_a, H6_b), 3.36 (1 H, ddd, br, $J_{2,3}$ 9.1, $J_{2,1}$ 7.8 Hz, H2). A second major compound eluted after **64** was found by NMR to be benzyl 3-*O*-(2'-nitro-4'-chlorophenyl)- β -D-glucopyranoside.

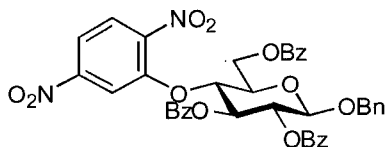
Benzyl 4-*O*-(4'-chloro-2'-nitrophenyl)- β -D-glucopyranosiduronic acid (8**)**



Prepared from **64** as described for **4**. Purified by column chromatography (PE:EtOAc 1:1 + 0.4% acetic acid) to give **8** as a white solid (78%). **8** was then passed down an ion exchange column (Bio-Rad[®] AG 50W-X2, 200-400 mesh, H^+ form), and freeze-dried: $^1\text{H NMR}$ (200 MHz, $(\text{CD}_3)_2\text{CO}$) (note: all signals are broad) δ 7.78 (1 H, d, $J_{3',5'}$ 2.5 Hz, H3'), 7.69 (1 H, d, $J_{6',5'}$ 9.1 Hz, H6'), 7.59 (1 H, dd, $J_{5',6'}$ 9.1, $J_{5',3'}$ 2.5 Hz, H5'), 7.40-7.20 (5 H, m, Ph), 4.84 (1 H, d, J 11.9 Hz, OCH_2Ph), 4.72-4.52 (3 H, m, OCH_2Ph , H1, H4), 4.18 (1 H, d, br, H5), 3.83 (1 H, dd, $J_{3,2} = J_{3,4}$ 9.0 Hz, H3), 3.42 (1 H, dd, $J_{2,3}$ 9.0, $J_{2,1}$ 7.8 Hz, H1); **HRMS** (LSIMS+, glycerol) m/z : 440.0751. Calc. For $\text{C}_{19}\text{H}_{19}\text{ClNO}_9$ $[\text{M} + 1]^+$ 440.0749; **Anal. calc. for** $\text{C}_{19}\text{H}_{18}\text{ClNO}_9 + 1 \text{ H}_2\text{O}$: C, 49.85; H, 4.40; N, 3.06. Found: C, 49.85; H, 4.1; N, 2.97.

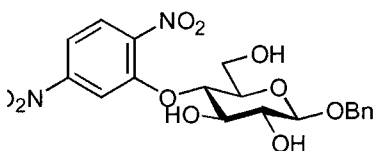
5.5.3 Benzyl 4-*O*-(2',5'-dinitrophenyl)- β -D-glucopyranosiduronic acid (**10**) (Scheme 3.8)

Benzyl 2,3,6-tri-*O*-benzoyl-4-*O*-(2',5'-dinitrophenyl)- β -D-glucopyranoside (**62**)

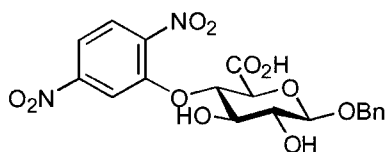


Prepared from **19** as described for **68** and **69**. Purified by column chromatography (PE:EtOAc 5:1) to give **62** as a foam (37%): ^1H NMR (200 MHz, CDCl_3) δ 8.12 (1 H, d, J 2.0 Hz, Ar), 8.00-7.88 (4 H, m, Ar), 7.80-7.68 (3 H, m, Ar), 7.63-7.34 (8 H, m, Ar), 7.30-7.16 (7 H, m, Ar), 5.89 (1 H, dd, $J_{3,2} = J_{3,4}$ 9.5 Hz, H3), 5.62 (1 H, dd, $J_{2,3}$ 9.5, $J_{2,1}$ 7.8 Hz, H2), 5.13 (1 H, dd, $J_{4,3} = J_{4,5}$ 9.5 Hz, H4), 4.93 (1 H, d, J 12.4 Hz, OCH_2Ph), 4.86 (1 H, d, $J_{1,2}$ 7.8 Hz, H1), 4.80-4.64 (3 H, m, OCH_2Ph , H6_a, H6_b), 4.17 (1 H, ddd, $J_{5,4}$ 9.5, $J_{5,6a} = J_{5,6b}$ 3.0 Hz, H5).

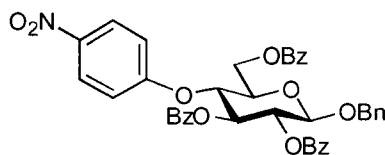
Benzyl 4-*O*-(2',5'-dinitrophenyl)- β -D-glucopyranoside (**65**)



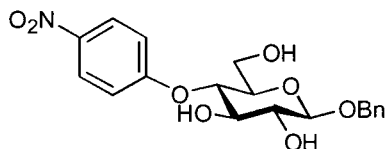
Zemplén deprotection of **62** with sodium methoxide was carried out according to the general scheme. Purified by column chromatography (PE:EtOAc 3:2) to give **65** as a pale yellow solid (26%): ^1H NMR (200 MHz, $(\text{CD}_3)_2\text{CO}$) δ 8.55 (1 H, d, $J_{6',4'}$ 2.2 Hz, H6'), 8.00 (1 H, d, $J_{3',4'}$ 9.0 Hz, H3'), 7.92 (1 H, dd, $J_{4',3'}$ 9.0, $J_{4',6'}$ 2.2 Hz, H4'), 7.41-7.18 (5 H, m, Ar), 4.87 (1 H, d, J 11.9 Hz, OCH_2Ph), 4.73 (1 H, dd, $J_{4,3}$ 9.1 Hz, H4), 4.61 (1 H, d, J 11.9 Hz, OCH_2Ph), 4.51 (1 H, d, $J_{1,2}$ 7.8 Hz, H1), 3.88-3.58 (4 H, m, H3, H5, H6_a, H6_b), 3.43 (1 H, dd, $J_{2,3}$ 9.1, $J_{2,1}$ 7.8 Hz, H2). A second major compound eluted after **65** was found by NMR to be benzyl 3-*O*-(2',5'-dinitrophenyl)- β -D-glucopyranoside.

Benzyl 4-O-(2',5'-dinitrophenyl)- β -D-glucopyranosiduronic acid (10)

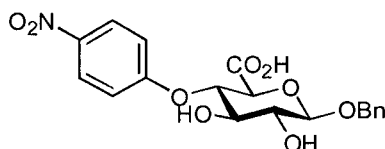
Prepared from **65** as described for **1**. Purified by column chromatography (PE:EtOAc 3:2 + 0.4% acetic acid) to give **10** as a white solid (76%). **10** was then passed down an ion exchange column (Bio-Rad[®] AG 50W-X2, 200-400 mesh, H⁺ form), and freeze-dried: ¹H NMR (200 MHz, (CD₃)₂CO) δ 8.56 (1 H, d, $J_{6',4'}$ 2.2 Hz, H6'), 8.01 (1 H, d, $J_{3',4'}$ 8.7 Hz, H3'), 7.94 (1 H, dd, $J_{4',3'}$ 8.7, $J_{4',6'}$ 2.2 Hz, H4'), 7.40-7.20 (5 H, m, Ar), 4.89 (1 H, d, J 11.7 Hz, OCH₂Ph), 4.78 (1 H, dd, $J_{4,5}$ = $J_{4,3}$ 9.1 Hz, H4), 4.67 (1 H, d, $J_{1,2}$ 7.8 Hz, H1), 4.64 (1 H, d, J 11.7 Hz, OCH₂Ph), 4.25 (1 H, d, $J_{5,4}$ 9.1 Hz, H5), 3.89 (1 H, dd, $J_{3,2}$ = $J_{3,4}$ 9.1 Hz, H3), 3.51 (1 H, dd, $J_{2,3}$ 9.1, $J_{2,1}$ 7.8 Hz, H2); **Anal. calc.** for C₁₉H₁₈N₂O₁₁ + 0.5 H₂O: C, 49.66; H, 4.17; N, 6.10. Found: C, 49.59; H, 4.22; N, 6.00.

5.5.4 Benzyl 4-O-(4'-nitrophenyl)- β -D-glucopyranosiduronic acid (12) (Scheme 3.8)**Benzyl 2,3,6-tri-O-benzoyl-4-O-(4'-nitrophenyl)- β -D-glucopyranoside (63)**

Prepared from **19** as described for **68** and **69**. Purified by column chromatography (PE:EtOAc 3.75:1 to 3:1) to give **63** as a white foam (44%): ¹H NMR (200 MHz, CDCl₃) δ 8.10-7.80 (6 H, m, Ar), 7.72-7.33 (9 H, m, Ar), 7.28-7.15 (7 H, m, Ar), 6.98 (2 H, d, J 9.3 Hz, Ar), 5.83 (1 H, dd, $J_{3,2}$ = $J_{3,4}$ 9.5 Hz, H3), 5.58 (1 H, dd, $J_{2,3}$ 9.5, $J_{2,1}$ 7.9 Hz, H2), 4.92 (1 H, d, J 12.5 Hz, OCH₂Ph), 4.92 (1 H, dd, $J_{4,5}$ = $J_{4,3}$ 9.5 Hz, H4), 4.84 (1 H, d, $J_{1,2}$ 7.9 Hz, H1), 4.71 (1 H, dd, $J_{6a,6b}$ 12.2, $J_{6a,5}$ 4.2 Hz, H6_a), 4.69 (1 H, d, J 12.5 Hz, OCH₂Ph), 4.58 (1 H, dd, $J_{6b,6a}$ 12.2, $J_{6b,5}$ 4.2 Hz, H6_b), 4.08 (1 H, ddd, $J_{5,4}$ 9.5, $J_{5,6a}$ = $J_{5,6b}$ 4.2 Hz, H5).

Benzyl 4-O-(4'-nitrophenyl)- β -D-glucopyranoside (66)

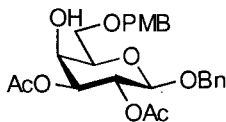
Zemplén deprotection of **63** with sodium methoxide was carried out according to the general scheme. Crystallization from EtOAc/PE gave **66** as a white solid (71%): ^1H NMR (200 MHz, $(\text{CD}_3)_2\text{CO}$) δ 8.18 (2 H, d, J 9.3 Hz, Ar), 7.46-7.26 (7 H, m, Ar), 4.92 (1 H, d, J 11.9 Hz, OCH_2Ph), 4.69 (1 H, d, J 4.4 Hz, OH), 4.66 (1 H, d, J 11.9 Hz, OCH_2Ph), 4.58 (1 H, dd, $J_{4,5} = J_{4,3}$ 9.0 Hz, H4), 4.54 (1 H, d, $J_{1,2}$ 7.8 Hz, H1), 3.95-3.72 (2 H, m), 3.68-3.56 (2 H, m), 3.43 (1 H, ddd, $J_{2,3}$ 9.0, $J_{2,1}$ 7.8, $J_{2,\text{OH}}$ 4.4 Hz, H2).

Benzyl 4-O-(4'-nitrophenyl)- β -D-glucopyranosiduronic acid (12)

Prepared from **66** as described for **1**. Purified by column chromatography (PE:EtOAc 2:3 + 0.4% acetic acid) to give **12** as a white solid (83%). **12** was then passed down an ion exchange column (Bio-Rad[®] AG 50W-X2, 200-400 mesh, H^+ form), and freeze-dried: ^1H NMR (200 MHz, $(\text{CD}_3)_2\text{CO}$) δ 8.12 (2 H, d, J 9.5 Hz, Ar), 7.42-7.18 (7 H, m, Ar), 4.88 (1 H, d, J 11.9 Hz, OCH_2Ph), 4.68 (1 H, dd, $J_{4,5} = J_{4,3}$ 9.1 Hz, H4), 4.63 (1 H, d, J 11.9 Hz, OCH_2Ph), 4.63 (1 H, d, $J_{1,2}$ 7.9 Hz, H1), 4.20 (1 H, d, $J_{5,4}$ 9.1 Hz, H5), 3.83 (1 H, dd, $J_{3,2} = J_{3,4}$ 9.1 Hz, H3), 3.49 (1 H, dd, $J_{2,3}$ 9.1, $J_{2,1}$ 7.9 Hz, H2); **Anal. calc. for** $\text{C}_{19}\text{H}_{19}\text{NO}_9 + 0.5 \text{H}_2\text{O}$: C, 55.07; H, 4.86; N, 3.38. Found: C, 55.33; H, 4.76; N, 3.31.

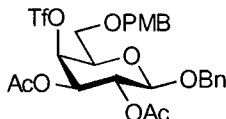
5.5.5 Benzyl 4-*O*-(3',4'-dinitrophenyl)- β -D-glucopyranosiduronic acid (**7**) (Scheme 3.9)

Benzyl 2,3-di-*O*-acetyl-6-*O*-paramethoxybenzyl- β -D-galactopyranoside (**67**)



Compound **67** was prepared from **17** as described for **47**, **48**, and **49**. Purified by column chromatography (CH_2Cl_2 :EtOAc 6:1) yielding a colourless syrup (43%): ^1H NMR (200 MHz, CDCl_3) δ 7.38-7.20 (7 H, m, Ar), 6.87 (2 H, d, J 8.5 Hz, Ar), 5.32 (1 H, dd, $J_{2,3}$ 10.0, $J_{2,1}$ 8.0 Hz, H2), 4.89 (1 H, d, J 12.2 Hz, OCH_2Ph), 4.88 (1 H, dd, $J_{3,2}$ 10.0, $J_{3,4}$ 3.2 Hz, H3), 4.62 (1 H, d, J 12.2 Hz, OCH_2Ph), 4.54 (1 H, d, J 11.7 Hz, OCH_2Ar), 4.48 (1 H, d, $J_{1,2}$ 8.0 Hz, H1), 4.47 (1 H, d, J 11.7 Hz, OCH_2Ar), 4.12 (1 H, d, $J_{4,3}$ 3.2 Hz, H4), 3.83-3.74 (2 H, m, H6_a, H6_b), 3.79 (3 H, s, OMe), 3.74-3.62 (1 H, m, H5), 2.07, 1.99 (6 H, 2 s, 2 Ac).

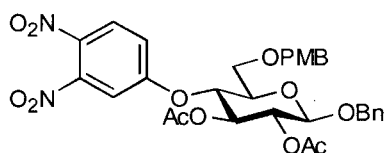
Benzyl 2,3-di-*O*-acetyl-6-*O*-paramethoxybenzyl-4-*O*-trifluoromethanesulfonyl- β -D-galactopyranoside (**68**)



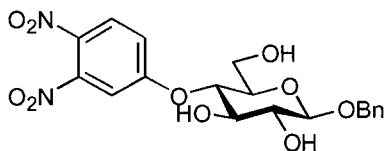
Trifluoromethanesulfonic anhydride (0.37 mL, 2.2 mmol, 3 eq) was added dropwise to a solution of **67** (348 mg, 0.73 mmol) in dry CH_2Cl_2 (3.5 mL) and dry pyridine (0.9 mL) at -15 to -20 $^\circ\text{C}$. After stirring for 15 min at this temperature the reaction was allowed to attain ambient temperature, and stirred for 2 h. The reaction mixture was diluted with H_2O and EtOAc, and the organic layer washed with 1 M HCl (3x). The combined aqueous phases were extracted with EtOAc (1x). The combined organic phases were washed with saturated NaHCO_3 (1x), H_2O (1x), dried over MgSO_4 , and concentrated under vacuum, leaving **68** as an amber syrup (420 mg, 94%). The compound is pure enough for further reactions, but can be purified by column chromatography (PE:EtOAc 7:2) to yield a colourless syrup: ^1H NMR (200 MHz, CDCl_3) δ 7.40-7.20 (7 H, m, Ar), 6.88 (2 H, d, J 8.5 Hz, Ar), 5.32 (1 H, d, $J_{4,3}$ 3.2 Hz,

H4), 5.26 (1 H, dd, $J_{2,3}$ 10.2, $J_{2,1}$ 7.8 Hz, H2), 5.04 (1 H, dd, $J_{3,2}$ 10.2, $J_{3,4}$ 3.2 Hz, H3), 4.88 (1 H, d, J 12.2 Hz, OCH₂Ar), 4.57 (1 H, d, J 12.2 Hz, OCH₂Ar), 4.54 (1 H, d, J 11.0 Hz, OCH₂Ar), 4.51 (1 H, d, $J_{1,2}$ 7.8 Hz, H1), 4.36 (1 H, d, J 11.0 Hz, OCH₂Ar), 3.85 (1 H, dd, $J_{5,6a}$ 8.8, $J_{5,6b}$ 5.4 Hz, H5), 3.80 (3 H, s, OMe), 3.69 (1 H, dd, $J_{6b,6a}$ 8.8, $J_{6b,5}$ 5.4 Hz, H6_b), 3.58 (1 H, dd, $J_{6b,6a} = J_{6b,5}$ 8.8 Hz, H6_a), 2.07, 1.99 (6 H, 2 s, 2 OAc); ¹⁹F NMR (188 MHz, CDCl₃) δ 2.05 (s).

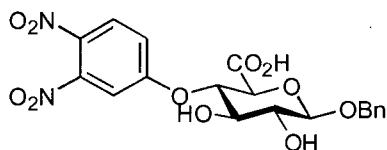
Benzyl 2,3-di-O-acetyl-4-O-(3',4'-dinitrophenyl)-6-O-paramethoxybenzyl- β -D-glucopyranoside (69)



A solution of **68** (497 mg, 0.82 mmol) and the potassium salt of 3,4-dinitrophenol (546 mg, 2.46 mmol, 3 eq) in dry DMF (5 mL) was heated to 80 °C for 2.5 h, cooled, diluted with EtOAc, and washed with H₂O (2x). The combined aqueous phases were extracted with EtOAc (3x). The combined organic phases were washed with saturated NaHCO₃ (8x), H₂O (1x), dried over MgSO₄, and concentrated in vacuo. The residue was purified by column chromatography (PE:EtOAc 3:1), to yield **69** as a light yellow foam (199 mg, 38%): ¹H NMR (200 MHz, CDCl₃) δ 7.86 (1 H, d, $J_{5',6'}$ 9.0 Hz, H5'), 7.38-7.25 (6 H, m, Ar), 7.13 (1 H, dd, $J_{6',5'}$ 9.0, $J_{6',2'}$ 2.7 Hz, H6'), 7.03 (2 H, d, J 8.8 Hz, Ar), 6.76 (2 H, d, J 8.8 Hz, Ar), 5.32 (1 H, dd, $J_{3,2} = J_{3,4}$ 9.5 Hz, H3), 5.07 (1 H, dd, $J_{2,3}$ 9.5, $J_{2,1}$ 7.8 Hz, H2), 4.92 (1 H, d, J 12.1 Hz, OCH₂Ph), 4.79 (1 H, dd, $J_{4,3} = J_{4,5}$ 9.5 Hz, H4), 4.64 (1 H, d, J 12.1 Hz, OCH₂Ph), 4.60 (1 H, d, $J_{1,2}$ 7.8 Hz, H1), 4.51 (1 H, d, J 11.4 Hz, OCH₂Ar), 4.25 (1 H, d, J 11.4 Hz, OCH₂Ar), 3.90-3.57 (3 H, m, H5, H6_a, H6_b), 3.77 (3 H, s, OMe), 1.99, 1.81 (6 H, 2 s, 2 Ac).

Benzyl 4-O-(3',4'-dinitrophenyl)- β -D-glucopyranoside (72)

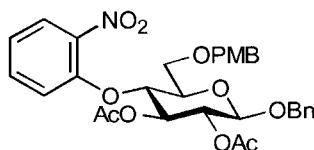
Compound **69** was deprotected with the general acetyl chloride in methanol deprotection strategy and purified by column chromatography (PE:EtOAc 1:1 to 1:2) to give **72** as a pale yellow syrup (82%): $^1\text{H NMR}$ (200 MHz, $(\text{CD}_3)_2\text{CO}$) δ 8.18 (1 H, d, $J_{5',6'}$ 9.0 Hz, H5'), 7.77 (1 H, d, $J_{2',6'}$ 2.7 Hz, H2'), 7.59 (1 H, dd, $J_{6',5'}$ 9.0, $J_{6',2'}$ 2.7 Hz, H6'), 7.42-7.18 (5 H, m, Ph), 4.87 (1 H, d, J 12.2 Hz, OCH_2Ph), 4.70-4.56 (2 H, m, H4, OCH_2Ph), 4.50 (1 H, d, $J_{1,2}$ 7.8 Hz, H1), 3.88-3.74 (2 H, m, H3, H6_a), 3.70-3.56 (2 H, m, H5, H6_b), 3.42 (1 H, dd, $J_{2,3}$ 9.0, $J_{2,1}$ 7.8 Hz, H2).

Benzyl 4-O-(3',4'-dinitrophenyl)- β -D-glucopyranosiduronic acid (7)

Prepared from **72** as described for **4**. Purified by column chromatography (PE:EtOAc 2:3 + 0.4% acetic acid) to give **7** as a white solid (85%). **7** was passed down an ion exchange column (Bio-Rad[®] AG 50W-X2, 200-400 mesh, H^+ form), and freeze-dried: $^1\text{H NMR}$ (200 MHz, $(\text{CD}_3)_2\text{CO}$) δ 8.13 (1 H, d, $J_{5',6'}$ 9.0 Hz, H5'), 7.70 (1 H, d, $J_{2',6'}$ 2.5 Hz, H2'), 7.52 (1 H, dd, $J_{6',5'}$ 9.0, $J_{6',2'}$ 2.5 Hz, H6'), 7.40-7.20 (5 H, m, Ph), 4.85 (1 H, d, J 12.0 Hz, OCH_2Ph), 4.79 (1 H, dd, $J_{4,5} = J_{4,3}$ 9.1 Hz, H4), 4.64 (1 H, d, $J_{1,2}$ 8.0 Hz, H1), 4.63 (1 H, d, J 12.0 Hz, OCH_2Ph), 4.25 (1 H, d, $J_{5,4}$ 9.1 Hz, H5), 3.86 (1 H, dd, $J_{3,2} = J_{3,4}$ 9.1 Hz, H3), 3.50 (1 H, dd, $J_{2,3}$ 9.1, $J_{2,1}$ 8.0 Hz, H2); **HRMS** (LSIMS⁺, glycerol) m/z : 451.0984. Calc. For $\text{C}_{19}\text{H}_{19}\text{N}_2\text{O}_{11}$ $[\text{M} + 1]^+$ 451.0989.

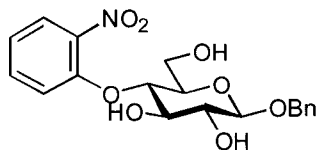
5.5.6 Benzyl 4-*O*-(2'-nitrophenyl)- β -D-glucopyranosiduronic acid (9) (Scheme 3.9)

Benzyl 2,3-di-*O*-acetyl-4-*O*-(2'-nitrophenyl)-6-*O*-paramethoxybenzyl- β -D-glucopyranoside (70)

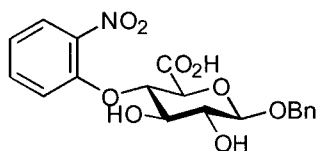


Prepared from **68** as described for **69**. Purified by column chromatography (PE:EtOAc 3:1 to 2.5:1) to give **70** as a colourless syrup (37%): ^1H NMR (200 MHz, CDCl_3) δ 7.72 (1 H, dd, $J_{3',4'} 8.1$, $J_{3',5'} 1.7$ Hz, $\text{H}_{3'}$), 7.44 (1 H, ddd, $J 8.5$, $J 7.1$, $J 1.7$ Hz, Ar), 7.36-7.26 (6 H, m, Ar), 7.08-6.98 (3 H, m, Ar), 6.73 (2 H, d, $J 8.8$ Hz, Ar), 5.33 (1 H, dd, $J_{3,2} = J_{3,4} 9.6$ Hz, H_3), 5.04 (1 H, dd, $J_{2,3} 9.6$, $J_{2,1} 7.8$ Hz, H_2), 4.91 (1 H, d, $J 12.4$ Hz, OCH_2Ph), 4.85 (1 H, dd, $J_{4,3} = J_{4,5} 9.6$ Hz, H_4), 4.63 (1 H, d, $J 12.4$ Hz, OCH_2Ph), 4.59 (1 H, d, $J_{1,2} 7.8$ Hz, H_1), 4.44 (1 H, d, $J 11.6$ Hz, OCH_2Ar), 4.24 (1 H, d, $J 11.6$ Hz, OCH_2Ar), 3.80-3.65 (3 H, m, H_5 , H_{6a} , H_{6b}), 3.77 (3 H, s, OMe), 1.98, 1.76 (6 H, 2 s, 2 Ac).

Benzyl 4-*O*-(2'-nitrophenyl)- β -D-glucopyranoside (73)



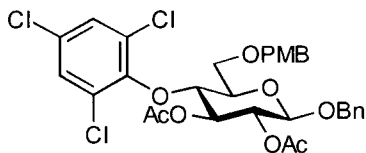
Compound **70** was deprotected with the general acetyl chloride in methanol deprotection strategy and purified by column chromatography (PE:EtOAc 1:1) to give **73** as a white foam (84%): ^1H NMR (200 MHz, $(\text{CD}_3)_2\text{CO}$) δ 7.77 (1 H, dd, $J 8.0$, $J 1.5$ Hz, Ar), 7.69 (1 H, dd, $J 8.8$, 1.5 Hz, Ar), 7.59 (1 H, ddd, $J 8.8$, $J 7.3$, $J 1.7$ Hz, Ar), 7.46-7.26 (5 H, m, Ph), 7.10 (1 H, ddd, $J 8.0$, $J 7.3$, $J 1.5$ Hz, Ar), 4.88 (1 H, d, $J 12.2$ Hz, OCH_2Ph), 4.61 (1 H, d, $J 12.2$ Hz, OCH_2Ph), 4.61 (1 H, d, $J 4.6$ Hz, OH), 4.53 (1 H, d, $J 4.4$ Hz, OH), 4.50 (1 H, dd, $J_{4,5} = J_{4,3} 8.8$ Hz, H_4), 4.49 (1 H, d, $J_{1,2} 7.8$ Hz, H_1), 3.90-3.52 (4 H, m, H_3 , H_5 , H_{6a} , H_{6b}), 3.36 (1 H, ddd, $J_{2,3} 9.0$, $J_{2,1} 7.8$, $J_{2,\text{OH}} 3.7$ Hz, H_2).

Benzyl 4-O-(2'-nitrophenyl)- β -D-glucopyranosiduronic acid (9)

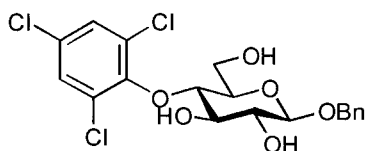
Prepared from **73** as described for **4**. Purified by column chromatography (PE:EtOAc 1:2 + 0.4% acetic acid), passed down a cation exchange column (Bio-Rad[®] AG 50W-X2, 200-400 mesh, H⁺ form), and freeze-dried to give **9** as a white solid (53%): ¹H NMR (200 MHz, (CD₃)₂CO) δ 7.71 (1 H, dd, J 8.0, J 1.6 Hz, Ar), 7.64 (1 H, dd, J 8.8, J 1.5 Hz, Ar), 7.54 (1 H, ddd, J 8.8, J 7.1, J 1.8 Hz, Ar), 7.40-7.20 (5 H, m, Ph), 7.06 (1 H, ddd, J 8.3, J 7.1, J 1.5 Hz, Ar), 4.88 (1 H, d, J 12.0 Hz, OCH₂Ph), 4.64 (1 H, dd, J_{4,5} = J_{4,3} 9.1 Hz, H₄), 4.63 (1 H, d, J_{1,2} 7.9 Hz, H₁), 4.62 (1 H, d, J 12.0 Hz, OCH₂Ph), 4.17 (1 H, d, J_{5,4} 9.1 Hz, H₅), 3.83 (1 H, dd, J_{3,4} = J_{3,2} 9.1 Hz, H₃), 3.44 (1 H, dd, J_{2,3} 9.1, J_{2,1} 7.9 Hz, H₂); **Anal. calc. for** C₁₉H₁₉NO₉ + 0.5 H₂O: C, 55.07; H, 4.86; N, 3.38. Found: C, 55.23; H, 4.85; N, 3.38.

5.5.7 Benzyl 4-O-(2',4',6'-trichlorophenyl)- β -D-glucopyranosiduronic acid (11)

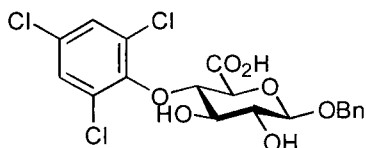
(Scheme 3.9)

Benzyl 2,3-di-O-acetyl-4-O-(2',4',6'-trichlorophenyl)-6-O-paramethoxybenzyl- β -D-glucopyranoside (71)

Prepared from **68** as described for **69**. Purified by column chromatography (PE:EtOAc 4:1) to give **71** as a syrup (47%): ¹H NMR (200 MHz, CDCl₃) δ 7.38-7.20 (9 H, m, Ar), 6.86 (2 H, d, J 8.8 Hz, Ar), 5.38 (1 H, dd, J_{3,2} = J_{3,4} 9.2 Hz, H₃), 5.00 (1 H, dd, J_{4,3} = J_{4,5} 9.2 Hz, H₄), 4.93 (1 H, dd, J_{2,3} 9.2, J_{2,1} 8.0 Hz, H₂), 4.90 (1 H, d, J 12.4 Hz, OCH₂Ph), 4.64 (1 H, d, J 12.4 Hz, OCH₂Ph), 4.62 (1 H, d, J_{1,2} 8.0 Hz, H₁), 4.46 (1 H, d, J 11.7 Hz, OCH₂Ar), 4.40 (1 H, d, J 11.6 Hz, OCH₂Ar), 3.96-3.80 (2 H, m, H₅, H_{6a}), 3.80 (3 H, s, OMe), 3.68 (1 H, dd, J_{6b,6a} 11.0, J_{6b,5} 5.3 Hz, H_{6b}), 1.98, 1.65 (6 H, 2 s, 2 Ac).

Benzyl 4-O-(2',4',6'-trichlorophenyl)- β -D-glucopyranoside (74)

Compound **71** was deprotected with the general acetyl chloride in methanol deprotection strategy and purified by recrystallization from EtOAc/PE to give **74** as a white solid (86%): mp 169-170 °C; ^1H NMR (200 MHz, $(\text{CD}_3)_2\text{CO}$) δ 7.40-7.17 (7 H, m, Ar), 4.90 (1 H, d, J 12.0 Hz, OCH_2Ph), 4.62 (1 H, d, J 12.0 Hz, OCH_2Ph), 4.55 (1 H, d, J 4.2 Hz, OH), 4.45 (1 H, d, $J_{1,2}$ 7.8 Hz, H1), 4.44 (1 H, dd, $J_{4,5} = J_{4,3}$ 8.7 Hz, H4), 4.12-3.62 (4 H, m, H3, H5, H6_a, H6_b), 3.20 (1 H, ddd, $J_{2,3}$ 8.8, $J_{2,1}$ 7.8, $J_{2,\text{OH}}$ 4.2 Hz, H2).

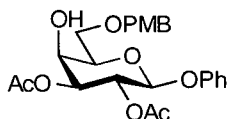
Benzyl 4-O-(2',4',6'-trichlorophenyl)- β -D-glucopyranosiduronic acid (11)

Prepared from **74** as described for **1**. Purified by column chromatography (PE:EtOAc 1:1 + 0.4% acetic acid) to give **11** as a white solid (82%): ^1H NMR (200 MHz, CDCl_3) δ 7.38-7.32 (5 H, m, Ph), 7.22 (2 H, s, H3',H5'), 4.96 (1 H, d, J 11.8 Hz, OCH_2Ph), 4.78 (1 H, dd, $J_{4,5}$ 8.8, $J_{4,3}$ 8.5 Hz, H4), 4.63 (1 H, d, J 11.8 Hz, OCH_2Ph), 4.55 (1 H, d, $J_{1,2}$ 7.6 Hz, H1), 4.28 (1 H, d, $J_{5,4}$ 8.8 Hz, H5), 4.12 (1 H, dd, $J_{3,2}$ 8.8, $J_{3,4}$ 8.5 Hz, H3), 3.52 (1 H, dd, $J_{2,3}$ 8.8, $J_{2,1}$ 7.6 Hz, H2).

5.6 Synthesis of the Fluorogenic Substrate

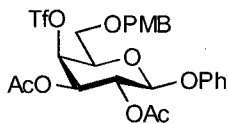
Phenyl 4-methylumbelliferyl- β -D-glucopyranosiduronic acid (**2**) (Scheme 3.10)

Phenyl 2,3-di-O-acetyl-6-O-paramethoxybenzyl- β -D-galactopyranoside (**75**)



A solution of **16** (2.69 g, 10.5 mmol), *p*-anisaldehyde dimethyl acetal (3.82 g, 21.0 mmol, 2 eq) and *p*-toluenesulfonic acid monohydrate (60 mg, 0.32 mmol, 0.03 eq) in dry DMF (15 mL) was rotated under aspirator pressure at 50 °C for 5 h. The temperature was then increased to 65 °C, and the reaction mixture concentrated under vacuum and poured slowly into a rapidly stirring mixture of water (10 mL), NaOH (35 mg), ice and ether (10 mL) causing phenyl 4,6-*O*-paramethoxybenzylidene- β -D-galactopyranoside to precipitate as a white solid (3.92 g 99%), which was filtered off and dried over P₂O₅ under vacuum. After acetylation of the remaining two hydroxyls via the general acetylation procedure, the benzylidene ring was selectively opened as for **49**, and the resulting crude material purified by column chromatography (CH₂Cl₂:EtOAc 6:1) giving **75** as a colourless syrup (81% for two steps): ¹H NMR (300 MHz, CDCl₃) δ 7.30-7.17 (3 H, m, Ar), 7.07-6.97 (3 H, m, Ar), 6.90-6.80 (3 H, m, Ar), 5.52 (1 H, dd, *J*_{2,3} 10.2, *J*_{2,1} 7.9 Hz, H2), 5.01 (1 H, d, *J*_{1,2} 7.9 Hz, H1), 4.99 (1 H, dd, *J*_{3,2} 10.2, *J*_{3,4} 3.2 Hz, H3), 4.50 (1 H, d, *J* 11.7 Hz, OCH₂Ar), 4.45 (1 H, d, *J* 11.7 Hz, OCH₂Ar), 4.18 (1 H, d, *J*_{4,3} 3.2 Hz, H4), 4.83-4.66 (6 H, m, H5, H6_a, H6_b, OMe), 2.10, 2.03 (6 H, 2 s, 2 Ac).

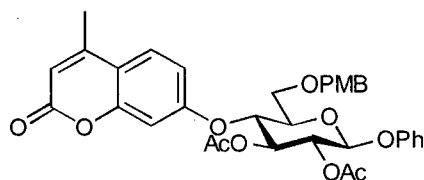
Phenyl 2,3-di-O-acetyl-6-O-paramethoxybenzyl-4-O-trifluoromethanesulfonyl- β -D-galactopyranoside (**76**)



Prepared from **75** as described for **68**. Purified by column chromatography (PE:EtOAc 7:2) to give **76** as a pale yellow syrup which crystallizes (66%): ¹H NMR

(300 MHz, CDCl_3) δ 7.35-7.22 (5 H, m, Ar), 7.10 (1 H, t, J 7.4 Hz, Ar), 7.00 (2 H, d, J 7.9 Hz, Ar), 6.90 (1 H, d, J 8.8 Hz, Ar), 5.51 (1 H, dd, $J_{2,3}$ 10.2, $J_{2,1}$ 7.9 Hz, H2), 5.40 (1 H, d, $J_{4,3}$ 2.8 Hz, H4), 5.20 (1 H, dd, $J_{3,2}$ 10.2, $J_{3,4}$ 2.8 Hz, H3), 5.08 (1 H, d, $J_{1,2}$ 7.9 Hz, H1), 4.55 (1 H, d, J 10.6 Hz, OCH_2Ar), 4.39 (1 H, d, J 10.6 Hz, OCH_2Ar), 4.04 (1 H, dd, $J_{5,6\text{ax}}$ 7.9, $J_{5,6\text{eq}}$ 6.5 Hz, H5), 3.83 (3 H, s, OMe), 3.74 (1 H, dd, $J_{6\text{eq},6\text{ax}}$ 9.2, $J_{6\text{eq},5}$ 6.5 Hz, H6_{eq}), 3.65 (1 H, dd, $J_{6\text{ax},6\text{eq}}$ 9.2, $J_{6\text{ax},5}$ 7.9 Hz, H6_{ax}), 2.14, 2.09 (6 H, 2 s, 2 Ac); ^{13}C NMR (100 MHz, CDCl_3) δ 169.95, 168.96 (2 C=O), 159.51, 156.74 (2 C), 129.71, 129.64 (2 CH), 123.47 (CH), 118.37 (q, J 320.9 Hz, CF_3), 116.98, 113.90 (2 CH), 99.70 (CH, C1), 80.62 (CH), 73.36 (CH_2), 71.75, 69.79, 68.21 (3 CH), 66.40 (CH_2), 55.27 (CH_3), 20.61, 20.46 (2 Ac); ^{19}F NMR (282 MHz, CDCl_3) δ 1.74.

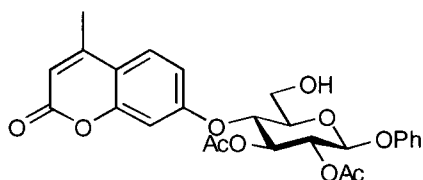
Phenyl 2,3-di-O-acetyl-4-methylumbelliferyl-6-O-paramethoxybenzyl- β -D-glucopyranoside (77)



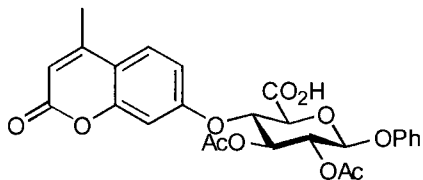
Prepared from **76** as described for **69**. Purified by column chromatography (CH_2Cl_2 :EtOAc 16:1 to 14:1) to give **77** as a white foam (29%); ^1H NMR (400 MHz, CDCl_3) δ 7.42 (1 H, d, J 8.8 Hz, Ar), 7.28 (1 H, dd, J 7.3, J 8.5 Hz, Ar), 7.06 (1 H, dd, J 7.6 Hz, Ar), 7.04-6.97 (5 H, m, Ar), 6.93 (1 H, d, J 2.4 Hz, Ar), 6.88 (1 H, dd, J 8.8, J 2.4 Hz, Ar), 6.70 (2 H, d, J 8.8 Hz, Ar), 6.16 (1 H, d, J 1.2 Hz, Ar), 5.44 (1 H, dd, $J_{3,2} = J_{3,4}$ 9.4 Hz, H3), 5.28 (1 H, dd, $J_{2,3}$ 9.4, $J_{2,1}$ 7.9 Hz, H2), 5.12 (1 H, d, $J_{1,2}$ 7.9 Hz, H1), 4.74 (1 H, dd, $J_{4,3} = J_{4,5}$ 9.4 Hz, H4), 4.42 (1 H, d, J 11.6 Hz, OCH_2Ar), 4.80 (1 H, d, J 11.6 Hz, OCH_2Ar), 3.84 (1 H, ddd, $J_{5,4}$ 9.4, $J_{5,6\text{ax}}$ 4.0, $J_{5,6\text{eq}}$ 1.8 Hz, H5), 3.74 (3 H, s, OMe), 3.72 (1 H, dd, $J_{6\text{eq},6\text{ax}}$ 11.0, $J_{6\text{eq},5}$ 1.8 Hz, H6_{eq}), 3.62 (1 H, dd, $J_{6\text{ax},6\text{eq}}$ 11.0, $J_{6\text{ax},5}$ 4.0 Hz, H6_{ax}), 2.38 (3 H, s, CH_3), 2.03, 1.80 (6 H, 2 s, 2 Ac); ^{13}C NMR (100 MHz, CDCl_3) δ 169.78, 169.48 (2 C=O), 161.15, 160.86, 159.18, 156.98, 154.91, 152.06 (6 C or C=O), 129.56 (CH), 129.38 (CH), 129.38 (C), 125.58, 123.20, 117.02 (3 CH), 114.70 (C), 113.58, 112.89, 112.78, 103.89, 99.18, 74.63, 74.36, 73.95 (8 CH), 73.20 (CH_2), 71.43 (CH),

67.21 (CH₂), 55.19 (OCH₃), 20.62, 20.57, 18.62 (3 CH₃); **Anal. calc. for** C₃₄H₃₄O₁₁: C, 66.01; H, 5.54. Found: C, 65.97; H, 5.48.

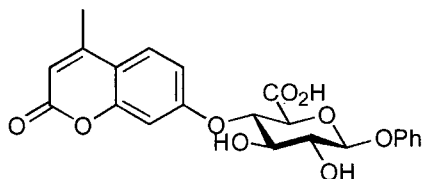
Phenyl 2,3-di-O-acetyl-4-methylumbelliferyl-β-D-glucopyranoside (78)



Ceric ammonium nitrate (C.A.N., 946 mg, 1.73 mmol, 2 eq) was added to a solution of **77** (534 mg, 0.86 mmol) in 9:1 CH₃CN:H₂O (8 mL) and stirred at rt for 1 h. TLC indicated incomplete reaction, so a further 300 mg C.A.N. was added and the reaction stirred for another 2 h. The solvent was evaporated under vacuum and the residue dissolved in EtOAc, washed with H₂O (1x), saturated NaHCO₃ (1x), H₂O (1x), dried over MgSO₄, and concentrated in vacuo. The residue was purified by column chromatography (PE:EtOAc 5:4 to 1:1) to give **78** as a white foam (375 mg, 87%): **mp** 102-103 °C; ¹H NMR (300 MHz, CDCl₃) δ 7.48 (1 H, d, J 8.8 Hz, Ar), 7.29 (1 H, dd, J 8.3, J 7.9 Hz, Ar), 7.06 (1 H, dd, J 7.4 Hz, Ar), 7.02-6.93 (5 H, m, Ar), 6.15 (1 H, d, J 0.9 Hz, Ar), 5.47 (1 H, dd, J_{3,4} 9.2, J_{3,2} 8.8 Hz, H₃), 5.29-5.18 (2 H, m, H₁, H₂), 4.71 (1 H, dd, J_{4,5} = J_{4,3} 9.2 Hz, H₄), 3.93 (1 H, dd, J_{6eq,6ax} 12.5, J_{6eq,5} 1.8 Hz, H_{6eq}), 3.78 (1 H, ddd, J_{5,4} 9.2, J_{5,6ax} 3.2, J_{5,6eq} 1.8 Hz, H₅), 3.70 (1 H, dd, J_{6ax,6eq} 12.5, J_{6ax,5} 3.2 Hz, H_{6ax}), 2.36 (3 H, s, CH₃), 2.03, 1.80 (6 H, 2 s, 2 Ac); ¹³C NMR (100 MHz, CDCl₃) δ 169.78, 169.49 (2 C=O), 161.14, 160.89, 156.73, 154.93, 152.11 (5 C or C=O), 129.68, 125.79, 123.34, 116.71 (4 CH), 114.85 (C), 112.91, 112.81, 103.93, 98.92, 74.73, 74.27, 73.70, 71.30 (8 CH), 60.54 (CH₂), 20.58, 20.53, 18.60 (3 CH₃); **Anal. calc. for** C₂₆H₂₆O₁₀: C, 62.65; H, 5.26. Found: C, 62.52; H, 5.31.

Phenyl 2,3-di-O-acetyl-4-methylumbelliferyl- β -D-glucopyranosiduronic acid (79)

A solution of **78** (222 mg, 0.445 mmol) and 1.1 mL of Jones reagent (1 g CrO_3 , 0.86 mL H_2SO_4 , 7.1 mL H_2O) in acetone (3.2 mL) was sonicated at 35–40 °C for 1.5 h and the reaction was quenched with isopropanol. The dark bottom layer of the reaction mixture was discarded, and any solid filtered off from the remaining liquid. The solvent was evaporated under vacuum and the residue purified by column chromatography (PE:EtOAc 1:3.25 to 100% EtOAc to EtOAc:MeOH 9:1) to give **79** as a glassy white solid (143 mg, 63%): ^1H NMR (400 MHz, CDCl_3) (Note all signals are very broad) δ 7.20 (3 H, s, Ar), 6.93 (5 H, s, Ar), 5.80 (1 H, s, Ar), 5.45 (1 H, s), 5.24 (2 H, s), 4.98 (1 H, s), 4.36 (1 H, s), 2.00 (6 H, m), 1.78 (3 H, s); ^{13}C NMR (100 MHz, CDCl_3) (Note all signals are very broad) δ 166.75, 166.17 (2 C=O), 158.71, 158.14, 154.11, 151.57, 150.37, 127.86, 123.91, 121.66, 115.34, 113.19, 110.78, 103.58, 98.62, 74.30, 73.53, 71.44, 22.48, 20.34; ESI-MS m/z 513.4 $[\text{M} + \text{H}]^+$; Anal. calc. for $\text{C}_{26}\text{H}_{24}\text{O}_{11} + 1 \text{ H}_2\text{O}$: C, 58.87; H, 4.94. Found: C, 58.83; H, 4.82.

Phenyl 4-methylumbelliferyl- β -D-glucopyranosiduronic acid (2)

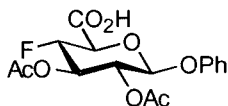
Zemplén deprotection of **79** with sodium methoxide was carried out according to the general procedure. The residue was purified by column chromatography (PE:EtOAc 1:4 to 100% EtOAc to EtOAc:MeOH 9:1 to EtOAc:MeOH 8:2) then HPLC (amide-80 column, linear gradient from 100% CH_3CN to $\text{CH}_3\text{CN}:\text{H}_2\text{O}$ 4:1 over 50 min, then $\text{CH}_3\text{CN}:\text{H}_2\text{O}$ 4:1 until completely eluted), to give **2** as a white solid (94%). **2** was then passed down a cation exchange column (Bio-Rad® AG 50W-X2, 200–400 mesh, H^+ form), and freeze-dried to give **2** as a white solid: ^1H NMR (400 MHz, CD_3OD) δ 7.57 (1

H, d, J 8.5 Hz, Ar), 7.20 (2 H, dd, J 8.5, J 7.3 Hz, Ar), 7.04-6.98 (4 H, m, Ar), 6.93 (1 H, t, J 7.3 Hz, Ar), 6.07 (1 H, d, J 1.2 Hz, Ar), 5.00 (1 H, d, $J_{1,2}$ 7.9 Hz, H1), 4.52 (1 H, dd, $J_{4,5}$ 9.7, $J_{4,3}$ 9.4 Hz, H4), 4.22 (1 H, d, $J_{5,4}$ 9.7 Hz, H5), 4.76 (1 H, dd, $J_{3,4}$ 9.4, $J_{3,2}$ 9.1 Hz, H3), 3.57 (1 H, dd, $J_{2,3}$ 9.1, $J_{2,1}$ 7.9 Hz, H2), 2.34 (3 H, s, CH₃); ¹³C NMR (100 MHz, CD₃OD) δ 164.12, 163.55, 158.84, 155.88, 155.60 (5 C or C=O), 130.41, 123.61, 117.82, 115.51 (4 CH), 115.18 (C), 112.18, 104.97, 80.70, 76.79, 74.83 (5 CH), 18.65 (CH₃); **Anal. calc.** for C₂₂H₂₀O₉ + 1 H₂O: C, 59.19; H, 4.97. Found: C, 59.15; H, 4.83.

5.7 Synthesis of the Substrates for the Deuterium Kinetic Isotope Effects

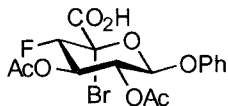
5.7.1 Phenyl 4-deoxy-4-fluoro-5-{²H}-β-D-glucopyranosiduronic acid (83) (Scheme 3.11)

Phenyl 2,3-di-O-acetyl-4-deoxy-4-fluoro-β-D-glucopyranosiduronic acid (80)



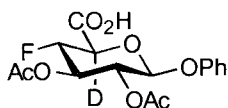
A solution of 4.3:1 acetic anhydride:sulfuric acid (35 μL) was added to a solution of **3** (656 mg, 2.41 mmol) in acetic anhydride (18 mL) and stirred at rt for 1.5 h, concentrated, added H₂O, extracted with CH₂Cl₂ (3x), EtOAc (3x). The combined organic phases were dried over MgSO₄, and concentrated. The residue was recrystallized from toluene/EtOAc/PE to give **80** as a white solid (681 mg, 79%): mp 175-176 °C; ¹H NMR (200 MHz, CDCl₃) δ 7.35-6.80 (5 H, m, Ar), 5.52-5.30 (1 H, m H3), 5.23 (1 H, dd, $J_{2,3}$ 9.6, $J_{2,1}$ 7.1 Hz, H2), 5.20 (1 H, d, $J_{1,2}$ 7.1 Hz, H1), 4.88 (1 H, ddd, $J_{4,F}$ 49.6, $J_{4,3} = J_{4,5}$ 9.0 Hz, H4), 4.31 (1 H, dd, $J_{5,4}$ 9.0, $J_{5,F}$ 5.8 Hz, H5), 2.11, 2.07 (6 H, 2 s, 2 Ac); ¹³C NMR (75 MHz, CDCl₃) δ 169.94, 169.81, 169.44 (3 C=O), 156.46 (C), 129.73, 123.77, 117.02 (3 CH), 99.12 (CH, C1), 86.86 (CH, d, $J_{4,F}$ 190.7 Hz, C4), 72.19 (CH, d, $J_{5,F}$ 25.2 Hz, C5), 71.70 (CH, d, $J_{3,F}$ 20.9 Hz, C3), 70.83 (CH, d, $J_{2,F}$ 7.2 Hz, C2), 20.64, 20.58 (2 Ac); ¹⁹F NMR (188 MHz, CDCl₃) δ -121.7 (ddd, $J_{F,4}$ 49.6, $J_{F,3}$ 14.0, $J_{F,5}$ 5.8 Hz); **Anal. calc.** for C₁₆H₁₇FO₈: C, 53.94; H, 4.81. Found: C, 53.64; H, 4.61.

Phenyl 2,3-di-O-acetyl-5-bromo-4-deoxy-4-fluoro- β -D-glucopyranosiduronic acid (81)

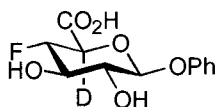


N-Bromosuccinimide (665 mg, 3.74 mmol, 2 eq) was added to a suspension of **80** in dry CCl_4 (20 mL) and irradiated with two 200 watt light bulbs (reflux) for 1 h, cooled, filtered, and concentrated. The residue was purified by column chromatography (EtOAc:MeOH 11: 1 + 0.4 % acetic acid) to yield **81** as a white solid (317 mg, 39%): ^1H NMR (300 MHz, CDCl_3) δ 7.30-6.80 (5 H, m, Ph), 5.75-5.45 (2 H, m, H1, H3), 5.40-5.20 (1 H, m, H2), 4.70 (1 H, d, br, $J_{\text{F},4}$ 48 Hz, H4), 2.05 (6 H, s, br, 2 Ac); ^{13}C NMR (75 MHz, CDCl_3) δ 169.72, 169.26, 169.20 (3 C=O), 156.55 (C), 129.86, 123.84, 116.56 (3 CH), 98.64 (CH, C1), 87.35 (CH, d, $J_{4,\text{F}}$ 202.9 Hz, C4), 70.76, 70.50, 69.65 (3 CH), 20.54, 20.50 (2 Ac).

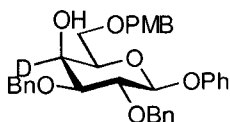
Phenyl 2,3-di-O-acetyl-4-deoxy-4-fluoro-5- $\{^2\text{H}\}$ - β -D-glucopyranosiduronic acid (82)



Tributyltin deuteride (250 μL , 0.93 mmol, 1.3 eq) was added to a solution of **81** (310 mg, 0.71 mmol) in dry toluene (15 mL) and heated to reflux for 1.5 h, cooled, and concentrated. The residue was dissolved in acetonitrile and washed with hexanes (5x), and then concentrated. Purification of the residue by column chromatography was problematic. Three silica columns were run (1. EtOAc:PE 9:1 + 0.4% acetic acid; 2. 100% EtOAc + 0.4% acetic acid; 3. EtOAc:toluene 6:1 + 0.4% acetic acid) to yield **82** as a white solid (13 mg, 5%): ^1H NMR (200 MHz, $(\text{CD}_3)_2\text{CO}$) δ 7.40-7.00 (5 H, m, Ph), 5.59 (1 H, d, $J_{1,2}$ 7.8 Hz, H1), 5.57 (1 H, ddd, $J_{3,\text{F}}$ 14.6, $J_{3,2}$ 9.5, $J_{3,4}$ 8.8 Hz, H3), 5.20 (1 H, dd, $J_{2,3}$ 9.5, $J_{2,1}$ 7.8 Hz, H2), 4.88 (1 H, dd, $J_{4,\text{F}}$ 50.0, $J_{4,3}$ 8.8 Hz, H4), 2.08, 2.03 (6 H, 2 s, 2 Ac); ^{13}C NMR (75 MHz, $(\text{CD}_3)_2\text{CO}$) δ 171.17 (2 x C=O), 170.71 (C=O), 158.93 (C), 131.51, 125.08, 118.70 (3 CH), 100.52 (CH, C1), 89.84 (CH, d, $J_{4,\text{F}}$ 187.9 Hz, C4), 73.80 (CH, d, $J_{3,\text{F}}$ 20.1 Hz, C3), 72.59 (CH, d, $J_{2,\text{F}}$ 8.0 Hz, C2), 21.57, 21.50 (2 Ac); ^{19}F NMR (188 MHz, $(\text{CD}_3)_2\text{CO}$) δ -123.47 (dd, $J_{\text{F},4}$ 50.0, $J_{\text{F},3}$ 14.6 Hz).

Phenyl 4-deoxy-4-fluoro-5- $\{^2\text{H}\}$ - β -D-glucopyranosiduronic acid (83**)**


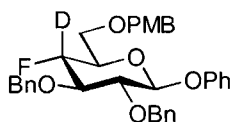
Zemplén deprotection of **82** was carried out with NaOMe- d_3 in CD_3OD according to the general procedure. The crude product was purified by column chromatography (EtOAc:PE 9:1 + 0.4% acetic acid) to give **83** as an oil which solidifies (92%). The residue was dissolved in H_2O and passed down a column of acid resin (Bio-Rad[®] AG 50W-X2, 200-400 mesh) and freeze-dried to give **83** as a fluffy white solid: ^1H NMR (200 MHz, $(\text{CD}_3)_2\text{CO}$) δ 7.35-6.90 (5 H, m, Ph), 5.22 (1 H, d, $J_{1,2}$ 7.8 Hz, H1), 4.57 (1 H, dd, $J_{4,F}$ 50.3, $J_{4,3}$ 8.8 Hz, H4), 3.90 (1 H, ddd, $J_{3,F}$ 16.1, $J_{3,4} = J_{3,2}$ 8.8 Hz, H3), 3.60 (1 H, dd, $J_{2,3}$ 8.8, $J_{2,1}$ 7.8 Hz, H2); ^{13}C NMR (75 MHz, $(\text{CD}_3)_2\text{CO}$) δ 168.79 (C=O), 158.41 (C), 130.24, 123.31, 117.45 (3 CH), 101.63 (CH, C1), 91.40 (CH, d, $J_{4,F}$ 183.9 Hz, C4), 74.92 (CH, d, $J_{3,F}$ 17.8 Hz, C3), 74.20 (CH, d, $J_{2,F}$ 8.8 Hz, C2); ^{19}F NMR (188 MHz, $(\text{CD}_3)_2\text{CO}$) δ -122.74 (dd, $J_{F,4}$ 50.3, $J_{F,3}$ 16.1 Hz); HRMS (LSIMS-, 3-NBA) m/z : 272.06846. Calc. For $\text{C}_{12}\text{H}_{11}\text{DFO}_6$ $[\text{M} - \text{H}]^-$ 272.0690.

5.7.2 Phenyl 4-deoxy-4-fluoro-4- $\{^2\text{H}\}$ - β -D-glucopyranosiduronic acid (87**) (Scheme 3.12)**
Phenyl 2,3-di-O-benzyl-6-O-paramethoxybenzyl-4- $\{^2\text{H}\}$ - β -D-galactopyranoside (84**)**


Sodium borodeuteride (374 mg, 8.94 mmol) was added to a mixture of **55** (2.48 g, 4.47 mmol) in dry MeOH (40 mL), and stirred for 40 min at rt. Water was added, and the reaction mixture was extracted with CH_2Cl_2 (3x). The combined organic phases were washed once with H_2O , dried over MgSO_4 , and concentrated under vacuum. The residue was purified by column chromatography (PE:EtOAc 3:1 to 2.75:1) to yield **84** as a colourless oil which crystallizes with time (2.33 g, 94%). A small sample was recrystallized from ethanol for elemental analysis: mp 89-90 °C; ^1H NMR (400 MHz, CDCl_3) δ 7.39-7.22 (14 H, m, Ar), 7.09 (2 H, m, Ar), 7.05 (1 H, m, Ar), 6.86 (2 H, d, J

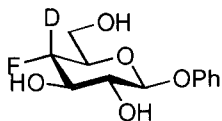
8.8 Hz, Ar), 5.01 (1 H, d, J 11.0 Hz, OCH₂Ar), 4.98 (1 H, d, J_{1,2} 7.6 Hz, H₁), 4.84 (1 H, d, J 11.0 Hz, OCH₂Ar), 4.75 (2 H, s, OCH₂Ar), 4.50 (2 H, s, OCH₂Ar), 3.96 (1 H, dd, J_{2,3} 9.4, J_{2,1} 7.6 Hz, H₂), 3.82 (1 H, dd, J_{6eq,6ax} 9.7, J_{6eq,5} 5.5 Hz, H_{6eq}), 3.80 (3 H, s, OMe), 3.75 (1 H, dd, J_{6ax,6eq} 9.7, J_{6ax,5} 5.8 Hz, H_{6ax}), 3.68 (1 H, dd, J_{5,6ax} 5.8, J_{5,6eq} 5.5 Hz, H₅), 3.59 (1 H, d, J_{3,2} 9.4 Hz, H₃); ¹³C NMR (100 MHz, CDCl₃) δ 159.25, 157.35, 138.34, 137.77, 130.05 (5 C), 129.41, 129.36, 128.44, 128.28, 128.14, 127.89, 127.80, 127.65, 122.55, 116.97, 113.78 (11 CH), 101.74 (CH, C1), 80.48, 78.56 (2 CH), 75.32 (CH₂), 73.55 (CH), 73.38, 72.43, 68.89 (3 CH₂), 55.21 (CH₃); **Anal. calc. for** C₃₄H₃₅DO₇: C, 73.23; H, 6.46. Found: C, 73.08; H, 6.52.

Phenyl 2,3-di-O-benzyl-4-deoxy-4-fluoro-6-O-*paramethoxybenzyl*-4-{²H}-β-D-galactopyranoside (85)



Prepared from **84** as for **23**. Purified by column chromatography (PE:EtOAc 8:1) to afford **85** as a white solid. A sample was recrystallized from ethanol/PE for elemental analysis: mp 69-70 °C; ¹H NMR (400 MHz, CDCl₃) δ 7.38-7.27 (12 H, m, Ar), 7.23 (2 H, d J 8.8 Hz, Ar), 7.10-7.04 (3 H, m, Ar), 6.85 (2 H, d, J 8.8 Hz, Ar), 5.02 (1 H, d, J_{1,2} 7.3 Hz, H₁), 5.01 (1 H, d, J 11.0 Hz, OCH₂Ar), 4.87 (1 H, d, J 11.3 Hz, OCH₂Ar), 4.83 (1 H, d, J 11.0 Hz, OCH₂Ar), 4.81 (1 H, d, J 11.3 Hz, OCH₂Ar), 4.52 (2 H, s, OCH₂Ar), 3.85-3.68 (4 H, m, H₂, H₃, H_{6a}, H_{6b}), 3.80 (3 H, s, OMe), 3.65 (1 H, ddd, J_{5,6ax} 10.7, J_{5,6eq} 6.1, J_{5,F} 1.8 Hz, H₅); ¹⁹F NMR (188 MHz, CDCl₃) δ -120.70 (s, br); **ESI-MS** m/z 582.2 [M + Na]⁺; **Anal. calc. for** C₃₄H₃₄DFO₆: C, 72.97; H, 6.30. Found: C, 72.65; H, 6.37.

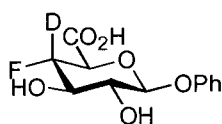
Phenyl 4-deoxy-4-fluoro-4-{²H}-β-D-glucopyranoside (86)



Prepared from **85** as described for **57**. The residue was purified by column chromatography (PE:EtOAc 4:5) giving **86** as a white solid (58%). A small sample was

recrystallized from EtOH/PE for elemental analysis: ^1H NMR (300 MHz, CD_3OD) δ 7.29 (2 H, dd, J 8.3, J 7.4 Hz, Ph_{meta}), 7.10 (2 H, dd, J 8.3, J 1.4 Hz, Ph_{ortho}), 7.01 (1 H, tt, J 7.4, J 1.4 Hz, Ph_{para}), 4.97 (1 H, d, $J_{1,2}$ 7.4 Hz, H1), 3.86 (1 H, ddd, $J_{6a,6b}$ 12.0, $J_{6a,5} = J_{6a,F} = 1.8$ Hz, H6_a), 3.81-3.64 (3 H, m, H3, H5, H6_b), 3.50 (1 H, dd, $J_{2,3}$ 9.2, $J_{2,1}$ 7.4 Hz, H2); ^{13}C NMR (75 MHz, CD_3OD) δ 159.02 (C), 130.43, 123.52, 117.78 (3 CH), 102.10 (CH, C1), 75.70 (CH, d, $J_{3,F}$ 18.1 Hz, C3), 75.27 (CH, d, $J_{5,F}$ 24.7 Hz, C5), 74.67 (CH, d, $J_{2,F}$ 8.4 Hz, C2), 61.50 (CH_2); ^{19}F NMR (188 MHz, CD_3OD) δ -122.79 (s, br); **Anal. calc. for** $\text{C}_{12}\text{H}_{14}\text{DFO}_5$: C, 55.60; H, 5.83. Found: C, 55.68; H, 5.91.

Phenyl 4-deoxy-4-fluoro-4- $\{^2\text{H}\}$ - β -D-glucopyranosiduronic acid (87)

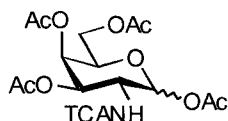


Prepared from **86** as described for **3** to give **87** as a white solid (50%): ^1H NMR (300 MHz, CD_3OD) δ 7.28 (2 H, dd, J 8.8, J 7.3 Hz, Ph_{meta}), 7.10 (2 H, dd, J 8.8, J 0.9 Hz, Ph_{ortho}), 7.02 (1 H, tt, J 7.3, J 0.9 Hz, Ph_{para}), 4.98 (1 H, d, $J_{1,2}$ 7.9 Hz, H1), 3.97 (1 H, d, $J_{5,F}$ 2.3 Hz, H5), 3.76 (1 H, dd, $J_{3,F}$ 15.7, $J_{3,2}$ 9.2 Hz, H3), 3.58 (1 H, dd, $J_{2,3}$ 9.2, $J_{2,1}$ 7.9 Hz, H2); ^{13}C NMR (75 MHz, CD_3OD) δ 174.72 (C=O), 158.96 (C), 130.39, 123.59, 117.89 (3 CH), 102.17 (CH, C1), 76.45 (CH, d, $J_{5,F}$ 25.3 Hz, C5), 75.72 (CH, d, $J_{3,F}$ 18.4 Hz, C3), 74.44 (CH, d, $J_{2,F}$ 8.6 Hz, C2); ^{19}F NMR (188 MHz, CD_3OD) δ -121.31 (s, br); **Anal. calc. for** $\text{C}_{12}\text{H}_{12}\text{DFO}_6 + 0.5 \text{H}_2\text{O}$: C, 51.07; H, 5.00. Found: C, 51.19; H, 4.91.

5.8 Synthesis of the Potential Inhibitors

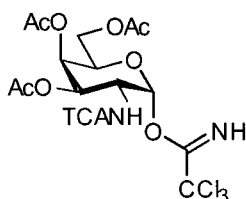
5.8.1 Methyl *O*-(2-acetamido-2-deoxy- β -D-galactopyranosyl)-(1 \rightarrow 4)- α -L-threo-hex-4-enopyranoside (88) (Schemes 4.1, 4.2, and 4.3)

1,3,4,6-Tetra-*O*-acetyl-2-deoxy-2-trichloroacetamido-D-galactopyranose (90)¹⁴¹



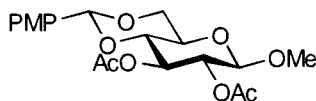
Trichloroacetyl chloride (3.9 mL, 34.88 mmol, 1.5 eq) was added dropwise to a stirred solution of galactosamine hydrochloride (5.00 g, 23.2 mmol) and NaHCO_3 (5.84 g, 69.6 mmol, 3 eq) in H_2O (55 mL) at rt. After 1.5 hr additional trichloroacetyl chloride (3.9 mL) and NaHCO_3 (5.84 g) were added, and the reaction stirred for a further 1.5 hr. The solvent was removed under vacuum, methanol (50 mL) was then added and the mixture stirred at 0 °C for 2 hr, filtered, and concentrated under vacuum. The residue was dissolved in pyridine (70 mL) and acetic anhydride (40 mL) and stirred overnight at rt. The reaction mixture was diluted with EtOAc and washed with H_2O (1x), 1 M HCl (6x), saturated NaHCO_3 (3x), H_2O (1x), dried over MgSO_4 and concentrated. The residue was purified by column chromatography (PE:EtOAc, 3:2), to yield **90** as an off-white foam (3.66 g, 32%): ^1H NMR (200 MHz, CDCl_3) (β anomer only) δ 7.08 (1 H, d, $J_{\text{NH},2}$ 7.5 Hz, NH), 5.84 (1 H, d, $J_{1,2}$ 8.8 Hz, H1), 5.38 (1 H, d, $J_{4,3}$ 3.4 Hz, H4), 5.25 (1 H, dd, $J_{3,2}$ 11.3, $J_{3,4}$ 3.4 Hz, H3), 4.15 (1 H, ddd, $J_{2,1}$ 8.8, $J_{2,3}$ 11.3, $J_{2,\text{NH}}$ 7.5 Hz, H2), 4.20-4.00 (3 H, m, H5, H6_a, H6_b), 2.16, 2.10, 2.02, 1.98 (12 H, 4 s, 4 Ac); ESI-MS m/z 516.0 $[\text{M} + \text{Na}]^+$.

3,4,6-Tri-O-acetyl-2-deoxy-2-trichloroacetamido- α -D-galactopyranosyl trichloroacetimidate (91)¹⁴¹



Hydrazine acetate (589 mg, 6.4 mmol, 1.5 eq) was added to a solution of **90** (2.1 g, 4.3 mmol) in dry DMF (19 mL) and stirred at rt for 1.5 hr. The reaction mixture was diluted with CH₂Cl₂, and washed with saturated NaHCO₃ (3x). The combined aqueous phases were extracted once with CH₂Cl₂. The combined organic phases were dried over MgSO₄, and the solvent was removed under vacuum. Trichloroacetonitrile (5.13 mL, 51 mmol, 12 eq) and 1,8-diazabicyclo[5.4.0]undec-7-ene (DBU) (0.16 mL, 1.1 mmol, 0.25 eq) were added to a solution of the residue in dry CH₂Cl₂ (30 mL) and stirred at rt for 1.5 hr. The solvent was removed under vacuum and the residue was purified by column chromatography (PE:EtOAc 3:1) to give **91** as a white foam (57%): ¹H NMR (200 MHz, CDCl₃) δ 8.80 (1 H, s, C=NH), 6.82 (1 H, d, J_{NH,2} 9.1 Hz, NH), 6.50 (1 H, d, J_{1,2} 3.8 Hz, H1), 5.52 (1 H, dd, J_{4,3} 3.4, J_{4,5} 0.9 Hz, H4), 5.40 (1 H, dd, J_{3,2} 11.4, J_{3,4} 3.4 Hz, H3), 4.70 (1 H, ddd, J_{2,3} 11.4, J_{2,NH} 9.1, J_{2,1} 3.8 Hz, H2), 4.39 (1 H, ddd, J_{5,6ax} 6.6, J_{5,6eq} 6.4, J_{5,4} 0.9 Hz, H5), 4.19 (1 H, dd, J_{6eq,6ax} 11.5, J_{6eq,5} 6.4 Hz, H6eq), 4.07 (1 H, dd, J_{6ax,6eq} 11.5, J_{6ax,5} 6.6 Hz, H6ax), 2.19, 2.02, 2.01 (9 H, 3 s, 3 Ac).

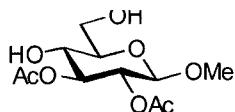
Methyl 2,3-di-O-acetyl-4,6-O-(4-methoxybenzylidene)- β -D-glucopyranoside (92)



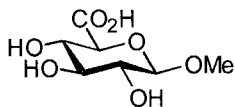
A solution of methyl β -D-glucopyranoside (10.0 g, 51.5 mmol), 4-methoxybenzaldehyde dimethyl acetal (14.0 g, 76.8 mmol, 1.5 eq), and *p*-toluenesulfonic acid monohydrate (200 mg, 1.0 mmol, 0.02 eq) in dry DMF (50 mL) was rotated under aspirator pressure at 50 °C for 4.5 h. The temperature was raised to 70 °C and the reaction mixture concentrated until a solid began to form. The mixture was poured into a stirred mixture of saturated NaHCO_{3(aq)} (50 mL), diethyl ether (50 mL) and ice. The

resulting solid was filtered off, washed successively with petroleum ether (PE) (bp 35-60 °C), and water, dried over P_2O_5 *in vacuo*. The solid was dissolved in pyridine (50 mL) and acetic anhydride (45 mL) and stirred at rt for 1.5 h. The reaction mixture was diluted with CH_2Cl_2 , washed with H_2O (1x), cold 1 M HCl (4x), saturated $NaHCO_3$ (5x), H_2O (1x), dried over $MgSO_4$ and concentrated under vacuum, leaving **92** (17.2 g, 80%) as a white solid: mp 190-191 °C; 1H NMR (200 MHz, $CDCl_3$) δ 7.33 (2 H, d, J 8.8 Hz, Ar), 6.85 (2 H, d, J 8.8 Hz, Ar), 5.44 (1 H, s, ArCH), 5.29 (1 H, dd, $J_{3,2} = J_{3,4}$ 9.3 Hz, H3), 4.96 (1 H, dd, $J_{2,3}$ 9.3, $J_{2,1}$ 7.8 Hz, H2), 4.49 (1 H, d, $J_{1,2}$ 7.8 Hz, H1), 4.35 (1 H, dd, $J_{6eq,6ax}$ 10.4, $J_{6eq,5}$ 4.8 Hz, H6eq), 3.84-3.72 (4 H, m, H6ax, ArOMe) 3.67 (1 H, dd, $J_{4,5} = J_{4,3}$ 9.3 Hz, H4), 3.50 (3 H, s, OMe), 3.49 (1 H, ddd, $J_{5,4} = J_{5,6ax}$ 9.3, $J_{5,6eq}$ 4.8 Hz, H5), 2.04, 2.01 (6 H, 2 s, 2 Ac).

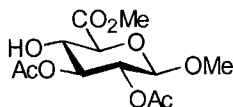
Methyl 2,3-di-O-acetyl- β -D-glucopyranoside (**93**)¹⁴⁴



A solution of **92** in 1% (w/v) of iodine in methanol (200 mL) was heated at reflux overnight. The solvent was removed under vacuum and the residue dissolved in ethyl acetate (EtOAc) and washed with saturated $Na_2S_2O_3$ (1x). The aqueous phase was extracted with EtOAc (5x), and the combined organic phases dried over $MgSO_4$ and concentrated. The residue was purified by column chromatography (PE:EtOAc 1:4 to 1:5) to yield **93** (3.40 g, 87%) as an oil which crystallized over time: 1H NMR (200 MHz, CD_3OD) δ 5.04 (1 H, dd, $J_{3,2}$ 9.5, $J_{3,4}$ 9.0 Hz, H3), 4.74 (1 H, dd, $J_{2,3}$ 9.5, $J_{2,1}$ 7.8 Hz, H2), 4.47 (1 H, d, $J_{1,2}$ 7.8 Hz, H1), 3.88 (1 H, dd, $J_{6eq,6ax}$ 12.0, $J_{6eq,5}$ 2.4 Hz, H6eq), 3.71 (1 H, dd, $J_{6ax,6eq}$ 12.0, $J_{6ax,5}$ 5.1 Hz, H6ax), 3.56 (1 H, dd, $J_{4,3} = J_{4,5}$ 9.0 Hz, H4), 3.48 (3 H, s, OMe), 3.37 (1 H, ddd, $J_{5,4}$ 9.0, $J_{5,6ax}$ 5.1, $J_{5,6eq}$ 2.4 Hz, H5), 2.02, 1.99 (6 H, 2 s, 2 Ac).

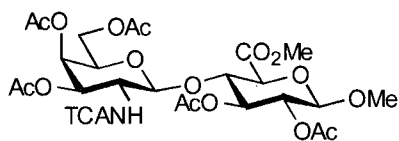
Methyl 2,3-di-O-acetyl- β -D-glucopyranosiduronic acid (94)

A solution of commercial bleach (30 mL, 6% w/v NaOCl, 23 mmol), saturated NaHCO₃ (15 mL), and saturated NaCl (30 mL) at 0 °C was added dropwise to a cooled solution of **93** (1.7 g, 6.1 mmol), sodium bromide (76 mg, 0.74 mmol, 0.12 eq), tetrabutylammonium bromide (135 mg, 0.42 mmol, 0.068 eq) and TEMPO (24 mg) in EtOAc (30 mL) and saturated NaHCO₃ (17 mL). The reaction was stirred for 2.5 h at 0 °C, diluted with EtOAc and water. The organic layer was extracted with half saturated NaHCO₃ (3x). The combined aqueous phases were acidified to pH 2 with 2 M HCl, then extracted with EtOAc (5x), CH₂Cl₂ (3x), dried over MgSO₄, and concentrated to give **94** (1.25 g, 70%) as a white solid: ¹H NMR (200 MHz, CDCl₃) δ 5.14 (1 H, dd, $J_{3,2} = J_{3,4}$ 9.5 Hz, H3), 4.93 (1 H, dd, $J_{2,3}$ 9.5, $J_{2,1}$ 7.6 Hz, H2), 4.51 (1 H, d, $J_{1,2}$ 7.6 Hz, H1), 4.06-3.85 (2 H, m, H4, H5), 3.50 (3 H, s, OMe), 2.07, 2.04 (6 H, 2 s, 2 Ac).

Methyl (methyl 2,3-di-O-acetyl- β -D-glucopyranosid)uronate (95)

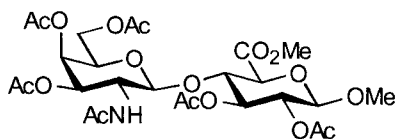
A solution of **94** (1.48 g, 5.06 mmol) in methanol (25 mL) was stirred with acid resin (Bio-Rad[®] AG 50W-X2, 200-400 mesh) for 3.5 h. The resin was removed by filtration and the reaction mixture was concentrated. The residue was dissolved in EtOAc, washed with saturated NaHCO₃ (2x), H₂O (1x), dried over MgSO₄ and concentrated. The residue was purified by column chromatography (PE:EtOAc 1:1) giving **95** (587 mg, 36%) as a colourless oil which crystallized over time: ¹H NMR (400 MHz, CDCl₃) δ 5.08 (1 H, ddd, $J_{3,2}$ 9.5, $J_{3,4}$ 7.4, $J_{3,OH}$ 1.6 Hz, H3), 4.89 (1 H, dd, $J_{2,3}$ 9.5, $J_{2,1}$ 7.7 Hz, H2), 4.44 (1 H, d, $J_{1,2}$ 7.7 Hz, H1), 3.97-3.88 (2 H, m, H4, H5), 3.81 (3 H, s, CO₂Me), 3.48 (3 H, s, OMe), 2.04, 2.01 (6 H, 2 s, 2 Ac).

Methyl [methyl O-(3,4,6-tri-O-acetyl-2-deoxy-2-trichloroacetamido- β -D-galactopyranosyl)-(1 \rightarrow 4)-2,3-di-O-acetyl- β -D-glucopyranosid]uronate (96**)**



A solution of **95** (578 mg, 1.89 mmol) and **91** (1.46 g, 2.45 mmol, 1.3 eq) in dry 1,2-dichloroethane (30 mL) was stirred over powdered 4 Å molecular sieves for 1.5 h before cooling to 0 °C and adding trimethylsilyl trifluoromethanesulfonate (68 μ L, 0.38 mmol, 0.2 eq). After 3 h an additional 100 mg of **91** was added, and the reaction mixture was stirred at 0 °C for another 45 min before triethylamine (0.37 mL) was added to quench. The reaction mixture was diluted with CH₂Cl₂, filtered, and concentrated. The residue was purified by column chromatography (PE:EtOAc 5:4 to 2:3) to give **96** (1.02 g, 73%) as a white foam: ¹H NMR (200 MHz, CDCl₃) δ 6.74 (1 H, d, $J_{\text{NH},2}$ 8.8 Hz, NH), 5.32 (1 H, d, $J_{4',3'}$ 2.5 Hz, H4'), 5.22-5.10 (2 H, m, H3, H3'), 4.93 (1 H, d, $J_{1',2'}$ 8.4 Hz, H1'), 4.88 (1 H, dd, $J_{2,3}$ 9.6, $J_{2,1}$ 7.1 Hz, H2), 4.44 (1 H, d, $J_{1,2}$ 7.1 Hz, H1), 4.15-3.88 (6 H, m, H2, H4, H5, H5', H6a', H6b'), 3.82 (3 H, s, CO₂Me), 3.48 (3 H, s, OMe), 2.14, 2.05, 2.03, 2.01, 1.95 (15 H, 5 s, 5 Ac); ESI-MS m/z 761.0 [M + Na]⁺.

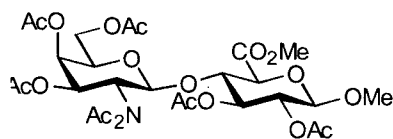
Methyl [methyl O-(2-acetamido-3,4,6-tri-O-acetyl-2-deoxy- β -D-galactopyranosyl)-(1 \rightarrow 4)-2,3-di-O-acetyl- β -D-glucopyranosid]uronate (97**)**



A solution of **96** (1.01 g, 1.37 mmol), tributyltin hydride (1.73 mL, 6.42 mmol, 4.7 eq), and 2,2'-azobisisobutyronitrile (AIBN, 36 mg, 0.22 mmol, 0.17 eq) in dry benzene (45 mL) was stirred at rt for 15 min, then heated to reflux for 40 min. The reaction mixture was then cooled, and concentrated *in vacuo*. The residue was dissolved in acetonitrile and washed with hexanes (5x) and concentrated leaving a white solid that was recrystallized from EtOAc/hexanes to yield **97** (677 mg, 78%) as fine colourless needles: decomposes at ~195 °C; ¹H NMR (400 MHz, CDCl₃) δ 5.42 (1 H, d, $J_{\text{NH},2'}$ 8.6 Hz, NH), 5.28 (1 H, d, $J_{4',3'}$ 3.4, H4'), 5.18 (1 H, dd, $J_{3',2'}$ 11.8, $J_{3',4'}$ 3.4 Hz, H3'), 5.16 (1

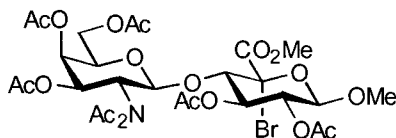
H, dd, $J_{3,4} = J_{3,2}$ 9.2 Hz, H3), 4.89 (1 H, dd, $J_{2,1}$ 7.5, $J_{2,3}$ 9.2 Hz, H2), 4.69 (1 H, d, $J_{1',2'}$ 8.4 Hz, H1'), 4.43 (1 H, d, $J_{1,2}$ 7.5 Hz, H1), 4.11-4.03 (3 H, m), 3.97 (1 H, d, $J_{5,4}$ 9.6 Hz, H5), 3.90-3.77 (2 H, m), 3.81 (3 H, s, CO₂Me), 3.42 (3 H, s, OMe), 2.12, 2.04, 2.03, 2.02, 1.96, 1.90 (18 H, 6 s, 6 Ac); ¹³C NMR (100 MHz, CDCl₃) δ 170.34 (2 x C=O), 170.23 (C=O), 170.10 (C=O), 169.81 (C=O), 169.48 (C=O), 168.60 (C=O), 102.04 (CH), 100.69 (CH), 76.14, 72.42, 71.39, 70.72, 70.05, 66.50, 61.16, 57.21, 53.03, 51.65, 23.26 (Ac), 20.72 (Ac), 20.59 (4 x Ac); ESI-MS m/z 635.8 [M]⁺; Anal. calc. for C₂₆H₃₇NO₁₈: C, 49.13; H, 5.87; N, 2.20. Found: C, 48.87; H, 5.98; N, 2.26.

Methyl [methyl O-(3,4,6-tri-O-acetyl-2-(N-acetylacetamido)-2-deoxy-β-D-galactopyranosyl)-(1→4)-2,3-di-O-acetyl-β-D-glucopyranosid]uronate (98)



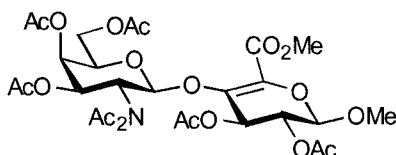
A suspension of **97** (595 mg, 0.94 mmol) and *p*-toluenesulfonic acid monohydrate (84 mg, 0.44 mmol, 0.47 eq) in isopropenyl acetate (12 mL) was heated to 65 °C under argon for 3.5 h (**97** has dissolved after ~ 1 h). Triethylamine (1.5 mL) was added to quench, and the solvent was removed under vacuum. The residue was purified by column chromatography (PE:EtOAc 2:3) giving **98** (622 mg, 98%) as a white foam: ¹H NMR (200 MHz, CDCl₃) δ 5.75 (1 H, dd, $J_{3',2'}$ 11.0, $J_{3',4'}$ 3.7 Hz, H3'), 5.38 (1 H d, $J_{4',3'}$ 3.7 Hz, H4'), 5.27 (1 H, d, $J_{1',2'}$ 7.6 Hz, H1'), 5.12 (1 H, dd, $J_{3,4} = J_{3,2}$ 9.5 Hz, H3), 4.94 (1 H, dd, $J_{2,1}$ 7.5, $J_{2,3}$ 9.5 Hz, H2), 4.40 (1 H, d, $J_{1,2}$ 7.5 Hz, H1), 4.18-4.08 (3 H, m, H4, H6_a', H6_b'), 3.95 (1 H, dd, $J_{5',6a'} = J_{5',6b'}$ 7.3 Hz, H5'), 3.86 (1 H, d, $J_{5,4}$ 9.8, H5), 3.80 (3 H, s, CO₂Me), 3.46 (3 H, s, OMe), 2.49, 2.29 (6 H, 2 s, NAc₂), 2.12 (3 H, s, Ac), 2.06 (6H, s, 2 Ac), 2.04, 1.93 (6 H, 2 s, 2 Ac); ¹³C NMR (75 MHz, CDCl₃) δ 174.38, 174.08, 170.34, 170.20, 169.63, 169.32, 169.10, 167.50 (8 C=O), 102.08, 97.66 (2 CH), 74.77, 74.26, 72.20, 70.80, 70.50, 67.32, 67.04, 60.79 (CH₂, C6'), 58.93, 57.24, 53.14, 27.71, 24.93, 20.90, 20.68, 20.62, 20.46, 20.36 (7 Ac); Anal. calc. for C₂₈H₃₉NO₁₈: C, 49.63; H, 5.80; N, 2.07. Found: C, 50.02; H, 5.81; N, 2.20.

Methyl [methyl O-(3,4,6-tri-O-acetyl-2-(N-acetylacetamido)-2-deoxy- β -D-galactopyranosyl)-(1 \rightarrow 4)-2,3-di-O-acetyl-5-bromo- β -D-glucopyranosid]uronate (99**)**



N-Bromosuccinimide (NBS) (309 mg, 1.74 mmol, 2 eq) was added to a solution of **98** (588 mg, 0.87 mmol) in dry CCl_4 (15 mL) and irradiated with two 200 watt light bulbs (reflux). After 45 min a further 140 mg of NBS was added and the reaction mixture irradiated for another 25 min. The mixture was cooled, filtered, and concentrated and the residue was dissolved in CH_2Cl_2 , washed with saturated NaHCO_3 (1x), H_2O (1x), dried over MgSO_4 , and concentrated. The residue was purified by column chromatography (PE:EtOAc 1:1) giving **99** (422 mg, 64%) as a white foam: ^1H NMR (200 MHz, CDCl_3) δ 5.86 (1 H, dd, $J_{3',2'} 11.0$, $J_{3',4'} 3.9$ Hz, $\text{H}_{3'}$), 5.56 (1 H, d, $J_{1',2'} 7.9$ Hz, $\text{H}_{1'}$), 5.46-5.33 (2 H, m, H_3 , $\text{H}_{4'}$), 5.06 (1 H, dd, $J_{2,3} 9.8$, $J_{2,1} 8.1$ Hz, H_2), 4.91 (1 H, d, $J_{1,2} 8.3$ Hz, H_1), 4.20-4.06 (3 H, m), 4.20-3.71 (2 H, m), 3.88 (3 H, s, CO_2Me), 3.50 (3 H, s, OMe), 2.36, 2.33, 2.12, 2.06, 2.05, 1.92 (21 H, 6 s, 7 Ac); ESI-MS m/z 756.2 $[\text{M}]^+$.

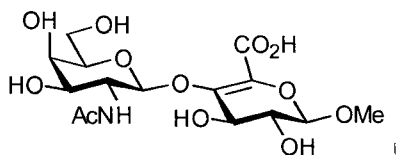
Methyl [methyl O-(3,4,6-tri-O-acetyl-2-(N-acetylacetamido)-2-deoxy- β -D-galactopyranosyl)-(1 \rightarrow 4)-2,3-di-O-acetyl- α -L-threo-hex-4-enopyranosid]uronate (100**)**



1,8-Diazabicyclo[5.4.0]undec-7-ene (DBU) (9 μL , 0.06 mmol, 1.5 eq) was added to a solution of **99** (30 mg, 0.04 mmol) in dry DMF (0.8 mL) at 0 $^\circ\text{C}$. The reaction was then allowed to attain ambient temperature and stirred for 2.5 h. The reaction mixture was diluted with CH_2Cl_2 , washed with H_2O (1x), 1 M HCl (2x), H_2O (1x), dried over MgSO_4 , and concentrated. The residue was purified by column chromatography (PE:EtOAc 2:3) giving **100** (20 mg, 75%) as a white foam: ^1H NMR (400 MHz, CDCl_3) δ 5.78 (1 H, dd, $J_{3',2'} 11.0$, $J_{3',4'} 3.5$ Hz, $\text{H}_{3'}$), 5.68 (1 H, d, $J_{1',2'} 7.6$ Hz, $\text{H}_{1'}$), 5.49 (1 H, d, $J_{1,2} 1.8$ Hz, H_1), 5.40 (1 H, d, $J_{4',3'} 3.5$ Hz, $\text{H}_{4'}$), 4.98 (1 H, dd, $J_{2,3} = J_{2,1} 2.4$ Hz, H_2), 4.92 (1 H, d, $J_{3,2} 2.4$,

H3), 4.18-4.08 (2 H, m, H2', H6eq'), 4.04 (1 H, dd, $J_{6ax',6eq'}$ 11.3, $J_{6ax',5'}$ 6.5, H6ax'), 3.93 (1 H, ddd, $J_{5',6ax'} = J_{5',6eq'}$ 6.5, $J_{5',4'}$ 0.7 Hz, H5'), 3.78 (3 H, s, CO₂Me), 3.46 (3 H, s, OMe), 2.42, 2.37, 2.13, 2.11, 2.06, 2.02, 1.94 (21 H, 7 s, 7 Ac).

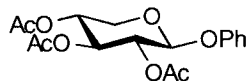
Methyl O-(2-acetamido-2-deoxy-β-D-galactopyranosyl)-(1→4)-α-L-threo-hex-4-enopyranoside (88)



3 M NaOH (3.4 mL) was added dropwise to stirred solution of **100** (250 mg, 0.37 mmol) in 5:1 MeOH:H₂O (7 mL). The reaction mixture was stirred at rt for 4 h, neutralized with dilute acetic acid, and concentrated *in vacuo*. The residue was purified by column chromatography (EtOAc:MeOH:H₂O 10:8:2 + 0.4% acetic acid to 5:4:2 + 0.4% acetic acid), concentrated to remove EtOAc and MeOH, then freeze-dried to yield 785 mg white solid (mostly salts). The solid was then dissolved in water (2 mL) and passed down a size exclusion column (Sephadex™ G-10, 1.6 x 60 cm). Fractions containing the desired product were pooled, concentrated, and re-purified by column chromatography (EtOAc:MeOH:H₂O 5:4:1 + 0.4% acetic acid) to yield **88** (72 mg, 48%) as a solid: ¹H NMR (400 MHz, D₂O) δ 4.91 (1 H, d, $J_{3,2} = 4.0$ Hz, H3), 4.67 (1 H, d, $J_{1',2'} = 8.4$ Hz, H1'), 4.09 (1 H, d, $J_{1,2} = 3.6$ Hz, H1), 3.98 (1 H, dd, $J_{2',3'} = 10.7$, $J_{2',1'} = 8.4$ Hz, H2'), 3.89 (2 H, m, H2, H4'), 3.79 (1 H, dd, $J_{6a',6b'} = 11.8$, $J_{6a',5'} = 8.2$ Hz, H6a'), 3.74 (1 H, dd, $J_{3',4'} = 3.3$, $J_{3',2'} = 10.7$ Hz, H3'), 3.69 (1 H, dd, $J_{6b',5'} = 4.0$, $J_{6b',6a'} = 11.8$ Hz, H6b'), 3.64 (1 H, dd, $J_{5',6a'} = 8.2$, $J_{5',6b'} = 4.0$ Hz, H5'), 3.46 (3 H, s, OMe), 2.01 (3 H, s, Ac) (assignments based on COSY experiment); ¹³C NMR (100 MHz, D₂O) δ 185.41, 179.60, 139.39, 132.73, 100.59, 100.21, 75.62, 71.29, 70.18, 68.08, 66.62, 61.21, 56.67, 52.68, 22.65; HRMS (LSIMS-, thioglycerol) m/z: 408.1142. Calc. For C₁₅H₂₂NO₁₂ [M - 1]⁺ 408.1141; IR (KBr) 3412, 2940, 1740, 1704, 1408, 1068 cm⁻¹.

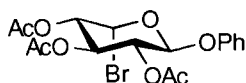
5.8.2 Phenyl (5S)-5-nitro- β -D-xylopyranoside (89) (Scheme 4.4)

Phenyl 2,3,4-tri-*O*-acetyl- β -D-xylopyranoside (**101**)¹⁵⁰



A solution of HBr (19 mL, 5.7 M in acetic acid) was added to a solution of 1,2,3,4-tetra-*O*-acetyl- β -D-xylopyranose (11.26 g, 35.4 mmol) in dry CH₂Cl₂ (30 mL) at 0 °C. The reaction mixture was then allowed to warm to ambient temperature, stirred for 3 h, and then poured into an ice/H₂O mixture and diluted with CH₂Cl₂. The aqueous phase was extracted once with CH₂Cl₂, and the combined organic phases washed with saturated NaHCO₃ (3x), H₂O (1x), dried over MgSO₄, and concentrated, yielding 2,3,4-tri-*O*-acetyl- β -D-xylopyranosyl bromide as a white solid (11.39 g, 95%). The bromide was then dissolved in CH₂Cl₂ (85 mL) to which was added phenol (6.32 g, 67.2 mmol, 2 eq), tetrabutylammonium hydrogensulfate (11.4 g, 33.6 mmol, 1 eq), and 1 M NaOH (85 mL). The mixture was rapidly stirred for 4 h, diluted with EtOAc, washed with 1 M NaOH (4x), H₂O (1x), brine (2x), dried over MgSO₄, and concentrated. The residue was recrystallized from ethanol to yield **101** (5.18 g, 42% overall) as plate-like crystals: ¹H NMR (300 MHz, CDCl₃) δ 7.27 (2 H, dd, J 7.9, J 8.8 Hz, Ph_{meta}), 7.03 (1 H, tt, J 7.9, J 0.9 Hz, Ph_{para}), 6.97 (2 H, dd, J 8.8, J 0.9 Hz, Ph_{ortho}), 5.26-5.13 (3 H, m, H1, H2, H3), 4.99 (1 H, ddd, J_{4,5ax} = J_{4,3} 7.9 Hz, J_{4,5eq} 5.1 Hz, H4), 4.20 (1 H, dd, J_{5eq,5ax} 12.0, J_{5eq,4} 5.1 Hz, H5eq), 3.50 (1 H, dd, J_{5ax,5eq} 12.0, J_{5ax,4} 7.9 Hz, H5ax), 2.05 (9 H, s, 3 Ac); ¹³C NMR (100 MHz, CDCl₃) δ 169.86, 169.73, 169.27 (3 C=O), 156.58 (C), 129.53, 123.04, 116.83 (3 CH), 98.56 (CH, C1), 70.75, 70.19, 68.49 (3 CH), 61.84 (CH₂), 20.65 (Ac); **Anal. calc.** for C₁₈H₂₀O₈: C, 57.95; H, 5.72. Found: C, 57.79; H, 5.74.

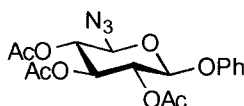
Phenyl (5S)-2,3,4-tri-*O*-acetyl-5-bromo- β -D-xylopyranoside (**102**)



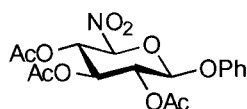
A mixture of **101** (4.82 g, 13.7 mmol) and NBS (7.30 g, 41.0 mmol, 3 eq) in dry CCl₄ (250 mL) was irradiated with one 250 watt heat lamp and one 200 watt light bulb (reflux). After 2.5 h an additional 2.4 g of NBS was added, the reaction mixture irradiated

for a further 2.5 h, cooled, filtered, and concentrated. The residue was dissolved in CH_2Cl_2 , washed with saturated NaHCO_3 (1x), H_2O (1x), dried over MgSO_4 , and concentrated under vacuum. The residue was purified by column chromatography (toluene:EtOAc 14:1) giving **102** (1.47 g, 25%) as a pale yellow solid: ^1H NMR (400 MHz, CDCl_3) δ 7.30 (2 H, dd, J 8.5, J 7.6 Hz, Ph_{meta}), 7.06 (1 H, tt, J 7.6, J 1.2 Hz, Ph_{para}), 6.99 (2 H, dd, J 8.5, J 1.2 Hz, Ph_{ortho}), 6.61 (1 H, d, $J_{5,4}$ 4.0 Hz, H5), 5.71 (1 H, dd, $J_{1,2}$ 8.2, $J_{1,3}$ 0.6 Hz, H1), 5.64 (1 H, dd, $J_{3,4} = J_{3,2}$ 9.7 Hz, H3), 5.33 (1 H, dd, $J_{2,3}$ 9.7, $J_{2,1}$ 8.2 Hz, H2), 4.91 (1 H, dd, $J_{4,3}$ 9.7, $J_{4,5}$ 4.0 Hz, H4), 2.10 (3 H, s, Ac), 2.05 (6 H, s, 2 Ac).

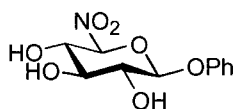
Phenyl (5S)-2,3,4-tri-O-acetyl-5-azido- β -D-xylopyranoside (**103**)



Sodium azide (265 mg, 4.08 mmol, 2 eq) was added to a solution of **102** (880 mg, 2.04 mmol) in dry DMF (6.5 mL) at 0 °C and stirred for 20 min, before the reaction was allowed to warm to ambient temperature and stirred for a further 1.5 h. The reaction was diluted with EtOAc, washed with H_2O (1x). The aqueous phase was extracted once with EtOAc, and the combined organic phases washed with H_2O (1x), brine (3x), dried over MgSO_4 , and concentrated under vacuum. The residue was purified by column chromatography (PE:EtOAc 3:1 to 2.75:1) giving **103** (359 mg, 45%) as a pale yellow syrup which crystallized over time: ^1H NMR (400 MHz, CDCl_3) δ 7.31 (2 H, dd, J 7.6, J 8.5 Hz, Ph_{meta}), 7.08 (1 H, tt, J 7.3, J 0.9 Hz, Ph_{para}), 7.02 (2 H, dd, J 8.5, J 0.9 Hz, Ph_{ortho}), 5.33 (1 H, dd, $J_{2,3}$ 8.8, $J_{2,1}$ 6.7 Hz, H2), 5.27 (1 H, d, $J_{1,2}$ 6.7 Hz, H1), 5.26 (1 H, dd, $J_{3,4} = J_{3,2}$ 8.8 Hz, H3), 5.12 (1 H, dd, $J_{4,3}$ 8.8, $J_{4,5}$ 7.6 Hz, H4), 4.87 (1 H, d, $J_{5,4}$ 7.6 Hz, H5), 2.07, 2.06, 2.04 (9 H, 3 s, 3 Ac); ^{13}C NMR (100 MHz, CDCl_3) δ 180.00, 179.21, 156.47, 129.70, 123.64, 118.14, 97.94, 85.46, 71.52, 70.91, 70.82, 20.57; IR (thin film) 2120 (N_3), 1857 (C=O) cm^{-1} .

Phenyl (5S)-2,3,4-tri-O-acetyl-5-nitro- β -D-xylopyranoside (104)

A solution of **103** (428 mg, 1.09 mmol) in EtOAc (14 mL) and ethanol (35 mL) was stirred with PtO₂ (Adam's catalyst, 175 mg) under 1 atm H₂ for 50 min. The catalyst was removed by filtration through a bed of Celite, and the solvent removed under vacuum, leaving a white solid that was dissolved in HPLC grade acetone (30 mL) and added dropwise to a freshly prepared solution of dimethyldioxirane (DMDO)¹⁵³ in acetone (250 mL, ~0.06 M). The reaction mixture was stirred at rt for 2.5 h, then concentrated under vacuum. The residue was purified by column chromatography (PE:EtOAc 3:1) giving **104** (182 mg, 42%) as a colourless solid. The product was then recrystallized from EtOAc/hexanes to give **104** as fine, colourless needles. Crystals were grown from ethanol for X-ray analysis (Note: **104** decomposes on a TLC plate to produce a spot with a larger R_f value, thus samples should be eluted immediately after spotting to avoid this decomposition): ¹H NMR (400 MHz, CDCl₃) δ 7.30 (2 H, dd, J 8.5, J 7.6 Hz, Ph_{meta}), 7.08 (1 H, tt, J 7.6, J 0.9 Hz, Ph_{para}), 7.03 (2 H, dd, J 8.5, J 0.9 Hz, Ph_{ortho}), 6.04 (1 H, dd, J_{4,3} 9.4, J_{4,5} 7.3 Hz, H4), 5.56 (1 H, d, J_{1,2} 2.1 Hz, H1), 5.51 (1 H, d, J_{5,4} 7.3 Hz, H5), 5.28 (1 H, dd, J_{3,4} 9.4, J_{3,2} 5.5 Hz, H3), 5.24 (1 H, dd, J_{2,3} 5.5, J_{2,1} 2.1 Hz, H2), 2.11, 2.09, 2.08 (9 H, 3 s, 3 Ac) (assignments based on NOE difference and COSY experiments); ¹³C NMR (75 MHz, CDCl₃) δ 179.83, 179.37, 178.62, 155.57, 129.65, 123.87, 117.49, 100.59, 99.13, 73.42, 70.30, 67.23, 20.64, 02.61, 02.44; **Anal. calc.** For C₁₈H₁₉NO₁₀: C, 51.39; H, 4.82; N, 3.53. Found: C, 51.51; H, 4.91; N, 3.57.

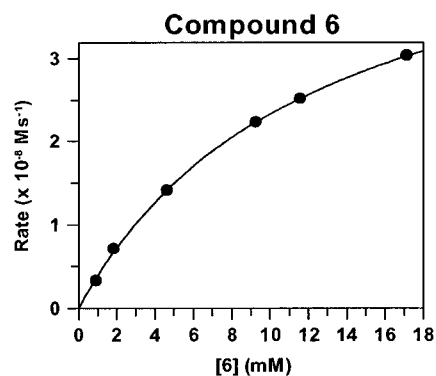
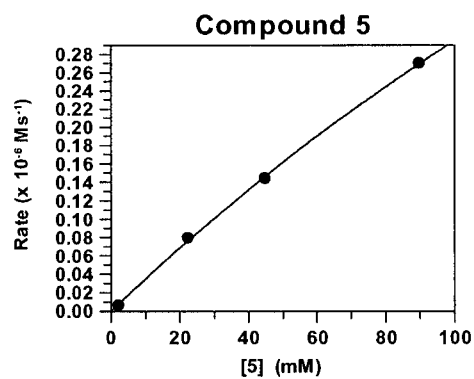
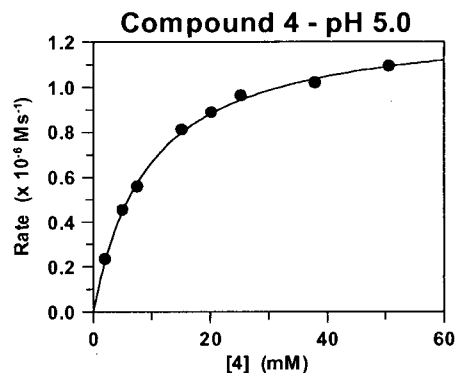
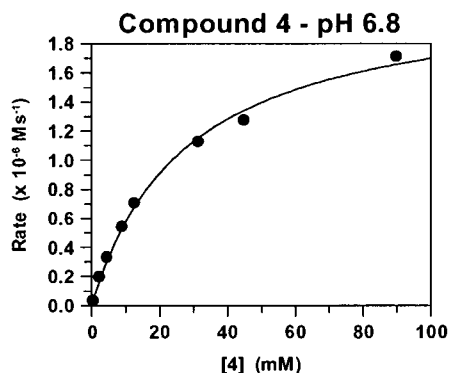
Phenyl (5S)-5-nitro- β -D-xylopyranoside (89)

To a solution of **104** (234 mg, 0.59 mmol) in dry MeOH (10 mL) at 0 °C was added acetyl chloride (1.0 mL). The reaction mixture was then stirred at 4 °C for 23 h, concentrated under vacuum and the residue was purified by column chromatography (PE:EtOAc 1:2 to 1:3) to yield **89** (124 mg, 78%) as a white foam: ¹H NMR (400 MHz,

CD₃OD) δ 7.33 (2 H, dd, J 7.3, 8.8 Hz, Ph_{meta}), 7.12 (2 H, dd, J 8.8, 1.2 Hz, Ph_{ortho}), 7.08 (1 H, tt, J 7.3, 1.2, Hz, Ph_{para}), 5.58 (1 H, d, J_{5,4} 8.8 Hz, H5), 5.30 (1 H, d, J_{1,2} 6.7 Hz, H1), 3.93 (1 H, dd, J_{4,3} = J_{4,5} 8.8 Hz, H4), 3.68 (1 H, dd, J_{2,3} 8.8, J_{2,1} 6.7 Hz, H2), 3.62 (1 H, dd, J_{3,2} = J_{3,4} 8.8 Hz, H3) (assignments based on NOE difference and COSY experiments); ¹³C NMR (75 MHz, CD₃OD) δ 158.39, 130.53, 124.10, 118.88, 105.65, 101.71, 75.23, 74.62, 73.27; **ESI-MS** m/z 294.2 [M + Na]⁺; Anal. calc. For C₁₁H₁₃NO₇: C, 48.71; H, 4.83; N, 5.17. Found: C, 48.48; H, 4.90; N, 5.05.

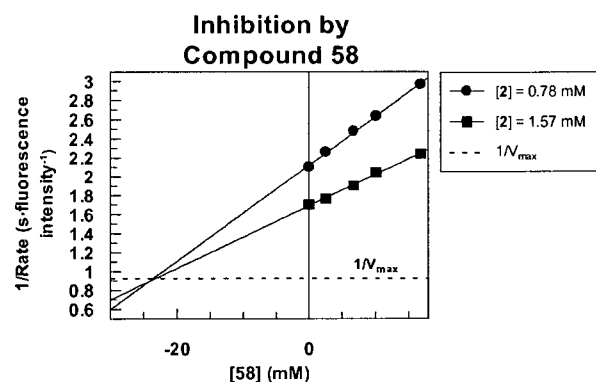
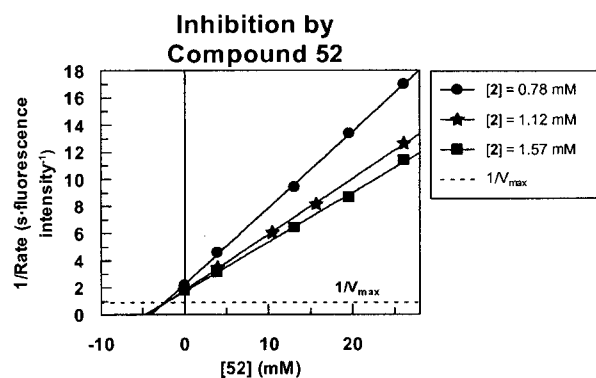
Appendix 1

Plots of reaction rate vs substrate concentration for the reaction of chondroitin AC lyase with the fluoride-releasing compounds **4**, **5**, and **6**. For compound **3**, see Chapter 1. (30°C, 50 mM buffer, 100 mM NaCl, pH 6.8 unless otherwise indicated)



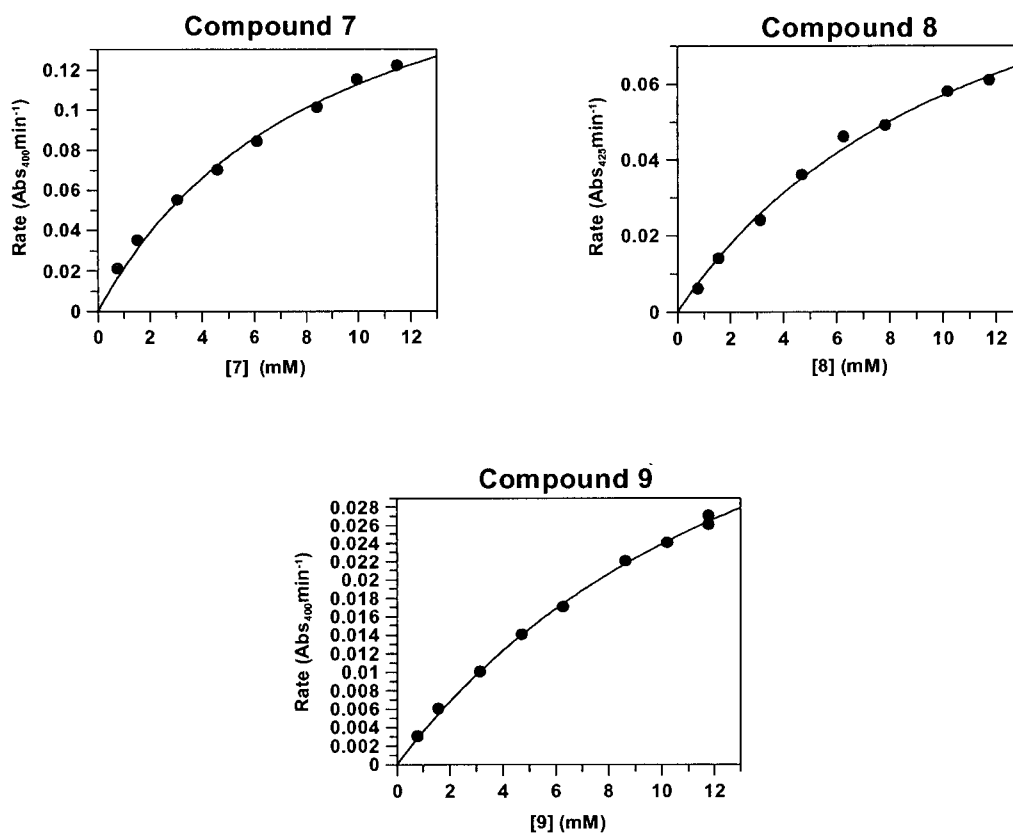
Appendix 2

Dixon plots ($1/\text{rate}$ vs [inhibitor]) showing the inhibition of chondroitin AC lyase by the incompetent fluorinated substrates **52** and **58**. The substrate used was the fluorogenic compound **2**. (30°C, 50 mM Tris buffer, 100 mM NaCl, pH 8.0)



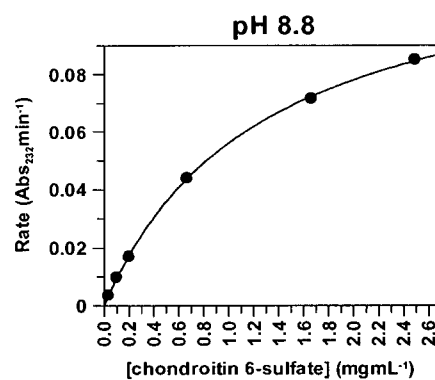
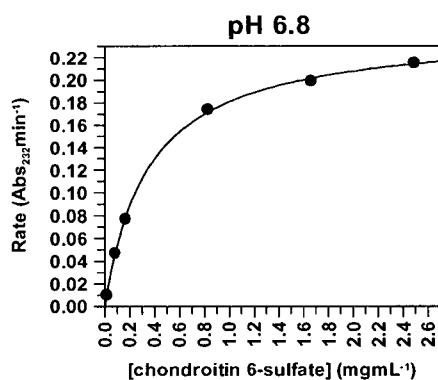
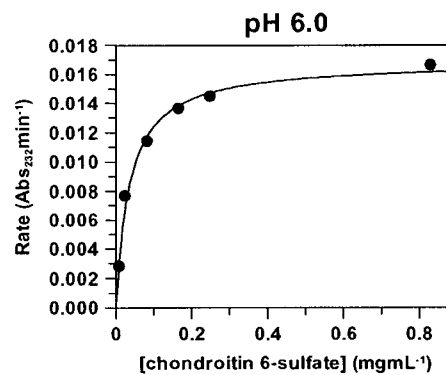
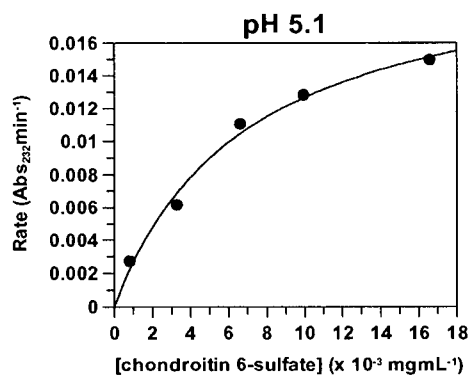
Appendix 3

Plots of reaction rate vs substrate concentration for the reaction of chondroitin AC lyase with compounds **7**, **8**, and **9** used to construct the linear free energy graph. For compound **1**, see Chapter 1. (30°C, 50 mM sodium phosphate buffer, 100 mM NaCl, pH 6.8)



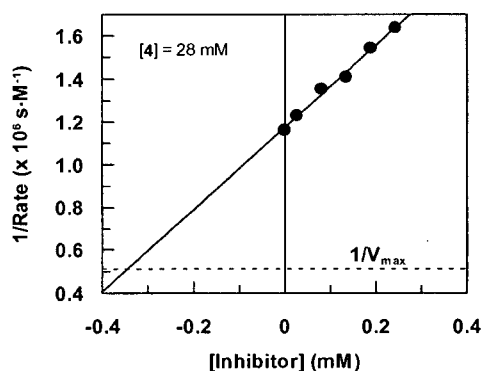
Appendix 4

Plots of reaction rate vs substrate concentration for the reaction of chondroitin AC lyase with chondroitin 6-sulfate at various pH values. (30°C, 50 mM buffer, 100 mM NaCl)



Appendix 5

Dixon plot (1/rate vs [inhibitor]) showing the inhibition of chondroitin AC lyase by the nitronate anion of compound **89** at pH 6.8. For inhibition data at pH 8.0 see Chapter 4. The concentration of the anion was calculated using a pK_a value of 8.8 for compound **89**. The substrate used was the fluoride-releasing compound **4**. (30°C, 50 mM sodium phosphate buffer, 100 mM NaCl, pH 6.8)



References

1. Laine, R. A. *Glycobiology* **1994**, *4*, 759-767.
2. Wolfenden, R.; Lu, X.; Young, G. *J. Am. Chem. Soc.* **1998**, *120*, 6814-6815.
3. Wolfenden, R.; Snider, M.; Ridgway, C.; Miller, B. *J. Am. Chem. Soc.* **1999**, *121*, 7419-7420.
4. Ernst, S.; Langer, R.; Cooney, C. L.; Sasisekharan, R. *Crit. Rev. Biochem. Mol. Biol.* **1995**, *30*, 387-444.
5. Yoder, M. D.; Jurnak, F. *Plant Physiol.* **1995**, *107*, 349-364.
6. Linhardt, R. J.; Galliher, P. M.; Cooney, C. L. *Appl. Biochem. Biotech.* **1986**, *12*, 135-76.
7. Wong, T. Y.; Preston, L. A.; Schiller, N. L. *Annu. Rev. Microbiol.* **2000**, *54*, 289-340.
8. Kjellen, L.; Lindahl, U. *Annu. Rev. Biochem.* **1991**, *60*, 443-75.
9. Lehninger, A. L.; Nelson, D. L.; Cox, M. M. *Principles of Biochemistry*; 2 ed.; Worth Publishers: New York, **1993**, p. 314.
10. Jandik, K. A.; Gu, K. A.; Linhardt, R. J. *Glycobiology* **1994**, *4*, 289-296.
11. Michelacci, Y. M.; Dietrich, C. P. *Biochem. J.* **1975**, *151*, 121-129.
12. Gu, K.; Linhardt, R. J.; Laliberte, M.; Zimmermann, J. *Biochem. J.* **1995**, *312*, 569-77.
13. Gu, K.; Liu, J.; Pervin, A.; Linhardt, R. J. *Carbohydr. Res.* **1993**, *244*, 369-377.
14. Scott, J. E. *FASEB J.* **1992**, *6*, 2639-45.
15. Meyer, K.; Palmer, J. W. *J. Biol. Chem.* **1934**, *107*, 629-634.
16. Jedrzejewski, M. J. *Crit. Rev. Biochem. Mol. Biol.* **2000**, *35*, 221-251.
17. Capila, I.; Linhardt, R. J. *Angew. Chem.-Int. Edit.* **2002**, *41*, 391-412.
18. Hook, M.; Woods, A.; Johansson, S.; Kjellen, L.; Couchman, J. R. in *Functions of the Proteoglycans*; Evered, D. and Whelan, J., Ed.; John Wiley & Sons: Toronto, **1986**, pp 143-157.
19. Paulsson, M.; Fujiwara, S.; Dziadek, M.; Timpl, R.; Pejler, G.; Backstrom, G.; Lindahl, U.; Engel, J. in *Functions of the Proteoglycans*; Evered, D. and Whelan, J., Ed.; John Wiley & Sons: Toronto, **1986**, pp 189-200.

20. Bourin, M. C.; Lindahl, U. *Biochem. J.* **1993**, 289, 313-330.
21. Davies, G.; Henrissat, B. *Structure* **1995**, 3, 853-859.
22. Davies, G.; Sinnott, M. L.; Withers, S. G. in *Comprehensive Biological Catalysis*; Sinnott, M. L., Ed.; Academic Press, **1998**; Vol. 1, pp 119-208.
23. McCarter, J.; Withers, S. G. *Curr. Opin. Struct. Biol.* **1994**, 4, 885-892.
24. White, A.; Rose, D. R. *Curr. Opin. Struct. Biol.* **1997**, 7, 645-651.
25. Zechel, D. L.; Withers, S. G. *Acc. Chem. Res.* **2000**, 33, 11-18.
26. Heightman, T. D.; Vasella, A. T. *Angew. Chem. Int. Ed.* **1999**, 38, 750-770.
27. Rye, C. S.; Withers, S. G. *Curr. Opin. Chem. Biol.* **2000**, 4, 573-580.
28. Sinnott, M. L. *Chem. Rev.* **1990**, 90, 1171-1202.
29. Tews, I.; Perrakis, A.; Oppenheim, A.; Dauter, Z.; Wilson, K. S.; Vorgias, C. E. *Nat. Struct. Biol.* **1996**, 3, 638-648.
30. Rao, V.; Cui, T.; Van Roey, P. *Prot. Sci.* **1999**, 8, 2338-2346.
31. Terwisscha van Scheltinga, A. C.; Armad, S.; Kalk, K. H.; Isogai, A.; Henrissat, B.; Dijkstra, B. *Biochemistry* **1995**, 34, 15619-15623.
32. Mark, B. L.; Vocadlo, D. J.; Knapp, S.; Triggs-Raine, B. L.; Withers, S. G.; James, M. N. G. *J. Biol. Chem.* **2001**, 276, 10330-10337.
33. Knapp, S.; Vocadlo, D.; Gao, Z. N.; Kirk, B.; Lou, J. P.; Withers, S. G. *J. Am. Chem. Soc.* **1996**, 118, 6804-6805.
34. Linker, A.; Meyer, K.; Hoffman, P. *J. Biol. Chem.* **1956**, 219, 13-25.
35. Gacesa, P. *FEBS Lett.* **1987**, 212, 199-202.
36. Bahnson, B. J.; Anderson, V. E. *Biochemistry* **1991**, 30, 5894-906.
37. Smith, P. J.; Westaway, K. C. *Can. J. Chem.* **1987**, 65, 2149-2153.
38. Fethiere, J.; Eggimann, B.; Cygler, M. *J. Mol. Biol.* **1999**, 288, 635-647.
39. Michelacci, Y. M.; Dietrich, C. P. *Biochim. Biophys. Acta* **1976**, 451, 436-443.
40. Huang, W. J.; Boju, L.; Tkalec, L.; Su, H. S.; Yang, H. O.; Gunay, N. S.; Linhardt, R. J.; Kim, Y. S.; Matte, A.; Cygler, M. *Biochemistry* **2001**, 40, 2359-2372.
41. Fethiere, J.; Shilton, B. H.; Li, Y.; Allaire, M.; Laliberte, M.; Eggimann, B.; Cygler, M. *Acta Cryst.* **1998**, D54, 279-280.

42. Li, S.; Kelly, S. J.; Lamani, E.; Ferraroni, M.; Jedrzejewski, M. J. *EMBO J.* **2000**, *19*, 1228-40.
43. Ponnuraj, K.; Jedrzejewski, M. J. *J. Mol. Biol.* **2000**, *299*, 885-895.
44. Silva, M. E.; Dietrich, C. P. *J. Biol. Chem.* **1975**, *250*, 6841-6846.
45. Dietrich, C. P.; Nader, H. B. *Biochim. Biophys. Acta* **1974**, *343*, 34-44.
46. Hiyama, K.; Okada, S. *J. Biochem.* **1977**, *82*, 429-436.
47. Hiyama, K.; Okada, S. *J. Biochem.* **1976**, *80*, 1201-1207.
48. Babbitt, P. C.; Hasson, M. S.; Wedekind, J. E.; Palmer, D. R. J.; Barrett, W. C.; Reed, G. H.; Rayment, I.; Ringe, D.; Kenyon, G. L.; Gerlt, J. A. *Biochemistry* **1996**, *35*, 16489-16501.
49. Gulick, A. M.; Palmer, D. R. J.; Babbitt, P. C.; Gerlt, J. A.; Rayment, I. *Biochemistry* **1998**, *37*, 14358-14368.
50. Blanchard, J. S.; Cleland, W. W. *Biochemistry* **1980**, *19*, 4506-4513.
51. Ngai, K. L.; Kallen, R. G. *Biochemistry* **1983**, *22*, 5231-5236.
52. Bach, R. D.; Badger, R. C.; Lang, T. J. *J. Am. Chem. Soc.* **1979**, *101*, 2845-2848.
53. Walsh, C. *Enzyme Reaction Mechanisms*; W.H. Freeman and Company: San Francisco, **1979**, pp. 542-547.
54. Madgwick, J.; Haug, A.; Larsen, B. *Acta. Chem. Scand.* **1973**, *27*, 711-712.
55. Stevens, R. A.; Levin, R. E. *Appl. Environ. Microbiol.* **1976**, *31*, 896-899.
56. Preiss, J.; Ashwell, G. *J. Biol. Chem.* **1962**, *237*, 309-316.
57. Hasegawa, S.; Nagel, C. W. *J. Biol. Chem.* **1962**, *237*, 619-621.
58. Nedjma, M.; Hoffmann, N.; Belarbi, A. *Anal. Biochem.* **2001**, *291*, 290-296.
59. Weissbach, A.; Hurwitz, J. *J. Biol. Chem.* **1959**, *234*, 705-709.
60. Boyd, J.; Turvey, J. R. *Carbohydr. Res.* **1977**, *57*, 163-171.
61. Wusteman, F. S.; Gacesa, P. *Carbohydr. Res.* **1993**, *241*, 237-244.
62. Yoshida, S.; Watanabe, S.; Takeuchi, T.; Murata, K.; Kusakabe, I. *Biosci. Biotech. Biochem.* **1997**, *61*, 357-358.
63. Reissig, J. L.; Strominger, J. L.; Leloir, L. F. *J. Biol. Chem.* **1955**, *217*, 959-966.
64. Kitamikado, M.; Lee, Y. Z. *Appl. Microbiol.* **1975**, *29*, 414-421.
65. Khan, M. Y.; Newman, S. A. *Anal. Biochem.* **1991**, *196*, 373-376.

66. Yang, V. C.; Linhardt, R. J.; Bernstein, H.; Cooney, C. L.; Langer, R. *J. Biol. Chem.* **1985**, *260*, 1849-1857.
67. Kempton, J. B. *A mechanistic investigation of Agrobacterium β -glucosidase*, PhD Thesis, University of British Columbia: Vancouver, BC, **1990**, pp 43.
68. Fersht, A. *Structure and Mechanism in Protein Science: A Guide to Enzyme Catalysis and Protein Folding*; W. H. Freeman and Company: New York, **1999**.
69. Sargent, A. L.; Rollog, M. E.; Almlöf, J. E.; Gassman, P. G.; Gerlt, J. A. *J. Mol. Struct.-Theochem.* **1996**, *388*, 145-159.
70. Gerlt, J. A.; Kozarich, J. W.; Kenyon, G. L.; Gassman, P. G. *J. Am. Chem. Soc.* **1991**, *113*, 9667-9669.
71. Cleland, W. W.; Frey, P. A.; Gerlt, J. A. *J. Biol. Chem.* **1998**, *273*, 25529-25532.
72. Gerlt, J. A.; Gassman, P. G. *J. Am. Chem. Soc.* **1992**, *114*, 5928-5934.
73. Gerlt, J. A.; Gassman, P. G. *J. Am. Chem. Soc.* **1993**, *115*, 11552-11568.
74. Cleland, W. W.; Kreevoy, M. M. *Science* **1994**, *264*, 1887-1890.
75. Frey, P. A.; Whitt, S. A.; Tobin, J. B. *Science* **1994**, *264*, 1927-1930.
76. Mader, M. M.; Bartlett, P. A. *Chem. Rev.* **1997**, *97*, 1281-1301.
77. Gerlt, J. A.; Gassman, P. G. *Biochemistry* **1993**, *32*, 11943-11952.
78. Guthrie, J. P.; Kluger, R. *J. Am. Chem. Soc.* **1993**, *115*, 11569-11572.
79. Guthrie, J. P. *Chem. Biol.* **1996**, *3*, 163-170.
80. Hilal, S. H.; Brewer, J. M.; Lebioda, L.; Carreira, L. A. *Biochem. Biophys. Res. Comm.* **1995**, *211*, 607-613.
81. Sinnott, M. L.; Souchard, I. J. L. *Biochem. J.* **1973**, *133*, 99-104.
82. Stoffyn, A.; Stoffyn, P. *J. Org. Chem.* **1967**, *32*, 4001-4006.
83. Königs, W.; Knorr, E. *Ber.* **1901**, *34*, 957.
84. Kobayashi, Y.; Shiozaki, M. *J. Org. Chem.* **1995**, *60*, 2570-2580.
85. Garegg, P. J.; Oscarson, S. *Carbohydr. Res.* **1985**, *137*, 270-275.
86. Wollwage, P. C.; Seib, P. A. *J. Chem. Soc.* **1971**, 3143-3155.
87. Leung, O. T.; Douglas, S. P.; Whitfield, D. M.; Pang, H. Y. S.; Krepinsky, J. J. *New. J. Chem.* **1994**, *18*, 349-363.
88. Petrakova, E.; Yeh, H. J. C.; Kovac, P.; Glaudemans, C. P. J. *J. Carbohydr. Chem.* **1992**, *11*, 407-412.

89. Davis, N. J.; Flitsch, S. L. *Tetrahedron Lett.* **1993**, *34*, 1181-1184.
90. Melvin, F.; McNeill, A.; Henderson, P. J. F.; Herbert, R. B. *Tetrahedron. Lett.* **1999**, *40*, 1201-1202.
91. Mintz, M. J.; Walling, C. *Organic Syntheses. Collective Volume 5*; Noland, W. E., Ed.; John Wiley & Sons, Inc., **1973**; Vol. 5, pp 184-187.
92. Kovac, P.; Taylor, R. B. *Carbohydr. Res.* **1987**, *167*, 153-173.
93. Garegg, P. J.; Hultberg, H. *Carbohydr. Res.* **1982**, *110*, 261-266.
94. Horton, D. *Methods in Carbohydrate Chemistry*; Whistler, R. L. and BeMiller, J. N., Ed.; Academic Press: New York, **1972**; Vol. VI, pp 282-285.
95. Gross, P. H.; Jeanloz, R. W. *J. Org. Chem.* **1967**, *32*, 2759-2763.
96. Rochepeau-Jobron, L.; Jacquinet, J. C. *Carbohydr. Res.* **1998**, *305*, 181-191.
97. Fraser-Reid, B.; Wu, Z.; Udodong, U. E.; Ottosson, H. *J. Org. Chem.* **1990**, *55*, 6068.
98. Wolfrom, M. L.; Thompson, A. *Methods in Carbohydrate Chemistry*; Whistler, R. L., Wolfrom, M. L. and BeMiller, J. N., Ed.; Academic Press: New York, **1963**; Vol. II, pp 211-215.
99. Ferro, V.; M., M.; Stick, R. V.; Tilbrook, D. M. G. *Aust. J. Chem.* **1988**, *41*, 813-815.
100. DeNinno, M. P.; Etienne, J. B.; Duplantier, K. C. *Tetrahedron Lett.* **1995**, *36*, 669-672.
101. Albright, J. D.; Goldman, L. *J. Am. Chem. Soc.* **1967**, *89*, 2416-2423.
102. Ley, S. V.; Norman, J.; Griffith, W. P.; Marsden, S. P. *Synthesis* **1994**, 639-666.
103. Allanson, N. M.; Liu, D. S.; Chi, F.; Jain, R. K.; Chen, A.; Ghosh, M.; Hong, L. W.; Sofia, M. J. *Tetrahedron Lett.* **1998**, *39*, 1889-1892.
104. Reed, A. E.; Schleyer, P. v. R. *J. Am. Chem. Soc.* **1987**, *109*, 7362-7373.
105. Schleyer, P. v. R.; Jemmins, E. D.; Spitznagel, G. W. *J. Am. Chem. Soc.* **1985**, *107*, 6393-6394.
106. Withers, S. G.; Street, I. P.; Percival, M. D. *Fluorinated Carbohydrates: Chemical and Biochemical Aspects*; Taylor, N. F., Ed.; American Chemical Society: Washington, DC, **1988**, pp 59-77.
107. Gran, G. *Anal. Chim. Acta* **1988**, *206*, 111-123.

108. Harris, D. C. *Quantitative Chemical Analysis*; 3 ed.; W. H. Freeman and Company: New York, **1991**.
109. Rossotti, F. J. C.; Rossotti, H. J. *Chem. Ed.* **1965**, *42*, 375-378.
110. Kempton, J. B.; Withers, S. G. *Biochemistry* **1992**, *31*, 9961-9969.
111. Klinman, J. P. *Transition States of Biochemical Processes*; Gandour, R. D. and Schowen, R. L., Ed.; Plenum Press: New York, **1978**, pp 165-200.
112. Northrop, D. B. *Biochemistry* **1975**, *14*, 2644-51.
113. Saunders, W. H. *Techniques of Chemistry. Investigations of Rates and Mechanisms of Reactions. Part I*; 4 ed.; Bernasconi, C. F., Ed.; John Wiley & Sons, Inc.: New York, **1986**; Vol. 6, pp 565-611.
114. Crooks, J. E. *Proton Transfer Reactions*; Caldin, E. and Gold, V., Ed.; Wiley: New York, **1975**, pp 153-177.
115. Bernasconi, C. F.; Terrier, F. *J. Am. Chem. Soc.* **1987**, *109*, 7115-7121.
116. Yoon, H. J.; Hashimoto, W.; Miyake, O.; Murata, K.; Mikami, B. *J. Mol. Biol.* **2001**, *307*, 9-16.
117. Shen, T. Y.; Westhead, E. W. *Biochemistry* **1973**, *12*, 3333-7.
118. Anderson, S. R.; Anderson, V. E.; Knowles, J. R. *Biochemistry* **1994**, *33*, 10545-55.
119. Taylor, E. A.; Palmer, D. R. J.; Gerlt, J. A. *J. Am. Chem. Soc.* **2001**, *123*, 5824-5825.
120. Morgan, P. M.; Sala, R. F.; Tanner, M. E. *J. Am. Chem. Soc.* **1997**, *119*, 10269-10277.
121. Shokat, K.; Uno, T.; Schultz, P. G. *J. Am. Chem. Soc.* **1994**, *116*, 2261-2270.
122. Hogg, J. L. *Transition States of Biochemical Processes*; Gandour, R. D. and Schowen, R. L., Ed.; Plenum Press: New York, **1978**, pp 201-224.
123. March, J. *Advanced Organic Chemistry. Reactions, Mechanisms, and Structure*; 4 ed.; John Wiley & Sons: New York, **1992**, pp. 991-992.
124. Blake, C. C. F.; Koenig, D. F.; Mair, G. A.; North, A. C. T.; Phillips, D. C.; Sarma, V. R. *Nature* **1965**, *206*, 757-761.
125. Pritchard, D. G.; Trent, J. O.; Li, X.; Zhang, P.; Egan, M. L.; Baker, J. R. *Proteins* **2000**, *40*, 126-34.

126. Akita, M.; Suzuki, A.; Kobayashi, T.; Ito, S.; Yamane, T. *Acta Cryst.* **2001**, D57, 1786-1792.
127. Sasisekharan, R.; Leckband, D.; Godavarti, R.; Venkataraman, G.; Cooney, C. L.; Langer, R. *Biochemistry* **1995**, 34, 14441-14448.
128. Godavarti, R.; Sasisekharan, R. *Biochem. Biophys. Res. Commun.* **1996**, 229, 770-777.
129. Yoon, H. J.; Choi, Y. J.; Miyake, O.; Hashimoto, W.; Murata, K.; Mikami, B. *J. Microbiol. Biotechnol.* **2001**, 11, 118-123.
130. Withers, S. G.; Namchuk, M.; Mosi, R. *Iminosugars as Glycosidase Inhibitors: Nojirimycin and Beyond*; Stutz, A. E., Ed.; Wiley-VCH: Weinheim, **1999**, pp 189-206.
131. Bolin, J. T.; Filman, D. J.; Matthews, D. A.; Hamlin, R. C.; Kraut, J. *J. Biol. Chem.* **1982**, 257, 13650-13662.
132. Werkheiser, W. C. *J. Biol. Chem.* **1961**, 236, 888-893.
133. Bartlett, P. A.; Marlowe, C. K. *Biochemistry* **1983**, 22, 4618-4624.
134. Anderson, V. E.; Weiss, P. M.; Cleland, W. W. *Biochemistry* **1984**, 23, 2779-2786.
135. Porter, D. J.; Bright, H. J. *J. Biol. Chem.* **1980**, 255, 4772-4780.
136. Schloss, J. V.; Porter, D. J.; Bright, H. J.; Cleland, W. W. *Biochemistry* **1980**, 19, 2358-2362.
137. Schloss, J. V.; Cleland, W. W. *Biochemistry* **1982**, 21, 4420-4427.
138. Crout, D. H. G.; Howarth, O. W.; Singh, S.; Swoboda, B. E. P.; Critchley, P.; Gibson, W. T. *J. Chem. Soc.-Chem. Commun.* **1991**, 1550-1551.
139. Crout, D. H. G.; Singh, S.; Swoboda, B. E. P.; Critchley, P.; Gibson, W. T. *J. Chem. Soc.-Chem. Commun.* **1992**, 704-705.
140. Singh, S.; Scigelova, M.; Critchley, P.; Crout, D. H. *Carbohydr. Res.* **1998**, 305, 363-70.
141. Bartek, J.; Muller, R.; Kosma, P. *Carbohydr. Res.* **1998**, 308, 259-273.
142. Johansson, R.; Samuelsson, B. *J. Chem. Soc. Perkin Trans. I* **1984**, 2371-2374.
143. Szarek, W. A.; Zamojski, A.; Tiwari, K. N.; Ison, E. R. *Tetrahedron Lett.* **1986**, 27, 3827-3830.

144. Oldham, J. W. H.; Rutherford, J. K. *J. Am. Chem. Soc.* **1932**, *54*, 366.
145. Blatter, G.; Beau, J. M.; Jacquinet, J. C. *Carbohydr. Res.* **1994**, *260*, 189-202.
146. Demchenko, A. V.; Boons, G. J. *Chem.-Eur. J.* **1999**, *5*, 1278-1283.
147. Ferrier, R. J.; Furneaux, R. H. *J. Chem. Soc. Perkin Trans. I* **1977**, 1996-2000.
148. Blattner, R.; Ferrier, R. J.; Tyler, P. C. *J. Chem. Soc. Perkin Trans. I* **1980**, 1535-1539.
149. Jacquinet, J. C. *Carbohydr. Res.* **1990**, *199*, 153-181.
150. Izumi, K. *Agric. Biol. Chem.* **1979**, *43*, 95-100.
151. Ferrier, R. J.; Tyler, P. C. *J. Chem. Soc. Perkin Trans. I* **1980**, 2767-2773.
152. Sugihara, J. M.; Teerlink, W. J.; MacLeod, R.; Dorrence, S. M.; Springer, C. H. *J. Org. Chem.* **1963**, *44*, 659-661.
153. Adam, W.; Hadjirapoglou, L. *Top. Curr. Chem.* **1993**, *164*, 45-62.
154. Corey, E. J.; Samuelsson, B.; Luzzio, F. A. *J. Am. Chem. Soc.* **1984**, *106*, 3682-3683.
155. Gilbert, K. E.; Borden, W. T. *J. Org. Chem.* **1979**, *44*, 659-661.
156. Leatherbarrow, R. J. *GraFit 4.0.15*, **2001**, Erithacus Software Ltd.
157. Piel, E. V.; Purves, C. B. *J. Am. Chem. Soc.* **1939**, *61*, 2978-2979.